

NASA Contractor Report 159228

Bifilar Analysis User's Manual—Volume II

Sebastian J. Cassarino
Timoleon Mouzakis

SIKORSKY AIRCRAFT
Stratford , Ct 06602

CONTRACT NASI-15612
AUGUST 1980



National Aeronautics and
Space Administration

Langley Research Center
Hampton, Virginia 23665
AC 804 827-3966

1. Report No. NASA CR-159228--Volume II	2. Government Accession No.	3. Recipient's Catalog No.	
4. Title and Subtitle Bifilar Analysis User's Manual - Volume II		5. Report Date August 1980	6. Performing Organization Code
7. Author(s) Sebastian J. Cassarino and Timoleon Mouzakis		8. Performing Organization Report No. SER-510036	10. Work Unit No.
9. Performing Organization Name and Address Sikorsky Aircraft Stratford, Connecticut 06602		11. Contract or Grant No. NAS1-15612	13. Type of Report and Period Covered
12. Sponsoring Agency Name and Address National Aeronautics and Space Administration Washington, D.C. 20546		14. Sponsoring Agency Code	
15. Supplementary Notes Technical Monitor: Dr. William F. White, Jr., The contract research effort which has led to the results in this report was financially supported by the Structures Laboratory, USARTL (AVRADCOM).			
16. Abstract This report describes the digital computer program developed to study the vibration response of a coupled rotor/bifilar/airframe coupled system. The theoretical development of the rotor/airframe system equations of motion is provided in Reference 1 while the fuselage and bifilar absorber equations of motion are discussed in Appendix D. The modular block approach used in the make-up of this computer program is described in Section 2. Section 3 provides descriptions of the input data needed to run the rotor and bifilar absorber analyses. Sample output formats are presented and discussed in Section 4. The results for four test cases, which use the major logic paths of the computer program, are presented in Section 5. In Section 6, the overall program structure is discussed in detail, including the segmentation procedure (overlay) needed to run the program on the NASA CDC computer system, the routine flow diagrams and a list of the COMMON blocks. Finally, in Section 7, the Fortran subroutines are described in detail.			
17. Key Words (Suggested by Author(s)) Coupled rotor/bifilar/airframe analysis, bifilar absorber, input, output, sample case, test cases		18. Distribution Statement Unclassified - Unlimited	
19. Security Classif. (of this report) Unclassified	20. Security Classif. (of this page) Unclassified	21. No. of Pages 359	22. Price*

TABLE OF CONTENTS

<u>Section</u>	<u>Page</u>
LIST OF FIGURES	v
LIST OF TABLES	vi
LIST OF APPENDICES	vii
1 SUMMARY	1
2 PROGRAM DESCRIPTION	2
2.1 Analytical Model	2
2.2 Program Execution	3
3 INPUT DESCRIPTIONS	5
3.1 Rotor Aeroelastic Analysis Input	5
3.2 Bifilar Analysis Input	22
3.3 Input Data Format	35
4 OUTPUT DESCRIPTIONS	36
4.1 Rotor Aeroelastic Analysis Output	36
4.2 Bifilar Analysis Output	40
5 TEST CASES RESULTS	45
5.1 Test Cases Description	45
5.2 Job Control Language	45
5.3 Test Cases Input Data	46
5.4 Test Cases Output Data	47
5.5 Test Cases Computer Time	47
6 OVERALL PROGRAM STRUCTURE	49
6.1 Segmentation Structure	49
6.2 Flow Diagrams	51

TABLE OF CONTENTS (CONTINUED)

<u>Section</u>	<u>Page</u>
6.3 Common Blocks	52
7 SUBROUTINE DESCRIPTIONS	53
REFERENCES	158
FIGURES	159
APPENDIX A: JOB CONTROL LANGUAGE	205
APPENDIX B. TEST CASES INPUT DATA	206
APPENDIX C: TEST CASES RESULTS	218
Case 1. Coupled Rotor/Linear Bifilar/Airframe	218
Case 2. Coupled Rotor/Non-Linear Bifilar/Airframe	241
Case 3. Coupled Linear Bifilar/Airframe	257
Case 4. Coupled Non-Linear Bifilar/Airframe	264
APPENDIX D: COUPLED ROTOR/BIFILAR/AIRFRAME ANALYSIS	277

LIST OF FIGURES

<u>Figure</u>		<u>Page</u>
1	Block Diagram of Bifilar Analysis	159
2	Output Format - Rotor Blade Input Data	160
3	Output Format - Rotor Blade Characteristics	161
4	Output Format - Rotor Blade Matrices	169
5	Output Format - Bifilar Linear Analysis Matrices	171
6	Output Format - Bifilar Linear Analysis Forced Response Results	182
7	Output Format - Bifilar Nonlinear Analysis Matrices	186
8	Output Format - Bifilar Nonlinear Analysis Time History Results	192
9	Bifilar Analysis Segmentation Structure	195
10	Flow Chart for the Main Program	196
11	Flow Chart for Subroutine PRELIM	197
12	Flow Chart for Subroutine MODES	198
13	Flow Chart for Subroutine DYNMAT	199
14	Flow Chart for Subroutine AERMAT	200
15	Flow Chart for The Bifilar Analysis	201
16	Flow Charts for Subroutines SYSCTL, CMPUTE, NLBIF	202
17	COMMON Blocks	203



LIST OF TABLES

<u>Table</u>		<u>Page</u>
1	Rotor Analysis Output Description	36
2	Program Multiple Cases Setup	46
3	Bifilar Analysis Test Cases Results	47
4	Segmentation Structure Description	49
5	Segmentation Structure Routines and COMMON Blocks	50
6	IMSL Routines	52
7	Program Subroutines Listing	53

LIST OF APPENDICES

<u>Appendix</u>		<u>Page</u>
A	Job Control Language	205
B	Test Cases Input Data	206
C	Test Cases Results	218
	Case 1. Rotor Results	218
	Case 1. Bifilar Results	234
	Case 2. Bifilar Results	241
	Case 3. Bifilar Results	257
	Case 4. Bifilar Results	264
D	Coupled Rotor/Bifilar Airframe Analysis	277

SECTION 1

SUMMARY

This report describes the digital computer program developed to study the vibration response of a coupled rotor/bifilar/airframe system.

The theoretical development of the rotor/airframe system equations of motion is provided in Reference 1 while the fuselage and bifilar absorber equations of motion are discussed in Appendix D.

The modular block approach used in the make-up of this computer program is described in Section 2. Section 3 provides descriptions of the input data needed to run the rotor and bifilar absorber analyses. Sample output formats are presented and discussed in Section 4. The results for four test cases, which use the major logic paths of the computer program, are presented in Section 5. In Section 6, the overall program structure is discussed in detail, including the segmentation procedure (overlay) needed to run the program on the NASA CDC computer system, the routine flow diagrams and a list of the COMMON blocks. Finally, in Section 7, the Fortran subroutines are described in detail.

The work was conducted under NASA contract NAS1-15612, "Bifilar Analysis Study".

SECTION 2

PROGRAM DESCRIPTION

The bifilar absorber analysis was developed to provide the engineer with an analytical tool capable of rapid parametric vibration evaluation of the entire helicopter. A block diagram of the vibration analysis program is shown in Figure 1, where it can be seen that a modular approach has been adopted to form the main program. Modularization is achieved when each component block outputs the mass, damping and stiffness matrices or force vectors with the pertinent degrees-of-freedom (d.o.f.) including the 6 d.o.f. of the attachment point, i.e. 6 d.o.f. at the hub for rotor or bifilar absorber attachment, or 6 d.o.f. in the cabin or cockpit for fixed-system absorber attachment. Where two blocks merge together, the degrees-of-freedom of the attachment point are eliminated and replaced by fuselage modal degrees-of-freedom.

2.1 Analytical Model

Derivation of the coupled analysis is shown in Appendix D.

A description of the analytical model which consists of primarily rotor, fuselage, rotating-system absorbers and fixed-system absorbers is given below.

Rotor

The rotor system is represented by a modal approach which utilizes the equations of motion from Reference 1. The rotor blade degrees-of-freedoms which can be incorporated in the analysis are: up to four blade elastic modes (coupled flatwise/edgewise), up to 2 blade torsional blade modes (first mode represents a rigid blade while the second one is an elastic mode) and rigid blade flapping and lead-lag motions - a total of 8 blade modes which correspond to 24 d.o.f. (each mode has one symmetric and two cyclic components). The rotor/airframe coupling terms are incorporated in the analysis using 5 airframe modes corresponding to uncoupled fuselage longitudinal (x), lateral (y), vertical (z), roll (θ_x) and pitch (θ_y) motions - yaw motion (θ_z) is not included.

The major assumptions made in the development of the rotor system model are listed below:

1. Dynamic and aerodynamic effects assume small perturbations about steady initial values of the system generalized coordinates.
2. Aerodynamic forces are developed using strip theory.
3. Number of rotor blades must be greater than two due to the polar symmetry assumption made in the rotating system generalized coordinate transformations.

4. The following effects are not included in the rotor analysis:

- a. Forward flight aerodynamics
- b. Rotor speed d.o.f.
- c. Variable inflow over the rotor disc
- d. Unsteady aerodynamics
- e. Airframe yaw motion

Fuselage

The fuselage dynamic model is a set of linear modal equations which are provided in Appendix D. The computer program accepts inputs of system modal properties of up to 16 airframe modes.

Rotating-System Absorbers

The bifilar analysis includes linear and non-linear inplane rotor-head absorbers and linear vertical absorbers. The forced response analysis can use up to 5 types of linear absorbers (inplane plus vertical). A maximum of 12 non-linear inplane pendulums can be employed in the time history analysis. Viscous damping of the absorbers is assumed.

Fixed-System Absorbers

Fixed system absorbers are modeled in the analysis as a simple unidirectional spring-mass-damper system. The absorbers attachment point must be at a defined modal vector point. Provisions for up to 5 absorbers are provided for in the analysis.

2.2 Program Execution

The rotor/bifilar coupled program starts by calculating the dynamic and aerodynamic rotor/airframe matrices (assuming that rotor coupling has been requested) and couples them with the bifilar analysis fixed system dynamic matrices. Then, it expands the matrices to include the contributions from the fixed system absorbers and the linear inplane and vertical bifilar pendulums. At this point, a decision is made on the type of solution to be calculated: forced response or time-history. If the forced response solution is requested, then the generalized forces are calculated followed by the evaluation of the forced response solution. If the time-history solution is required, then the program proceeds to calculate the dynamic matrices of the non-linear inplane bifilars, adds them to the matrices from the linear analysis, solves for the acceleration vector and integrates it to obtain the velocity and displacement vectors. The final results are harmonically analyzed (up to 10 harmonics can be obtained) and printed out.



Multiple cases, in which any number of input variables are changed, can be easily run (a detailed discussion can be found in Section 5 - TEST CASES RESULTS). If the rotor blade characteristics are not changed, then the rotor matrices are calculated only once, stored and used at a later time as needed.

Computer running time is highly dependent on the total system degrees-of-freedom used and the type of solution requested. The time-history solution requires considerably greater computer time than the forced response solution. Typical computer running times for the time history solution range from one to seven minutes while the forced response execution usually requires from a few seconds to one-half a minute (see Section 5.5 for more details).

When a nonsystem error occurs during the execution of a case, the program attempts to continue using the best data available; if the error is too fundamental for the case to be meaningful, then a partial data printout, followed by an error message, is given before job termination.

SECTION 3

INPUT DESCRIPTION

3.1 Rotor Aeroelastic Analysis Input

3.1.1 Computer Listing of Input for Rotor Aeroelastic Analysis

<u>Symbol</u>	<u>Location</u>	<u>Input Item</u>	<u>Units</u>
RHO	1	Air mass density	Lb sec**2/ft**4
VS	2	Speed of sound	Ft/sec
TL	3	Tip loss factor	Nd
VIP	4	Rotor axial velocity	Knots
OMEGAI	5	Rotor rotational speed	RPM
RIP	6	Rotor radius	Ft
EIP	7	Blade offset	Ft
BLADES	8	No. of blades - must be greater than 2	Nd
KBETA	9	Blade flapping hinge spring constant	Lb-in/rad
KGAMMA	10	Blade lag hinge spring constant	Lb-in/rad
GAMOI	11	Blade prelag angle - lag positive	Deg
BETOI	12	Blade precone angle - up positive	Deg
THETAO	13	Blade collective pitch angle at 75% radius	Deg
EB	14	Blade Young's modulus	Lb/in**2
YPH2	15	Distance along blade axis from center of rotation to push rod	
PHL	16	Distance from blade elastic axis to push rod - positive toward leading edge	In
ZETGAM	17	Fraction of critical lag damping	Nd
ZETPIT	18	Fraction of critical blade pitch damping - based on rotor speed	Nd
OMGI	19	Reference rotor speed for defining percent critical lag damping in ground resonance studies	RPM
XNEMOD	20	Number of blade bending modes - up to 4	Nd
---	21	Open	
ZETBLD	22-25	Fraction of critical damping of blade bending modes - based on mode frequencies	Nd
---	26-105	Open	
ALPHA1	106	Blade pitch/lag coupling	Nd

Control Switches

DUM1(1)	107	Printout of 30 X 30 rotor dynamic (3) and aerodynamic (2) matrices 0 - no ; 1 - yes
DUM1(2)	108	Printout of KXK (compressed) rotor matrices (dyn. + aero.) 0 - no ; 1 - yes
DUM1(3)	109	Punch out of KXK (compressed) rotor matrices (dyn. + aero.) 0 - no ; 1 - yes
DUM1(4)	110	Use of rotor matrices in bifilar analysis 0. do not use 1. use new rotor matrices -1. use previous rotor matrices
ROTEST	111	1. for main rotor 2. for tail rotor
---	112	Open
SYSDEF	113	System definition - ABCDEFGH. A - blade bending B - blade rigid body pitching C - blade rigid body flapping D - blade rigid body lagging E - fixed system modes F - blade elastic pitching G - set to 1 H - set to 1 Element = 0 to include = 1 to exclude
ROTDEF	114	Rotor definition - X. X = 1. - blade hinged flatwise and edgewise = 2. - blade cantilevered flatwise and edgewise = 3. - blade hinged flatwise, cantilevered edgewise = 4. - blade cantilevered flatwise, hinged edgewise = 5. - gimbaled rotor
ARTIC	115	Blade pitch input control - XY. X = 1 - pitch bearing follows blade out-of-plane root slope = 0 - pitch bearing remains in plane of hub or preconed position Y = 1 - pitch bearing follows blade inplane root slope = 0 - pitch bearing remains in vertical plane or prelagged position
---	116-118	Open
PRINT	119	Main printout control - X. X = 3. - A, basic calculations + dyn. and aero. integrals = 4. - B, A + blade frequency input = 5. - C, basic calculations only = 6. - D, B + blade frequency output = 7 or greater - same as for X = 3.

DUM2(1)	120	Propeller moment option in dynamic stiffness matrix 0. include propeller moment (default value) 1. exclude propeller moment
---	121-	Open
	124	
LAGKII	125	Blade lag damper option 0. include lag damper 1. exclude lag damper

Lag damper physical characteristics

L1	126	L1, inches
L2	127	L2, inches
L3	128	L3, inches
L4	129	L4, inches
L5	130	L5, inches
L6	131	L6, inches
CLD	132	Damper damping coefficient, lb-sec/in.
KLD	133	Damper stiffness coefficient, lb/in.
ZETELP	134	Blade elastic pitch modal damping, nd
CP	135	Effective radius to cantilevered point in torsion (defaults to value of blade offset in location 7) , in.
---	136-	Open
	199	
BN	200	Number of elements in blade segment chart - up to 20. These are defined over the length of the blade only - the first segment is at the root of the blade-normally the last segment should be no more than 3 percent radius.
RR	201- 249	Segment lengths, inches

The following blade properties are input from the center
of rotation to the blade tip at specified radial positions

NCHI	250	Number of elements in blade chord chart
CHORD	251-	Radius - in : chord - in
	349	
NATWI	350	Number of elements in blade aerodynamic twist chart
ATWIST	351-	Radius - in : twist - deg
	449	(twist down is positive and is zero at 75 percent radius)

17308
16447

NSTWI	450	Number of elements in blade structural twist chart
STWIST	451- 549	Radius - in : twist - deg (twist down is positive. The twist at 75 percent radius is defined by the blade geometry consistent with the definition of aerodynamic twist)
NCGI	550	Number of elements in blade center of gravity chart
CG	551- 649	Radius - in : CG - in (CG is positioned relative to and positive ahead of elastic axis)
NACI	650	Number of elements in blade aerodynamic center chart
AC	651- 749	Radius - in : AC - in (AC is positioned relative to and positive ahead of elastic axis)
NEAI	750	Number of elements in blade elastic axis chart
EA	751- 849	Radius - in : EA - in (EA is positioned relative to and positive aft of semi-chord)

The following blade properties are defined for a specified radial segment

NGJFI	850	Number of elements in flexbeam torsional stiffness (cross-beam rotor design) chart
RGJF	851- 949	GJ - lb-in**2 : segment length - in
NMBI	950	Number of elements in blade weight chart
RMB	951- 1049	Weight - lb/in : segment length - in
NIEI	1050	Number of elements in blade edgewise second moment of area chart
RIE	1051- 1149	IYY - In**4 : segment length - in
NIFI	1150	Number of elements in blade flatwise second moment of area chart
RIF	1151- 1249	IXX - In**4 : segment length - in
NFM	1250	Number of elements in blade flatwise mass moment of inertia chart (about CG)
RFM&FMI	1251- 1349	IF - lb-in-sec**2/in : segment length - in
NEM	1350	Number of elements in blade edgewise mass moment of inertia chart (about CG)
REM&EMI	1351- 1449	IE - lb-in-sec**2/in : segment length - in
NTM	1450	Number of elements in blade torsional mass moment of inertia chart (about CG)
RTM&TMI	1451- 1549	IT - lb-in-sec**2/in : segment length - in
NGJI	1550	Number of elements in blade torsional stiffness - GJ chart
RGJ	1551- 1649	GJ - lb-in**2 : segment length - in

XBR Parameters

YA	1650	Distance from center of rotation to outer snubber, in.
YB	1651	Distance from center of rotation to inner snubber, in.
FRR	1652	Distance from center of rotation to flexbeam root, in.
---	1653-	Open
	1669	

Tail Rotor Control System Parameters

PBM	1670	Weight at blade pushrod, 1b.
---	1671-	Open
	1674	
C1	1675	Damping associated with weight above, 1b-sec/in.
---	1676-	Open
	1679	
PBK	1680	Stiffness associated with weight above, 1b/in.
---	1681-	Open
	1766	

Main Rotor Control System Parameters

PBMM	1767	Weight at blade pushrod, 1b.
---	1768	Open
C1M	1769	Damping associated with weight above, 1b-sec/in.
---	1770-	Open
	1772	
PBKM	1773	Stiffness associated with the weight above, 1b/in.
---	1774-	Open
	1778	
RSB	1779	Distance from center of rotation to pushrod connection on swashplate, in.
RS	1780	Distance from center of rotation to servo actuator connections on swashplate, in.
---	1781-	Open
	1849	

Blade Section Aerodynamic Data

DRGDAT	1850-	Drag data
	2749	
LIFDAT	2750-	Lift data
	3649	
PMDAT	3650-	Pitching moment data
	4548	

3.1.2 Description of Input for Rotor Aeroelastic Analysis

Additional information on the input parameters is provided in this section.

Each input quantity is given in the following format:

Location No., Quantity, Units.

Important details and comments.

1. Air Mass Density, $\text{lb sec}^2/\text{ft}^4$.

If set to zero, all aerodynamic calculations are omitted.

2. Speed of Sound, ft/sec.

Used to compute local blade Mach number for lift, drag, and pitching moment calculations.

3. Tip Loss Factor, Nondimensional.

Provides lift and pitching moment loss in the blade tip region. Drag is not affected.

Value should be equal to or greater than one minus the non-dimensional length of the blade tip segment. A value of one constitutes no loss.

4. Rotor Axial Velocity, Knots.

Represents climb or sideslip velocity for a main or tail rotor respectively. For propellers this is the forward speed of the aircraft. Positive velocities are in the same direction as the thrust.

5. Rotor Rotational Speed, rpm.

When calculating blade bending frequencies at low rpm's, computer time is greatly increased. It is suggested that rpm not be less than 50 cpm.

6. Rotor Radius, ft.

Measured from center of rotation.

7. Blade Offset, ft.

Distance from center of rotation to flap and lag hinge. These hinges are assumed to be coincident.

8. Number of Blades, Nondimensional.

Any number greater than 2 since the analysis assumes that the rotors have polar symmetry. The analysis will execute for $N = 2$ but the results are incorrect.

9. Blade Flapping Hinge Spring Constant, lb in/rad.

If the rotor definition, location 114, stipulates a hinged root boundary condition, the flapping spring provides root flapping restraint in the calculation of the blade elastic modes. It is also used in the rigid-body flapping equation.

10. Blade Lag Hinge Spring Constant, lb in/rad.

Same comments as above with "lagging" substituted for "flapping".

11. Blade Prelag Angle, Degrees.

Lag positive.

12. Blade Precone Angle, Degrees.

Up positive.

13. Blade Collective Pitch, Degrees.

Aerodynamic blade angle at 75% radius. Leading edge up positive. If affects blade thrust and blade bending frequencies and mode shapes.

14. Blade Young's Modulus, lb/in².

Used in calculation of blade elastic modes and steady elastic deflections. Appears explicitly in steady elastic deflection calculations and therefore must have a value if the blades are flexible.

15. Distance Along Blade Axis From Center of Rotation to Blade Pushrod, in.

Used in calculation of pitch/flap coupling for rigid-body flapping and for pitch/flap and pitch/lag coupling for elastic blades.

16. Distance From Blade Elastic Axis to Pushrod, in.

Used in calculation of pitch/flap coupling for rigid body flapping, pitch/lag coupling for rigid body lagging, and pitch/flap and pitch/lag coupling for elastic blades. Positive toward leading edge.



17. Fraction of Critical Lag Damping, Nondimensional.
Used only in the rigid-body lag equation. Based on uncoupled lag frequency. This value is ignored if the lag damper option is exercised (loc 125 set to 0).
18. Fraction of Critical Blade Pitch Damping, Nondimensional.
Used only in the blade pitch equation. Based on rotor speed. If, for example, at a given rotor speed the blade torsional frequency is 5 per rev and we wish to incorporate 10% critical damping, we would input 0.5.
19. Reference Rotor Speed, RPM.
Holds the rigid-body lag and pitch damping coefficients, C, constant at the value corresponding to that at the chosen reference rotor speed. If actual rotor speed variations are made, the percentage of critical damping will vary. If this is not desired, a zero should be input.
20. Number of Blade Bending Modes, Nondimensional.
Up to four elastic modes can be used. If rigid-body modes are also being used, the program automatically recognizes this and will provide the correct elastic modes. For example, if two bending modes are requested and rigid-body flapping is being used, the program finds the first three blade modes, eliminates that mode which corresponds to rigid-body flapping, and provides the remaining two modes. A zero locks out elastic modes.
- 22.-25. Fraction of Critical Damping of Blade Bending Modes, Nondimensional.
Used only in the blade bending equations. Based on modal frequencies.
106. Blade Pitch-Lag Coupling, Nondimensional.
Defined as degrees pitch-up per degree lead for rigid-body lagging motion, or degrees pitch-up per degree blade tip inplane lead angle measured at blade root for elastic modes. Lead/pitch-up positive.

107. Printout option for 30 X 30 rotor matrices. The dynamic stiffness, damping and mass matrices and the aerodynamic damping and stiffness matrices are printed out if switch is set to 1.
108. Printout option for compressed rotor matrices. Same as above except that only those degrees-of-freedom requested are printed out if switch is set to 1.
109. Punchout option for compressed rotor matrices. This option was used before rotor was coupled to bifilar analysis internally in the program. It is excercised if set to 1.
110. Coupling switch governing use of rotor matrices in the bifilar analysis.
 0. = do not use rotor matrices in the bifilar analysis
 1. = calculate and use rotor matrices in the bifilar analysis
 - 1. = use previously calculated rotor matrices in the bifilar analysis
111. Control Switch for Main or Tail Rotor.
 - 1 = Main Rotor
 - 2 = Tail Rotor
113. System Definition.

Exercises primary control in the program. Overrides any contradictory controls. There is one exception: when location 114 equals 5, i.e., a gimbaled rotor. In this case location 114 has executive control whereby digits 1, 3 and 4 of the system definition are ignored. Up to 8 blade degrees-of-freedom (4 bending modes plus 2 torsional modes plus rigid body flapping and inplane motions) can be used in the rotor analysis.
114. Rotor Definition.

When equal to 1, 3, or 4, motion at the hinges is restrained by the springs in locations 9 and 10 as appropriate.

When equal to 5, gimbaled rotor, the program automatically uses rigid-body flapping, and 4 elastic modes with boundary conditions suitably selected to correctly define the first 5 gimbaled rotor modes. See Reference 1 for a complete explanation of this.

Rotor Definition - X.

- X = 1 - Blade Hinged Flatwise & Edgewise
- = 2 - Blade Cantilevered Flatwise & Edgewise
- = 3 - Blade Hinged Flatwise, Cantilevered Edgewise
- = 4 - Blade Cantilevered Flatwise, Hinged Edgewise
- = 5 - Gimbaled Rotor

115. Blade Pitch Input Control.

This simply determines whether inboard or outboard blade feathering is being employed. The feathering bearing is always at the root of the blade.

Blade Pitch Input Control - XY.

- X = 1 - Pitch Bearing Follows Blade Out of Plane Root Slope
- = 0 - Pitch Bearing Remains In Plane of Hub or Preconed Position
- Y = 1 - Pitch Bearing Follows Blade Inplane Root Slope
- = 0 - Pitch Bearing Remains In Vertical Plane or Prelagged Position

119. Main Printout Control.

Provides a graduated printout capability for debugging, etc.

It is generally good practice to use option 5 for the first case of any run in order to establish that all of the input is correct.

Main Printout Control - X.

- X = 3. - A, Basic Calculations + Dynamic & Aerodynamic Integrals
- = 4. - B, A + Blade Frequency Input
- = 5. - C, Basic Calculations Only
- = 6. - D, B + Blade Frequency Output
- > 7. - A (Same as X = 3.)

120. Propeller Moment Option - X.

The propeller moment contribution to the blade rigid torsion degree-of-freedom can be accounted for or neglected depending on the rotor blade design. Removal of the propeller moment is necessary when the rotor design employs blade counterweight devices. The propeller moment is given by:

$$M_p = \Omega^2 I_p \theta \text{ where}$$

$$I_p = \int_0^1 (I_E - I_F) dx$$

The inertia, I_p , is the difference between the blade edgewise and flatwise mass moments of inertia integrated along the blade span. Rotor speed is Ω and blade torsional deflection is given by θ . The moment affects only the dynamic stiffness matrix.

- $X = 0.$ - Include Propeller Moment
- $= 1.$ - Do Not Include Propeller Moment

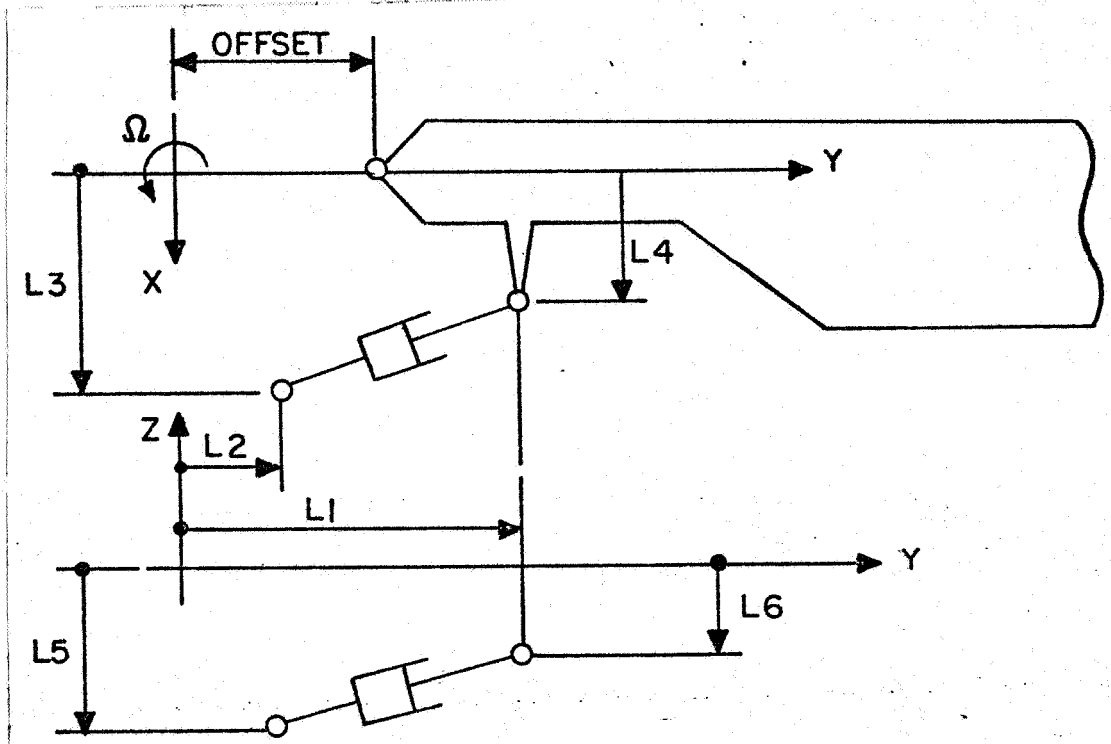
125. Blade Lag Damper Option - X.

- $X = 0.$ - Include Lag Damper
- $= 1.$ - Do Not use Lag Damper

This option allows the use of a blade lag damper which includes all blade motions kinematics and damping and stiffness constants.

A typical arrangement is shown in the sketch below.

The positive convention for the lag damper distances is also shown in the sketch.



Blade Lag Damper Schematic

It should be noted that if a lag damper is used, then input to location 17 is ignored.

126.-134. Refer to the lag damper sketch above.

135. Effective radius to cantilevered point in torsion, in.

All elastic deformation of the blade occurs outboard of this point. For example, in a conventional blade this might be the radius to the pitch horn; in a crossbeam design, it may be the radius to the outboard snubber (if the torque tube is assumed rigid) or it may be the radius to the push rod connection for a torsionally flexible torque tube. The user must use his own judgement in deciding where the cantilever point is situated. If the input cantilever point radius is less than the offset, it is set equal to the offset.

200. Number of Elements in Blade Segment Chart.

Up to 20 may be used. The choice of elements is important, particularly in relation to cross-beam type rotors where it is generally necessary to have smaller elements inboard where the spar is highly twisted. Thus, we may have, for example, 10 elements describing the inboard 25% of the blade, and 10 elements describing the remaining 75%.

201.-220. Segment Lengths, in.

These are defined over the length of the blade only. That is, their sum should equal the blade radius minus the offset. The tip segment should generally be of the order of (1-tip loss factor) times the blade radius.

General Comments for Inputs 250 to 849.

All of these quantities are input as values corresponding to a radial position. The first value is always at the center of rotation and the last at the tip. Linear interpolation is used between adjacent values. Each chart can have up to 49 pairs of radius/value coordinates.

250.-349. Blade Chord, in.

350.-449. Blade Aerodynamic Twist, deg.

Defined positive nose down and must be zero at 75% radius. This distribution is used in the calculation of aerodynamic effects.



450.-549. Blade Structural Twist, deg.

Defined positive nose down and will have a value at 75% radius consistent with the geometric properties of the blade. This distribution is used in the calculation of the blade elastic modes, steady elastic deflections, and blade center of gravity offset effects.

550.-649. Blade Center of Gravity, in.

Positioned relative to, and defined positive ahead of, elastic axis.

650.-749. Blade Aerodynamic Center, in.

Positioned relative to, and defined positive ahead of, elastic axis.

750.-849. Blade Elastic Axis, In.

Positioned relative to, and defined positive aft of, blade semi-chord (for a normal blade, input = - chord/4).

General Comments for Inputs 850 to 1649.

All of these quantities are input as values over a segment length. If an offset exists, the first pair should be "zero, offset". The total of the segment lengths should equal the rotor radius. The weight and stiffness charts can have up to 49 value/segment length pairs. The mass moment of inertia charts can have up to 24 value/segment length pairs.

850.-949. Flexbeam Torsional Stiffness Distribution.

Stiffness: $lb\cdot in^2$, Segment Length: in.

If an effective offset is input, stiffness may be set to zero over this distance.

- 950.-1049. Blade Weight Distribution.
Weight: 1b/in, Segment Length: in.
- 1050.-1149. Blade Flatwise Area Moment Distribution.
Area Mom: in⁴, Segment Length: in.
- 1150.-1249. Blade Edgewise Area Moment Distribution:
Area Mom: in⁴, Segment Length: in.
- 1250.-1299. Blade Edgewise Mass Moment of Inertia Distribution.
Edg. Mass Mom: 1b in sec²/in, Segment Length: in.
- 1350.-1399. Blade Flatwise Mass Moment of Inertia Distribution.
Flat. Mass Mom: 1b in sec²/in, Segment Length: in.
- 1450.-1499. Blade Torsional Mass Moment of Inertia Distribution.
Tors. Mass Mom: 1b in sec²/in, Segment Length: in.
- 1550.-1649. Blade Torsional Stiffness Distribution.
Stiffness: 1b-in², Segment Length: in.
Zeros may be input up to the cantilever point radius (loc. 135). Do not include flexbeam stiffness in this chart.
1650. Distance From Center of Rotation to Outer Snubber, in.
1651. Distance From Center of Rotation to Inner Snubber, in.
Locations 1650 and 1651 have a value other than zero only when cross-beam type rotors are being treated. Nonzero values instruct the program to apply the collective pitch at the outer snubber location. The spar, or structural, blade angle inboard of the outer snubber location is then made equal to the sum of the collective pitch (which is reduced linearly from the value at the outer snubber to zero at the blade root) and the input structural twist. The aerodynamic blade angle inboard of the outer snubber is made equal to the value at the outer snubber.
The torque tube is assumed to be rigid in calculations of pitch/flap coupling.

1652. Distance From Center of Rotation to Flexbeam Root, in.

This is the radius at which torsional deformations of the flexbeam may be assumed to be zero. This radius is also used in defining the twist distribution for blade bending mode computations.

Tail Rotor Control System Parameters

1670. Weight at Blade Pushrod, 1b.

1675. Damping Associated With Weight Above, 1b-sec/in.

1680. Series Stiffness of One Arm of Pitch Beam, Pushrod, and Pitch Horn for Pitch Beam Assumed Cantilevered at its Center, 1b/in.

Main Rotor Control System Parameters

1767. Weight at Blade Pushrod, 1b.

1769. Damping Associated With Weight Above, 1b-sec/in.

1773. Stiffness Associated With Pushrod, Swashplate Connection, Pitch Horn, etc..., 1b/in.

1779. Distance From Center of Rotation to Pushrod Connection on Swash Plate, in.

1780. Distance From Center of Rotation to Servo Actuator Connection on Swash Plate, in.

Blade Section Aerodynamic Data

Drag, lift, and pitching moment data are each input in sets of CD, CL, or CM pairs corresponding to up to 12 Mach numbers.

Any or all of the data charts can be omitted.

In each chart there are up to 35 pairs of angle-of-attack and CD, CL, or CM data corresponding to each Mach number.

A total of 75 locations are allocated to each Mach number.

Mach numbers and angles-of-attack are input in ascending order.

If charts are employed use no less than 2 Mach numbers and 5 pairs of data per chart.

The input angle-of-attack range should exceed the expected range for the condition being analyzed.

Unsymmetric airfoil data can be used.

Only one set of airfoil data can be used.

Example of input format:

1850	Number of pairs for first Mach number
1851	First Mach number
1852-1924	Angle-of-attack: CD pairs
1925	Number of pairs for second Mach number
1926	Second Mach number
1927-1999	Angle-of-attack: CD pairs
Etc.	
1850.-2749.	Drag Data.
2750.-3649.	Lift Data.
3650.-4549.	Pitching Moment Data.

3.2 Bifilar Analysis Input

3.2.1 Computer Listing of Input for Bifilar Analysis

COMPUTER LISTING OF INPUT TO THE BIFILAR ANALYSIS

SYMBOL	LOCATION	DESCRIPTION	UNITS	
NINBF	1	KINDS OF INPLANE BIFILARS	=< 5	
NAP	2	NUMBER OF AIRCRAFT STATION POINTS TO EVALUATE RESPONSE	=< 4	
WF	3	FORCING FREQUENCY	CYCLES/REV	
NIMP	4	DIMENSION OF IMPEDANCE MATRIX (LOC 4 = LOC 9 * 2)		
-----	5	OPEN		
XNARM	6	TOTAL NUMBER OF INPLANE BIFILARS	=< 10	
OMEGAR	7	ROTOR SPEED	RPM	
NFABS	8	NUMBER OF FIXED SYSTEM ABSORBERS	=< 5	
NF	9	NUMBER OF FIXED SYSTEM MODES	=< 16	
IWRITE	10	=1. GET EXTENSIVE PRINTOUT		
-----	11	OPEN		
NVBIF	12	KINDS OF VERTICAL BIFILARS	=< 5	
XNARM	13	TOTAL NUMBER OF VERTICAL BIFILARS	=< 10	
RHM	14	=1. CALCULATE ROTOR HEAD MOTION ONLY		
ICHECK	15	=1. WRITE M,C,K MATRICES AND IMPEDANCE		
-----	16	OPEN		
ROTPNT	17	=0. NO PRINTOUT OF ROTOR MATRICES =1. GET PRINTOUT OF ROTOR MATRICES		
NLBFSW	18	=0. NO NON-LINEAR INPLANE BIFILARS =1. USE NON-LINEAR INPLANE BIFILARS		
-----	19	OPEN		
FIXED SYSTEM ABSORBER DATA				
FABSM	20-29	FIXED SYSTEM ABSORBER MASS	ARRAY	BUGS
FABSWN	30-39	FIXED SYSTEM ABSORBER FREQUENCY	ARRAY	CPM
FABSD	40-49	FIXED SYSTEM ABSORBER DAMPING	ARRAY	
FIXED SYSTEM MODAL DATA				
XMG	50-69	GENERALIZED MODAL MASS	ARRAY	BUGS
XWN	70-89	GENERALIZED MODAL FREQUENCY	ARRAY	CPM
XDP	90-109	GENERALIZED MODAL DAMPING	ARRAY	
FORCES AND MOMENTS DATA				
FHC	110-119	COSINE COMPONENT OF HUB FORCES & MOMENTS	LB & IN-LB	
FHS	120-129	SINE COMPONENT OF HUB FORCES & MOMENTS	"	
FTC	130-139	COSINE COMPONENT OF TAIL ROTOR LOADS	"	

FTS	140-149	SINE COMPONENT OF TAIL ROTOR LOADS	"
FFC	150-159	COSINE COMPONENT OF HORIZONTAL TAIL LOADS	"
FFS	160-169	SINE COMPONENT OF HORIZONTAL TAIL LOADS	"
FEC	170-179	COSINE COMPONENT OF LOADS OF ANOTHER POINT	"
FES	180-189	SINE COMPONENT OF LOADS OF ANOTHER POINT	"

INPLANE BIFILAR PENDULUMS DATA

BIFM	190-199	INPLANE BIFILAR MASS ARRAY	BUGS
BARM	200-209	BIFILAR ARM FROM CENTER OF ROTATION	IN
BIFWN	210-219	INPLANE BIFILAR TUNING FREQUENCY ARRAY	CYCLES/REV
BIFDAM	220-229	INPLANE BIFILAR DAMPING ARRAY	

VERTICAL BIFILAR PENDULUMS DATA

BIFM	230-239	VERTICAL BIFILAR MASS ARRAY	BUGS
BIFARM	240-249	BIFILAR ARM FROM CENTER OF ROTATION	IN
BIFWN	250-259	VERTICAL BIFILAR TUNING FREQUENCY ARRAY	CYCLES/REV
BIFDAM	260-269	VERTICAL BIFILAR DAMPING ARRAY	

----- 270-449 OPEN
 XPHI 450-549 TRANSFER MATRIX TO MODAL COORDINATES
 FOR MAIN ROTOR IMPEDANCE (6 X NF)

MODE SHAPES OF 2 AIRCRAFT STATIONS WHERE LOADS ARE APPLIED

XPF	550-649	FIRST AIRCRAFT STATION (6 X NF)	
XPE	650-749	SECOND AIRCRAFT STATION (6 X NF)	

MODE SHAPES OF FIXED SYSTEM ABSORBERS & TAIL ROTOR HUB

XPHABS	750-849	FIXED SYSTEM ABSORBER COUPLING MATRIX (NFABS X NF) <small>(20 SPACES RESERVED FOR EACH ABSORBER)</small>	
XPT	850-949	TAIL ROTOR HUB TRANSFER MATRIX	
-----	950-999	OPEN	

MODE SHAPES OF AIRCRAFT STATION POINTS

XPHAP	1000-1399	COUPLING MATRIX OF AIRCRAFT STATION POINTS <small>(6 X NF X NAP)</small>	
	1000-1099	FOR FIRST AIRCRAFT STATION	
	1100-1199	FOR SECOND AIRCRAFT STATION	
	1200-1299	FOR THIRD AIRCRAFT STATION	
	1300-1399	FOR FOURTH AIRCRAFT STATION	
-----	1400-1489	OPEN	

PRINTOUT OPTIONS

=0. PRINTOUT IS NOT WANTED
 =1. PRINTOUT IS WANTED

FSPNT	1490	A = FIXED SYSTEM MATRICES	
FSRPNT	1491	B = A + ROTOR MATRICES	
FSAPNT	1492	C = B + FIXED SYSTEM ABSORBERS	
IBPPNT	1493	D = C + INPLANE BIFILAR PENDULUMS	
VBPPNT	1494	E = D + VERTICAL BIFILAR PENDULUMS	
IBQPNT	1495	INPLANE BIFILAR MATRICES ONLY (9 X 9)	
VBQPNT	1496	VERTICAL BIFILAR MATRICES ONLY (9 X 9)	
IGAMMA	1497	PRINTOUT OF "GAMMAS" (DEGREES-OF-FREEDOM)	
ICUSE	1498	=0. DO NOT USE INITIAL CONDITIONS OPTION	

=I. USE INITIAL CONDITIONS FROM PREVIOUS CASE
(SEE LOCATIONS 1720-1939)

----- 1499 OPEN

***** END OF INPUT FOR LINEAR BIFILAR ANALYSIS *****

***** INPUT FOR NON-LINEAR INPLANE BIFILARS ANALYSIS *****

INPLANE BIFILAR PENDULUMS CHARACTERISTICS

BM	1500-1519	BIFILAR WEIGHTS	LBS
DP	1520-1539	BIFILAR DAMPING	
WP	1540-1559	BIFILAR NATURAL FREQUENCIES	CYCLES/REV
BR	1560-1579	ARM DISTANCES FROM CENTER OF ROTATION	IN
PSIR	1580-1599	RELATIVE AZIMUTH LOCATIONS	DEGREES

HUB FORCES & MOMENTS HARMONICS INPUT

FORMAT IS " COS(K*PSI) + SIN(K*PSI) "
WHERE K=1 THROUGH A MAXIMUM VALUE OF 10

FXX	1600-1619	LONGITUDINAL HUB FORCE (X)	LBS
FYY	1620-1639	LATERAL HUB FORCE (Y)	LBS
FZZ	1640-1659	VERTICAL HUB FORCE (Z)	LBS
XXM	1660-1679	ROLL HUB MOMENT (THETAX)	IN-LB
YYM	1680-1699	PITCH HUB MOMENT (THETAY)	IN-LB
ZZM	1700-1719	YAW HUB MOMENT (THETAZ)	IN-LB

GAMMA	1720-1739	INITIAL BIFILAR ANGULAR DISPLACEMENT	RADIANS
GAMMAD	1740-1759	INITIAL BIFILAR ANGULAR VELOCITY	RAD/SEC
PSIP	1760	FORCE RAMP FACTOR (3. IS RECOMMENDED)	
DPSI	1761	DELTA AZIMUTH ANGLE	DEGREES
FPSI	1762	MAXIMUM AZIMUTH ANGLE	DEGREES
NBIF	1763	NUMBER OF BIFILARS (MAX=12)	
NHFH	1764	NO. OF INPUT HUB FORCE HARMONICS (MAX=10)	
XNH	1765	NO. OF OUTPUT STATE VARIABLES HARMONICS(MAX=10)	
PSI	1766	INTEGRATION VARIABLE (NOT AN INPUT ITEM)	
NFP	1767	NUMBER OF POINTS ON AIRCRAFT WHERE FORCE IS APPLIED BESIDES ROTOR HEAD (<= 2) (MODE SHAPES ARE INPUT IN LOC. 550-749)	

HUB & STATE VARIABLES INITIAL VALUES

HUBD	1768-1773	HUB INITIAL DISPLACEMENTS
HUBV	1774-1779	HUB INITIAL VELOCITIES
STDP	1780-1859	STATE VARIABLES INITIAL DISPLACEMENTS
TVL	1860-1939	STATE VARIABLES INITIAL VELOCITIES

FORCES & MOMENTS HARMONICS INPUT OF 2 ADDITIONAL AIRCRAFT POINTS

FORMAT IS " COS(K*PSI) + SIN(K*PSI) "
WHERE K=1 THROUGH A MAXIMUM VALUE OF 10
(MODE SHAPES ARE INPUT IN LOC. 550-749)

P1FX	1940-1959	POINT 1 LONGITUDINAL (X)	LBS
P1FY	1960-1979	" LATERAL (Y)	LBS
P1FZ	1980-1999	" VERTICAL (Z)	LBS
P1MX	2000-2019	" ROLL (THETAX)	IN-LB
P1MY	2020-2039	" PITCH (THETAY)	IN-LB

P1MZ	2040-2059	"	YAW	(THETAZ)	IN-LB
P2FX	2060-2079	POINT 2	LONGITUDINAL	(X)	LBS
P2FY	2080-2099	"	LATERAL	(Y)	LBS
P2FZ	2100-2119	"	VERTICAL	(Z)	LBS
P2MX	2120-2139	"	ROLL	(THETAX)	IN-LB
P2MY	2140-2159	"	PITCH	(THETAY)	IN-LB
P2MZ	2160-2179	"	YAW	(THETAZ)	IN-LB
----	2180-2199	OPEN			

SUCCESSIVE CASES CONTROL SWITCH

CODE 2200 =1. COMPLETES LAST CASE
 =0. GOES BACK TO ROTOR ANALYSIS FOR NEXT CASE

***** END OF INPUT LOCATIONS *****



3.2.2 Description of Input for Bifilar Analysis

Additional information on the input parameters is provided in this section.

Each input quantity is given in the following format:

Location No., Quantity, Units
Important Details and Comments

Linear Analysis Input (Loc 1-1498)

1. Kinds of Inplane Bifilars, Nondimensional.

Up to 5 kinds of inplane bifilars can be used in the analysis if no vertical bifilars are present. The combined number of kinds of inplane and vertical bifilars cannot be greater than 5. This corresponds to a maximum number of 15 degrees-of-freedom (including collective and 2 cyclic motions). Ex. loc 1=2 if one set of 3P and one set of 5P inplane bifilars are employed.

2. Aircraft Station Points, Nondim.

Due to computer storage requirements, a maximum of 4 points can be used.

3. Forcing Frequency, Cycles/Rev.

Frequency at which the bifilars will respond divided by the rotor speed.

4. Impedance Matrix Dimension, Nondim.

This location is 2 times the number of fixed system modes loaded in location 9.

6. Number of Inplane Bifilars, Nondim.

The actual number of inplane bifilars present in each kind as defined in loc. 1. It should be noted that, if more than one kind of inplane bifilars is used, then the number of bifilars in each kind has to be the same. The maximum number allowed is 10.

7. Rotor Speed, RPM.

Used to non-dimensionalize frequency units.

8. Number of Fixed System Absorbers, Nondim.

The total number of fixed system absorbers is limited to 5.

9. Number of Fixed System Modes, Nondim.

The maximum number of fixed system modes is 16 which allows for 6 rigid body modes (if desired) and 10 flexible modes.

Rigid airframe modes should not be used in the non-linear bifilar analysis.

Program will not execute if number of modes is zero.

10. Extensive Printout Option, Nondim.

Set this location to 1. to obtain additional printout for debugging use.

12. Kinds of Vertical Bifilars, Nondim.

Up to 5 kinds of vertical bifilars can be used if no inplane bifilars are present. Otherwise, the total of the two kinds is 5.

13. Number of Vertical Bifilars, Nondim.

Actual number of vertical bifilars present in each kind as defined in loc. 12. Same number of bifilars is assumed for each kind. Maximum number is 10.

14. Rotor Head Motion Switch, Nondim.

If this control is set to 1. then only the rotor head motion will be calculated.

15. Additional Printout Option, Nondim.

If set to 1., stiffness, damping and mass matrices are printed out for debugging purposes.

17. Rotor Matrices Printout Option, Nondim.

If set to 1., the input matrices to the bifilar analysis from the rotor aeroelastic program are printed out. Order is stiffness, damping and mass. The stiffness and damping matrices include aerodynamics if air density is non-zero.

18. Linear/Non-Linear Analysis Option, Nondim.

If set to zero, then linearized inplane bifilar equations

of motion are used and the forced response of all components is calculated. Sample runs using 16 and 28 degrees-of-freedom required 3 seconds and 25 seconds respectively.

If set to 1., then the full non-linear inplane bifilar equations of motion are used and a time history solution is calculated. Computer time for the non-linear option is highly dependent on the number of degrees-of-freedom used. A sample run with 17 d.o.f. took 1 minute and 8 seconds requiring 13 rotor revolutions for convergence of the bifilar motions. A sample run with 29 d.o.f. took 7 minutes and 7 seconds of computer time and required 16 rotor revolutions for convergence.

20.-29. Fixed System Absorber Masses, Lb-sec²/in. or Bugs

Absorber weight in pounds divided by 386.4. Although 10 locations are provided, only 5 can be used (see loc. 8).

30.-39. Fixed System Absorber Frequencies, Cpm

40.-49. Fixed System Absorber Damping, Nondim.

Damping associated with the absorber i.e., .01 corresponding to 1% critical.

50.-69. Fixed System Generalized Masses, Lb-sec²/in or Bugs

Maximum number of masses is actually 16 (see loc. 9) although 20 computer locations have been allowed.

70.-89. Fixed System Generalized Frequencies, Cpm

90.-109. Fixed System Generalized Damping, Nondim.

Forces and Moments Data - General Comments, Lb & In-lb

110.-189. The Forces and Moments are Defined in the Fixed System.

The order of the forces and moments input data is: x, y, z, θ_x , θ_y , θ_z , which correspond to longitudinal, lateral, vertical, roll, pitch and yaw motions respectively. The coordinate system used is a right-handed (system with the x-axis defined as positive aft and y-axis as positive out of the right wing).

Thus only six locations are needed to define an input force or moment although 10 computer locations have been allocated.

Examples of input of hub forces (loc. 110-129):

- a) For a 4P inplane bifilar, to load a pure 5P hub force, then F_x (cosine) = $-F_y$ (sine) (loc. 110 = - loc. 121) and F_y (cosine) = F_x (sine) (loc. 111 = loc. 120).
- b) To load a pure 3P hub force, then F_x (cosine) = F_y (sine) (loc. 110 = loc. 121) and F_y (cosine) = $-F_x$ (sine) (loc. 111 = - loc. 120).

Additional forces/moment inputs can be specified for the tail rotor (loc. 130-149), the horizontal tail (150-169) and one other arbitrary point (loc. 170-189).

190.-199. Inplane Bifilar Masses, Lb-sec²/in. or Bugs

Bifilar weights divided by 386.4 are loaded for each kind of bifilar used (see loc. 1). The limit on the number of bifilar kinds which can be used is 5 although 10 computer locations are available.

200.-209. Inplane Bifilar Arm From Center of Rotation, In.

210.-219. Inplane Bifilar Tuning Frequency, Cycles/Rev

The linear inplane bifilar tuning frequency is defined by

$$F^2 = R/r \text{ where } R = \text{bifilar arm (loc. 200-209)} \\ r = \text{bifilar distance from hinge to} \\ \text{bifilar center of mass}$$

Example: Given $R = 18.22$ in, $r = 2.02444$, then $F = 3.0$ per rev

220.-229. Inplane Bifilar Damping, Nondim.

230.-239. Vertical Bifilar Masses, Lb-sec²/in. or Bugs

Same comment as for inplane bifilar (see loc. 12).

240.-249. Vertical Bifilar Arm From Center of Rotation, In.

250.-259. Vertical Bifilar Tuning Frequency, Cycles/Rev

The linear vertical bifilar tuning frequency is defined by
 $F^2 = (R+r)/r$ where $R = \text{bifilar arm (loc. 240-249)}$
 $r = \text{bifilar distance from hinge to}$
 $\text{bifilar center of mass}$

Example: Given $R = 18.50$ in, $r = 1.23333$ in, then $F = 4.0$ per rev

260.-269. Vertical Bifilar Damping, Nondim.

450.-549. Transfer Matrix to Modal Coordinates for Main Rotor Impedance, In/in & Rad/in.

The main rotor hub transfer matrix has the dimensions 6 X NF (where NF is the number of fixed system modes defined in loc. 9). Since the maximum value of NF is 16, then 96 computer locations are necessary to define the largest transfer matrix.

The first mode is loaded into locations 450-455, the second mode into locations 456-461, etc. .. until the last or 16th mode into locations 540-545.

For each mode, the order of input is $x, y, z, \theta_x, \theta_y, \theta_z$. The units of the linear motions are in/in while rotations are in rad/in. The user must be careful to load the mode shapes corresponding to the fixed system modes masses, frequencies and damping values from locations 50-109.

550.-649. Mode Shapes for First Aircraft Station Where Loads Are Applied, In/in. & Rad/in

650.-749. Mode Shapes for Second Aircraft Station Where Loads Are Applied, In/in & Rad/in

Same comments as for the main rotor hub transfer matrix above apply for these inputs.

750.-849. Fixed System Absorber Coupling Matrix, In/in & Rad/in

The fixed absorber coupling matrix has the dimension NFABS X NF (where NFABS is the number of fixed system absorbers from location 8). The modal response in one direction (vertical, lateral or longitudinal) for each fixed system mode (as defined in location 9) is loaded in locations 750-769 for the first absorber, in locations 770-789 for the second, and so on.

850.-949. Tail Rotor Hub Transfer Matrix, In/in & Rad/in

Same comments as above for main rotor hub transfer matrix (loc. 450-549).

1000.-1399. Mode Shapes of Aircraft Station Points, In/in & Rad/in

The response of 4 aircraft stations can be analyzed according to the mode shapes input in locations 1000-1099 for the first station, 1100-1199 for the second, 1200-1299 for the third, and 1300-1399 for the fourth station.

The mode shapes are loaded in the same manner as described above for the main rotor hub (loc. 450-549).

1490.-1494. Printout Options, Nondim.

If any printout option switch is set to 0., then the printout of the corresponding matrices is suppressed. If printout of the matrices is desired, then the proper switch should be loaded as 1.

The build-up of the matrices is as follows:

- (loc. 1490) 1. Fixed system matrices (16 X 16 max)
- (loc. 1491) 2. Add rotor matrices (24 X 24 max → 40 X 40 max total)
- (loc. 1492) 3. Add fixed system absorbers (5 X 16 max → 45 X 45 max. total)
- (loc. 1493) 4. Add linear inplane bifilars
- (loc. 1494) 5. Add vertical bifilars (combined with inplane bifilars, the matrices are 15 X 15 max → 60 X 60 max. total)

Thus, the maximum number of degrees-of-freedom which can be handled at the present time with the linear rotor/bifilar coupled program is 60.

Location 1493 also controls the printout of the "Final Combined Mass Matrix" for the non-linear analysis option.

1495.-1496. Bifilar Pendulums Printout Switches, Nondim.

The individual contributions to the coupled system matrices from the inplane and vertical bifilars can be obtained through the use of the printout options as defined in locations 1495 and 1496 respectively.

1497. The results of the forced response analysis for all the system degrees-of-freedom can be printed out through this switch.

1498. Initial Conditions Option, Nondim.

This option applies only when the non-linear analysis is requested (loc. 18 = 1.). If set to 1.0, then the initial conditions to be used should be loaded in locations 1720-1939. Input to these locations is printed out at the end of a non-linear analysis run.

Non-Linear Analysis Input (Loc. 1500-2179)

1500.-1519. Inplane Bifilar Pendulum Weights, Lbs.

The weight of each bifilar pendulum in pounds is loaded according to the number of pendulums from loc. 1763. The maximum number of pendulums allowed is 12.

1520.-1539. Inplane Bifilar Pendulum Damping, Nondim.

1540.-1559. Inplane Bifilar Pendulum Frequencies, Cycles/Rev

Same comments as provided for the linear inplane bifilars (loc. 210-219) apply here.

1560.-1579. Inplane Bifilar Pendulum Arms From Center of Rotation, In.

1580.-1599. Relative Azimuth Locations of Inplane Bifilar Pendulums, Deg

Example: If four inplane pendulums are analyzed, then locations 1580-1583 are respectively 0., 90., 180., 270.

1600.-1719. Hub Forces and Moments Input, Lbs and in.-lb

For the non-linear analysis, the fixed system hub forces and moments are input in harmonics format. Up to 10 harmonics can be used. Cosine and sine components of each harmonic are input alternately.

Ex. Loc 1600 - Longitudinal motion - cosine component of first harmonic

Loc 1601 - Longitudinal motion - sine component of first harmonic

Loc 1602 - Longitudinal motion - cosine component of second harmonic

Etc...

Location 1764 is used in conjunction with the input loads.

1720.-1739. Initial Bifilar Angular Displacements, Radians

These locations are used if the initial conditions switch (loc. 1498) is 1. These values are printed out at the end of a converged time history solution for each inplane bifilar.

1740.-1759. Initial Bifilar Angular Velocity, Rad/Sec

Same comments as above for the initial displacements.

1760. Force Ramp Factor, Nondim.

The hub loads are imposed on the rotor/bifilar/fixed system coupled system as a ramp input dependent on the maximum azimuth angle (loc. 1762) for the time history solution and the ramp factor.

Example: If loc. 1762 = 4320 degrees (or 12 revolutions) and loc. 1760 = 3.0, then the hub loads (loc 1600-1719) are applied linearly in the azimuth interval from zero to $4320/3$ (which equals 1440 degrees or 4 revolutions).

1761. Azimuthal Increment For Time History Solution, Degrees

A value of 2 degrees is recommended. However, if the time history does not converge, lower values can be tried to eliminate what may possibly be a numerical instability. It should be noted that the computer execution time is directly proportional to the size of this input quantity.

1762. Maximum Azimuth Angle, Degrees

It is recommended that values corresponding to 10 to 20 rotor revolutions (3600 and 7200 degrees respectively) be used in this location. As for loc. 1761 above, the computer execution time is also dependent on this input. If the time history does not meet the convergence criteria, then it will terminate when the integration azimuthal angle equals the input value in loc. 1762.

1763. Number of Inplane Bifilar Pendulums, Nondim.

A maximum number of 12 bifilars can be used.

1764.

Number of Input Hub Force Harmonics, Nondim.

A maximum number of 10 harmonics, corresponding to the input loads in loc. 1600-1719, can be used.

1765.

Number of Output State Variables Harmonics, Nondim.

This location governs the number of harmonics analyzed and printed out for the following variables:

1. Bifilar pendulum response, degrees
2. Hub response ($x, y, z, \theta_x, \theta_y, \theta_z$), g's
3. Aircraft stations response (x, y, z), g's

Up to 10 harmonics may be requested.

1767.

Number of Aircraft Additional Points Where Loads Are Applied, Nondim.

This number is equal or less than 2. If non-zero, then load appropriate mode shapes in locations 550-749.

1768.-1773.

Hub Initial Displacements, In or Rad

At the completion of the time history solution, the hub displacements are printed out to be used for successive cases if desired. The output yields, in order, the longitudinal, lateral, vertical, roll, pitch and yaw motions.

1774-1779.

Hub Initial Velocities, In/sec or Rad/sec

Same comments as above for the hub initial displacements.

1780.-1859.

State Variables Initial Displacements, In or Rad

The initial displacements of all the degrees-of-freedom (except the non-linear inplane bifilar pendulums) are printed out for use in successive cases. The order of printout is:

1. Fixed system
2. Rotor (if required)
3. Fixed system absorbers
4. Linear inplane bifilars
5. Linear vertical bifilars

1860.-1939. State Variables Initial Velocities, In/sec or rad/sec.

Same comments as made above for the initial displacements.

1940.-2179. Aircraft Additional Points Forces and Moments Input, Lbs and in-lb.

Refer to comments on hub forces (locations 1600-1719).

2200. Successive Cases Control Switch, Nondim.

If successive runs are to be made, then location 2200 is set to zero. The program then goes back to the rotor aeroelastic analysis and starts execution of the next case. The last bifilar analysis case must have a 1. in location 2200 for proper termination of the computer run.

The maximum number of degrees-of-freedom which can handled by the linear and non-linear analyses are respectively 60 and 72. A breakdown of the individual component maximum d.o.f. is presented in the chart below.

Component Description	Maximum No. of D.O.F.		Input Location(s)
	Linear	Non-Linear	
1. Linear Bifilars (inplane + vertical)	15	15	1 & 12
2. Fixed System Absorbers	5	5	8
3. Fixed System Modes	16	16	9
4. Rotor Blade	24	24	-
5. Non-linear Inplane Bifilars	-	12	1763
Total →	60	72	

3.3 Input Data Format

All data is input via cards or card-like images with the following (loader) format. Column 2 represents the number of data values on the card, columns 3-6 give the location numbers of the first data values, successive data values are loaded into successive locations, and columns 7-66 contain the data values in fields of 12, the default format being 5E12.4. A minus sign in column 1 indicates the end of a case. Subsequent cases are loaded immediately after this card in the same format. See subroutine LOADIT for a more detailed description of data cards.

SECTION 4

OUTPUT DESCRIPTIONS

4.1 Rotor Aeroelastic Analysis Output

If the rotor coupling option is exercised (location 110 is not zero), then a listing of the input rotor data is first printed out. A sample page of this output can be seen in Figure 2. The input cards are listed out as read by the computer. For successive cases, only the new input items will be printed out to reflect the changes made between runs. This information is provided for all printout options.

The output formats which follow are obtained for all printout options, as provided in location 119. Additional printout of blade bending frequency calculations and dynamic and aerodynamic integrals evaluations can be obtained if the printout switch is not equal to 5. These formats are not shown here for sake of brevity - they are mainly used for debugging purposes.

Input and calculated dynamic and aerodynamic characteristics of the rotor blade and fixed system are presented in Figures 3a through 3h. Additional explanations are provided in Table 1 below. Some differences may appear in the output formats from the input data due to corrections applied by the computer program to eliminate possible inconsistencies in the input control options.

The abbreviations used in the output formats are listed and discussed in the table below. It should be noted that some input quantities have been preset within the computer program since some program capabilities were not needed for the coupling of the rotor and bifilar systems.

TABLE 1. Rotor Analysis Output Description

<u>Output Symbol</u>	<u>Quantity Description</u>	<u>Input Location</u>	<u>Present Value</u>	<u>Figure Number</u>
PHIXPH	Blade Bending Mode Coupling Factors	-	-	3a
PHIZPH	Blade Bending Mode Coupling Factors	-	-	
<u>..... Lag Damper Quantities</u>				
PHELD	Edgewise Bending Mode at Lag Damper	-	-	
PHEPLD	Edgewise Bending Mode Slope at Lag Damper	-	-	
PHFLD	Flatwise Bending Mode at Lag Damper	-	-	
PHFPLD	Flatwise Bending Mode Slope at Lag Damper	-	-	
QEOLD	Edgewise Steady Deflection at Lag Damper	-	-	

<u>Output Symbol</u>	<u>Quantity Description</u>	<u>Input Location</u>	<u>Present Value</u>	<u>Figure Number</u>
QEOPLD	Edgewise Steady Slope at Lag Damper	-	-	3a
QFOLD	Flatwise Steady Deflection at Lag Damper	-	-	
QFOPLD	Flatwise Steady Slope at Lag Damper	-	-	
PHLD	Torsional Mode Shape at Lag Damper	-	-	
THTLD	Blade Twist at Lag Damper	-	-	
PHOS	Torsional Mode Shape at Outboard Snubber	-	-	
XNAMOD	Number of Fixed System Modes	-	5.	3b
VF	Forward Flight Speed	-	0.	
<u>..... Control Switches</u>				
ROTEST	Rotor Definition	111	-	
FTEST	Flight Definition	-	1.	
SYSDEF	System Definition	113	-	
ROTDEF	Rotor Definition	114	-	
ARTIC	Blade Pitch Input Control	115	-	
PHASE	Phasing Matrix Printout Control	-	0.	
VECT	Eigenvector Printout Control	-	0.	
TRMASC	Tail Rotor Main Mass Control	-	1.	
SUMASC	Tail Rotor Subsidiary Mass Control	-	111.	
TSERVC	Tail Rotor Servo Control	-	1.	
MRMASC	Main Rotor Mass Control	-	1.	
MSERVC	Main Rotor Servo Control	-	111.	
CIR	Circulatory Unsteady Aerodynamics Control	-	1.	
CIRN	Noncirculatory Unsteady Aerodynamics Control	-	1.	
LAGKII	Lag Damper Control	125	-	
ZETBLD	Fraction of Critical Damping of Blade Bending Modes	22-25	-	
<u>..... Fixed System Modes</u>				
ZETG	Fraction of Critical Damping of Fixed System Modes	-	0.	
MG	Generalized Mass of Fixed System Modes	-	0.	
OMF	Frequency of Fixed System Modes	-	0.	
PHY	Lateral Fixed System Mode Shape (Second Mode Only Equals 1.0)	-	0. & 1.	
PHX	Longitudinal Fixed System Mode Shape (First Mode Only Equals 1.0)	-	0. & 1.	
PHZ	Vertical Fixed System Mode Shape (Third Mode Only Equals 1.0)	-	0. & 1.	

<u>Output Symbol</u>	<u>Quantity Description</u>	<u>Input Location</u>	<u>Present Value</u>	<u>Figure Number</u>
PHTY	Pitch Fixed System Mode Shape (Fifth Mode Only Equals 1.0)	-	0. & 1.	3b
PHTX	Roll Fixed System Mode Shape (Fourth Mode Only Equals 1.0)	-	0. & 1.	
R	Radius of the Blade Element Mid- Points From Center of Rotation	201-220	-	3c
AC	Blade Aerodynamic Center	650-749	-	
CG	Blade Center of Gravity	550-649	-	
EA	Blade Elastic Axis	750-849	-	
QEO	Blade Edgewise Steady Deflection	-	-	
QFO	Blade Flatwise Steady Deflection	-	-	
QEOP	Derivative of QEO with respect to R	-	-	
QFOP	Derivative of QFO with respect to R	-	-	
DT	Elemental Thrust	-	-	3d
DH	Elemental Drag	-	-	
DM	Elemental Pitching Moment	-	-	
D	Derivative with Respect to	-	-	
D(UT)	Tangential Velocity	-	-	
D	Derivative with Respect to	-	-	
D(UP)	Vertical Velocity	-	-	
D	Derivative with Respect to	-	-	
D(θ T)	Angle-of-Attack	-	-	
CL	Coefficient of Lift	2750-3649	-	3e
CD	Coefficient of Drag	1850-2749	-	
CM	Coefficient of Pitching Moment	3650-4548	-	
D	Derivative with Respect to	-	-	
DA	Angle-of-Attack	-	-	
D	Derivative with Respect to Mach	-	-	
DM	Number	-	-	
θ STRUC- TURAL	Structural Twist	450-549	-	
θ AERO- DYNAMIC	Aerodynamic Twist	350-449	-	
UP	Hover Inflow Velocity	-	-	
UT	Tangential Velocity	-	-	
U	Total Velocity	-	-	
θ	Inflow Angle	-	-	
ALPHA	Angle-of-Attack	-	-	
PHE(I)	Edgewise Part of i^{th} Blade Bend- ing Mode	-	-	3f
PHF(I)	Flatwise Part of i^{th} Blade Bend- ing Mode	-	-	
PHEP(I)	Edgewise Slope Part of i^{th} Blade Bending Mode	-	-	
PHFP(I)	Flatwise Slope Part of i^{th} Blade Bending Mode	-	-	

The rotor blade radial distributions of edgewise, flatwise and torsional mass moments of inertia, mass, and edgewise and flatwise area moments of inertia are shown in Figure 3g. Care must be exercised in the input of these quantities to make sure that the sum of the blade segments equals the blade radius (location 6).

If either rigid blade flapping or inplane motion is used in the rotor analysis, then the rotor blade flapping mass, first and second moments of inertia and the blade lag frequency are printed out as can be seen in Figure 3h. In this figure are also shown calculations of the blade bending mode generalized masses (defined as the blade mass times the sum of the squares of the flatwise and edgewise components) and of other blade parameters.

The total number of degrees-of-freedom used in the rotor analysis is indicated in Figure 3h. The individual degrees-of-freedoms are identified by integers according to the schedule given below.

<u>Number</u>	<u>Degree-of-Freedom</u>	<u>Motion</u>
1-4	Blade Bending Modes (up to 4)	Symmetric
5-6	Blade Torsional Modes (up to 2)	
7	Blade Rigid Body Flapping	
8	Blade Rigid Body Lead-Lag	
9-16	Blade Bending Modes	Cyclic
17-20	Blade Torsional Modes	
21-22	Blade Rigid Body Flapping	
23-24	Blade Rigid Body Lead-Lag	
25-29	Fixed System Modes (Fixed at 5)	-

Thus, for the example in Figure 3h, it is seen that two blade bending modes, rigid body flapping and lead-lag and five fixed system modes are employed for a total of 17 degrees-of-freedom.

The maximum number of rotor/fixed system degrees-of-freedom is 29 (8 blade modes times 3 plus 5 fixed system modes).

A sample output matrix is presented in Figure 4. For this case, location 108 was set to 1. to yield the printout of the compressed (17 X 17) rotor/fixed system matrices. The complete 29 X 29 matrices can be displayed if location 107 is set to 1. The order of the elements in each column follows the schedule shown above. For example, the fourth element in the second row corresponds to the lead-lag symmetric stiffness contribution to the second blade bending mode symmetric equation of motion.

The compressed matrices include rotor aerodynamic contributions. They are coupled directly to the bifilar analysis. If no rotor coupling is desired, then the compressed matrices are stored for future use.

4.2 Bifilar Analysis Output

Typical output formats presenting results from the bifilar analysis are shown in Figures 5 through 8. The output parameters from Figures 5a through 5k are common for both linear and non-linear bifilar analyses. The final linear analysis results are presented in Figure 6 while the non-linear results can be seen in Figures 7 and 8.

Figure 5a shows the number of degrees-of-freedom utilized in a given computer run, the number of aircraft stations where the response is calculated and the printout options requested. For the example shown, it is seen that nine fixed system modes, one fixed system absorber and one kind each of inplane and vertical bifilars are requested. In addition, rotor coupling is employed and the response of four aircraft stations is to be analyzed. All printout switches have been activated (set at 1.0) to show examples of the output generated.

The bifilar analysis starts off with the fixed system degrees-of-freedom. Then, it expands the fixed system stiffness, damping and mass matrices to include in sequence the contributions from the rotor, fixed system absorbers, linear inplane bifilars and finally the linear vertical bifilars. Then, either a forced response or a time-history solution is calculated depending on the input to location 18. The build-up of the degrees-of-freedom is shown in Figures 5b through 5k for the stiffness matrix only. The damping and mass matrices are handled in an identical manner.

The basic fixed system stiffness matrix is presented in Figure 5b. It is seen that for this example the stiffness matrix is a square diagonal matrix of order 9. This printout is governed by location 1490.

The rotor/fixed system stiffness matrix to be coupled with the bifilar analysis is shown in Figure 5c and d and is of order 18. This matrix is basically the same as that from Figure 4 except that now the fixed system degrees-of-freedom appear first and include an extra equation corresponding to the yaw degree-of-freedom (which is not present in the rotor aeroelastic analysis). Consequently, the total number of degrees-of-freedom is 18. This printout option is controlled by location 17.

Every time a new system component is added, the printout shown in Figure 5e is automatically obtained. It shows what the present number of degrees-of-freedom (d.o.f.) is (for this example, 9 fixed system d.o.f.), the number to be added (12 rotor d.o.f.) and the final system d.o.f. (a total of 21 d.o.f.).

The combined fixed system/rotor stiffness matrix is displayed in Figure 5f. Only the first nine equations are shown here for brevity. This output is obtained if location 1491 is set to 1.0.

Next, the fixed system/rotor coupled system is expanded to include the contribution of the fixed system absorber. In this example, only one absorber is used and thus the number of d.o.f. becomes 22, as can be seen in Figure 5g. Location 1492 controls this printout option.

If linear inplane bifilar pendulums are used (see location 1), then the fixed system/bifilar coupled matrices (mass, damping and stiffness) can be obtained for each kind of bifilar (see loc. 1495). The output matrices in all cases are square matrices of order 9. The first 6 d.o.f. correspond to the hub motions (x , y , z , θ_x , θ_y and θ_z respectively) and the next three to the inplane bifilar symmetric and two cyclic modes. In Figure 5h, the coupled stiffness (QQK) matrix is presented.

The system matrices are now expanded to include the contribution of the inplane bifilar pendulums. The stiffness matrix of the fixed system/rotor/fixed system absorber/inplane bifilar coupled system can be seen in Figure 5i. Since only one kind of inplane bifilar is used in this example, the final number of d.o.f. is increased by 3 for a total of 25. This output is generated if location 1493 is set to 1.

If linear vertical bifilar pendulums are employed in the analysis (see loc. 12), the corresponding fixed system/vertical bifilar matrices can be displayed (see loc. 1496) as seen in Figure 5j. The format is the same as that for the inplane bifilars.

Now the vertical bifilar d.o.f. are added to the system. The final stiffness matrix for this example is shown in Figure 5k. The total d.o.f. to be analyzed is 28. This output format is controlled through location 1494.

The results of the linear bifilar analysis are presented in Figure 6. The cosine and sine components of the generalized forces appearing near the top of Figure 6a are obtained by multiplication of the hub forces/moment vectors (see loc 110-119 for the cosine component and loc 120-129 for the sine component) by the transpose of the rotor hub transfer matrix (located in loc. 450-549). The units are lbs and inch-lbs.

The "GAMMAS" printed out in Figure 6a are the generalized coordinates of the rotor/fixed system absorber/bifilar coupled system and are obtained from the forced response solution. First, the cosine component for all d.o.f. is printed out and then the sine component. For this example, the total number of d.o.f. of the rotor, the fixed system absorber and the inplane and vertical bifilars equals 19. Thus, 38 values of "GAMMAS" are printed out; the printout switch is location 1497. The units are in inch for the fixed system absorber and non-dimensional for the rotor and bifilars.



The "GAMMAS" are sorted out according to the system components present and printed out accordingly, as shown in Figure 6a and 6b. The calculated amplitudes are in inch for the fixed system absorber and in degrees for both inplane and vertical bifilar pendulums, all phase angles are shown in degrees. The method used to calculate the bifilar amplitudes is shown below.

OUTPUT FORMAT

	<u>Cosine</u>	<u>Sine</u>	<u>Amplitude</u>	<u>Phase</u>
Symmetric Equation	A_{OC}	A_{OS}	A_N	Φ_{IN}
Cyclic Equation - sine	A_{SC}	A_{SS}	A_{N-1}	Φ_{IN-1}
Cyclic Equation - cosine	A_{CC}	A_{CS}	A_{N+1}	Φ_{IN+1}

$$A_N = A_{OC}^2 + A_{OS}^2 * 57.30/NB$$

$$A_{N-1} = A_1^2 + A_2^2 * 57.30/NB \text{ where } A_1 = A_{CC} + A_{SS} \text{ & } A_2 = A_{CS} - A_{SC}$$

$$A_{N+1} = A_3^2 + A_4^2 * 57.30/NB \text{ where } A_3 = A_{CC} - A_{SS} \text{ & } A_4 = A_{CS} + A_{SC}$$

and NB = number of bifilar pendulums

The input frequencies are listed out in Figure 6b; the units are in Hz.

The forcing frequency in Hz is obtained by multiplying the forcing frequency in cycles/rev (loc 3) by the rotor speed (loc 7) and dividing by 60.

The conversion factor to g's is obtained by dividing the square of the forcing frequency in rad/sec by the factor 386.40.

The fixed system generalized coordinates are also shown in Figure 6b. The units are inch. They are utilized to calculate the dynamic response of the aircraft stations and of the rotor head which are shown in Figures 6b through 6d. As indicated in the printout, the aircraft and hub response is in g's.

Sample results from the time history solution when non-linear inplane bifilar absorbers are employed (loc 18 is 1.) are printed in Figures 7 and 8. If the total number of degrees-of-freedom exceeds 72, then a message will be printed out to that effect and the non-linear analysis proceeds to the next case to be analyzed.

In Figure 7a, the top line lists out the different components degrees-of-freedom requested in a specific computer run. For the example shown, the total number of d.o.f. is 29 which is obtained as follows:

<u>System Component</u>	<u>D.O.F.</u>
1. Fixed system modes (NF)	9
2. Rotor d.o.f. (KROTOR)	12
3. Fixed system absorber (NFABS)	1
4. Kinds of (linear) inplane bifilars (0X3)	0
5. Kinds of vertical bifilar (1X3)	3
6. Number of non-linear inplane bifilars	4
	29

The time history solution proceeds at first to collect all the acceleration terms on the left hand side of the equations of motion. The right hand side contains the stiffness and damping terms and the forcing functions. Successive integrations of the accelerations yield the velocity and displacement vectors at the next time increment. Then, the system accelerations are computed again and the procedure continues until a converged time history is obtained or the maximum azimuthal position (specified in location 1762) is reached.

The output formats presented in Figures 7a through 7e are for zero azimuth. The initial right hand side (r.h.s.) terms are displayed in Figure 7a. They are all zero to start since no initial conditions of the state variables displacements and velocities have been located in the input locations 1780 through 1939. This printout appears for azimuth positions up to 3 degrees.

The next printout shown in Figure 7a is that of the left-hand-side mass matrix whose order is the sum of the six hub d.o.f. and the number of non-linear inplane bifilars (loc. 1763) which for this example is four. The bifilar force vector is also listed out in this figure. Small values appear in this vector due to coupling terms between the fixed system and the bifilar pendulums. These outputs are presented for azimuth positions up to 5 degrees.

The rotor head mode shapes appear in Figure 7b. This matrix is an image of the input in locations 450 through 549. It is shwon only for azimuth positions up to 2 degrees.

The next printout in Figure 7b is that of the "Expanded Bifilar Mass Matrix" whose order is the sum of the number of fixed system modes (loc 9) and the non-linear bifilars (loc 1763). Similarly, the "Expanded Bifilar Force Vector" is printed out in Figure 7c. Both output formats are generated for azimuth angles up to 5 degrees.



The contributions of the remaining system components are now added to the fixed system/non-linear inplane bifilar system. The resulting mass matrix and force vector can be seen in Figures 7d and 7e respectively. The final matrix order is 29, as previously stated in Figure 7a. These printouts are obtained for azimuth angles up to 15 degrees.

The solution vector of the state variables and the non-linear bifilar displacements and velocities at zero azimuth is shown in Figure 7e. It is printed out for azimuth angles up to 30 degrees. This vector is now used to calculate the right-hand-side terms at the next azimuth position (as defined in location 1761) which are displayed at the bottom of Figure 7e.

The time history solution proceeds around the rotor azimuth until either the convergence criterion set on the bifilar motions is satisfied or the maximum azimuth value (loaded in location 1762) is reached. At the end of each rotor revolution, bifilar displacements and hub motions are printed out as exhibited in Figure 7f. For the example shown, 16 rotor revolutions were necessary before the convergence criterion was met, i.e. the angular displacements of the first two bifilars (G1 and G2) for two successive revolutions must be within .002 radian (or .1146 degree).

The rotor/bifilar analysis then proceeds to calculate the harmonic response of the non-linear bifilar pendulums displacements, the hub six degrees-of-freedom (the order is x , y , z , θ_x , θ_y and θ_z) and the aircraft station(s) linear motions (x , y and z), as can be seen in Figures 8a and 8b. The pendulum output is in degrees while the hub and A/C station(s) output is in g's. All phase angles are in degrees. The four rows of output describing the hub and A/C response are respectively the cosine and sine components, the total amplitude and phase angle. For the example shown, the bifilar motions are about 9.8 degrees each; the longitudinal (x) hub response is .13864 g's.

The final output format of the non-linear analysis results consists of the initial values of bifilar, hub and state variables displacements and velocities. These results can be loaded into locations 1720 through 1939 and will be used as initial conditions for the subsequent computer run provided location 1498 is set to 1.0.

Additional information can be printed out if the control switches in locations 10 and 15 are activated. This is only needed if debugging of the bifilar analysis calculations is desired.

SECTION 5

TEST CASES RESULTS

5.1 Test Cases Description

The rotor/bifilar coupled analysis has been executed for the following four test cases:

- Case 1. Includes rotor and uses linear bifilar analysis.
- Case 2. Includes rotor and uses non-linear bifilar analysis.
- Case 3. Doesn't include rotor and uses linear bifilar analysis.
- Case 4. Doesn't include rotor and uses non-linear bifilar analysis.

These cases test the major program logic paths.

For each case, the component degrees-of-freedom utilized are listed in the chart below.

COMPONENT D.O.F.

<u>Test Case</u>	<u>Rotor Blade</u>	<u>Fixed System</u>	<u>Fixed Absorber</u>	<u>Linear Inplane</u>	<u>Bifilar Vertical</u>	<u>Non-Linear Bifilars</u>	<u>Total D.O.F.</u>
1	12	9	1	3	3	0	28
2	12	9	1	0	3	4	29
3	0	9	1	3	3	0	16
4	0	9	1	0	3	4	17

The rotor degrees-of-freedom include two blade bending modes and rigid body flapping and lead-lag motion. Only one kind of inplane and vertical linear bifilars is used in the test cases. However, the analysis has been checked out for cases utilizing several kinds of bifilar pendulums. The inplane bifilars are tuned to 4 per rev.

5.2 Job Control Language

The Job Control Language (JCL) needed to execute the coupled program on the IBM 370/169 computer system is presented in Appendix A. This JCL must be modified for use on the NASA CDC computer system. A brief description of the JCL setup is discussed below.

<u>Card Number</u>	<u>Description</u>
1	Describes job name and characteristics (class, time, etc.).
2	Executes program module E90BCFIN.
3	Locates program module in ET473.SEBBY.LOAD.
4	Reads input data from ET473.BIFILAR.DATA (NASARUN) using Unit 5.
5	Provides paper output using Unit 6.
6	Provides punched cards output using Unit 7.
7	Stores calculated data internally in Unit 8.
8	Stores input data for first case in Unit 11 to be used for successive cases.
9	Ends JCL setup.

5.3 Test Cases Input Data

The input data needed to run the four test cases is listed in Appendix B.

The input format which must be followed to run multiple cases is described in Table 2 below.

TABLE 2. Program Multiple Cases Setup

<u>Data Block</u>	<u>Input Data Description</u>	<u>Case Number</u>
1	Rotor blade data (loc. 1-4549)	1
2	Last rotor blade data card (minus sign in column 1)	
3	Title for rotor blade data	
4	Title for bifilar data	
5	Bifilar data (loc. 1-2199)	
6	Last bifilar data card (loc 2200 = 0. - not last case)	
7	Rotor blade data	2 (last)
8	Last rotor blade data card (minus sign in column 1)	
9	Bifilar data	
10	Last bifilar data card (loc 2200 = 1. - last case)	

The format above is shown for two cases only for brevity. Data blocks 7 through 10 are repeated for each case.

If the first case does not use rotor data, then the data blocks numbered 1 through 3 above are replaced by a single card as follows:

-1 110 0.

5.4 Test Cases Output

The results of the rotor/bifilar coupled program for the four test cases are presented in Appendix C. Only the important results are shown in the Appendix to minimize the size of this report (the actual run consisted of 165 pages of output with only the most important printout switches being activated).

Some important results from the bifilar analysis are summarized in the Table 3 below.

TABLE 3. Bifilar Analysis Test Cases Results

Test Case Number	Inplane Bifilar Response		Rotor		Hub Response			
	AmpL (deg)	Phase (deg)	Longitudinal (X)	Lateral (Y)	Ampl. (g's)	Phase (deg)	Vertical (Z)	
1	9.29	-77	.134	113	.094	178	.006	132
2	1. 9.76	96	.139	-84	.100	-20	.008	-53
↓	2. 9.77	-174						
3	3. 9.80	-84						
↓	4. 9.80	6						
3	9.52	-86	.184	113	.081	137	.010	46
4	9.57	88	.193	-79	.086	-56	.010	-134
↓	9.58	177						
	9.63	-93						
	9.62	-2						

For all test cases, the input force is a 4 per rev fixed system force with lateral sine and longitudinal cosine components of 500 pounds. For the non-linear bifilar analysis results, the response of each of the four inplane bifilars is shown in the table above (cases 2 and 4).

5.5 Test Cases Computer Time

The computer total running time for the four test cases was 8 minutes and 43 seconds. The break-down in computer time per case is shown in the following table.

Test Case Number	Number of D.O.F.	Bifilar Analysis	Computer Time	
			Minutes	Seconds
1	28	Linear	0	25
2	29	Non-linear	7	07
3	16	Linear	0	03
4	17	Non-linear	1	08
		Total	8	43

From the table above, a comparison between cases 1 and 2 and between cases 3 and 4 reveals that the time history analysis requires considerable greater computer time for a complete converged solution than the linear analysis. Also, the computer running time increases tremendously as the number of system degrees-of-freedom is increased when comparing cases 1 and 3 and 2 and 4.

SECTION 6
OVERALL PROGRAM STRUCTURE

The rotor/bifilar program is basically made up of two parts: the rotor aeroelastic analysis and the fixed system/fixed absorber/bifilar pendulums analysis. The bifilar analysis can be executed with and without coupling with the rotor analysis while the opposite is not possible. In addition, the bifilar portion of the program can use either a forced response solution for linear inplane bifilar pendulums or a time history solution for non-linear inplane bifilars. The main purpose of the rotor aeroelastic analysis is to provide the rotor blade stiffness, damping and mass matrices for coupling with the bifilar analysis.

6.1 Segmentation Structure

Due to the large size of the coupled program, it was necessary to implement a segmentation structure to permit operation within a 64K (decimal) for CDC computer use. A basic breakdown of the 10 control segments needed is shown in Table 4 below and in the schematic of Figure 9.

TABLE 4. Segmentation Structure Description

<u>Segment Number</u>	<u>Leading Fortran Routine</u>	<u>Number of Segment Routines</u>	<u>Segment Description</u>
1	SHAKIT	4	Controls overall program logic and specifically the rotor analysis program flow.
2	PRELIM	34	Reads rotor input, initializes data and performs many basic rotor calculations.
3	DYNMAT	12	Calculates rotor dynamic matrices.
4	AERMAT	17	Calculates rotor aerodynamic matrices.
5	EIGER	2	Combines dynamic and aerodynamic rotor matrices, compresses and links them to the bifilar analysis.
6	MAINSV	3	Controls bifilar analysis program flow.
7	SYSCTL	6	Calculates contributions from fixed system modes, fixed absorber, inplane and vertical linear bifilar and couples rotor matrices.
8	HUBIMP	1	Computes rotor hub impedance and transfer matrices.
9	CMPUTE	4	Controls generalized forces calculations and solves for the forced response for the linear bifilar analysis option.

10

NLBIF

9

Performs time-history
solution for the non-linear
bifilar analysis option.

Total = 92

A total of 92 Fortran routines have been developed for this program: 69 of them comprise the rotor analysis portion while 23 make up the bifilar analysis portion.

From the schematic presented in Figure 9, it seen that the rotor aeroelastic analysis is performed in segments 1 through 5 while the bifilar analysis is handled by segments 6 through 10. There is no lateral transfer of data between any two segments; data can only be transferred in a vertical sense to segment 1 for the rotor portion and to segments 1 and 6 for the bifilar portion.

Table 5 below lists in alphabetical order the Fortran sub-routines and the common blocks needed for each segment.

TABLE 5. Segmentation Structure Routines and COMMON Blocks

<u>Segment Number</u>	<u>Fortran Subroutine Name</u>			<u>COMMON Block Name</u>
1	SHAKIT			DYNINP LAGDAM
	INTEG			EOF6 NIMIC
	LOADIT			INDAT PRNTSW
	QTFG			INEIG TMDS
2				INEIGN
	PRELIM	MATEO	PINT	CONT
	BLIN4	MATF	POUT	DAT
	ELI	MATR	PRODM	EMATI
	ELO	MIND	PROUT	EMATO
	EXTEND	MISC	REMOVE	FMAT
	E159X	MODES	ROOTX	FREQ
	FILL	MSHAPE	SECAER	PHTNO
	FOLL	ORTHOG	SIMLIN	PMAT
	FREQUN	OVUN	SKIPLN	PRAM1
	FULL	PFMULT	SORTAB	TORFIN
	GMPRDD	PICK	STDEFL	WORKA
3	MATEI			
	DYNMAT	DMATEX	DYNINT	DYNOUT
	BLELPD	DMDMAT	DYNIN1	NAMIC
	DISCON	DMMMAT	DYNIN2	
4	DISINT	DMSMAT	DYNLST	
	AERMAT	AERIN5	AEROII	AERO1
	AERINT	AERIN6	AMATEX	AERO2
	AERIN1	AERIN7	AMDMAT	AERO3
	AERIN2	AERIN8	AMSMAT	AERO4
	AERIN3	AERLST	BLELPA	AERO5
	AERIN4	AEROI		CDCAER

<u>Segment Number</u>	<u>Fortran Subroutine Name</u>	<u>COMMON Block Name</u>	
5 ↓	EIGER		
6 ↓	COMPRSS		
7 ↓	MAINSV	NDOF	TOTMAT
	INCOND	NLDAT1	XFRDAT
	INPUTV	PRSWTH	
	SYSCTL		
	ADDOFR		
	FIXABS		
	FIXSYS		
	LINBIF		
	LVBIF		
	HUBIMP		
	CMPUTE		
	FORCR		
	GENFOR		
	OUTPUT		
8 ↓	NLBIF	HARMON	HARM
9 ↓	BIFEXP	INTEQ	NLDAT2
	BIFILR	OUT	
	COMBIN	RHS	
	CONVER		

All the Fortran sub-routines listed above except four are computer independent. The computer dependent routines are: SHAKIT (segment 1), LOADIT (segment 1), PRELIM (segment 2) and MAINSV (segment 6). This is due to CDC computer requirements for identification of the main routine, file read error and end of file transfers and word size definition for alpha-numeric read statements. The program coding allows the programmer to convert easily to the IBM 370/168 computer system by commenting out the appropriate block(s) of statements.

6.2 Flow Diagrams

Computer logic flow diagrams are presented in Figures 10 through 16 for the 10 segments. A summary of the flow charts is provided in the table below.

<u>Figure Number</u>	<u>Flow Chart Description</u>	<u>Segment Number(s)</u>
10	Main Program Flow Chart	1 & 5
11	"PRELIM" Flow Chart	2
12	"MODES" Flow Chart	2
13	"DYNMAT" Flow chart	3
14	"AERMAT" Flow Chart	4
15	Bifilar Analysis Flow Chart	6 & 8
16a	"SYSCTL" Flow Chart	7
16b	"CMPUTE" Flow Chart	9
16c	"NLBIF" Flow Chart	10



It should be noted that "IMSL" routines are needed for the calculations performed in "HUBIMP" and "NLBIF". Table 6 below lists the 10 "IMSL" routines used in the bifilar analysis portion of the coupled program:

TABLE 6. IMSL Routines

No.	<u>IMSL Routine Name</u>
1	LEQT2F
2	LINV2F
3	LUDATF
4	LUELMF
5	LUREFF
6	UERTST
7	UGETIO
8	VXADD
9	VXMUL
10	VXSTO

These routines must be supplied by the government for successfull operation of the rotor/bifilar coupled program.

6.3 "COMMON" Blocks

The "COMMON" blocks used in the rotor/bifilar analysis are presented in Figure 17 as they appear in each Fortran sub-routine. Both routines and "COMMON" blocks are listed alphabetically for easy reference.

SECTION 7

SUBROUTINE DESCRIPTIONS

The Fortran subroutines needed to execute the rotor/bifilar coupled program are described in detail in this section. For each routine, the following information is provided, where applicable:

1. Name
2. Purpose
3. Method
4. Usage
5. Subroutines Called
6. Error Returns
7. Restrictions

In addition, an alphabetical listing of the routines and the corresponding page numbers are shown in Table 7 below for easy reference.

TABLE 7. Program Subroutines Listing

No.	Name	Page	No.	Name	Page	No.	Name	Page	No.	Name	Page
1	ADDOFR	24	CMPUTE	47	FORCER	70	NLBIF	131			
2	AERINT	25	COMBIN	48	FREQUN	71	ORTHOG	132			
3	AERIN1	26	CONVER	49	FULL	72	OUT	133			
4	AERIN2	27	DISCON	50	GENFOR	73	OUTPUT	134			
5	AERIN3	28	DISINT	51	GMPRDD	74	OVUN	135			
6	AERIN4	29	DMATEX	52	HARMON	75	PFMULT	136			
7	AERIN5	30	DMDMAT	53	HUBIMP	76	PICK	138			
8	AERIN6	31	DMMMAT	54	INCOND	77	PINT	139			
9	AERIN7	32	DMSMAT	55	INPUTV	78	POUT	140			
10	AERIN8	33	DYNINT	56	INTEG	79	PRELIM	141			
11	AERLST	34	DYNIN1	57	INTEQ	80	PRODM	144			
12	AERMAT	35	DYNIN2	58	LINBIF	81	PROUT	145			
13	AEROI	36	DYNLST	59	LOADIT	82	QTFG	146			
14	AEROII	37	DYNMAT	60	LVBIF	83	REMOVE	147			
15	AMATEX	38	EIGER	61	MAINSV	84	RHS	148			
16	AMDMAT	39	ELI	62	MATEI	85	ROOTX	149			
17	AMSMAT	40	ELO	63	MATEO	86	SECAER	150			
18	BIFEXP	41	EXTEND	64	MATF	87	SHAKIT	151			
19	BIFILR	42	E159X	65	MATR	88	SIMLIN	152			
20	BLELPA	43	FILL	66	MIND	89	SKIPLIN	153			
21	BLELPD	44	FIXABS	67	MISC	90	SORTAB	154			
22	BLIN4	45	FIXSYS	68	MODES	91	STDEFL	155			
23	CMPRSS	46	FOLL	69	MSHAPE	92	SYSCTL	157			

NAME: ADDOFR

PURPOSE: To add degrees-of-freedom to the mass, damping and stiffness system matrices in the bifilar analysis.

METHOD: The new matrices to be added of order NL X NL are split up in four parts:

1. An upper diagonal matrix of order (NL-NA)X(NL-NA)
2. A lower diagonal matrix of order NA X NA
3. An upper off diagonal matrix of order (NL-NA) X NA
4. A lower off diagonal matrix of order NA X (NL-NA)

The lower diagonal matrices are added to the original matrices of order NP X NP, which now become of order (NP + NA) X (NP + NA). The upper off diagonal matrix is pre-multiplied by the fixed system transfer matrix XPH (locations 450-549) while the lower off diagonal matrix is post-multiplied by XPH. The upper diagonal matrix is pre-multiplied and post-multiplied by XPH.

USAGE: CALL ADDOFR (NL, NA, NP)

NL = Order of matrices to be added

NA = Number of degrees-of-freedom to be added

NP = Present order of matrices (after ADDOFR,
order of matrices is NP + NA)

SUBROUTINES
CALLED: None

ERROR RETURNS: None

RESTRICTIONS: None

NAME: AERINT

PURPOSE: To set initial values of all blade aerodynamic integrals to zero and to control the calculation of the aerodynamic integrals needed to construct the aerodynamic damping and stiffness matrices.

METHOD: Aerodynamic integrals independent of the number of bending modes are calculated by calls of AERIN1 and AERIN7 for lift, AERIN3 and AERIN8 for drag, and AERIN4 for pitching moment. Integrals involving bending mode dependent functions are calculated in AERIN2, AERIN5 and AERIN6 for lift, drag and pitching moment respectively.

USAGE: CALL AERINT

SUBROUTINES CALLED: AERIN1, AERIN2, AERIN3, AERIN4, AERIN5, AERIN6, AERIN7, AERIN8

ERROR RETURNS: None

RESTRICTIONS: Due to computer storage restrictions, the aerodynamic integrals had to be calculated in 8 separate routines, i.e. AERIN1 through AERIN8.

NAME: AERIN1

PURPOSE: To calculate the aerodynamic integrals which contain thrust derivatives and are independent of the number of blade bending modes.

METHOD: These integrals are formed in AEROI from the product of 5 radial functions, and are referred to as un-subscripted ATK and AT1K integrals.
Since all the integrals involve thrust derivatives, the upper limit of integration is the blade radius multiplied by the tip loss factor.

USAGE: CALL AERIN1

SUBROUTINES CALLED: AEROII, AEROI

ERROR RETURNS: None

RESTRICTIONS: None

NAME: AERIN2

PURPOSE: To calculate the aerodynamic integrals which contain bending mode dependent functions and thrust derivatives.

METHOD: These integrals are formed in AEROI from the product of 5 radial functions. They are referred to as AT1I and AT2I for doubly subscripted integrals and ATJ, AT1J, AT2J, AT3J for singly subscripted integrals. Since all the integrals involve thrust derivatives, the upper limit of integration is the blade radius multiplied by the tip loss factor.

USAGE: CALL AERIN2

SUBROUTINES CALLED: AEROII, AEROI

ERROR RETURNS: None

RESTRICTIONS: None

NAME:	AERIN3
PURPOSE:	To calculate the aerodynamic integrals which contain drag derivatives and are independent of the number of blade bending modes.
METHOD:	These integrals are formed in AEROI from the product of 5 radial functions, and are referred to as un-subscripted ADK and AD1K integrals. Since all the integrals involve drag derivatives, they are computed over the whole blade.
USAGE:	CALL AERIN3
SUBROUTINES CALLED:	AEROII, AEROI
ERROR RETURNS:	None
RESTRICTIONS:	None

NAME: AERIN4

PURPOSE: To calculate the aerodynamic integrals which contain pitching moment derivatives and are independent of the number of blade bending modes.

METHOD: These integrals are formed in AEROI from the product of 5 radial functions, and are referred to as un-subscripted AM1K, AM2K, AM3K integrals.
Since all the integrals involve pitching moment derivatives, the upper limit of integration is the blade radius multiplied by the tip loss factor.

USAGE: CALL AERIN4

SUBROUTINES CALLED: AEROII, AEROI

ERROR RETURNS: None

RESTRICTIONS: None



NAME:	AERIN5
PURPOSE:	To calculate the aerodynamic integrals which contain bending mode dependent functions and drag derivatives.
METHOD:	These integrals are formed in AEROI from the product of 5 radial functions. They are referred to as AD1I and AD2I for doubly subscripted integrals and ADJ, AD1J, AD2J and AD3J for singly subscripted integrals. Since all the integrals involve drag derivatives, they are computed over the whole blade.
USAGE:	CALL AERIN5
SUBROUTINES CALLED:	AEROII, AEROI
ERROR RETURNS:	None
RESTRICTIONS:	None

NAME: AERIN6

PURPOSE: To calculate the aerodynamic integrals which contain one bending mode dependent functions and pitching moment derivatives.

METHOD: These integrals are formed in AEROI from the product of 5 radial functions, and are referred to as singly subscripted AM1J and AM2J integrals. Since all the integrals involve pitching moment derivatives, the upper limit of integration is the blade radius multiplied by the tip loss factor.

USAGE: CALL AERIN6

SUBROUTINES CALLED: AEROII, AEROI

ERROR RETURNS: None

RESTRICTIONS: None



NAME: AERIN7

PURPOSE: To calculate the aerodynamic integrals which contain thrust derivatives and are independent of the number of blade bending modes.

METHOD: These integrals are formed in AEROI from the product of 5 radial functions, and are referred to as unsubscripted AT2K and AT3K integrals.

Since all the integrals involve thrust derivatives, the upper limit of integration is the blade radius multiplied by the tip loss factor.

USAGE: CALL AERIN7

SUBROUTINES
CALLED: AEROII, AEROI

ERROR RETURNS: None

RESTRICTIONS: None

NAME:	AERIN8
PURPOSE:	To calculate the aerodynamic integrals which contain drag derivatives and are independent of the number of bending modes.
METHOD:	These integrals are formed in AEROI from the product of 5 radial functions, and are referred to as unsubscripted AD2K and AD3K integrals. Since all the integrals involve drag derivatives, they are calculated over the whole blade.
USAGE:	CALL AERIN8
SUBROUTINES CALLED:	AEROII, AEROI
ERROR RETURNS:	None
RESTRICTIONS:	None



NAME: AERLST

PURPOSE: To print the aerodynamic integrals.

METHOD: If the print option is set at 3 or 4, then the integrals are printed. Otherwise control is returned to AERMAT with no integrals printed.
Only those integrals calculated are printed.

USAGE: CALL AERLST

SUBROUTINES CALLED: None

ERROR RETURNS: None

RESTRICTIONS: None

NAME: AERMAT

PURPOSE: To control the calculation of the aerodynamic damping and stiffness matrices.

METHOD: The aerodynamic integrals needed to calculate the matrices are evaluated in AERINT, stored in COMMON blocks AERO1 through AERO5, and printed out by AERLST. AERMAT then makes calls to AMDMAT to calculate the damping matrix, and to AMSMAT to calculate the stiffness matrix. Then, it extends the matrices to include blade torsional bending mode terms in AMATEX and calls BLELPA to calculate elastic torsional contributions.

USAGE: CALL AERMAT

SUBROUTINES CALLED: AERINT, AERLST, AMDMAT, AMSMAT, AMATEX, BLELPA

ERROR RETURNS: None

RESTRICTIONS: None

NAME:	AEROI
PURPOSE:	To calculate the integral of the function $y = F1(R)*F2(R)*F3(R)*F4(R)*F5(R)$ in the interval $(r1, r2)$.
METHOD:	The 5 radial functions are multiplied together at each radial station specified. It should be noted that the second argument in the AEROI calling sequence is designated complex and corresponds to an aerodynamic derivative function. The integral is evaluated in two parts, real and imaginary, by calls to INTEG. If there are no unsteady aerodynamic corrections, then the imaginary part of the integral is set to zero.
USAGE:	CALL AEROI (F1, F2, F3, F4, F5, ANS) F1, F3, F4, F5 = Real functions defined at the radii in R from AEROII. One or more may be equal to 1.0 at every R. F2 = Complex function defined at the radii in R. If no unsteady aerodynamic correction has been applied, the imaginary part will be zero. ANS = The complex integral of the product of F1 through F5. If no unsteady aerodynamic corrections have been applied, then the imaginary part will be zero.
SUBROUTINES CALLED:	INTEG
ERROR RETURNS:	None
RESTRICTIONS:	None

NAME:	AEROII
PURPOSE:	To set up calculations of the integral of the function $y = a(R)*b(R)*c(R)*d(R)*e(R)$ over the interval (r_1, r_2) .
METHOD:	This routine sets the radial values where the functions are defined, the limits of integration, the number of subdivisions to be used in the trapezoidal rule integration method and the switches for unsteady aerodynamics. Subsequent calls to AEROI supply the 5 functions whose product is to be integrated.
USAGE:	CALL AEROII (R, N, RL, RU, K, CIR, CIRN) R = Array of radii at which the functions are defined. N = The number of points in R and in each function array. RL = The lower limit of integration. RU = The upper limit of integration. K = The number of subdivisions to be used in performing the integration by the trapezoidal rule. CIR = 1 No circulatory unsteady aerodynamics used. CIRN = 1 No noncirculatory unsteady aerodynamics used.
SUBROUTINES CALLED:	None
ERROR RETURNS:	None
RESTRICTIONS:	1. N must be equal or less than 25. 2. CIR and CIRN have been set to 1 for no unsteady aerodynamics.



91783

NAME:	AMATEX
PURPOSE:	To expand the aerodynamic matrices to include the blade elastic torsional mode.
METHOD:	The original aerodynamic damping (AMD) and stiffness (AMS) matrices are increased by 3 rows and columns and redefined as AMDN and AMSN to accomodate one collective and two cyclic modes associated with the blade elastic torsional mode.
USAGE:	CALL AMATEX
SUBROUTINES CALLED:	None
ERROR RETURNS:	None
RESTRICTIONS:	The matrices are limited to 30 x 30.

NAME:	AMDMAT
PURPOSE:	To calculate the aerodynamic damping matrix.
METHOD:	The matrix is calculated from the expressions given in Reference 1 using the aerodynamic integrals calculated in AERINT.
USAGE:	CALL AMDMAT
SUBROUTINES CALLED:	None
ERROR RETURNS:	None
RESTRICTIONS:	None



NAME: AMSMAT

PURPOSE: To calculate the aerodynamic stiffness matrix.

METHOD: The elements are calculated from the expressions given in Reference 1 using the aerodynamic integrals calculated in AERINT.

USAGE: CALL AMSMT

SUBROUTINES CALLED: None

ERROR RETURNS: None

RESTRICTIONS: None

NAME: BIFEXP

PURPOSE: To transfer the non-linear bifilar mass matrix and the bifilar and rotor hub force vector to fixed system coordinates.

METHOD: The bifilar mass (square matrix of order 6+NBIF) and the force vector (of order 6+NBIF) are transferred to the fixed system coordinates by proper multiplications with the fixed system mode shapes vector (loc. 450-549). The final expanded mass matrix and force vector have the dimensions of NF + NBIF. The method used is similar to that discussed in routine ADDOFR. The expanded mass and force vector are passed through labelled COMMON/NLDAT2.

They are printed out for azimuth positions up to 5 degrees. The fixed system mode shapes vector is printed out for azimuths up to 2 degrees.

USAGE: CALL BIFEXP (NRHS, NF)

NRHS = Total number of non-linear bifilars plus 6
(maximum is 18).

NF = Number of fixed system modes (maximum is 16).

SUBROUTINES CALLED: None

ERROR RETURNS: None

RESTRICTIONS: Expanded matrix and force vector cannot have dimensions greater than 28.

NAME: BIFILR

PURPOSE: To calculate the non-linear bifilar mass matrix and the bifilar and rotor hub force vector.

METHOD: For the time history solution, the bifilar acceleration terms are left on the left-hand-side of the equations of motion while the r.h.s. contains the bifilar damping and stiffness terms and the input hub forces. The bifilar mass matrix, S (dimensioned 6+NBIF), is calculated and stored in labelled COMMON/INEIGN. Then, the bifilar damping and stiffness terms are used to develop the r.h.s. vector, T (dimensioned 6+NBIF). Next, the rotor hub forces, loaded in locations 1600 through 1719, are evaluated and added to the bifilar contributions in vector T. The hub forces are added to the system gradually according to the ramp factor (location 1760) and the azimuth position. The vector T is passed through labelled COMMON/NLDAT2. The order of the degrees-of-freedom in this routine is: 6 fixed system d.o.f. ($x, y, z, \theta_x, \theta_y, \theta_z$) and non-linear bifilars d.o.f. (NBIF-location 1763). Thus, the maximum number of d.o.f. is 18. For azimuth positions up to 5 degrees, the mass matrix and the force vector are printed out.

USAGE: CALL BIFILR (NREV)

NREV = Revolution number-location 1762 divided by 360.

SUBROUTINES CALLED: None

ERROR RETURNS: None

RESTRICTIONS: Number of input harmonics of rotor hub forces is limited to 10.

NAME: BLELPA

PURPOSE: To calculate the blade elastic pitch aerodynamic contributions.

METHOD: The aerodynamic damping and stiffness matrix elements are calculated using the appropriate expressions for blade pitch in Reference 1. All the terms are multiplied by the torsional mode shape, $\Phi(r)$, which is a function of blade radius, except the blade pitch terms which are multiplied by the square of the mode shape.

USAGE: CALL BLELPA

SUBROUTINES CALLED: None

ERROR RETURNS: None

RESTRICTIONS: None

NAME: BLELPD

PURPOSE: To calculate the blade elastic pitch dynamic contributions.

METHOD: The dynamic mass, damping and stiffness matrix elements are calculated using the equation for the blade pitch in Reference 1. All the terms are multiplied by the torsional mode shape, $\Phi_H(r)$, which is a function of blade radius, except the blade pitch terms which are multiplied by the square of the mode shape.

USAGE: CALL BLELPD

SUBROUTINES CALLED: None

ERROR RETURNS: None

RESTRICTIONS: None

NAME: BLIN4

PURPOSE: To provide a bivariant table lookup with linear interpolation for the airfoil data.

METHOD: The Mach number entries are searched to find K such that

$$M_{K-1} < M < M_K$$

The angles of attack in the M_{K-1} and M_K tables are searched to find I and J such that

$$\alpha_{K-1,I-1} < \alpha < \alpha_{K-1,I}$$

and

$$\alpha_{K,J-1} < \alpha < \alpha_{K,J}$$

Then the coefficient at M_{K-1} and α is given by

$$c_{K-1} = (\alpha - \alpha_{K-1,I-1}) * (c_{K-1,I} - c_{K-1,I-1}) / \\ (\alpha_{K-1,I} - \alpha_{K-1,I-1}) + c_{K-1,I-1}$$

and the coefficient at M_K and α is given by

$$c_K = (\alpha - \alpha_{K,J-1}) * (c_{K,J} - c_{K,J-1}) / (\alpha_{K,J} - \alpha_{K,J-1}) + \\ c_{K,J-1}$$

Finally, the coefficient at M and α is obtained from

$$c = (M - M_{K-1}) * (c_K - c_{K-1}) / (M_K - M_{K-1}) + c_{K-1}$$

$$\frac{dc}{dm} = \frac{c_K - c_{K-1}}{M_K - M_{K-1}}$$

USAGE: CALL BLIN4 (T, M, K, X, Y, Z, D, L)

T = A two-dimensional array containing the coefficient, angle of attack pairs. The first point in each column represents the number of pairs, the second point in each column represents the Mach number, and the remaining points in the column are the pairs for that Mach number.

M,K = The dimensions of T
M is the maximum number of Mach numbers in the table.
K is the maximum column length.

X = Angle of attack.

Y = Mach number.

Z = Returned coefficient.

D = Derivative with respect to M.

L = Error switch.
1 No error
2 Mach number not spanned
3 Angle of attack not spanned

SUBROUTINES CALLED: None

ERROR RETURNS: See above

RESTRICTIONS:

1. Number of Mach numbers specified must be equal or greater than 2 and cannot be greater than 12.
2. Number of coefficient/angle of attack pairs must be equal or greater than 5 and cannot be greater than 35.

NAME:	CMPRSS
PURPOSE:	To compress a square matrix.
METHOD:	The returned matrix of dimension L x L is produced by taking the first L rows and columns of the input matrix of dimension N x N.
USAGE:	CALL CMPRSS (A, N, B, L) A = Input matrix. N = Dimensions of A. B = Output matrix, which may have the same location as A. L = Dimensions of B.
SUBROUTINES CALLED:	None
ERROR RETURNS:	None
RESTRICTIONS:	If L is equal or greater than N, no matrix compression is done.



NAME: CMPUTE

PURPOSE: To control calculations of the generalized forces and of the forced response for the linear bifilar analysis.

METHOD: First, the generalized forces are calculated in GENFOR. Then, the forced response of the linear system of equations is obtained in FORCER. The results of the analysis are printed out in a call to OUTPUT.

USAGE: CALL CMPUTE

SUBROUTINES CALLED: GENFOR, FORCER, OUTPUT

ERROR RETURNS: None

RESTRICTIONS: None

NAME:	COMBIN
PURPOSE:	To combine the non-linear bifilar mass matrix and the force vector developed for the non-linear bifilar analysis with the corresponding matrix and vector from the Linear bifilar analysis.
METHOD:	<p>The mass matrix and force vector calculated in BIFEXP are added to the results of the linear analysis from SYSCTL. The fixed system d.o.f. are affected. The combined mass matrix and force vector include all the degrees-of-freedom (up to the maximum of 72).</p> <p>If forces are input to one or two additional aircraft stations (as specified in locations 1767 and 1940 through 2179), their corresponding contributions to the final force vector are included by pre-multiplying the input forces by the appropriate aircraft station mode shapes (see locations 550-749).</p> <p>The final combined mass matrix and force vector are stored in labelled COMMON/NLDAT2.</p>
USAGE:	<pre>CALL COMBIN (NBML, NRHS, NF, NREV)</pre> <p>NBML = Fixed system modes plus non-linear bifilars (maximum is 28).</p> <p>NRHS = Total number of d.o.f. not including non-linear bifilars (maximum is 60).</p> <p>NF = Number of fixed system modes (maximum is 16).</p> <p>NREV = Revolution number - loc 1762 divided by 360.</p>
SUBROUTINES CALLED:	None
ERROR RETURNS:	None
RESTRICTIONS:	<ol style="list-style-type: none"> 1. Total number of degrees-of-freedom is 72 (60 from linear analysis and 12 for the maximum number of non-linear bifilars). 2. Harmonic force inputs are possible for only 2 aircraft stations.

NAME:

CONVER

PURPOSE:

To test on the convergence of the time history solution for two successive revolutions.

METHOD:

This routine checks the difference in the displacements of the first two non-linear bifilar pendulums obtained for two successive revolutions. If both differences are within .002 radian (corresponding to .1146 degree), then the convergence criterion is satisfied; IER (see below) is set to 1 and the program returns to NLBIF to calculate one more revolution after which the harmonic analysis is performed and printed out. If one of the differences is greater than .002 radian, the time history analysis proceeds to the next revolution.

The revolution number, the two bifilar displacement differences and the rotor hub x , y , θ_z , \dot{x} , \dot{y} motions are all listed out for each revolution.

USAGE:

CALL CONVER (I, IER)

I = Rotor revolution number - location 1762 divided by 360.

IER = Convergence criterion - it is met if equal to 1.

SUBROUTINES
CALLED:

None

ERROR RETURNS:

None

RESTRICTIONS:

None

NAME:	DISCON
PURPOSE:	To adjust a blade stepwise function so that it is defined only over the blade.
METHOD:	The input segments are extended or truncated so that the first segment starts at the offset and the final segment finishes at the blade radius. Function values are unaltered but may be discarded if the segment they refer to is completely outside the blade.
USAGE:	CALL DISCON (KSTAR, DELTAR, NSTAR, E, R, RBAR, KBAR, N1BAR) KSTAR = Array of input stepwise function values. DELTAR = Array of segment lengths over which KSTAR is defined. NSTAR = Number of entries in KSTAR and DELTAR. E = Blade offset. R = Blade radius. RBAR = Array of adjusted segment lengths. KBAR = Array of stepwise function values defined over RBAR. N1BAR = Number of entries in RBAR and KBAR.
SUBROUTINES CALLED:	None
ERROR RETURNS:	None
RESTRICTIONS:	None

NAME: DISINT

PURPOSE: To perform the integration of the product of a step function and a radial function over the blade length.

METHOD: The stepwise function is first adjusted by DISCON so that it is defined over a segment distribution which starts at the offset and finishes at the blade radius. The integration of the radial function is then performed separately over each of these segments and multiplied by the value of the stepwise function for that segment. The final answer is the sum of these results.

$$\text{i.e. } \int_E^{R_N} f(r)S(r)dr = S_1 \int_E^{R_1} f(r)dr + S_2 \int_{R_1}^{R_2} f(r)dr + \dots$$

$$S_k \int_{R_{K-1}}^{R_K} f(r)dr + \dots + S_N \int_{R_{N-1}}^{R_N} f(r)dr$$

where

S_K = the value of the stepwise function over the K^{th} segment.

$f(r)$ = the radial function

USAGE: CALL DISINT (COMP, R, N, FPPP, RPPP, NM2, E, CR, SUM)

COMP = Array of radial function values.

R = Array of radii at which COMP is defined

N = Number of points in COMP and R.

FPPP = Array of stepwise function values.

RPPP = Array of segment lengths over which FPPP is defined.

USAGE: NM2 = Number of entries in FPPP and RPPP.
 E = Blade offset.
 CR = Blade radius.
 SUM = Integral of the product of the two functions.

SUBROUTINES
CALLED: DISCON, INTEG

ERROR RETURNS: None

RESTRICTIONS: None

48490

NAME:	DMATEX
PURPOSE:	To expand the dynamic matrices to include the blade elastic torsional mode.
METHOD:	The original dynamic mass (DMM), damping (DMD) and stiffness (DMS) matrices are increased by 3 rows and columns and redefined as DMMN, DMDN and DMSN respectively to accomodate one collective and two cyclic modes associated with the blade elastic torsional mode.
USAGE:	CALL DMATEX
SUBROUTINES CALLED:	None
ERROR RETURNS:	None
RESTRICTIONS:	The matrices are limited to 30 x 30.

NAME: DMDMAT

PURPOSE: To calculate the dynamic damping matrix.

METHOD: The matrix is calculated from the expressions given in Reference 1, using the dynamic integrals calculated in DYNINT.

USAGE: CALL DMDMAT

SUBROUTINES CALLED: None

ERROR RETURNS: None

RESTRICTIONS: None



NAME:	DMMMAT
PURPOSE:	To calculate the dynamic mass matrix.
METHOD:	The matrix is calculated from the expressions given in Reference 1, using the dynamic integrals calculated in DYNINT.
USAGE:	CALL DMMMAT
SUBROUTINES CALLED:	None
ERROR RETURNS:	None
RESTRICTIONS:	None

NAME:	DMSMAT
PURPOSE:	To calculate the dynamic stiffness matrix.
METHOD:	The matrix is calculated from the expressions given in Reference 1, using the dynamic integrals calculated in DYNINT.
USAGE:	CALL DMSMAT
SUBROUTINES CALLED:	None
ERROR RETURNS:	None
RESTRICTIONS:	None



NAME: DYNINT

PURPOSE: To set the initial values of the dynamic integrals to zero and to control the calculation of the integrals needed to construct the dynamic mass, damping, and stiffness matrices.

METHOD: The dynamic integrals are obtained from the integration of the product of a radial function and a stepwise function over the blade length. All integrals have the blade mass or the edgewise, flatwise, and torsional mass moments of inertia as their stepwise function.
If the radial function is independent of the blade bending modes, then the integrals are calculated in DYNIN1. Integrals with singly and doubly subscripted radial functions are handled in DYNIN2.

USAGE: CALL DYNINT

SUBROUTINES CALLED: DYNIN1, DYNIN2

ERROR RETURNS: None

RESTRICTIONS: None

NAME:	DYNIN1
PURPOSE:	To calculate the dynamic integrals whose setwise function is either the blade mass or the edgewise, flatwise, or torsional mass moment of inertia and whose radial functions contain no blade bending mode dependent quantities.
METHOD:	These integrals are formed in DISINT from the product of a radial function and a stepwise function integrated over the blade length. The radial function may itself be a product of radial functions. The integrals which are a function of blade mass are referred to as unsubscripted BMK. The integrals dependent on the blade mass moments of inertia are referred to as unsubscripted BIK.
USAGE:	CALL DYNIN1
SUBROUTINES CALLED:	DISINT
ERROR RETURNS:	None
RESTRICTIONS:	None



NAME:	DYNIN2
PURPOSE:	To calculate the dynamic integrals whose stepwise function is either the blade mass or the edgewise, flatwise, or torsional mass moment of inertia and whose radial function contains one or two blade bending mode dependent quantities.
METHOD:	These integrals are formed in DISINT from the product of a radial function and a stepwise function. The integrals which are a function of blade mass are referred to as BMJ and BMI for singly and doubly subscripted values respectively. The integrals dependent on the blade mass moments of inertia are referred to as BIJ and BII for singly and doubly subscripted values respectively.
USAGE:	CALL DYNIN2
SUBROUTINES CALLED:	DISINT
ERROR RETURNS:	None
RESTRICTIONS:	None

NAME: DYNLST

PURPOSE: To print out the dynamic integrals.

METHOD: If the print option is set to 3 or 4, the integrals are printed. Otherwise, control is returned to DYNMAT.
Only those integrals calculated are printed.

USAGE: CALL DYNLST

SUBROUTINES CALLED: None

ERROR RETURNS: None

RESTRICTIONS: None

NAME:	DYNMAT
PURPOSE:	To control the calculation of the dynamic mass, damping and stiffness matrices.
METHOD:	<p>The dynamic integrals needed to calculate the elements of the matrices are evaluated in DYNINT, stored in labelled COMMON/DYNOUT, and printed out by DYNLST. DYNMAT then makes calls to DMMMAT, DMDMAT and DMSMAT to calculate the mass, damping and stiffness matrices respectively. Then, it expands the matrices in DMATEX to include the blade torsional elastic mode terms, which are calculated in BLELPD.</p> <p>In addition, several blade parameters are calculated and printed out according to the degrees-of-freedom being used.</p>
USAGE:	CALL DYNMAT
SUBROUTINES CALLED:	DYNINT, DYNLST, DMMMAT, DMDMAT, DMSMAT, DMATEX, BLELPD
ERROR RETURNS:	None
RESTRICTIONS:	None

NAME: EIGER

PURPOSE: To compress and link the rotor matrices to the bifilar analysis.

METHOD: The degrees-of-freedom not utilized are eliminated from the rotor dynamic and aerodynamic matrices. The dynamic and aerodynamic damping and stiffness matrices are added together. Then, the 30 x 30 matrices are compressed to K X K in CMRSS. The final compressed matrices (3) are stored in labelled COMMON/INEIG for coupling with the bifilar analysis. The matrices can be printed out and/or punched out in cards if desired.

USAGE: CALL EIGER

SUBROUTINES CALLED: CMRSS

ERROR RETURNS: None

RESTRICTIONS: None

NAME: ELI

PURPOSE: To calculate the forces and moments needed to create the elastic matrix associated with the inboard half of a segment.

METHOD: The forces and moments are calculated using the expressions derived in Reference 2.

USAGE: CALL ELI(I)
I = Blade segment number.

SUBROUTINES CALLED: None

ERROR RETURNS: None

RESTRICTIONS: None

NAME: ELO

PURPOSE: To calculate the forces and moments needed to create the elastic matrix associated with the outboard half of a segment.

METHOD: The forces and moments are calculated using the expressions derived in Reference 2.

USAGE: CALL ELO(I)

I = Blade segment number.

SUBROUTINES
CALLED: None

ERROR RETURNS: None

RESTRICTIONS: None

NAME: EXTEND

PURPOSE: To find the values of a function at a set of points, given the function values at a different set of points.

METHOD: The value of the function at a new point is obtained by linear interpolation between the two closest old points.

USAGE: CALL EXTEND (F, R, M, RSTAR, N)

F = On input, the old function values.
On output, the new function values.

R = The set of points at which F is defined on input.

M = Number of points in F and R.

RSTAR = The set of points at which F is defined on output.

N = The number of points in RSTAR and F on output.

SUBROUTINES CALLED: None

ERROR RETURNS: None

RESTRICTIONS: N must be less than or equal to 400.

NAME: E159X

PURPOSE: To calculate the blade elastic torsional frequency.

METHOD: The torsional frequency is found from repeated calls to ROOTX which calculates the torsional mode shape. The frequency trials start at zero frequency and proceed in steps of 10 rad/sec up to a maximum of 1990 rad/sec. After each trial, a check is made on the sign of the root mode shape. If a change in sign is found, then the frequency has been found. Three more iterations are performed to zero-in the frequency value (difference in 2 successive values of the root mode shape is within .0001).

USAGE: CALL E159X

SUBROUTINES CALLED: ROOTX

ERROR RETURNS: If after 200 trials no sign change in the root mode shape has been found, then an error message is printed out as follows:
'OUT OF RANGE'
followed by the last frequency trial value and the root mode shape value.

RESTRICTIONS:

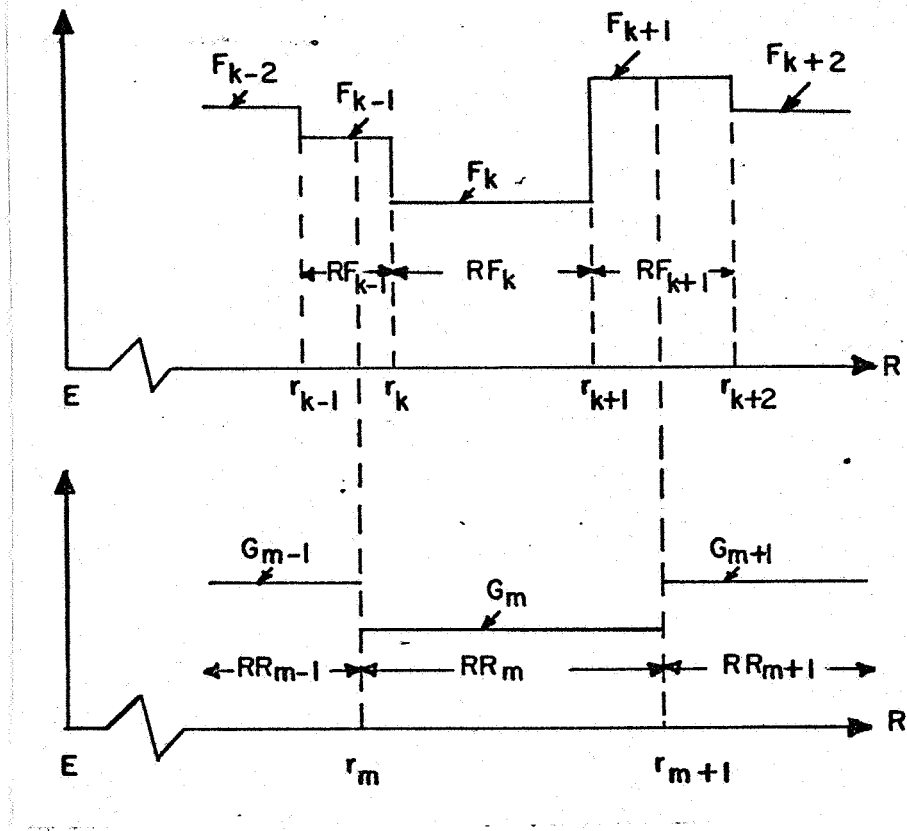
1. Frequency upper limit is 1990 rad/sec.
2. Only the first elastic torsional frequency is found.
3. Three trials allowed to zero-in the final frequency value.

NAME: FILL

PURPOSE:

To find the value/length of a second moment of area function over each of the blade segments, given the function/length values over some other segment distribution.

METHOD:



The redistributed function G_m is defined below for new segment RR_m :

$$\frac{RR_m}{G_m} = \frac{r_k - r_m}{F_{k-1}} + \frac{r_{k+1} - r_k}{F_k} + \frac{r_{m+1} - r_{k+1}}{F_{k+1}}$$

Where:

- F_k = Old function values
- RF_k = Old blade segments
- r_k = Radial positions of function from hinge (E)
- G_m = New function values
- RR_m = New blade segments

USAGE: CALL FILL (RR, NSEG, F, RF, NF, E)

RR = An array containing the blade segment lengths.

NSEG = The number of segments in RR.

F = On input, the function values over RF.
On output, the function values over RR.

RF = An array containing the segment lengths over
which F is defined on input.

NF = The number of segments in RF.

E = The offset of the blade from the center of
rotation.

SUBROUTINES CALLED: None

ERROR RETURNS: None

RESTRICTIONS: NSEG must be less than or equal to 25.

NAME: FIXABS

PURPOSE: To calculate the fixed system absorber matrices in the bifilar analysis.

METHOD: This routine initializes the matrices to zero. Then, it defines needed parameters from the input vector, V, and proceeds to evaluate the mass damping and stiffness elements according to the equations from Reference 3.
Printout of final matrices is controlled by location 10.

USAGE: CALL FIXABS

SUBROUTINES CALLED: None

ERROR RETURNS: None

RESTRICTIONS: Number of fixed system absorber cannot be greater than 5.

NAME: FIXSYS

PURPOSE: To calculate the fixed system modes matrices in the bifilar analysis.

METHOD: The fixed system modal mass, damping and stiffness elements are calculated according to the expressions in Reference 3.
A printout of the matrices can be obtained if location 10 is set to 1.

USAGE: CALL FIXSYS

SUBROUTINES CALLED: None

ERROR RETURNS: None

RESTRICTIONS: None

NAME: FOLL

PURPOSE: To convert a blade function from value/length to an equivalent radial function.

METHOD: The input function is first converted into a cumulative function with values at the end points of the input segment distribution. The value then assigned to a radial point is derived by finding the cumulative values at the end points of the segment that the radial point represents and subtracting them.

USAGE: CALL FOLL (RAD, F, NF, RB, NB, E, RR)

RAD = Segment lengths of input distribution.

F = Input stepwise function.

NF = Number of elements in RAD and F.

RB = The radial points at which values are required.

NB = The number of elements in RB.

E = The blade offset.

RR = The segment lengths to be associated with the radial points in RB.

SUBROUTINES CALLED: EXTEND

ERROR RETURNS: None

RESTRICTIONS: None

NAME: FORCER

PURPOSE: To solve for the forced response of the linear bifilar analysis.

METHOD: At first, this routine combines the generalized force cosine and sine vectors and prints out the final vector, FRC, of dimension $2*NF$. Then, it inverts the hub impedance matrix, T, by a call to LINV2F and forms the fixed system generalized coordinates vector, XQ, of dimension $2*NF$. The generalized coordinates vector of all the system degrees-of-freedom, GAMMA, of dimension 90, is calculated from a multiplication of the transfer matrix, TRANSF, and the XQ vector. The final vector GAMMA is used to calculate and print out the forced response amplitudes and phase angles of the fixed system absorbers and bifilar pendulums.

The GAMMA vector is printed out if location 1497 is set to 1.0.

USAGE: CALL FORCER

SUBROUTINES CALLED: LINV2F
(This is an "IMSL" package routine which must be supplied by the Army).

ERROR RETURNS: None

RESTRICTIONS: Refer to subroutine HUBIMP.

NAME: FREQUN

PURPOSE: To calculate the blade natural frequencies.

METHOD:
The natural frequencies are the eigenvalues of the matrix formed by applying suitable boundary conditions to the matrix relating forces, etc., at the blade tip to the blade root.

The eigenvalues are found by assuming an initial frequency and then increasing it by a predetermined increment until a change in sign of the determinant occurs. Newton's method is then used to improve the answer until $|F_{i+1} - F_i| < .001$.

The search for further natural frequencies continues until either the requested number has been found or the upper frequency limit is reached.

The starting values for the frequency trials is $.15\Omega$ where Ω is the rotor speed in rad/sec.

The frequency scan interval is $.10\Omega$.

USAGE: CALL FREQUN

SUBROUTINES
CALLED: PRODM, MIND

ERROR RETURNS:
1. 'EXCEEDED UPPER FREQUENCY LIMIT'

The program will search for the number of frequencies requested up to a frequency of 75 cycles/rev.

The program continues using the number of natural frequencies that have been found.

2. 'DID NOT CONVERGE AFTER SIGN CHANGE - 100 TRIALS'

Having located a change in sign of the determinant, the program was unable to improve the eigenvalue sufficiently to satisfy the convergency test in 100 trials. The program continues using the last estimate.

3. 'FAILED TO LOCATE SIGN CHANGE AFTER 500 TRIALS'

An eigenvalue was not detected in the frequency range 0.0 to 75 cycles/rev. The program continues with a frequency of 75 cycles/rev.

4. 'AN EVEN NUMBER OF FREQUENCIES HAVE BEEN MISSED'

Two frequencies differ by less than $.0015\omega - .00001$ (ω is the rotor speed). The program treats them as one frequency and continues.

RESTRICTIONS:

1. Frequencies cannot be calculated at zero rotor speed. It is suggested that rotor speed be lowered gradually to about 50 rad/sec. Computer time increases tremendously as rotor speed decreases since the scan interval is set at $.10\omega$.
2. See notes on "ERROR RETURNS".



NAME: FULL

PURPOSE: To find the values of an area function over each of the blade segments, given the function/length values over some other segment distribution.

METHOD: Same method as discussed for subroutine "FILL".

USAGE: CALL FULL (RR, NSEG, F, RF, NF, E)

RR = An array containing the blade segment lengths.

NSEG = The number of segments in RR.

F = On input, the function values/length over L.
On output, the function values/length over RR.

RF = An array containing the segment lengths over which F is defined on input.

NF = The number of segments in RF.

E = The offset of the blade from the center of rotation.

SUBROUTINES
CALLED: None

ERROR RETURNS: None

RESTRICTIONS: NSEG must be less than or equal to 25.

NAME: GENFOR

PURPOSE: To calculate the generalized forces for the linear bifilar analysis.

METHOD: The generalized force vectors for the cosine (FQC) and sine component (FQS) are calculated from the force input vectors (locations 110-289) provided for the main and tail rotor hubs and 2 additional aircraft points and their appropriate mode shapes (locations 450-749 and 850-949).
The force vectors of dimension NF (location 9) are passed through labelled COMMON/XFRDAT.

USAGE: CALL GENFOR

SUBROUTINES CALLED: None

ERROR RETURNS: None

RESTRICTIONS: None

NAME: GMPRDD

PURPOSE: To multiply two general matrices to form a resultant general matrix.

METHOD: The M X L matrix B is premultiplied by the N X M matrix A and the result is stored in the N X L matrix R.

RESULT:

$$\begin{matrix} R \\ \text{NXL} \end{matrix} = \begin{matrix} A \\ \text{NXM} \end{matrix} \times \begin{matrix} B \\ \text{MXL} \end{matrix}$$

USAGE: CALL GMPRDD (A, B, R, N, M, L)

A = First input matrix.

B = Second input matrix.

R = Output matrix.

N = Number of rows in A.

M = Number of columns in A and rows in B.

L = Number of columns in B.

SUBROUTINES CALLED: None

ERROR RETURNS: None

RESTRICTIONS: None

NAME: HARMON

PURPOSE: To perform harmonic analysis of the time history solution.

METHOD: The solution acceleration vector calculated in INTEQ and passed through labelled COMMON/NLDAT2 is harmonically analyzed once the convergence criterion is met in routine CONVER.
The harmonics are stored in labelled COMMON/HARM.

USAGE: CALL HARMON (IC, N1)
IC = Rotor revolution number - location 1762 divided by 360.
N1 = Total number of degrees-of-freedom (maximum is 72).

SUBROUTINES CALLED: None

ERROR RETURNS: None

RESTRICTIONS: The number of harmonics output is limited to 10.

NAME:

HUBIMP

PURPOSE:

To develop the transfer and hub impedance matrices for the linear bifilar analysis.

METHOD:

At first, the final mass (XMFC) and stiffness (XKFC) are combined to form matrix A ($= XKFC - W_F^2 * XMFC$), where W_F is the forcing frequency. Then, the damping matrix (XCFC) is used to form matrix B ($= W_F * XCFC$). If no fixed system absorbers and no linear bifilars are present in the system, the routine calculates the hub impedance matrix, E, from matrices A and B and then returns to MAINSV; otherwise, it proceeds to calculate the transfer matrix, TRANSF, after a call to LINV2F, and subsequently the hub impedance matrix E. (Additional information can be obtained in Ref. 3).

The transfer and hub impedance matrices are passed through labelled COMMON/XFRDAT.

Throughout the matrix calculations performed, the resulting matrices can be printed out using the control switches in locations 10 and 15.

USAGE:

CALL HUBIMP

SUBROUTINES
CALLED:

LINV2F

(This is an "IMSL" package routine which must be supplied by the government)

ERROR RETURNS:

None

RESTRICTIONS:

1) Number of degrees-of-freedom of the final system matrices (XMFC, XKFC, XCFC) is limited to 60 as follows:

a.	Fixed system modes	16
b.	Fixed system absorbers	5
c.	Linear bifilars (5X3)	15
d.	Rotor Modes	24
		60 = Total

- 2) The transfer matrix (TRANSF) maximum dimensions are (90X32) where 90 represents 2 times the maximum d.o.f. of the fixed system absorber plus the bifilar and rotor modes and 32 is 2 times the maximum number of fixed system d.o.f.
- 3) The hub impedance matrix (E) has maximum dimensions of (32X32) obtained from 2 times the maximum fixed system d.o.f.

NAME: INCOND

PURPOSE: To initialize quantities to zero in the bifilar analysis.

METHOD: The system mass, damping and stiffness matrices (XMFC, XCFC, XKFC respectively) of dimensions 60X60 are set to zero. In addition, the matrices (10X75) used to store the harmonic results (CHARM and SHARM) are zeroed out. The input location 1498 controls the initialization of the bifilar pendulums, the rotor hub and the state variables displacements and velocities.

USAGE: CALL INCOND

SUBROUTINES
CALLED: None

ERROR RETURNS: None

RESTRICTIONS: None

NAME: INPUTV

PURPOSE: To provide a description of the input locations to the bifilar analysis and to read the input data.

METHOD: Locations 1 through 2200 are listed and discussed - all lines of code are of course commented out. Then, a call is made to LOADIT to read the input data.

USAGE: CALL INPUTV

SUBROUTINES CALLED: LOADIT

ERROR RETURNS: None

RESTRICTIONS: None

NAME:	INTEG
PURPOSE:	To convert a function defined at unequally spaced argument points, to an equal function defined at a set number of equally spaced points in a given interval and integrate it using the trapezoidal rule.
METHOD:	The length of the interval is divided by the number of divisions required to obtain the argument spacing. Function values at these subdivision points are obtained by linearly interpolating between the two nearest existing function values. The redistributed function is then passed to QTFG for integration.
USAGE:	<pre>CALL INTEG (F, R, NSEG, RBAR1, RBAR2, N, XI)</pre> <p>F = Array of function values. R = Array of argument values at which F is defined. NSEG = Number of blade segments RBAR1 = Lower limit of the interval of integration. RBAR2 = Upper limit of the interval of integration. N = Number of subdivisions to be used. XI = Integral.</p>
SUBROUTINES CALLED:	QTFG
ERROR RETURNS:	None
RESTRICTIONS:	N must be less than or equal to 100.

NAME: INTEQ

PURPOSE: To calculate the time history solution of the non-linear equations of motion.

METHOD: The combined mass matrix (XMT) and force vector (FT) of dimensions NT developed in COMBIN are used to obtain the time history response of the non-linear system. The procedure is discussed below.

$$\text{Given } [XMT] \{ \ddot{q} \} = \{ FT \},$$

first, the matrix and vectors are partitioned as follows:

$$\left[\begin{array}{c|c} XMT_A & XMT_B \\ \hline \hline XMT_C & I \end{array} \right] \left[\begin{array}{c} \ddot{q}_1 \\ \vdots \\ \ddot{q}_2 \end{array} \right] = \left[\begin{array}{c} FT_1 \\ \vdots \\ FT_2 \end{array} \right]$$

where the square matrix, $[XMT_A]$, the acceleration vector part, $\{ \ddot{q}_1 \}$, and the force vector part, $\{ FT_1 \}$, have dimensions (NT-ND) and include only the degrees-of-freedom associated with the fixed system and rotor modes, while the unity matrix, $[I]$, the acceleration vector part, $\{ \ddot{q}_2 \}$, and the force vector part, $\{ FT_2 \}$, have dimensions ND and include the rest of the d.o.f. of the system.

Next, the accelerations are solved for as shown below:

$$1) [XMT_A] \{ \ddot{q}_1 \} + [XMT_B] \{ \ddot{q}_2 \} = \{ FT_1 \}$$

$$2) [XMT_C] \{ \ddot{q}_1 \} + [I] \{ \ddot{q}_2 \} = \{ FT_2 \}$$

Solve for $\{ \ddot{q}_2 \}$ from equation 2) above.

$$3) \{ \ddot{q}_2 \} = \{ FT_2 \} - [XMT_C] \{ \ddot{q}_1 \}$$

Then, the solution vector \dot{q}_1 is given by substituting 3) into 1) above.

$$4) \left([XMT_A] - [XMT_B] [XMT_C] \right) \{ \ddot{q}_1 \} = \{ FT_1 \} - [XMT_B] \{ FT_2 \}$$

which can be written as,

$$5) \quad [XXT] \quad \{ \ddot{q}_1 \} = \{ \dot{X} \}$$

The routine forms the matrix $[XXT]$ and the vector $\{ \dot{X} \}$ (note that the maximum dimensions of (NT-ND) are 40).

The acceleration vector, $\{ \ddot{q}_1 \}$, is solved for in the IMSL routine LEQT2F. Subsequently, the acceleration vector, $\{ \ddot{q}_2 \}$, is evaluated from expression 3) above.

The analysis proceeds next to integrate the combined acceleration vector, $\{ \ddot{q} \}$, to obtain the velocity and displacement vectors using the expressions below:

$$6) \quad \{ \dot{q} \}_{t+\Delta t} = \{ \dot{q} \}_t + \Delta t \{ \ddot{q} \}_t$$

$$7) \quad \{ q \}_{t+\Delta t} = \{ q \}_t + \Delta t \{ \dot{q} \}_t$$

where the time increment, Δt , is defined from

$$8) \quad \Delta t = \frac{\Delta\psi (\text{deg-loc } 1761)}{\Omega (\text{rpm-loc } 7)} * 6, \text{ seconds}$$

The resulting velocity vector is loaded into the input vector, V, in locations 1740-1759 for the non-linear bifilar and in locations 1860-1939 for the remaining d.o.f., while the displacement vector is loaded similarly into locations 1720-1739 and locations 1780-1859. The rotor hub velocities and displacements are also calculated by pre-multiplying the resulting vectors by the transfer matrix (input in locations 450-549). The resulting velocity and displacement vectors are printed out at every azimuth position up to 30 degrees. The final step in INTEQ is to increment the azimuthal angle and return to NLBIF.

The final results are passed through labelled COMMON/INDAT for the input vector V and through labelled COMMON/NLDAT2 for the solution acceleration vector $\{ \ddot{q} \}$.

USAGE:

CALL INTEG (NT, ND)

NT = Total number of d.o.f. (72 maximum).

ND = NT minus number of d.o.f. of fixed system
(16 maximum) and rotor (24 maximum); maximum
value of ND is 32.

SUBROUTINES
CALLED:

LEQT2F

(This is an "IMSL" package routine which must be supplied by the Army).

ERROR RETURNS:

None

RESTRICTIONS:

The maximum order of the solution vector (as obtained from LEQT2F) is 40.

NAME: LINBIF

PURPOSE: To calculate the linear inplane bifilar matrices

METHOD: This routine defines needed parameters from the input vector, V, to start. Then, it initializes the matrices to zero and proceeds with the calculations of the mass, damping and stiffness elements according to the expressions published in Ref. 3. The matrices are of order 9X9 and consist of the following degrees-of-freedom:

1. Fixed system longitudinal
2. Fixed system lateral
3. Fixed system vertical
4. Fixed system roll
5. Fixed system pitch
6. Fixed system yaw
7. Bifilar symmetric mode
8. Bifilar cyclic (sine) mode
9. Bifilar cyclic (cosine) mode

A printout of the bifilar matrices can be obtained by setting location 1495 to 1.0.

USAGE: CALL LINBIF

SUBROUTINES CALLED: None

ERROR RETURNS: None

RESTRICTIONS:

1. Number of bifilars in each kind is limited to 10.
2. Number of different bifilar kinds (inplane and vertical) cannot be greater than 5.

NAME: LOADIT

PURPOSE: To read a data card, and then after checking the characters, to store the data in the specified locations.

METHOD: Each card in the input stream is read and printed out before any interpretation is attempted. Each character on the card is then checked for validity. Column one must be -, +, 0 or blank; column two must be 1 through 5; columns three through six must be +, 0 - 9, or blank; and columns seven through sixty-six can be -, +, 1, 0 - 9, E or blank.
 A minus in column one indicates end of input data for that case.
 Column two contains the number of values to be read in.
 Columns three through six contain the input location at which to start storing the values. If the address is zero or blank, the next location is used.
 Columns seven through sixty-six contain the values to be stored. A format of 5E12.4 is assumed.

USAGE: CALL LOADIT(X,NFILE)
 X = An array into which the data is placed.
 In the rotor analysis, X = INPUT (which is equivalent to blank COMMON).
 In the bifilar analysis, X=V (which is equivalent to labelled COMMON/INDAT).
 NFILE = 5. The read unit file for both rotor and bifilar analyses.

SUBROUTINES CALLED: None

ERROR RETURNS: Any error results in the card that caused the error being ignored.

RESTRICTIONS:

- *1) LOADIT is one of four routines which are computer dependent. Coding for both IBM and CDC computer systems is retained with appropriate lines commented out.
- 2) The maximum number of input locations is 8100 for the rotor analysis and 2200 for the bifilar analysis.

NAME: LVBIF

PURPOSE: To calculate the linear vertical bifilar matrices

METHOD: This routine defines needed parameters from the input vector, V, to start. Then, it initializes the matrices to zero and proceeds with the calculations of the mass, damping and stiffness elements according to the expressions published in Ref. 3. The matrices are of order 9X9 and consist of the following degrees-of-freedom:

1. Fixed system longitudinal
2. Fixed system lateral
3. Fixed system vertical
4. Fixed system roll
5. Fixed system pitch
6. Fixed system yaw
7. Bifilar symmetric mode
8. Bifilar cyclic (sine) mode
9. Bifilar cyclic (cosine) mode

A printout of the bifilar matrices can be obtained by setting location 1496 to 1.0.

USAGE: CALL LVBIF

SUBROUTINES
CALLED: None

ERROR RETURNS: None

RESTRICTIONS:

1. Number of bifilars in each kind is limited to 10.
2. Number of different bifilar kinds (inplane and vertical) cannot be greater than 5.

NAME:	MAINSV
PURPOSE:	To control the principal logic flow of the bifilar analysis portion of the rotor/bifilar coupled program.
METHOD:	<p>MAINSV first calls INPUTV which calls LOADIT to read the input data for the case at hand. Then, the bifilar matrices and other quantities are set to zero in INCOND. The contributions of the fixed system modes, the rotor (if used), the fixed system absorbers, and the linear inplane and vertical bifilar pendulums to the final system mass, damping and stiffness matrices are added in SYSCTL. The program then proceeds to calculate the hub impedance and transfer matrices in HUBIMP, and the generalized forces and the forced response in CMPUTE for the linear analysis case.</p> <p>If non-linear inplane bifilars are to be analyzed, the program bypasses HUBIMP and CMPUTE and instead it activates NLBIF to calculate the time-history response of the system.</p>
USAGE:	<p>CALL MAINSV (I927SW, NCASE)</p> <p>I927SW = \neq 0 Include rotor contributions. 0 Do not include rotor contributions.</p> <p>NCASE = 1 Input vector, V(2200), is initialized to zero and the bifilar analysis title (second one) is read in.</p> <p><u>>2</u> Input vector is not set to zero and the second title card is not read.</p>
SUBROUTINES CALLED:	INPUTV, INCOND, SYSCTL, HUBIMP, CMPUTE, NLBIF
ERROR RETURNS:	None
RESTRICTIONS:	None

NAME: MATEI

PURPOSE: To calculate the elastic matrix associated with the inboard half of a rotor blade segment.

METHOD: The 13 X 13 matrix is calculated using the expressions derived in Reference 2 and the forces and moments calculated in ELI.

USAGE: CALL MATEI(I)

I = Blade segment number.

SUBROUTINES CALLED: MIND, GMPRDD

ERROR RETURNS: None

RESTRICTIONS: None



NAME: MATEO

PURPOSE: To calculate the elastic matrix associated with the outboard half of a rotor blade segment.

METHOD: The 13 X 13 matrix is calculated using the expressions derived in Reference 2 and the forces and moments calculated in ELO.

USAGE: CALL MATEO(I)

I = Blade segment number.

SUBROUTINES CALLED: MIND, GMPRDD

ERROR RETURNS: None

RESTRICTIONS: None

NAME:	MATF
PURPOSE:	To calculate the mass transfer matrix which relates the blade forces across a concentrated mass.
METHOD:	The 13 X 13 matrix is calculated using the expressions derived in Reference 2.
USAGE:	CALL MATF(I,W) I = Blade segment number. W = Rotational speed.
SUBROUTINES CALLED:	None
ERROR RETURNS:	None
RESTRICTIONS:	None

NAME:

MATR

PURPOSE:

To calculate the transformation matrix associated with a discontinuity in blade twist.

METHOD:

The 13 X 13 matrix is calculated using the expression derived in Reference 2 and represents the change in twist from segment I to segment I-1.

USAGE:

CALL MATR(I)

I = Blade segment number.

SUBROUTINES
CALLED:

None

ERROR RETURNS:

None

RESTRICTIONS:

None

NAME: MIND

PURPOSE: To invert a matrix and calculate its determinant.

METHOD: The routine is an adaption of the routine MINV from the IBM Scientific Subroutine Package, which uses the standard Gauss-Jordan reduction to obtain the inverse. The value of the determinant is obtained simultaneously as the product of the pivot.
To avoid possible overflow conditions, the value of the determinant is expressed in the form $D \times 10^I$, where D is between 1.0 and 10.0, by repeated calls to OVUN.

USAGE: CALL MIND (A, N, D, L, M, IE)
A = The matrix to be inverted; it is destroyed during the computation.
N = The dimensions of A.
D = Determinant value.
L = Work vector of length N.
M = Work vector of length N.
IE = Power of 10 to be associated with D.

SUBROUTINES CALLED: OVUN

ERROR RETURNS: A determinant of zero indicates a singular matrix.

RESTRICTIONS: None

NAME: MISC

PURPOSE: To perform initial calculations on the input data for the blade frequency and mode shape calculations.

METHOD: The input segment lengths are used to construct an array of radii to the segment centers, and the local twist distribution is used to construct the twist discontinuities.

USAGE: CALL MISC

SUBROUTINES CALLED: None

ERROR RETURNS: The sum of the segment lengths is checked against the blade radius; a difference of more than 10% produces the following warning:
'INCOMPATABILITY BETWEEN RADIUS AND SUM OF SEGMENTS'.
The program continues with the input values.

NAME:	MODES
PURPOSE:	To control the calculations of the rotor blade fully-coupled frequencies and mode shapes.
METHOD:	<p>The blade is assumed to consist of a number of spanwise segments with the inertial loading on each segment concentrated at the center. Each segment is then divided into two parts: one inboard and one outboard of the concentrated mass. The half segments are treated as weightless, with the concentrated mass being located at the junction between them. The elastic properties are assumed to be constant within the inboard and outboard halves of the segment. The built-in blade twist is incorporated in the model by permitting angle changes at the junction between segments.</p> <p>Relationships between blade forces, moments, and elastic deformations at the tip and at the root of the blade can be obtained by considering the changes in these variables over the blade segments. Elastic matrices are used to give the change across the inboard and outboard sections of the segments. Transformation matrices account for the change due to an abrupt change in twist at the segment junctions, and mass transfer matrices give the change from a position just outboard to just inboard of a concentrated mass at the center of a segment. The product of these matrices for all segments will relate the variables at the tip to those at the root.</p> <p>By applying suitable boundary conditions and iterating on frequency, the blade natural frequencies and hence the mode shapes can be derived.</p>
USAGE:	CALL MODES
SUBROUTINES CALLED:	MISC, PINT, FREQUN, MSHAPE, POUT, ORTHOG
ERROR RETURNS:	None
RESTRICTIONS:	None

NAME: MSHAPE

PURPOSE: To calculate the blade mode shapes and their first and second derivatives.

METHOD: This routine first determines whether the mode shape will be predominantly flatwise, edgewise, or torsional by examining the size of the determinant of the matrix relating the tip properties to the root properties at a frequency just less than the natural frequency.
This knowledge is used in setting up a series of simultaneous equations whose solutions yield the required mode shape on substitution into expressions derived in Reference 2.

USAGE: CALL MSHAPE

SUBROUTINES CALLED: PRODM, MIND, OVUN, SIMLIN, MATF, ELO, MATEO, MATR, ELI, MATEI, GMPRDD

ERROR RETURNS: None

RESTRICTIONS: None

NAME: NLBIF

PURPOSE: To control the non-linear bifilar analysis calculations.

METHOD: The non-linear bifilar analysis is performed if the control switch in location 18 is set to 1 and the number of non-linear bifilars in location 1763 is greater than zero.

At first, the routine calculates the total number of degrees-of-freedom and proceeds with the calculations if it is equal or less than 72. Then, it calculates the time history response by calling, in sequence, the routines RHS, BIFILR, BIFEXP, COMBIN, INTEQ for each rotor revolution until either the maximum azimuth angle (input location 1762) is reached or the convergence criterion is met, as specified in CONVER. In either case, the analysis proceeds to analyze the harmonic response of the bifilar pendulums, the rotor hub and the aircraft stations in HARMON. The results are printed out in the routine OUT. The initial values of the bifilar, hub and state variables displacements and velocities are then listed to be used as starting values for the next case.

USAGE: CALL NLBIF

SUBROUTINES CALLED: RHS, BIFILR, BIFEXP, COMBIN, INTEQ, HARMON, CONVER, OUT

ERROR RETURNS: If the number of degrees-of-freedom is greater than 72, then the non-linear bifilar analysis is not activated and the following message is printed out:
 'TIME HISTORY SOLUTION WAS NOT PERFORMED SINCE TOTAL NUMBER OF D.O.F. = , I.E. > 72'.

RESTRICTIONS:

1. Number of non-linear inplane bifilars is limited to 12.
2. Total number of d.o.f. is 72 (60 from linear analysis plus 12 for non-linear analysis).

NAME: ORTHOG

PURPOSE: To test the orthogonality of the blade mode shapes.

METHOD: The orthogonality relation is shown below.

$$\text{ORTH}(i,j) = \frac{\sum_k m_k \phi_{i,k} \phi_{j,k}}{\sqrt{\sum_k m_k (\phi_{i,k}^2 + \phi_{j,k}^2)}}$$

where m_k = Mass of segment k.

$\phi_{i,k}$ = i^{th} mode shape for segment k.

$\phi_{j,k}$ = j^{th} mode shape for segment k.

USAGE: CALL ORTHOG

SUBROUTINES
CALLED: None

ERROR RETURN: None

RESTRICTIONS: None

NAME: OUT

PURPOSE: To print out the harmonic results for the non-linear bifilar analysis.

METHOD: At first, this routine calculates some parameters from the input vector V. Then, it uses the harmonic analysis results from HARMON to calculate the amplitudes and phase angles of the harmonic response of the non-linear bifilar pendulums, the rotor head and the aircraft stations. Appropriate multiplications with the mode shapes input for the fixed system and the aircraft stations are performed.

USAGE: CALL OUT (NTOT, N1)

NTOT = Total number of system d.o.f.
excluding the number of non-linear bifilars.

N1 = Total number of system d.o.f.

SUBROUTINES
CALLED: None

ERROR RETURNS: None

RESTRICTIONS:

1. Maximum number of output harmonics is 10.
2. Maximum number of aircraft stations whose response is harmonically analyzed is 4.

NAME: OUTPUT

PURPOSE: To calculate and print the aircraft and rotor hub forced response.

METHOD: This routine uses the results from FORCER (specifically vector XQ) to calculate the forced response at specific aircraft stations (up to 4) where mode shapes are loaded in locations 1000 through 1399 and at the rotor head using the mode shape in locations 450 through 549.

USAGE: CALL OUTPUT

SUBROUTINES CALLED: None

ERROR RETURNS: None

RESTRICTIONS: The response of the aircraft can be evaluated at a maximum of 4 stations.

NAME: OVUN

PURPOSE: To express A in the form $B \times 10^I$, where
 $1.0 \leq B < 10.0$.

METHOD: If A is greater than 10.0, it is continually divided by 10.0 until it is less than 10.0. If A is less than 1.0, it is continually multiplied by 10.0 until it is greater than 1.0.

USAGE: CALL OVUN (A, B, I)

A = Input number to be transformed.

B = Part of A which is greater than or equal to 1.0 and less than or equal to 10.0.

I = The power of 10 which is associated with B to form A.

SUBROUTINES CALLED: None

ERROR RETURNS: None

RESTRICTIONS: None



NAME: PFMULT

PURPOSE: To generate a point field matrix, relating the steady deflections of the center of a blade segment to those of the previous segment center.

METHOD: The point matrix is defined as W(5X5):

<u>Column</u>	1	2	3	4	5	<u>Row</u>
W =	1	L/A	-L*J/2	-L ² *J/6	C*J*L/2 + L*γ*B	1
	0	2/A-1	-J	-A*J*L*(1/A+0.5)/3	C*A*J*(B+2)+2*γ*B	2
	0	-2B/(A*J)	1/A	L*(1/A+2)/3	-C*(B+6)-2*γ*B/(A*J)	3
	0	0	0	1	-L*D	4
	0	0	0		1	5

Where:

- 1) D = Thrust or drag derivative/unit length between segment centers.
- 2) EI = Flatwise or edgewise segment stiffness.
- 3) L = Segment length.
- 4) M = Segment mass.
- 5) R = Segment radial position.
- 6) r = Blade lag or coning angle.
- 7) Ω = Rotor speed.
- 8) A = $\left[1-L^2*\Omega^2/(2*EI)\right] * \sum_i^N M_i R_i$
- 9) B = 1/A-1
- 10) C = L²*D/12
- 11) J = L/(EI*A)

For inplane deflections, a point mass matrix is added to the fourth row whose elements then become

$$W(4,I) = W(4, I) - M * \Omega^2 * [W(1,I) + R * \gamma * W(5,I)]$$

Conditions at the next center are obtained by pre-multiplying W by the matrix representing conditions at the previous center.

USAGE:

CALL PFMULT (PFIN, PFOUT, LS, AS, EIS, DS, MOMG2S, GAMOS, RS, ISWTCH)

PFIN = 5x5 matrix corresponding to previous center.

PFOUT = 5x5 matrix corresponding to next outboard center.

LS = Distance between centers.

$$AS = \left[1 - L * \Omega^2 / (2 * EI) \right] * \sum_i^N M_i R_i .$$

EIS = Flatwise or edgewise second moment of area between centers.

DS = Thrust or drag derivative/unit length between centers.

MOMG2S = $M * \Omega^2$ (centrifugal force).

GAMOS = γ - calculated lag or coning angle.

RS = Distance of next center from the blade root.

ISWTCH = 0 for inplane deflections.

= 1 for out-of-plane deflections.

**SUBROUTINES
CALLED:**

GMPRDD

ERROR RETURNS:

None

RESTRICTIONS:

None

NAME: PICK

PURPOSE: Given 3 points on the curve $y=f(x)$, choose the best 2 to use for an estimate of the solution of $y=f(x)$.

METHOD: The 3 points are rearranged such that

$$y_1 - x_1 \geq y_2 - x_2 \geq y_3 - x_3$$

If $y_2 - x_2 \leq 0$, then points 1 and 2 in the rearranged order are used.

If $y_2 - x_2 > 0$, then points 2 and 3 in the rearranged order are used.

USAGE: CALL PICK (TT, CT)

TT = Array of argument values.

CT = Array of function values.

SUBROUTINES
CALLED: None

ERROR RETURNS: None

RESTRICTIONS: None

NAME: PINT

PURPOSE: To print the input data used in the blade natural frequency and mode shape calculations.

METHOD: If the print option is set to 4, the input is printed. Otherwise, control is returned to MODES with no printing.

USAGE: CALL PINT

SUBROUTINES CALLED: None

ERROR RETURNS: None

RESTRICTIONS: None

NAME:	POUT
PURPOSE:	To print the output of the blade mode subsegment of the program.
METHOD:	This routine is not used by the rotor stability program, but has been included for completeness.
USAGE:	CALL POUT
SUBROUTINES CALLED:	None
ERROR RETURNS:	None
RESTRICTIONS:	None

NAME: PRELIM

PURPOSE: To prepare the data for use by the rotor aeroelastic analysis.

METHOD: The two main tasks of PRELIM are to standardize the data tables so that all the data tables are defined over the same segment lengths or at the same radial points, and to control the calculation of other quantities needed throughout the remainder of the program.

Transfer of data between the program segments is achieved through 3 COMMON blocks. Blank COMMON is used primarily to store input data. Quantities calculated by PRELIM from the input are stored in labelled COMMON/DYNINP. Printout control is maintained by switches set in labelled COMMON /PRNTSW. All other labelled COMMON blocks are used for the transfer of data within the PRELIM segment.

The following is a more detailed breakdown of the tasks performed.

1. The input data are read into blank COMMON via subroutine LOADIT and immediately stored on a temporary work file (Unit 11). Prior to each subsequent case in the run, this temporary file is read into blank COMMON; thus, only those variables which differ from the previous case need be input.

It should be noted that PRELIM is the third computer dependent routine due to different requirements for reading input data. Coding for both IBM and CDC systems is retained in the program with the appropriate lines commented out.

2. The coupling matrix terms needed for the bifilar analysis portion are initialized to zero to start. For subsequent cases, the coupling matrices are retained and used again if the rotor is not changed or recalculated if a new rotor is employed.

3. Specific input locations are set for the coupling with the bifilar analysis portion.
4. Control switches are set and, where applicable, inputs are converted from generally accepted engineering units to standard units for program calculations.
5. The input blade segments, which form the basis of all radial distributions used by the program, are adjusted to include a 0.1 segment to accommodate pitch horn effects. They are then used to set up a radius vector representing the distance of the mid-points of each segment from the center of rotation. The offset is automatically included if it exists.
6. All input tables are extended or redefined over the distributions obtained in 3 above.
7. Pitch horn effects are added to the blade center of gravity and blade weight tables.
8. The thrust for the input pitch angle is calculated for hover or vertical flight.
9. An input vector used by MODES to calculate mode shapes and frequencies is set up. In multiple cases, if this input has not changed from the previous case, then no call is made to MODES and the program uses the values obtained in the previous case.
10. Pitch-lag and pitch-flap coupling effects are calculated using the blade bending modal components at the pitch horn.
11. Blade lag damper coupling terms are calculated from the input blade damper geometry.
12. The aerodynamic derivatives and steady deflections are calculated in hover.
13. Control system inputs are checked to eliminate contradictions.
14. Blade torsional properties are calculated including cross-beam blade characteristics.

15. Selected portions of the input and calculated data are printed out by subroutine PROUT.

USAGE:

CALL PRELIM (NCASE, NMODE)

NCASE = 0 Input vector, INPUT (8100), is initialized to zero and the rotor analysis title (first one) is read in.

> 1 Input vector is not set to zero, original input vector is read from Unit 11 and the first title card is not read in.

NMODE = Switch for calculating mode shapes and frequencies.

SUBROUTINES
CALLED:

LOADIT, SORTAB, EXTEND, FILL, SECAER, QTFG, PICK,
MODES, REMOVE, STDEFL, FOLL, FULL, E159X, PROUT

ERROR RETURNS:

None

RESTRICTIONS:

None

NAME: PRODM

PURPOSE: To calculate the matrix relating blade forces, moments and elastic deformations at the tip to the blade root and to apply the boundary conditions.

METHOD: Since the elastic matrices and twist transformation matrices are independent of the frequency, they are calculated once for each segment and stored on a work file. For the given frequency, the mass transfer matrices are calculated and combined with the matrices on the work file to produce the tip-to-root relation matrix. Boundary conditions are applied, and the resulting 8 X 8 matrix is returned.

Some data are stored in a temporary work file (Unit 8).

USAGE: CALL PRODM (A, NEQ)

A = The returned 8 X 8 matrix.

NEQ = The dimensions of A.

SUBROUTINES CALLED: ELO, MATEO, MATR, ELI, MATEI, GMPRDD, MATF

ERROR RETURNS: None

RESTRICTIONS: None

NAME: PROUT

PURPOSE: To print selected input and calculated quantities.

METHOD: All significant input and calculated quantities are printed out depending on the setting of the print switch.

USAGE: CALL PROUT (NBLD, NSEG, IE, IF, GJ, T, BETOD, GAMOD)

NBLD = Number of blades.

NSEG = Number of blade segments.

IE = Blade edgewise second moment of area.

IF = Blade flatwise second moment of area.

GJ = Blade torsional stiffness.

T = Blade thrust.

BETOD = Blade steady coning angle.

GAMOD = Blade steady lag angle.

SUBROUTINES CALLED: SKIPLN

ERROR RETURNS: None

RESTRICTIONS: None

NAME:	QTFG
PURPOSE:	To compute the vector of integral values for a given table of argument and function values by the trapezoidal rule.
METHOD:	This routine is a copy of QTFG, and is obtained from IBM System/360 Scientific Subroutine Package.
USAGE:	<pre>CALL QTFG (X, Y, Z, NDIM)</pre> <p>X = The input vector of argument values. Y = The input vector of function values. Z = The resulting vector of integral values. NDIM = The dimensions of X, Y, and Z.</p>
SUBROUTINES CALLED:	None
ERROR RETURNS:	None
RESTRICTIONS:	None

NAME: REMOVE

PURPOSE: To delete a blade flatwise or edgewise mode from an array of mode shapes and frequencies.

METHOD: The characteristics of each mode are examined until the required mode is found. Then, the mode shape and its frequency are deleted and the remaining modes are compressed in the array.

USAGE: CALL REMOVE (SHAPE, MODE, TYPE, N)

SHAPE = An array containing the type of each mode.

MODE = Number of modes to be examined.

TYPE = The type of mode to be removed.

N = The occurrence of type which is removed, i.e., the 2nd flatwise.

SUBROUTINES CALLED: None

ERROR RETURNS: A message is printed if the requested mode could not be deleted.

RESTRICTIONS: None

NAME:	RHS
PURPOSE:	To shift the damping and stiffness contributions to the right-hand-side of the non-linear bifilar equations of motion.
METHOD:	The stiffness and damping matrices obtained at the completion of the calling sequence in SYSCTL are post-multiplied respectively by the initial values of the state variables displacements and velocities. The resulting vector, FRHS, is shifted to the r.h.s. by a change in sign and transferred through labelled COMMON/NLDAT2. It is dimensioned NRHS (see below).
USAGE:	CALL RHS (NRHS)
	NRHS = Total number of degrees-of-freedom not including number of non-linear bifilars (maximum values is 60).
SUBROUTINES CALLED:	None
ERROR RETURNS:	None
RESTRICTIONS:	None

NAME: ROOTX

PURPOSE: To calculate the blade elastic torsional mode shape.

METHOD: The blade torsional mass moment of inertia and stiffness distributions are used to calculate the torsional mode shape using a given frequency trial and the input value of rotor speed.
The frequency and mode shape trials are printed out if location 119 is 6.

USAGE: CALL ROOTX (W2, XHI, O2, YTI, YTK)

W2 = Square of frequency trial, $(\text{rad/sec})^2$

XHI = Calculated blade torsional mode shape, non-dimensional

O2 = Square of rotor speed, $(\text{rad/sec})^2$

YTI = Blade torsional mass moment of inertia, in-lb-sec^2

YTK = Blade torsional stiffness, $\text{lb-in}^2/\text{in}$

SUBROUTINES CALLED: None

ERROR RETURNS: None

RESTRICTIONS: None

NAME:	SECAER
PURPOSE:	To calculate blade section coefficients and derivatives.
METHOD:	<p>Lift, drag, and pitching moment coefficients are input against angle of attack for various Mach numbers. For a given angle of attack and Mach number, the required coefficients and their derivatives with respect to Mach number and angle of attack are obtained from the corresponding table by linear interpolation.</p> <p>The routine assumes airfoil data to be non-symmetric if the first input angle of attack value is negative.</p> <p>For angles of attack greater than 30°, a Mach number of 0.0001 is assumed.</p>
USAGE:	<pre>CALL SECAER (ALPHA, AMACH, I, M, FF, DFF, DM)</pre> <p>ALPHA = Angle of attack (radians).</p> <p>AMACH = Mach number.</p> <p>I = Not used by this program.</p> <p>RFM = 1 for lift coefficient. = 2 for drag coefficient. = 3 for pitching moment coefficient.</p> <p>FF = Returned coefficient.</p> <p>DFF = Derivative with respect to angle of attack.</p> <p>DM = Derivative with respect to Mach number.</p>
SUBROUTINES CALLED:	BLIN4
ERROR RETURNS:	Any error termination from BLIN4 stops execution with the message 'TROUBLE IN BLIN4', followed by 6 numbers which represent angle of attack in radians, angle of attack in degrees, input Mach number, Mach number used, the error switch L from BLIN4 and the switch M respectively. See BLIN4 for description of errors.
RESTRICTIONS:	See locations 1850-4548 of rotor stability input description and BLIN4.

NAME:	SHAKIT
PURPOSE:	To control the principal logic flow of the rotor/bifilar coupled program.
METHOD:	<p>MAIN first calls subroutine PRELIM, which controls the input, conversion and adjustment of the blade data. Then, the rotor blade dynamic and aerodynamic matrices are obtained from calls to DYNMAT and AERMAT respectively. The dynamic and aerodynamic matrices are cleaned out, added together, compressed and stored for coupling with the bifilar analysis portion in EIGER. The bifilar analysis is subsequently executed by calling MAINSV.</p> <p>After PRELIM is called, the rotor analysis calculations are bypassed if input location 110 is zero or -1.</p> <p>It should be added that SHAKIT is the fourth computer dependent routine. For CDC use, the first line of code is</p> <p>"PROGRAM SHAKIT (INPUT, OUTPUT, TAPE1, TAPE2, TAPE3)".</p> <p>For IBM use, this card is not needed; thus, the first line contains blank COMMON input data.</p>
USAGE:	Program SHAKIT is never referenced in a CALL statement.
SUBPROGRAMS CALLED:	PRELIM, DYNMAT, AERMAT, EIGER, MAINSV
ERROR RETURNS:	None
RESTRICTIONS:	None



NAME:	SIMLIN
PURPOSE:	To solve a system of linear simultaneous equations.
METHOD:	The solution is obtained by elimination using largest pivotal division. The determinant of the coefficient matrix is produced during the process.
USAGE:	CALL SIMLIN (A, B, X, N, NX, C)
	A = Coefficient matrix (destroyed during computations) of dimensions XN by XN.
	B = Vector of right-hand value, destroyed during the computations. On return, B(1) contains the determinant of the coefficient matrix.
	X = Solution vector.
	N = The number of rows in A.
	NX = Dimensions of matrix A.
	C = Work vector.
SUBROUTINES CALLED:	None
ERROR RETURNS:	None
RESTRICTIONS:	None

NAME: SKIPLN

PURPOSE: To skip a given number of lines during printing.

METHOD: In an effort to prevent the printout of output tables going over a page boundary, SKIPLN is used to center tables within a page or part of a page.

USAGE: CALL SKIPLN(J)

J = Number of lines to be skipped.

SUBROUTINES CALLED: None

ERROR RETURNS: None

RESTRICTIONS: None



NAME: SORTAB

PURPOSE: To unscramble an array of alternating X and Y points into an array of X points and an array of Y points.

METHOD: Even subscripted values in the input array are moved to another array. Both arrays are then compressed.

USAGE: CALL SORTAB (G, M, KSTAR, NSTAR)

G = On input, G contains the alternating X and Y values.
On output, G contains only X values.

M = The number of points in G on input.

KSTAR = The unscrambled Y points.

NSTAR = The number of points in G and KSTAR on output.

SUBROUTINES CALLED: None

ERROR RETURNS: None

RESTRICTIONS: None

NAME: STDEFL

PURPOSE: To calculate the inplane and out-of-plane blade steady deflections and slopes.

METHOD: Blade deflections are calculated by successively calculating the deflection of each segment relative to the previous one. This is done by constructing a point matrix from the mass, stiffness, and geometric properties of the segment to relate the displacement of the center of a segment relative to the previous center. The process is started by assuming suitable conditions at the root of the blade. A correction is made to these deflections if the pitch bearing does not follow the blade root slope.

USAGE: CALL STDEFL (QEO, XEO, E, RB, MB, NB, RR, D, IE, IF, TH, OMEGA, EB, GAMOT, KGAMA, GAMO, KASE, IEF, ROTDEF)

- QEO = Returned inplane or out-of-plane steady deflections.
- XEO = Returned slope for inplane or out-of-plane deflections.
- E = Blade offset.
- RB = Array of distances of the blade segment centers from the center of rotation.
- MB = Mass of each segment.
- NB = Number of radii in RB.
- RR = Blade segment lengths.
- D = Drag derivative for inplane deflections or thrust derivative for out-of-plane deflections.
- IE = Blade edgewise second moment of area.
- IF = Blade flatwise second moment of area.
- TH = Blade twist.
- OMEGA = Rotational speed.



EB = Blade Young's modulus.

GAMOT = Calculated lag angle for inplane deflections or calculated coning angle for out-of-plane deflections.

KGAMA = Blade lag hinge spring constant for inplane deflections or blade flapping hinge spring constant for out-of-plane deflections.

GAMO = Blade prelag angle for inplane deflections or blade precone angle for out-of-plane deflections.

KASE = Blade pitch input control (derived from input location 115).

IEF = 0 for inplane deflections.
= 1 for out-of-plane deflections.

ROTDEF = Rotor definition (input location 114).

SUBROUTINES
CALLED: PFMULT

ERROR RETURNS: None

RESTRICTIONS: None

NAME:	SYSCTL
PURPOSE:	To include the contributions of the fixed system modes, rotor (if used), the fixed system absorbers and the linear inplane and vertical bifilars to the final system mass, damping and stiffness matrices in the bifilar analysis.
METHOD:	At first, SYSCTL calls FIXSYS to obtain the fixed system modes matrices. Then, if rotor contributions are desired, it restructures the rotor matrices and adds the rotor elements to the fixed system matrices using ADDOFR. Subsequently, it includes contributions due to fixed system absorbers from FIXABS, linear inplane bifilars from LINBIF and finally linear vertical bifilars from LVBIF. In all cases, the matrices are increased systematically by repeated calls to ADDOFR. Printout of the matrices is governed by the switches in locations 17 and 1490 through 1496.
USAGE:	CALL SYSCTL
SUBROUTINES CALLED:	FIXSYS, ADDOFR, FIXABS, LINBIF, LVBIF
ERROR RETURNS:	None
RESTRICTIONS:	None

REFERENCES

1. R. A. Johnston, "Helicopter Rotor Stability Analysis", USAAMRDL-TR-75-40, January 1976.
2. R. Piziali, "An Investigation of the Structural Dynamics of Helicopter Rotors", USAAVLABSTR-70-24, April 1970. AD872715.

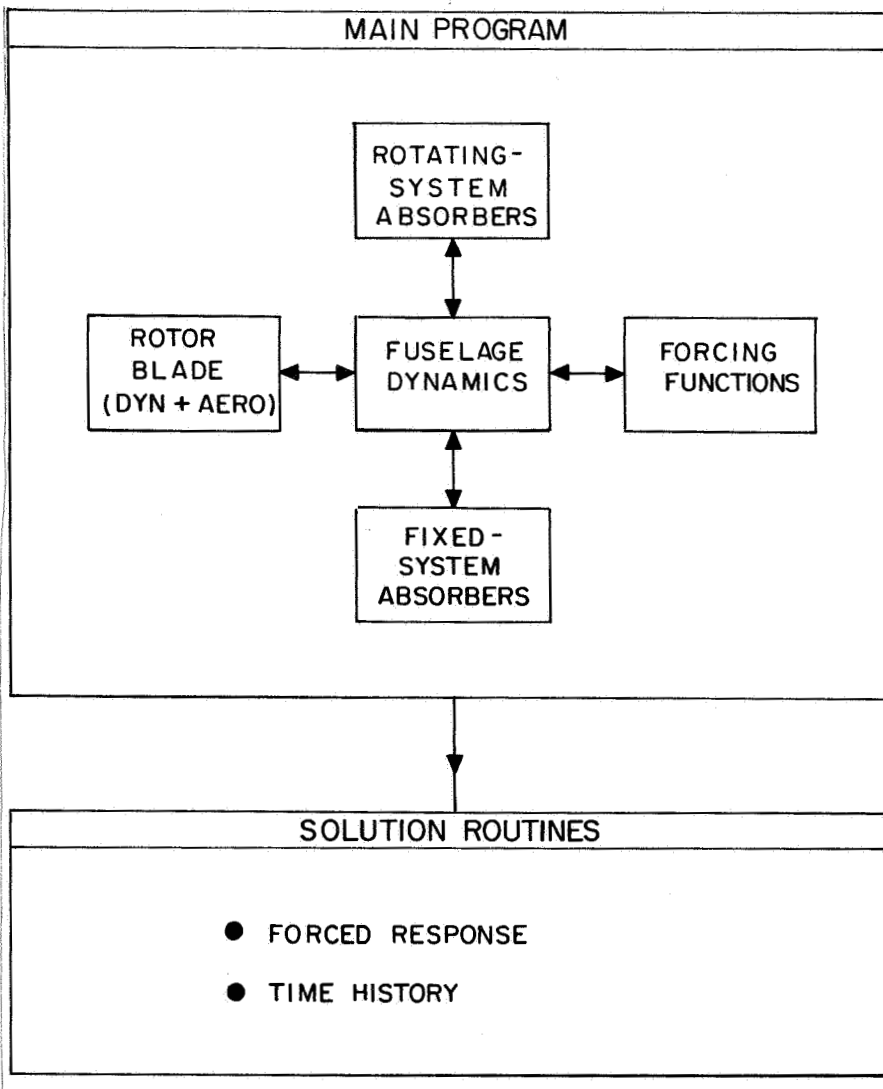


Figure 1. Block Diagram of Bifilar Analysis.

```

***** INPUT DATA *****

***** 5.1. -237800-02 -1116.0 -590000 4.0000 0.0000 258.00 *****
***** 5.13 .0 1.2500 1.0000 15.127 7.2500 .35000 *****
***** 5.107 2.19 258.00 1.0000 0.0000 1.0000 *****
***** 5.111 1.0000 0.0000 0.0000 0.0000 0.0000 *****
***** 5.113 .110000+06 1.0000 11.0000 11.0000 *****
***** 5.119 5.0000 1.0000 0.0000 0.0000 0.0000 *****
***** 5.125 1.0000 0.0000 0.0000 0.0000 0.0000 *****
***** 5.131 -1.0000 0.0000 0.0000 0.0000 0.0000 *****
***** 5.166 27.074 11.236 9.1780 6.8200 .35500 *****
***** 5.201 17.500 17.500 15.000 16.800 16.800 *****
***** 5.206 16.800 16.800 16.800 17.490 17.490 *****
***** 5.211 17.490 17.490 15.900 15.900 15.900 *****
***** 5.216 12.970 12.970 7.7000 7.7000 7.7000 *****
***** 5.251 20.000 0.0000 0.0000 0.0000 0.0000 *****
***** 4.251 15.010 8.1000 15.000 0.0000 4.0000 *****
***** 4.255 50.010 20.760 228.76 20.160 20.160 *****
***** 4.259 228.97 228.97 228.97 22.317 22.317 *****
***** 4.263 276.67 276.67 276.67 20.760 20.760 *****
***** 4.267 276.67 276.67 276.67 20.760 20.760 *****
***** 1.350 14.000 9.5000 50.000 0.0000 0.0000 *****
***** 4.351 .0 1.2000 290.00 2.8000 2.8000 *****
***** 4.355 270.00 1.2000 290.00 1.2000 1.2000 *****
***** 4.359 305.00 3.8000 316.00 316.00 316.00 *****
***** 2.363 322.00 1.2000 0.0000 0.0000 0.0000 *****
***** 1.450 14.000 0.0000 0.0000 0.0000 0.0000 *****
***** 4.451 0.0 -2.5000 50.000 0.0000 0.0000 *****
***** 4.455 270.00 1.2000 290.00 2.8000 2.8000 *****
***** 4.459 305.00 3.8000 316.00 316.00 316.00 *****
***** 2.463 322.00 1.2000 0.0000 0.0000 0.0000 *****
***** 1.550 58.000 0.0000 0.0000 0.0000 0.0000 *****
***** 4.551 0.0 0.0000 58.000 0.0000 0.0000 *****
***** 4.555 75.000 -.82200 159.00 -.82200 0.0000 *****
***** 4.559 159.01 -.66700 192.00 -.66700 0.0000 *****
***** 4.563 192.01 -.46800 210.00 -.46800 0.0000 *****
***** 4.567 210.01 -.67500 220.00 -.67500 0.0000 *****
***** 4.571 220.01 -.69900 224.00 -.69900 0.0000 *****
***** 4.575 228.96 -.55600 228.97 -.55600 0.0000 *****
***** 4.579 240.00 -.29900 270.30 -.29900 0.0000 *****
***** 4.583 270.31 -.80000-02 276.66 -.80000-02 0.0000 *****
***** 4.587 276.67 -.36800 289.00 -.36800 0.0000 *****
***** 4.591 290.00 1.2335 291.00 1.2335 2.0990 *****
***** 4.595 299.00 2.0920 299.50 2.0920 2.1247 *****
***** 4.599 301.25 1.7592 303.75 1.7592 0.6920 *****
***** 4.603 306.69 -.33590 318.00 -.33590 0.0000 *****
***** 2.607 322.00 -.45600 318.00 -.45600 0.0000 *****
***** 1.650 18.000 0.0000 0.0000 0.0000 0.0000 *****
***** 4.651 0.0 0.0000 50.000 0.0000 0.0000 *****
***** 4.655 50.010 -.35000 28.96 -.35000 0.0000 *****
***** 4.659 288.97 .0 276.66 .0 276.66 *****
***** 4.663 276.67 -.35000 302.60 -.35000 0.0000 *****
***** 2.667 322.00 -.74110 318.00 -.74110 0.0000 *****
***** 1.750 20.000 0.0000 0.0000 0.0000 0.0000 *****

```

FIGURE 2. Output Format - Rotor Blade Input Data.

TITLE 1 - TEST MAIN ROTOR DATA - COUPLED WITH BIFLAR ANALYSIS 000663					
HOVER					
MAIN ROTOR					
PITCH ANGLE AT 75% RADIUS	= 6.400 DEG	ANGLE OF ATTACK	= 6.400 DEG		
CALCULATED THRUST	= 16364.911 LB				
CALCULATED CONING ANGLE	= 3.369 DEG				
CALCULATED LAG ANGLE	= 5.180 DEG				
CALCULATED BLADE TORSIONAL FREQUENCY	= 0.0 RAD/SEC				
CALCULATED BLADE BENDING FREQUENCIES : MODE 1 = 77.5 RAD/SEC					
MODE 2 = 126.7 RAD/SEC					
STEADY DEFLECTIONS (IN)					
RADIUS (IN) FLATWISE EDGEWISE					
6.0	0.0	0.0	0.0	-74.100	
15.000	0.0	0.0	0.0	-33.210	
23.750	-0.004	0.011	0.011	-20.206	
41.250	-0.009	0.106	0.106	-6.880	
62.500	0.041	0.285	0.285	-0.199	
83.400	0.156	0.505	0.505	2.542	
100.200	0.256	0.699	0.699	3.650	
117.000	0.356	0.904	0.904	6.212	
133.800	0.455	1.119	1.119	6.447	
150.600	0.546	1.343	1.343	6.446	
167.745	0.626	1.582	1.582	4.277	
185.235	0.688	1.835	1.835	3.980	
202.725	0.723	2.098	2.098	3.588	
220.215	0.728	2.371	2.371	3.124	
236.910	0.696	2.661	2.661	2.627	
252.810	0.631	2.907	2.907	2.116	
268.710	0.542	3.181	3.181	1.574	
284.165	0.456	3.437	3.437	0.647	
290.115	0.397	3.670	3.670	-0.156	
306.450	0.368	3.957	3.957	-0.315	
312.150	0.353	3.997	3.997	1.274	
320.000	0.344	4.103	4.103	2.101	
ROTATIONAL MODE NO.					
1	PHIXPH	PHIZPH	PHELD	PHFLD	PHFLD
2	1.0000	-0.0009	0.0	0.0	0.0
	-1.0000	0.0010	0.0	0.0	0.0
ROTATIONAL MODE NO.					
1	QEOFLD	QEFOLD	QFOLD	PHFLD	THFLD
2	0.0	0.0	0.0	(a)	PHOS

FIGURE 3. Output Format - Rotor Blade Characteristics.

CASE DEFINITION							
AIR DENSITY LB.SEC.^-SQ.IN.^4TH	SPEED OF SOUND FT./SEC.	TIP LOSS FACTOR	AXIAL VEL. KNOTS	ROTOR SPEED R.P.M.	BLADE RADIUS FEET	PRELAG ANGLE RADIAN	PRELAG SPRING LB.IN./RAD.
1116.00000	0.99000	0.0	258.00000	26.03333	0.0	0.0	0.0
1.25000	4	0.0	0.0	258.00000	0.0	0.0	0.0
BLADE YOUNG'S MOD. LB./IN.^-SQ	RADIUS OF PUSH ROD INCHES	LAG DAMPING FRACT CRITICAL	RIGID PITCH DAMP. FRACT CRITICAL	REF. ROTOR SPEED R.P.M.	BLADE BENDING MODES		
0.10000D+07	15.12450	0.35000	0.0	0.50000D+05	0.0	0.0	258.00000
FIXED SYSTEM MODES PITCH-LAG COUPLING WEIGHT AT PUSHROD, PITCH BEAM STIFFNESS ACTUATOR HOM. STIFFNESS PITCH BEAM RADIUS INCHES LB-IN./RAD.							
5	0.0	0.0	0.0	0.50000D+05	0.0	0.0	0.0
PITCH HORN LENGTH INCHES	FORWARD FLIGHT SPEED KNOTS	ELASTIC PITCH DAMP. FRACT. CRITICAL	LAG DAMPER COEFFICIENT LB-SEC./IN.	LAG DAMPER STIFFNESS LB/IN.	FLEXBEAM ROOT (XBR) INCHES		
7.25000	0.0	0.0	676.00000	0.0	0.0		
CONTROL SWITCHES							
ROTEST	FTEST	SYSDEF	ROTOFF	ARTIC	PHASE		
1.	1.	1.000111...	1.	11.	0.		
VECT	TRMASC	SUMASC	TSERV	MRMASC	MSERV		
0.	1.	111.	1.	1.	111.		
CIR	CIRN	LAGR1	LAGR2				
1.	1.	1.	1.				
MODE NO.	ZETBD	ZETG	MG	CMF	PHY	PHZ	PHY
1	0.0	0.0	0.0	0.0	0.0	0.0	0.0
2	0.0	0.0	0.0	0.0	1.0000	0.0	0.0
3	0.0	0.0	0.0	0.0	0.0	1.0000	0.0
4	0.0	0.0	0.0	0.0	0.0	0.0	1.0000
5	0.0	0.0	0.0	0.0	0.0	0.0	0.0

(b)

FIGURE 3. Continued.

R	CHORD	STRUCTURAL			AEROdynamic	AC	C6	TORSIONAL	EA	MODE SHAPE
		TWIST	TWIST	EA	AC	EA	SHAPE	SHAPE	EA	SHAPE
0.0	0.0	-9.50000	-9.50000	0.0	0.0	0.0	0.0	0.0	0.0	0.0
15.00000	0.0	-9.50000	-9.50000	0.0	0.0	0.0	0.0	0.0	0.0	0.0
23.75000	8.30000	-9.50000	-9.50000	0.0	0.0	0.0	0.0	0.0	0.0	0.0
41.25000	8.30000	-9.50000	-9.50000	0.0	0.0	0.0	0.0	0.0	0.0	0.0
62.50000	20.76000	-8.89205	-8.89205	-0.35000	-0.21759	0.0	0.0	0.0	0.0	-5.19000
83.40000	20.76000	-7.87555	-7.87555	-0.35000	-0.19000	0.0	0.0	0.0	0.0	-5.19000
100.20000	20.76000	-7.05645	-7.05645	-0.35000	-0.19000	0.0	0.0	0.0	0.0	-5.19000
117.00000	20.76000	-6.24136	-6.24136	-0.35000	-0.19000	0.0	0.0	0.0	0.0	-5.19000
133.80000	20.76000	-5.44247	-5.44247	-0.35000	-0.19000	0.0	0.0	0.0	0.0	-5.19000
150.60000	20.76000	-4.60118	-4.60118	-0.35000	-0.19000	0.0	0.0	0.0	0.0	-5.19000
167.75000	20.76000	-3.77331	-3.77331	-0.35000	-0.19000	0.0	0.0	0.0	0.0	-5.19000
185.23500	20.76000	-2.92266	-2.92266	-0.35000	-0.19000	0.0	0.0	0.0	0.0	-5.19000
202.72500	20.76000	-2.07201	-2.07201	-0.35000	-0.19000	0.0	0.0	0.0	0.0	-5.19000
220.21500	20.76000	-1.22336	-1.22336	-0.35000	-0.19000	0.0	0.0	0.0	0.0	-5.19000
236.91000	22.31700	-0.40938	-0.40938	0.0	0.0	0.0	0.0	0.0	0.0	-5.58000
252.81000	22.31700	0.36394	0.36394	0.0	0.0	0.0	0.0	0.0	0.0	-5.58000
268.71000	22.31700	1.13726	1.13726	0.0	0.0	0.0	0.0	0.0	0.0	-5.58000
283.14500	20.76000	2.25160	2.25160	0.0	0.0	0.0	0.0	0.0	0.0	-5.19000
296.11500	20.76000	3.20767	3.20767	0.0	0.0	0.0	0.0	0.0	0.0	-5.19000
306.45000	20.76000	3.51000	3.51000	0.0	0.0	0.0	0.0	0.0	0.0	-5.19000
314.15000	20.76000	1.97000	1.97000	0.0	0.0	0.0	0.0	0.0	0.0	-5.19000
320.00000	20.76000	1.20000	1.20000	0.0	0.0	0.0	0.0	0.0	0.0	-5.19000
R	QEO	QFO	QEP	QEOP	QEOP	QFOP	QFOP	QFOP	QFOP	QFOP
0.0	0.0	0.0	0.0	0.0	0.0	0.0	0.0	0.0	0.0	0.0
15.00000	0.0	0.0	0.0	0.0	0.0	0.0	0.0	0.0	0.0	0.0
23.75000	0.01108	-0.00402	0.0	0.0115	0.0	0.01151	0.0	0.0	0.0	0.0
41.25000	0.01392	-0.00914	0.00659	0.00659	0.0	-0.00127	0.0	0.0	0.0	0.0
62.50000	0.28471	0.01123	0.00918	0.00918	0.0	0.00136	0.0	0.0	0.0	0.0
83.40000	0.50523	0.15567	0.01101	0.01101	0.0	0.00444	0.0	0.0	0.0	0.0
100.20000	0.69359	0.55515	0.01110	0.01110	0.0	0.00453	0.0	0.0	0.0	0.0
117.00000	0.90412	0.35611	0.01231	0.01231	0.0	0.00450	0.0	0.0	0.0	0.0
133.80000	1.11881	0.45498	0.01290	0.01290	0.0	0.00450	0.0	0.0	0.0	0.0
150.60000	1.34309	0.54645	0.01347	0.01347	0.0	0.00351	0.0	0.0	0.0	0.0
167.74500	1.56162	0.62265	0.01404	0.01404	0.0	0.00256	0.0	0.0	0.0	0.0
185.23500	1.83470	0.88764	0.01460	0.01460	0.0	0.00133	0.0	0.0	0.0	0.0
202.72500	2.09751	0.72338	0.01516	0.01516	0.0	0.00032	0.0	0.0	0.0	0.0
220.21500	2.37055	0.72764	0.01577	0.01577	0.0	0.00018	0.0	0.0	0.0	0.0
236.91000	2.64091	0.69591	0.01635	0.01635	0.0	0.00016	0.0	0.0	0.0	0.0
252.81000	2.90789	0.63050	0.01689	0.01689	0.0	0.00010	0.0	0.0	0.0	0.0
268.71000	3.18148	0.54180	0.01741	0.01741	0.0	0.000672	0.0	0.0	0.0	0.0
283.14500	3.43658	0.45651	0.01779	0.01779	0.0	0.00611	0.0	0.0	0.0	0.0
296.11500	3.66970	0.39675	0.01806	0.01806	0.0	0.00370	0.0	0.0	0.0	0.0
306.45000	3.85659	0.36786	0.01815	0.01815	0.0	0.00217	0.0	0.0	0.0	0.0
314.15000	3.99675	0.35395	0.01816	0.01816	0.0	0.00171	0.0	0.0	0.0	0.0
320.00000	4.10300	0.34363	0.01816	0.01816	0.0	0.00167	0.0	0.0	0.0	0.0

(c)

FIGURE 3. Continued.

R	D(DT1)/D(U) D(DH1)/D(U) D(DM1)/D(U)	D(DT1)/D(U) D(DH1)/D(U) D(DM1)/D(U)	D(DT1)/D(U) D(DH1)/D(U) D(DM1)/D(U)	D(DT1)/D(U) D(DH1)/D(U) D(DM1)/D(U)	D(DT1)/D(U) D(DH1)/D(U) D(DM1)/D(U)	D(DT1)/D(U) D(DH1)/D(U) D(DM1)/D(U)
0.0	0.0 0.0 0.0	0.0 0.0 0.0	0.0 0.0 0.0	0.0 0.0 0.0	0.0 0.0 0.0	0.0 0.0 0.0
15.00000	-0.00040	-0.00073	-0.0001	-0.00001	-0.00021	-0.16268
23.75000	-0.00040	-0.00073	-0.0001	-0.00001	-0.00021	-0.1837
41.25000	0.00140	-0.00216	6.5270	0.00034	-0.00030	1.1837
62.50000	0.0014	-0.01307	23.85057	0.00109	-0.00327	6.46567
83.75000	-0.0010	-0.01753	41.71377	0.01037	-0.00644	8.75891
100.20000	0.00745	-0.02118	59.83550	0.00103	-0.00180	10.4751
117.00000	0.00859	-0.02683	81.23057	0.00100	-0.00133	14.24987
133.80000	0.00954	-0.02651	105.97088	0.00096	-0.00090	14.26927
150.60000	0.01102	-0.03221	134.44925	0.00100	-0.00056	16.16053
167.74500	-0.01195	-0.03662	169.58804	0.00098	-0.00051	18.4051
185.23500	0.01269	-0.04126	210.32202	0.00095	-0.00015	20.76338
202.72500	0.01218	-0.04602	255.52919	0.00083	-0.00014	23.23199
220.21500	0.01210	-0.05052	304.00663	0.00078	-0.00027	25.63136
236.91000	0.01266	-0.05901	381.23640	0.00078	-0.00053	29.98935
252.81000	0.01374	-0.06689	447.37186	0.00099	-0.00125	35.26863
268.71000	0.01276	-0.07412	541.85065	0.00064	-0.00173	38.29369
285.14500	0.00678	-0.07731	593.92714	0.00055	-0.00250	36.35645
296.11500	-0.00529	-0.08701	697.52274	0.00039	-0.00370	38.61169
306.45000	0.01024	-0.09279	771.89581	0.00079	-0.00067	41.73612
314.15000	0.01896	-0.09562	817.74876	0.00168	-0.00694	74.68638
320.00000	0.02305	-0.08673	756.49209	0.00288	-0.00730	110.98781
<hr/>						
R	D(DM1)/D(U) D(DH1)/D(U) D(DM1)/D(U)	D(DM1)/D(U) D(DH1)/D(U) D(DM1)/D(U)	D(DM1)/D(U) D(DH1)/D(U) D(DM1)/D(U)	D(DM1)/D(U) D(DH1)/D(U) D(DM1)/D(U)	D(DM1)/D(U) D(DH1)/D(U) D(DM1)/D(U)	D(DM1)/D(U) D(DH1)/D(U) D(DM1)/D(U)
0.0	0.0 0.0 0.0	0.0 0.0 0.0	0.0 0.0 0.0	0.0 0.0 0.0	0.0 0.0 0.0	0.0 0.0 0.0
15.00000	-0.00044	-0.00073	-0.00054	-0.00072	-0.00591	0.31287
23.75000	-0.00048	-0.00082	-0.00053	-0.02561	-0.11705	0.28950
41.25000	-0.00011	0.00040	-0.62797	0.43551	0.15563	0.19019
62.50000	0.00014	0.00051	-1.08320	2.76689	0.63633	0.27625
83.75000	0.00017	0.00060	-1.54369	5.12692	0.97858	0.36383
100.20000	0.00011	-0.00514	16.77181	7.77250	1.27528	0.54370
117.00000	0.00120	-0.00588	21.82340	1.53142	0.79426	1.17383
133.80000	0.00351	-0.00625	27.06373	13.41433	1.74900	2.61195
150.60000	0.00655	-0.00613	29.93084	16.53055	1.95691	4.59828
167.74500	0.00674	-0.00640	29.70216	19.55134	2.12254	5.50461
185.23500	-0.00210	-0.0021	30.45112	22.08643	2.22559	6.18703
202.72500	-0.0021	-0.00339	19.66104	23.68544	2.24479	5.39755
220.21500	-0.00107	-0.00339	30.45112	26.27911	2.30051	5.25127
236.91000	-0.00210	-0.00102	5.55683	22.08643	2.22559	6.18703
252.81000	0.00324	-0.00114	2.46606	26.27911	2.30051	5.25127
268.71000	0.00322	-0.00193	37.29655	25.32963	2.20955	6.39222
285.14500	0.00189	-0.00551	65.92044	16.159756	1.59790	5.49964
306.45000	0.00052	-0.01268	101.65111	8.78590	1.13260	6.52287
314.15000	-0.00627	-0.0125	148.14500	7.69074	1.13389	2.42666
320.00000	-0.0125	-0.08714	-765.20654	46.48986	4.15306	2.40927

(d)

—Continued.

STRUCTURAL AERODYNAMIC										MACH NUMBER		
R	CL	CD	CM	D(CL)/DA	D(CD)/DA	D(CM)/DA	D(CL)/DM	D(CD)/DM	D(CM)/DM	ALPHA		
0.0	-0.42608	1.86000	0.47020	-0.74305	0.0	-0.30558	0.0	0.0	0.0	0.0	0.0	
15.00000	-0.74466	0.17050	0.74305	-2.04628	-0.47795	-0.0	0.0	0.0	0.0	0.0	0.0	
23.75000	-0.90206	0.44392	0.12548	0.57296	-0.08962	-0.10657	0.0	0.0	0.0	0.0	0.0	
41.25000	-0.62922	0.08167	0.00516	9.31056	-0.02625	-5.36861	0.0	0.0	0.0	0.0	0.0	
62.50000	0.12646	0.00913	0.00251	6.76090	-0.03820	-0.00828	0.0	0.0	0.0	0.0	0.0	
83.40000	0.44991	0.0964	0.00211	6.76090	0.01432	-0.00828	0.0	0.0	0.0	0.0	0.0	
100.00000	0.58070	0.00991	0.00195	6.76090	0.01432	-0.00828	0.0	0.0	0.0	0.0	0.0	
117.00000	0.64789	0.01013	0.00215	6.76090	0.01432	-0.00828	0.0	0.0	0.0	0.0	0.0	
133.80000	0.67479	0.01027	0.00242	6.76090	0.01438	-0.00828	0.0	0.0	0.0	0.0	0.0	
150.60000	0.67739	0.01025	0.00242	6.76090	0.01438	-0.00828	0.0	0.0	0.0	0.0	0.0	
167.74500	0.67371	0.01004	0.00511	6.90300	0.03591	-0.05834	0.48216	-0.00304	0.01112	0.0	0.0	
185.23500	0.65583	0.00974	0.00736	7.05707	0.03627	-0.047210	-0.00315	0.07172	0.0	0.0	0.0	
202.72500	0.61204	0.00917	0.00829	7.15287	0.03870	0.045377	-0.00342	0.07250	0.0	0.0	0.0	
220.21500	0.56106	0.00897	0.00625	7.15546	0.04038	0.04078	-0.00675	-0.00201	-0.05261	0.0	0.0	
236.91000	0.49999	0.00854	0.00459	7.25523	0.04000	0.02234	-0.00522	-0.00240	-0.04836	0.0	0.0	
252.81000	0.43973	0.00838	0.00392	7.46130	0.07675	0.00186	0.35840	-0.00343	-0.03682	0.0	0.0	
268.71000	0.37532	0.00850	0.00423	8.02034	0.04954	0.02468	0.1998	0.01149	0.01686	0.0	0.0	
283.14500	0.24356	0.00379	0.00808	8.50984	0.0	0.02468	0.1998	0.01149	0.01686	0.0	0.0	
296.11500	0.11559	0.00808	0.00285	9.13770	-0.02865	0.04540	-0.07334	0.0	-0.00143	0.0	0.0	
306.45000	0.09663	0.00852	0.00143	9.44286	-0.02314	0.06405	-0.31458	0.0	-0.01143	0.0	0.0	
314.15000	0.37295	0.01086	0.00060	9.50400	0.03454	0.08717	0.51367	0.01827	-0.06202	0.0	0.0	
320.00000	0.52222	0.01837	0.00130	8.52200	0.78367	0.02461	0.96091	0.06649	-0.11108	0.0	0.0	
							1.14977	1.14977	0.16673	0.16405	0.0	0.0
0.0	15.90000	15.90000	468.02342	0.0	468.02342	90.00000	-74.10000	-0.03495	0.0	0.0	0.0	
15.00000	15.90000	15.90000	468.02342	468.02342	468.02342	619.10159	49.11037	-33.21037	0.04623	0.0	0.0	
23.75000	15.90000	15.90000	468.02342	641.67180	641.67180	794.22202	36.10631	-26.10631	0.05931	0.0	0.0	
41.25000	15.90000	15.90000	468.02342	1104.48260	1104.48260	1209.76689	22.77982	-6.87982	0.09026	0.0	0.0	
62.50000	15.29205	15.29205	468.02342	1689.61000	1752.25986	1752.25986	15.49151	-0.1996	0.13084	0.0	0.0	
83.40000	14.27555	14.27555	468.02342	2201.21116	2301.23194	2301.23194	11.73392	2.54433	0.17105	0.0	0.0	
100.00000	13.45845	13.45845	468.02342	2701.17955	2741.33817	2741.33817	9.80947	3.64998	0.20515	0.0	0.0	
117.00000	11.82427	11.82427	468.02342	3151.53744	3195.53744	3195.53744	8.42192	4.21944	0.23862	0.0	0.0	
133.80000	11.07178	11.07178	468.02342	4058.87466	4099.70347	4099.70347	7.37693	4.44734	0.27219	0.0	0.0	
150.60000	10.17331	10.17331	468.02342	4532.09415	4532.09415	4532.09415	5.65613	4.44556	0.30583	0.0	0.0	
167.74500	9.32266	9.32266	468.02342	5006.65277	5026.47144	5026.47144	5.89596	4.27735	0.34022	0.0	0.0	
185.23500	8.47201	8.47201	468.02342	5477.17540	5497.13528	5497.13528	5.32665	3.98001	0.37533	0.0	0.0	
202.72500	7.662136	7.662136	468.02342	5949.71602	5968.09573	5968.09573	4.49780	3.58796	0.41048	0.0	0.0	
220.21500	6.80938	6.80938	468.02342	6400.77752	6417.86560	6417.86560	4.18501	3.12356	0.44565	0.0	0.0	
236.91000	6.03616	6.03616	468.02342	6830.35991	646.37586	646.37586	3.91984	2.11622	0.51123	0.0	0.0	
252.81000	5.26774	5.26774	468.02342	7259.94229	7275.01258	7275.01258	3.68856	1.57418	0.64324	0.0	0.0	
268.71000	4.14860	4.14860	468.02342	7649.94366	7664.27712	7664.27712	3.50099	0.64741	0.57230	0.0	0.0	
286.11500	3.19233	3.19233	468.02342	8000.36400	8014.04206	8014.04206	3.34800	-0.15567	0.59842	0.0	0.0	
306.45000	2.89000	2.89000	468.02342	8279.57255	8292.81006	8292.81006	3.25534	-0.34534	0.61924	0.0	0.0	
314.15000	4.43000	4.43000	468.02342	8487.65930	8500.52334	8500.52334	3.15620	-1.27380	0.63475	0.0	0.0	
320.00000	5.20000	5.20000	468.02342	8645.68320	8658.34187	8658.34187	3.09661	2.10139	0.64653	0.0	0.0	

(e)

FIGURE 3. Continued.

R	PHE(1,I)	PHE(1,I)	PHE(2,I)	PHE(2,I)	PHE(3,I)	PHE(3,I)	PHE(4,I)	PHE(4,I)
0.0	0.0	0.0	0.0	0.0	0.0	0.0	0.0	0.0
15.00000	0.00000	0.00000	-0.00000	-0.00000	-0.00000	-0.00000	-0.00000	-0.00000
23.75000	0.01443	0.01443	-0.06550	-0.11533	-0.31780	-0.50707	-0.69035	-0.87997
41.25000	0.06265	0.06265	-0.19033	-0.31780	-0.51612	-0.69542	-0.87997	-0.87997
62.50000	0.04366	0.04366	-0.34180	-0.54193	-0.71296	-0.89571	-0.98226	-0.98226
83.40000	0.09119	0.09119	-0.46391	-0.64142	-0.81232	-0.98226	-0.98226	-0.98226
100.20000	0.11385	0.11385	-0.54193	-0.69542	-0.81232	-0.98226	-0.98226	-0.98226
117.00000	0.13553	0.13553	-0.59983	-0.71296	-0.87997	-0.98226	-0.98226	-0.98226
133.80000	0.18788	0.18788	-0.63489	-0.71296	-0.87997	-0.98226	-0.98226	-0.98226
150.60000	0.12652	0.12652	-0.64339	-0.646607	-0.646607	-0.646607	-0.646607	-0.646607
162.74500	0.11893	0.11893	-0.62318	-0.56598	-0.56598	-0.56598	-0.56598	-0.56598
185.23500	0.10502	0.10502	-0.56974	-0.48154	-0.33437	-0.23437	-0.17723	-0.13980
202.72500	0.04497	0.04497	-0.48154	-0.35641	-0.19443	-0.05044	-0.02332	-0.01755
220.21500	0.05895	0.05895	-0.35641	-0.20108	-0.05044	-0.05044	-0.05044	-0.05044
236.91000	0.08880	0.08880	-0.20108	-0.02128	-0.09481	-0.44739	-0.44739	-0.44739
252.81000	-0.04119	-0.04119	-0.02128	-0.02128	-0.02128	-0.02128	-0.02128	-0.02128
268.71000	-0.06047	-0.06047	0.18855	0.24475	0.24475	0.24475	0.24475	0.24475
283.14500	-0.05552	-0.05552	0.39359	0.38317	0.38317	0.38317	0.38317	0.38317
296.11500	-0.10802	-0.10802	0.59156	0.50845	0.32125	0.32125	0.32125	0.32125
306.45000	-0.13423	-0.13423	0.75377	0.60848	0.61391	0.61391	0.61391	0.61391
314.15000	-0.15381	-0.15381	0.87562	0.68303	0.80485	0.80485	0.80485	0.80485
320.00000	-0.16870	-0.16870	0.96331	0.73966	0.95027	0.95027	0.95027	0.95027

R	PHEP(1,I)	PHEP(1,I)	PHEP(2,I)	PHEP(2,I)	PHEP(3,I)	PHEP(3,I)	PHEP(4,I)	PHEP(4,I)
0.0	0.0	0.0	0.0	0.0	0.0	0.0	0.0	0.0
15.00000	0.01665	0.01665	-0.0750	-0.0750	-0.1336	-0.1336	-0.0793	-0.0793
23.75000	0.01164	0.01164	-0.0766	-0.0766	-0.1283	-0.1283	-0.0791	-0.0791
41.25000	0.01158	0.01158	-0.0724	-0.0724	-0.1060	-0.1060	-0.0697	-0.0697
62.50000	0.01133	0.01133	-0.0637	-0.0637	-0.0765	-0.0765	-0.0298	-0.0298
83.40000	0.01100	0.01100	-0.05312	-0.05312	-0.0430	-0.0430	-0.0192	-0.0192
100.20000	0.00970	0.00970	-0.0496	-0.0496	-0.0201	-0.0201	-0.0038	-0.0038
117.00000	0.00339	0.00339	-0.0265	-0.0265	-0.0012	-0.0012	-0.0012	-0.0012
133.80000	0.0006	0.0006	-0.0117	-0.0117	0.0213	0.0213	-0.0109	-0.0109
150.60000	-0.0030	-0.0030	0.0052	0.0052	0.0356	0.0356	-0.0093	-0.0093
167.74500	0.00664	0.00664	-0.0235	-0.0235	0.0466	0.0466	-0.0466	-0.0466
185.23500	-0.0101	-0.0101	0.0429	0.0429	0.0674	0.0674	-0.0855	-0.0855
202.72500	-0.0136	-0.0136	0.0637	0.0637	0.0767	0.0767	-0.0508	-0.0508
220.21500	-0.0169	-0.0169	0.0854	0.0854	0.0839	0.0839	-0.0009	-0.0009
236.91000	-0.0198	-0.0198	0.0662	0.0662	0.0892	0.0892	-0.0580	-0.0580
252.81000	-0.0221	-0.0221	0.0246	0.0246	0.0930	0.0930	0.0181	0.0181
268.71000	-0.0239	-0.0239	0.0160	0.0160	0.0953	0.0953	0.0174	0.0174
283.14500	-0.0249	-0.0249	0.0507	0.0507	0.0963	0.0963	0.0156	0.0156
306.45000	-0.0253	-0.0253	0.0563	0.0563	0.0967	0.0967	0.0392	0.0392
314.15000	-0.0255	-0.0255	0.0581	0.0581	0.0968	0.0968	0.0471	0.0471
320.00000	-0.0255	-0.0255	0.0585	0.0585	0.0968	0.0968	0.02486	0.02486

(f)

FIGURE 3. Continued.

	BLADE EDGENESS M. OF I. ABOUT C.G. LB./IN. SEC-SQ/IN.	DELTA R IN.	BLADE FLATWISE M. OF I. ABOUT C.G. LB./IN. SEC-SQ/IN.	DELTA R IN.	BLADE TORSIONAL M. OF I. ABOUT C.G. LB./IN. SEC-SQ/IN.	DELTA R IN.
		0.0	15.000	0.0	15.000	
	0.00269	6.300	0.00269	6.300	0.00269	6.300
	0.00679	2.800	0.00679	2.800	0.00679	2.800
	0.00823	3.900	0.00823	3.900	0.00823	3.900
	0.01842	15.830	0.01842	15.830	0.01842	15.830
	0.02398	29.170	0.02398	29.170	0.02398	29.170
	0.03180	89.000	0.03180	89.000	0.03180	89.000
	0.03474	61.000	0.03474	61.000	0.03474	61.000
	0.03971	8.960	0.03971	8.960	0.03971	8.960
	0.04650	11.060	0.04650	11.060	0.04650	11.060
	0.04356	35.460	0.04356	35.460	0.04356	35.460
	0.03881	12.340	0.03881	12.340	0.03881	12.340
	0.06848	2.000	0.06848	2.000	0.06848	2.000
	0.05861	8.000	0.05861	8.000	0.05861	8.000
	0.05723	9.500	0.05723	9.500	0.05723	9.500
	0.03805	13.500	0.03805	13.500	0.03805	13.500

	BLADE MASS LB./SEC-SQ/IN.-SQ.	DELTA R IN.	BLADE EDGENESS SECOND MOMENT OF AREA-IN.4TH	DELTA R IN.	BLADE FLATWISE SECOND MOMENT OF AREA-IN.4TH	DELTA R IN.
	0.0	15.0000	0.88567E+02	17.50000	0.87855E+02	17.50000
	0.00744	17.5000	0.37941E+03	17.50000	0.35636E+02	17.50000
	0.00423	17.50000	0.46303E+03	25.00000	0.27052E+02	25.00000
	0.00168	25.00000	0.71842E+03	16.80000	0.23430E+02	16.80000
	0.00144	16.80000	0.85000E+03	16.80000	0.23430E+02	16.80000
	0.00138	16.80000	0.85000E+03	16.80000	0.23430E+02	16.80000
	0.00137	16.80000	0.85000E+03	16.80000	0.23430E+02	16.80000
	0.00137	16.80000	0.85000E+03	16.80000	0.23430E+02	16.80000
	0.00145	17.49000	0.90000E+03	17.49000	0.27430E+02	17.49000
	0.00146	17.49000	0.84272E+03	17.49000	0.27227E+02	17.49000
	0.00150	17.49000	0.73952E+03	17.49000	0.27150E+02	17.49000
	0.00162	17.49000	0.64334E+03	15.90000	0.27116E+02	15.90000
	0.00190	15.90000	0.59000E+03	15.90000	0.26920E+02	15.90000
	0.00186	15.90000	0.56444E+03	15.90000	0.25433E+02	15.90000
	0.00176	12.97000	0.53000E+03	12.97000	0.22950E+02	12.97000
	0.00343	12.97000	0.53000E+03	12.97000	0.22950E+02	12.97000
	0.00223	7.70000	0.53000E+03	7.70000	0.22950E+02	7.70000
	0.00139	7.70000	0.53000E+03	7.70000	0.22950E+02	7.70000
	0.00036	4.00000	0.53000E+03	4.00000	0.22950E+02	4.00000

(g)

FIGURE 3. Continued.

IBM 2301

FINAL STIFFNESS MATRIX

FIGURE 4. Output Format - Rotor Blade Matrices.

IBM Z30687

12	.0	.0	.0	-859.306	369.188	-391.228	-1781.58	-.217900D+07	242365.
	.272896D+07	-.123781D+08	.0	.0	.0	-.161588D+07	208639.		
13	.0	.0	.0	-33.0894	1.71156	-8.99605	-5.12357	-1732.55	-4083.65
	.756.359	753.296	.0	.0	.0	125.043	-16335.3		
14	.0	.0	.0	.0	.0	1.71156	33.0894	-5.12357	-8.49605
	753.296	756.359	.0	.0	.0	16335.3	-125.043		
15	.0	-112.808	-10129.7	3611.79	.0	.0	.0	.0	.0
	.0	.0	.0	.0	.0	.0			
16	.0	.0	.0	.0	7143.69	-3206.0	-3102.89	-35682.5	.17431D+08
	-.235881D+07	.118284D+07	.0	.0	.0	-153513.	-515291.		
17	.0	.0	.0	-32606.9	-7143.69	-35682.5	3102.89	-.415679D+07	-.17431D+08
	.118284D+07	.235881D+07	.0	.0	.0	130248.	-153513.		

(b)

FIGURE 4. Concluded.

IBM 2301 F

BIFLAR ANALYSIS RESULTS

ALL DISPLACEMENTS ARE IN G AND ALL ANGLES ARE IN DEGREES

NUMBER OF FIXED SYSTEM MODES	IS 9
NUMBER OF FIXED SYSTEM ABSORBERS	IS 1
NUMBER OF INPLANE BIFLARS	IS 1
NUMBER OF VERTICAL BIFLARS	IS 1
TOTAL NO. OF DEGREES-OF-FREEDOM (WITH NO ROTOR)	IS 16
NUMBER OF A.C. STATIONS	IS 4
ROTOR COUPLING SWITCH.....(0=NO,1=OR-1=YES) IS 1	
ROTOR MATRICES PRINTOUT(0=NO,1=YES) IS 1	
FIXED SYSTEM MATRICES PRINTOUT " IS 1	
ADD ROTOR MATRICES PRINTOUT " IS 1	
ADD FIX.SYS. ABSORBER PRINTOUT " IS 1	
ADD INPLANE BIFLAR PRINTOUT " IS 1	
ADD VERTICAL BIFLAR PRINTOUT " IS 1	
INPLANE BIFLAR (9X9) PRINTOUT " IS 1	
VERTICAL BIFLAR (9X9) PRINTOUT " IS 1	
GATHAS PRINTOUT " IS 1	

(a)

FIGURE 5. Output Format - Bifilar Linear Analysis Matrices.

IBM Z 30687

FIXED SYSTEM STIFFNESS MATRIX OF ORDER 9

FIXED SYSTEM STIFFNESS MATRIX									
1	1856.52	0	0	0	0	0	0	0	0
2	0	4949.75	0	0	0	0	0	0	0
3	0	0	47608.9	0	0	0	0	0	0
4	0	0	0	18302.4	0	0	0	0	0
5	0	0	0	0	20652.7	0	0	0	0
6	0	0	0	0	0	10311.0	0	0	0
7	0	0	0	0	0	0	11560.1	0	0
8	0	0	0	0	0	0	0	56774.3	0
9	0	0	0	0	0	0	0	0	110572.

(b)

FIGURE 5. Continued.

IBM 230687

ROTOR NO. OF DEGREES-OF-FREEDOM IS 12

TOTAL NO. OF DEGREES-OF-FREEDOM IS 28

ROTOR BLADE MATRICES

(INCLUDING 6 RIGID FIX.SYS. MODES) OF ORDER 16

ROTOR STIFFNESS MATRIX

1	.0 -13.0894	.0 1.71156	.0 -6.49605	125.043 -5.12357	-16335.3 -1732.55	.0 -4083.65	.0 756.359	.0 753.296	.0 .753.296	.0 0	.0 0
2	.0 1.71156	.0 33.0894	.0 -5.12357	-16335.3 8.49605	125.043 -4083.65	.0 1732.55	.0 753.296	.0 756.359	.0 0	.0 0	.0 0
3	.0 .0	.0 .0	.0 .0	.0 .0	.0 .0	.0 .0	.0 .0	.0 .0	-112.326 .0	-112.806 .0	-10229.7 3811.79
4	.0 7143.69	.0 -32606.9	.0 -3102.89	-163513. -35682.5	-515291. .17411n+08	.0 -415679D+07	.0 -235681D+07	.0 .118284D+07	.0 0	.0 0	.0 0
5	.0 -32606.9	.0 -7143.69	.0 -35682.5	130248. 3102.89	-153513. -1.915679n+07	.0 -1.74311n+08	.0 .118284D+07	.0 -.235681D+07	.0 0	.0 0	.0 0
6	.0 .0	.0 .0	.0 .0	.0 .0	.0 .0	.0 .0	.0 .0	.0 .0	.0 0	.0 0	.0 0
7	.0 .0	.0 .0	.0 .0	.0 .0	.0 .0	.0 .0	.0 .0	.0 .0	714.170 .0	-74.3204 .0	-1222.21 760.385
8	.0 .0	.0 .0	.0 .0	.0 .0	.0 .0	.0 .0	.0 .0	.0 .0	-1.41149 .0	3330.19 .0	-2364.16 -1473.63
9	.0 .0	.0 .0	.0 .0	.0 .0	.0 .0	.0 .0	.0 .0	.0 .0	-1339.02 .0	-1795.95 .0	.108472D+08 .108102D+07

10

IBM 230687

(c)

FIGURE 5. Continued.


```

PRESENT NO. OF DEGREES-OF-FREEDOM (NP) = 9
ADDITIONAL NO. DEGREES-OF-FREEDOM (NA) = 12
TOTAL NO. OF DEGREES-OF-FREEDOM (NP+NA) = 21
ORDER OF MATRIX TO BE ADDED (NL) = 16
ORDER D.O.F. OF ADDED MATRIX (NL-NA) = 6

```

FIGURE 5. Continued.
IBM 230687
(e)

..... FIXED SYSTEM + ROTOR STIFFNESS MATRIX

FIXED SYSTEM + ROTOR STIFFNESS MATRIX									
1	1840.85	-13.7054	29.0877	-40.2377	-36.7691	-5.31752	-5.31752	59.0887	21.5091
	-1181808	-10.1297	3.81179	-51.8077	168.526	-1.80373	185.435	-91831.7	-11276.2
	-4821.86								12750.0
2	6.55250	4916.60	-43.4811	-7.79660	-15.3611	-2.18325	148.156	-2.92543	-12.3561
	-12.4069	-1114.27	419.297	179.396	40.3897	188.198	-10.0499	92234.3	-5599.71
	-12623.0								
3	2.5770	115.453	-4449.4	-235.7540	-92.7525	-13.6929	-13.6929	-513.012	-21.1438
	34.9706	3140.20	-1181.65	235.837	-384.257	143.606	-486.442	247642.	35837.3
	3428.88								36.8218
									-37848.8
4	-39.6206	31.1830	124.255	18373.5	35.5950	-5.72737	-144.004	42.8766	.112328
	.112808	10.1297	-3.81179	85.0983	-378.529	-43.1991	-428.364	205086.	-59877.6
	14951.0								-28138.7
5	-11.1006	-58.4978	-18.7667	39.7876	20530.5	-9.29177	258.778	22.8854	12.3561
	-12.4059	1114.27	-419.297	62.3753	288.688	143.541	279.060	-126021.	91883.3
	-17334.8								15464.5
6	4.68930	.687792	-11.4586	-11.2524	7.78050	10312.2	1.20479	-2.50523	-5.90571
	-2.48178	-222.853	63.8594	4.77058	41.8767	20.6461	42.1130	-19539.3	-2.47123
	-2598.68								2288.10
7	10.2006	16.9931	-12.4257	-28.0608	28.8399	4.37561	11564.4	-74.3508	-15.2570
	-2.48178	-222.853	63.8594	-1.66189	39.3893	19.4673	40.4173	-19521.4	-2.47123
	-2519.84								2080.36
8	-66.4519	75.7296	231.326	139.692	-44.5378	-7.39395	56429.8	70.3950	-14.0411
	-16.1010	-1266.21	476.474	-775.992	-144.332	-82.661	75.0061	-100576.	27351.1
	55326.4								
9	-16.6906	12.4415	47.6708	31.8761	-13.1562	-2.12151	-57.0478	110588.	-112328
	-112808	-10.1297	3.81179	40.2200	-201.431	-28.2559	-233.776	108961.	-2965.1
	8158.73								-14544.7

IBM 230687

(f)

FIGURE 5. Continued.

FIXED...SYSTEM †...ROTOR ‡...FIXED...ABSORBERS...MATRICES OF ORDER 22

FIXED...SYSTEM †...ROTOR ‡...FIXED...ABSORBERS...STIFFNESS...MATRIX

1	1840.85	-13.7054	29.0877	40.2377	-51.8077	168.526	-1.80373	185.435	-5.31752	-59.0887	21.5081	-112328	.0
2	6.53520	4916.60	-63.4811	-7.79460	-15.3811	179.396	40.3897	188.198	-2.18325	148.156	-2.92543	-12.3561	.0
3	2.57701	115.453	-47495.4	-32.7940	92.755	-384.257	143.606	-486.442	-13.6929	-513.012	-21.1438	-34.8218	.0
4	38.6706	31.3830	124.255	1893.5	-35.5950	-378.559	-43.191	-428.364	-5.72737	-144.084	42.8766	.112328	.0
5	11.1006	-58.4978	-18.7467	39.7876	20590.5	288.688	143.541	279.060	-9.29177	-258.778	22.0254	12.3561	.0
6	4.66930	.687792	-11.4586	-11.2524	7.78050	10312.2	1.20479	42.1130	-2.50523	-5.90571	-2.47123	.15464.5	.0
7	10.2006	-16.9931	-12.4257	-28.0668	-1.66189	28.8399	4.37561	11564.4	-74.3508	-152570	-2.47123	.0	
8	-2.44178	-222.853	-63.6594	-28.0668	-1.66189	39.3593	19.4673	40.4173	-19521.4	-12176.0	2080.36	.0	
9	-14.6906	12.4415	47.6708	31.8761	-13.1522	-2.12151	-223.776	-26.3559	-57.0478	110588.	-112328	.0	

(g) Continued.

IBM 23068 /

INPLANE_BIFILAR_QSK MATRIX									
1	0	0	0	0	0	0	0	0	0
2	0	0	0	0	0	0	0	0	0
3	0	0	0	0	0	0	0	0	0
4	0	0	0	0	0	0	0	0	0
5	0	0	0	0	0	0	0	0	0
6	0	0	0	0	0	0	0	0	0
7	0	0	0	0	0	0	0	6562.60	0
8	0	0	0	0	0	0	0	0	5839.65
9	0	0	0	0	0	0	0	0	43.7974
									5839.65

(h)

IBM Z30687

FIGURE 5. Continued

FIXED SYSTEM + ROTOR + FIXED ABSORBERS + INPLANE PENDULUM MATRICES OF ORDER 25

..... FIXED SYSTEM + ROTOR + FIXED ABSORBERS + INPLANE PENDULUMS STIFFNESS MATRIX.

1	1840.85	-13.7054	29.0877	-40.2377	-34.7691	-5.31752	-59.0887	-21.5081	-112328
	-.112808	-10.1297	3.81179	-.0	168.5526	-1.80373	185.435	-91831.7	13276.2
	-.4823.88	.0	.0	.0	.0				12750.0
2									
	6.53520	4916.60	-43.4811	-7.79460	-15.3811	-2.1835	148.156	-2.92543	-12.3561
	-.12.4689	-1114.27	419.297	179.396	40.3897	186.198	-10.0499	20037.9	92234.3
	-.12623.0	.0	.0	.0	.0				-5689.71

3	2.57701	115.453	-97495.4	-32.7940	92.7525	13.6929	-513.012	-21.1438	34.8218
	34.9706	3140.20	-1181.65	235.837	-384.257	145.606	-486.442	247642.	35837.3
	3428.88	.0	.0	.0	.0				-37648.6
4									
	38.6206	31.3630	124.255	18393.5	-35.5950	-5.72737	-144.084	42.8766	.112328
	-.112808	10.1297	-3.81179	85.0983	-378.529	-43.1991	-428.364	20906.	-50877.6
	-.14351.0	.0	.0	.0	.0				-28138.7

5	11.1006	-56.4978	-18.7467	39.7876	20590.5	-9.29177	-258.778	22.8254	12.3561
	12.4689	-1114.27	-419.297	62.3753	288.668	143.541	279.060	-126021.	91883.3
	-.17334.8	.0	.0	.0	.0				15464.5
6									
	4.68930	.687792	-11.4586	-11.2524	7.78050	10312.2	1.20479	-2.50823	-5.90571
	-2.48178	-222.853	83.8594	4.77058	41.8767	20.6461	42.1130	-1539.3	13099.2
	-.2528.68	.0	.0	.0	.0				2288.10

7	10.2006	16.9331	-12.4257	-28.0608	28.8399	4.37561	11564.4	-78.3508	-15.2570
	-.2.48178	-222.853	83.8594	-.66169	39.3893	19.4673	40.4173	-19521.4	12176.0
	-.2519.64	.0	.0	.0	.0				2080.36
8									
	66.4519	75.7296	231.326	139.692	-44.5378	-7.39395	56429.8	70.3950	-14.0411
	-14.1010	-1266.21	476.474	-775.992	-144.332	-832.661	75.0631	-100578.	-404325.
	-.55326.4	.0	.0	.0	.0				27351.1

9	-.14.6906	12.4415	47.6708	31.8761	-13.1522	-2.12151	-57.0678	110588.	-112328
	-.112808	-10.1297	3.81179	40.2206	-201.431	-28.2559	-223.776	108961.	-23645.1
	0158.73	.0	.0	.0	.0				14514.7
									(i)

IBM 230687

FIGURE 5. Continued.

VERTICAL_BIFILAR_90%_MATRIX

1	.0	.0	.0	.0	.0	.0	.0	.0	.0
2	.0	.0	.0	.0	.0	.0	.0	.0	.0
3	.0	.0	.0	.0	.0	.0	.0	.0	.0
4	.0	.0	.0	.0	.0	.0	.0	.0	.0
5	.0	.0	.0	.0	.0	.0	.0	.0	.0
6	.0	.0	.0	.0	.0	.0	.0	.0	.0
7	.0	.0	.0	.0	.0	.0	.0	11679.3	.0
8	.0	.0	.0	.0	.0	.0	.0	.0	-58.3965
9	.0	.0	.0	.0	.0	.0	.0	.0	10949.3
									10949.3

(j)

FIGURE 5. Continued.

IBM 230687

FIXED SYSTEM + ROTOR + FIXED ABSORBERS + INPLANE + VERTICAL PENDULUM MATRICES OF ORDER 28

FIXED SYSTEM + ROTOR + FIXED ABSORBERS + INPLANE + VERTICAL PENDULUM MATRICES OF ORDER 28									
1	1890.85	-13.7054	29.0877	-40.2377	-34.7691	-5.31752	-59.0881	21.5081	-111328
	-112808	-10.1297	3.81179	-51.8077	168.526	-1.80373	185.435	-91.831.7	13276.2
	-4823.88	.0	.0	.0	.0	.0	.0	.0	12750.0
2	6.53520	4916.60	-43.4811	-7.79460	-15.3811	-2.18325	148.156	-2.92543	-12.3561
	-62.4089	-1114.27	419.297	179.396	40.3897	168.198	-10.099	92234.3	-589.71
	-12623.0	.0	.0	.0	.0	.0	.0	.0	.0
3	2.57701	115.453	-47495.4	-32.7980	92.7525	-13.6929	-513.012	-21.1438	34.8218
	34.9706	3140.20	-1181.65	235.837	-384.257	163.606	-686.442	247642.	-37846.8
	3428.88	.0	.0	.0	.0	.0	.0	.0	.0
4	-38.6206	31.3830	124.255	18393.5	-35.5950	-5.72737	-144.084	42.8766	-112328
	-112808	10.1297	-3.81179	85.0933	-378.5529	-43.1591	-828.364	20986.	-50877.6
	-14951.0	.0	.0	.0	.0	.0	.0	.0	-28138.7
5	51.1006	-58.4978	-18.7467	39.7876	20590.5	-9.29177	-258.778	22.8254	12.3561
	-12.4089	1114.27	-419.297	62.3753	288.688	143.541	279.060	-126621.	91883.3
	-17334.8	.0	.0	.0	.0	.0	.0	.0	15464.5
6	6.68930	.687792	-11.4586	-11.2554	7.78050	10312.2	1.20479	-2.50523	-5.90571
	-2.49178	-222.653	83.8594	4.77058	41.8767	20.6661	42.1130	-19539.3	13039.2
	-2519.84	.0	.0	.0	.0	.0	.0	.0	2288.10
7	30.2096	-16.9931	-12.4257	-28.0608	28.8399	6.37561	11564.4	-74.3508	-15.2570
	-2.49178	-222.653	83.8594	-1.66189	39.3893	19.4673	40.4173	-19521.4	12176.0
	-2519.84	.0	.0	.0	.0	.0	.0	.0	2080.36
8	-66.45119	75.7296	231.326	139.692	-44.5378	-7.39395	56429.8	70.3950	-14.0411
	-14.1010	-1266.21	476.474	-775.992	-144.332	-332.661	75.0061	-100378.	-40325.
	55326.4	.0	.0	.0	.0	.0	.0	.0	27551.1
9	-14.6906	12.4415	47.6768	31.8761	-13.1522	-2.12151	-57.0478	110588.	-112328
	-112808	-10.1297	3.81179	40.2200	-201.431	-223.776	10861.	-29645.1	-14514.7
	8158.73	.0	.0	.0	.0	.0	.0	.0	IBM Z30687

FIGURE 5. Concluded.

```

GENERALIZED FORCES - ORDER IS = 9

COSINE COMPONENT
.500000 -170.000 500.000 .500000 -201.000 25.000 120.000 350.000
-25.0000

SINE COMPONENT
75.0000 .500000 .500000 270.000 75.0000 -32.5000 -75.0000 260.000
110.0000

(GAMMAS)

.420508D-03 -.320688D-03 .257314D-05 .100956D-06 -.123203D-02 .397414D-02 -.915847D-02 .270562D-02 .666964D-04
-.548605D-04 -.160107D-04 -.544875D-02 .705332D-03 .315306 .50356D-01 -.235034D-01 .510356D-02 -.122553D-02 .030800D-02
.291655D-04 -.300370D-05 .705246D-07 -.137627D-02 -.377319D-07 -.137627D-02 -.192891D-02 -.177153D-03 .176337D-05 .228122D-05
.750412D-04 -.150106D-02 .691230D-03 .718392D-01 -.317137 -.213538D-01 .326855D-02 .391056D-02

(GAMMAS)

COSINE - SINE - AMPLITUDE - PHASE(DEG)
ROTOR

.420508D-03 .103080D-02
.320688D-03 .291653D-04
.257314D-05 -.300397D-05
.100956D-06 .705546D-07
.123203D-02 .977913D-02
.397414D-02 -.137627D-02
.915847D-02 .563780D-02
.270562D-02 .192891D-02
.122553D-02 -.14733D-05
.666964D-04 .176337D-05
.030800D-02 .228122D-05
.177153D-03 -.213538D-01
.176337D-05 .326855D-02
.391056D-02 .391056D-02

FIXED SYSTEM ABSORBER(S)

.344875D-02 -.150106D-02 .376126D-02 -156.479
.705332D-03 .691230D-03 .141059D-01 44.4215
.315306 .718392D-01 9.28677 -77.2864

```

(a) IBM Z30687

FIGURE 6. Output Format - Bifilar Linear Analysis Forced Response Results

708454D-01 -317137.....2984380-01 -118.491
 VERTICAL BIFILAR PENDULUM(S) (AMP & PHASE ORDER IS:N,N-1,N+1)
 (EQT ORDER IS:0,SIN,COS) (AMP & PHASE ORDER IS:N,N-1,N+1)
 DEG & DEG

-255034D-01	-213536D-01	.45860	-137.744
.510358D-02	.326655D-02	.358881D-01	-30.2823
.1822553D-02	.391058D-02	.148276	116.499

INPUT FIXED SYSTEM FREQUENCIES (HZ)
 5.10000 6.40000 15.3000 14.3000 13.8000 11.6000 12.1000 17.4000 21.1000
 FORCING FREQUENCY (HZ) = 17.2000

THE CONVERSION FACTOR TO G = 30.2259

FUSELAGE NO. OF DEGREES OF FREEDOM = 9

COSINE COMPONENT

-214190D-03	-448165D-04	.369518D-03	.295426D-02	-567524D-03	.284549D-03	.641759D-03	-2586691D-02
.214395D-03							

SINE COMPONENT

-236794D-03	-109046D-03	.122252D-02	-224671D-02	-105094D-02	.310558D-03	.889165D-03	.331319D-02
.2352297D-03							

FIRST A.C. STATION DISPLACEMENT IN G

	X	Y	Z		
COSINE	SINE	COSINE	SINE	COSINE	SINE
.106454D-01	-.131066D-01	-.208498D-01	-.159455D-01	-.143570D-01	.182978D-02

FIRST A.C. STATION TOTAL DISPLACEMENT IN G

	X	Y	Z
	.168852D-01	.262483D-01	.144732D-01

IBM 2301r/h

FIGURE 6. Continued.
(b)

SECOND A.C. STATION DISPLACEMENT IN G						
X	COSINE	SINE	COSINE	SINE	COSINE	SINE
-50.9158	.112625D-01	-.152813D-01	-.891726D-02	.894320D-02	-.978861D-02	-.282865D-01
SECOND A.C. STATION TOTAL DISPLACEMENT IN G						
X	Y	Z	X	Y	Z	
.189832D-01	.124878D-01	.299323D-01				
SECOND A.C. STATION PHASE ANGLE IN DEG						
-53.6093	134.916	-109.066				
THIRD A.C. STATION DISPLACEMENT IN G						
X	COSINE	SINE	COSINE	SINE	COSINE	SINE
.566726D-02	-.669938D-02	.130642D-02	.746452D-02	.160931D-01	.684755D-02	
THIRD A.C. STATION TOTAL DISPLACEMENT IN G						
X	Y	Z	X	Y	Z	
.877494D-02	.757798D-02	.171225D-01				
THIRD A.C. STATION PHASE ANGLE IN DEG						
-49.7768	99.9272	19.9690				
FOURTH A.C. STATION DISPLACEMENT IN G						
X	COSINE	SINE	COSINE	SINE	COSINE	SINE
.175254D-01	.101492D-01	.224446D-01	.275227D-01	-.131746D-01	.320180D-02	
FOURTH A.C. STATION TOTAL DISPLACEMENT IN G						
X	Y	Z	X	Y	Z	
.202524D-01	.355603D-01	.135581D-01				

IBM 230687

FIGURE 6. (c)
Continued.

FOURTH A.C. STATION PHASE ANGLE IN DEG

30.075 - 50.8648 - 166.240

ROTOR HEAD DISPLACEMENT IN G

X	Y	Z			
COSINE	SINE	COSINE	SINE	COSINE	SINE
-5285340-01	.123521	-.941640D-01	.374169D-02	-.398021D-02	.438087D-02

ROTOR HEAD TOTAL DISPLACEMENT IN G

X	Y	Z			
COSINE	SINE	COSINE	SINE	COSINE	SINE
.134354	.962383D-01	.591696D-02			

ROTOR HEAD DISPLACEMENT PHASE ANGLES IN DEG

113.166 - 177.725 - 132.256

FIGURE 6. Concluded.
(d) IBM 2301.

D.O.F.=29,NFE=.9,KRTRD= 12, NFABS=.1,KINDS OF INPL.BIF= 0,KINDS OF VERT. BIF=.1,NUIBS OF N.L. INPL.BIF= 4

FIXED SYSTEM + ROTOR + FIXED ABSORBERS (R.H.S.) OF ORDER 25

THE JOURNAL OF CLIMATE

THE MASS (L.H.S.) MATRIX OF ORDER 18

THE BIFILAR FORCE VECTOR OF ORDER 10

IBM Z30687

FIGURE 7. Output Format - Bifilar Nonlinear Analysis Matrices.

THE ROTOR HEAD MODE SHAPES, TRANSPOSE(PHI), OF ORDER 9 X 6

.10000D-02	.15000	.10000D-02	-.51200D-02	.47400D-03	.15680D-02
-.34000	.10000D-02	.11000	-.12000D-03	-.51830D-02	.28000D-03
1.00000	.10000D-02	.31000	.13020D-01	.55950D-02	.15000D-03
.10000D-02	.54000	-.10000D-02	.12140D-01	.77200D-04	.36830D-03
-.40200	.15000	-.11000	-.60100D-02	-.35220D-02	.43820D-03
.50000D-01	-.65000	.22000D-01	-.12440D-02	-.47300D-03	-.60000D-02
-.24000	-.15000	.22000D-01	-.12440D-02	-.47300D-03	.60000D-02
.70000	.52000	.12500	-.70000D-04	.23100D-01	.15000D-03
-.50000D-01	.22000	.10000D-02	.63500D-02	.22000D-03	-.12700D-02

THE EXPANDED BIPLAR MASS MATRIX OF ORDER = 13

.57749D-02	-.24725D-05	.30618D-03	.19956D-01	.53592D-02	-.33300D-02	-.64115D-02	.19357D-01	.78938D-02	.22596D-01.
.38222D-02	-.14703D-01	.40709D-02	.59513D-04	.33600D-01	-.43612D-02	-.20251D-01	-.58333D-01	.41943D-02	.82907D-03
-.24725D-05	.28406D-01	-.83517D-01	.41567D-01	.36387D-03	-.98722D-01	.12176D-01	-.58829D-01	.17209	.50167D-03.
.42976D-01	.58641D-03	-.41567D-01	.24565	.25322D-03	.12470				
.30618D-01	-.83517D-01	.24565							
-.12395									
.19956D-01	.59513D-04	.38387D-03	.71646D-01	.19783D-01	-.88356D-02	-.20061D-01	.69157D-01	.29112D-01	.68064D-01.
.80266D-03	-.66210D-01	.10513D-02							
.53592D-02	.33600D-01	-.98722D-01	.19783D-01	.45245D-01	-.70660D-02	-.28963D-01	-.49972D-01	.13100D-01	.17546D-01.
.46877D-01	-.19752D-01	-.51062D-01							
.33300D-02	-.43612D-02	.86332D-02	-.70660D-02	.52764D-02	.89673D-02	.20617D-03	-.23163D-02	-.33596D-02	
-.21318D-01	-.70203D-02	-.86853D-02							
-.64115D-02	-.20251D-01	.58829D-01	-.20061D-01	-.28963D-01	-.89673D-02	-.23301D-01	-.22018D-01	-.10287D-01	-.33751D-01
.19357D-01	-.58333D-01	.17209	.69157D-01	-.49972D-01	.20417D-03	.22018D-01	.18680	.19486D-01	.65028D-01
-.86652D-01	-.64273D-01	.87407D-01							
-.15186D-01	-.17075								
1.00000	.0	.0							
.78938D-02	.41943D-02	-.12246D-01	.29112D-01	.13100D-01	-.33598D-02	-.10287D-01	.19486D-01	.12666D-01	.24155D-01
.30199D-02	-.30549D-01	-.94129D-02							
.89774D-01	.32948D-02	.19948D-02	.27042	.9712D-01	-.92108D-01	-.13409	.25636	.95972D-01	1.0000
.0	.0	.0							
-.15186D-01	-.17075								
1.00000	.0	.0							
-.58614D-01	.23060D-02	.10061D-02	-.26306	-.78476D-01	-.27892D-01	-.14094D-01	.25536	-.12137	.0
0	1.00000	1.0000							
.16174D-01	-.16151	.49546	.41770D-02	-.20295	(b)	-.35302D-01	.58551D-01	.34727	-.37396D-01
0	.0								

IBM Z30687

FIGURE 7. Continued.

THE EXPANDED BIPLANE FORCE VECTOR OF ORDER = 13

- .36036D-05 - .87050D-05 .25502D-04 - .13759D-04 - .14691D-04 .29357D-05 .99556D-05 - .45950D-05 - .68925D-05 .0

FIGURE 7. (c) Continued.
IBM Z30687

FINAL COMBINED MASS MATRIX OF ORDER 29 FOR PSI = .0												
1												
	3.0344	-81765D-01	-2.9687	-2.3651	1.7839	.22636	.17970	.79122	-1.2707	-.94238D-04		
	.38577D-05	.86147D-01	.0	-.34010D-02	.66786D-02	.17445D-01	.19518D-01	.33621	-101.32	-18.629		
	.73043	.10999D-02	.74987D-04	-.75765D-02	-.70140D-03	.22596D-01	.38222D-02	-.14703D-01	.40709D-02			
2												
	.41765D-01	4.6785	-.11174	-.77927D-01	1.2008	.60433D-01	-.16217	.6.0335	-.12199D-01	-.10366D-01		
	.42234D-03	9.4761	.0	.56962D-02	.68219D-02	.18770D-01	-.40917D-01	.102.89	7.3631	2.8095		
	35.048	-.17236D-01	.82485D-02	-.47757D-03	-.76635D-02	-.82907D-03	-.42976D-01	.580941D-03	-.41567D-01			
3												
	-2.9687	16.746	6.5549	-.4.9101	-.44102	.15529	-2.9867	.3.2545				
	-.11959D-02	-.26.705	9.1664	-.3.6371	-.7238.	-.64336	-.3.5180					
	-.80.063	-.19410D-02	-.23246D-01	.19266D-01	.79832D-02	.50187D-03	.12335	.263.46	-.29214D-01	5.5910		
	-.23246D-03	-.79832D-03	-.11442D-03	.68064D-01	.80266D-03	-.25220D-03	.12470					
4												
	2.3651	-.77927D-01	6.5549	-.3.6371	-.75966D-02	.58028D-01	-.49290D-01	24.190	23.26	-.32.934		
	-.38577D-05	-.86147D-01	.0	-.10372D-01	-.17984D-01	.48877D-01	.80266D-03	-.66210D-01	.10513D-02			
	4.5767	-.64700D-03	-.74987D-04	-.17984D-01	-.11442D-03	.68064D-01						
5												
	1.7839	1.2008	-4.9101	-.3.6371	6.7034	.38845	.76440D-01	-.3.9865	-.2.0075	-.150.60	-.18.270	
	-.44434D-03	-.9.4761	.0	.11460D-02	.14920D-01	.31152D-01	-.17411D-01	.80.374				
	39.574	-.64700D-01	-.82485D-02	-.11853D-01	.48121D-02	.175446D-01	-.48877D-01	-.19752D-01	-.51086D-01			
6												
	22634	.60633D-01	-.44102	-.72238	.38845	2.0415	.16325	-.41731	-.37584	-.20732D-02	3.7638	
	.86866D-04	1.8952	.0	.14237D-02	-.22647D-03	-.50120D-02	-.10771D-01	.11.265	-.22.983			
	4.3971	-.32350D-02	-.16437D-02	-.18408D-02	-.69599D-03	-.23183D-01	-.24318D-01	-.70203D-02	-.88852D-02			
7												
	.17970	-.16217	.15529	-.84336	.76440D-01	.14325	2.3217	-.47330D-01	.45179	-.20732D-02		
	-.84866D-04	1.8952	.0	-.23020D-02	-.42724D-02	-.14042D-01	-.25221D-01	.30.528				
	-21.450	-.64700D-03	-.16497D-02	-.18408D-02	-.69599D-03	-.33751D-01	-.44940D-01	-.35475D-02	-.14737D-01			
8												
	.79122	-.6.0335	-.2.9867	-.78956	-.3.9865	-.4.1731	-.47330D-01	.30.528	.35510	-.11760D-01		
	-.48221D-03	10.748	.0	-.31467D-01	-.11927D-01	-.2075	-.37584	-.45179	.35510	8.1061		
	-81.393	-.12940D-01	.93733D-02	-.10358D-03	-.34182D-01	.65920D-01	-.86652D-01	-.64273D-01	.87407D-01	-.47226	-.51.089	
9												
	-1.2707	-.21990D-01	3.2945	3.5180	-.2.0075	-.37584	-.45179					
	.38577D-05	-.86147D-01	.0	-.41449D-02	-.34414D-02	.22166D-01	-.31427D-01	.15.882	122.01	-.11.405		
	5.9875	-.12940D-02	.74987D-04	.93983D-02	-.35550D-03	.241555D-01	.30193D-02	-.30549D-01	-.94129D-02			
10												
	-.37605D-03	-.41465D-01	.11685	.37695D-03	.41465D-01	-.82928D-02	-.47119D-01	-.37695D-03	.12486			
	-.25186D-03	.62960	-.90689D-01	.0	.0	.0	.0	.0	.0	.0		
	0	0	0	0	0	0	0	0	0	0		
11												
	.15431D-04	.16374D-02	-.47835D-02	-.15431D-04	-.16974D-02	.33947D-03	.19288D-02	.15431D-04	-.25186D-03			
	.20956	-.3.9559	.75778	.0	.0	.0	.0	.0	.0	.0		
12												

IBM Z30687

(d)

FIGURE 7. Continued.

FINAL COMBINED FORCE VECTOR OF ORDER 29 FOR PSI = .0

-.38035D-05	-.870500-05	.25502D-04	-.13759D-04	-.14091D-04	.29357D-05	.99558D-05	.45950D-05	-.68925D-05	.0
.0	.0	.0	.0	.0	.0	.0	.0	.0	.0
.0	.0	.0	.0	.0	.0	.0	.0	.0	.0

STATE VARIABLES (DISP&VEL) FOR PSI = .0

-.25266D-11	-.19571D-08	-.20489D-08							
-.26472D-11									
-.46431D-11	-.35933D-08								
-.71134D-11	-.55290D-08								
-.52201D-11	-.50463D-08								
.16185D-11	.12527D-08								
.51322D-11	.39723D-08								
.23660D-12	.18313D-09								
-.12291D-11	-.75307D-09								
-.30384D-11	-.23517D-08								
.41981D-12									
.18716D-13	.32493D-09								
.30790D-16	.14486D-10								
-.11559D-11	.23987D-13								
.36247D-11	-.89465D-09								
.63628D-11	.28055D-08								
-.10919D-10	-.49403D-08								
-.18112D-13	-.84510D-08								
-.31698D-13	-.14801D-10								
-.50001D-13	-.24534D-10								
.93811D-13	-.36701D-10								
.44214D-11	.72610D-10								
.31637D-11	.34222D-08								
-.40165D-12	.24487D-08								
-.18834D-12	-.31088D-09								
	.14578D-09								

IBM 230687

BIFFLAR INITIAL DISP & VEL FOR PSI = .0

.34172D-11	.26449D-08								
.49642D-11	.38443D-08								
-.25322D-11	-.19754D-08								
-.40992D-11	-.31728D-08								

FIXED SYSTEM + ROTOR + FIXED ABSORBERS (R.H.S.) OF ORDER 25
(PSI = 2 DEG)

-.13624D-07	.44860D-07	.22938D-06	.23800D-06	.13370D-06	-.28845D-07	-.92330D-07	-.10342D-06	.20289D-06	.41828D-06
.27024D-09	-.50329D-06	.80167D-06	.94019D-06	.19417D-07	-.12205D-06	-.45731D-08	.14607D-05	-.36007D-05	.73651D-04
-.30834D-04	-.70800D-07	-.42243D-07	.50807D-06	-.23538D-08					

(e)

FIGURE 7. Continued

```

..... NREV= 5, G1= .462D-02, G2= .344D-01, XHUB= .333D-02, YHUB= .592D-02, THZH= .122D-04, DXHUB= -.770 ..., DYHUB= .486D-01

..... NREV= 6, G1= .168D-02, G2= .301D-01, XHUB= .321D-02, YHUB= .601D-02, THZH= .131D-04, DXHUB= -.612 ..., DYHUB= .176D-01

..... NREV= 7, G1= .437D-02, G2= .219D-01, XHUB= .109D-02, YHUB= .526D-02, THZH= .146D-04, DXHUB= -.749 ..., DYHUB= -.140

..... NREV= 8, G1= .128D-01, G2= .984D-02, XHUB= .271D-03, YHUB= .371D-02, THZH= .128D-04, DXHUB= -.614 ..., DYHUB= .183

..... NREV= 9, G1= .124D-01, G2= .213D-02, XHUB= .247D-03, YHUB= .261D-02, THZH= .103D-04, DXHUB= -.468 ..., DYHUB= .148

..... NREV= 10, G1= .653D-02, G2= .821D-02, XHUB= .454D-03, YHUB= .226D-02, THZH= .844D-05, DXHUB= -.382 ..., DYHUB= .608D-01

..... NREV= 11, G1= .454D-03, G2= .141D-02, XHUB= .191D-02, YHUB= .257D-02, THZH= .723D-05, DXHUB= -.361 ..., DYHUB= .573D-01

..... NREV= 12, G1= .452D-02, G2= .419D-02, XHUB= .312D-02, THZH= .781D-05, DXHUB= -.399 ..., DYHUB= .573D-01

..... NREV= 13, G1= .481D-02, G2= .310D-02, XHUB= .201D-02, YHUB= .356D-02, THZH= .846D-05, DXHUB= -.450 ..., DYHUB= .477D-01

..... NREV= 14, G1= .252D-02, G2= .296D-02, XHUB= .174D-02, YHUB= .374D-02, THZH= .932D-05, DXHUB= -.483 ..., DYHUB= .131D-01

..... NREV= 15, G1= .193D-03, G2= .309D-02, XHUB= .147D-02, YHUB= .371D-02, THZH= .969D-05, DXHUB= -.486 ..., DYHUB= .195D-01

```

THE NUMBER OF REVOLUTIONS REQUIRED TO CONVERGE = 16

INPUT FIXED SYSTEM MODES FREQUENCIES IN HZ

5.10 6.40 15.3 16.3 13.8 11.6 12.1 17.4 21.1

THE CONVERGENCE FACTOR TO G = 30.2

BIFFILAR HARMONIC OUTPUT - AMPLITUDE AND PHASE

1

卷之三

1	- .535387D-03	- .713332D-03	- .107830D-02	.135130-01	.111270-01	.43362D-03	.25521D-03	.59209D-03	.93772D-04
2	.717840-04	.157370-03	.156350D-03	- .13798	.199540-02	.688499D-03	.466885D-03	.214467D-03	.27708D-03
3	.361945D-03	.730450D-03	.108666D-02	.113864	.111314D-01	.985515D-03	.506063D-03	.62981D-03	.295510-03
4	168.53	167.56	172.90	-84.407	10.156	-63.896	-64.214	-19.929	-71.303
5	.840535D-04	- .172840D-03	- .410975D-03	.947630D-01	- .980150D-02	.106481D-03	.62883D-04	.22187D-03	.38572D-04
6	.12153D-03	- .114595D-03	- .505350D-03	- .319350D-01	.164420D-02	- .19251D-03	- .16555D-04	- .223391D-03	.30311D-04
7	.14776D-03	.20757D-03	.682150D-03	.99985D-01	.100117D-01	.219190-03	.65056D-04	.31522D-03	.49135D-04
8	55.331	-166.37	-126.92	-18.623	9.44668	-61.433	-16.750	-45.263	38.090
9	.18633D-03	.124650D-03	- .20801D-03	.43658D-02	.29709D-02	.36247D-03	.16057D-03	.73188D-04	.68470D-04
10	- .20863D-04	- .20787D-04	- .10308D-03	.65451D-02	.67828D-02	- .10717D-03	- .29959D-04	- .29408D-04	.33223D-05
11	.18633D-03	.12689D-03	.23232D-03	.81157D-02	.70494D-02	.37798D-03	.16333D-03	.78859D-04	.60566D-04
12	-173.82	-170.53	-153.60	-52.813	66.346	-16.471	-10.552	-21.891	-3.0290
13	.111922D-04	.18351D-04	- .20946D-04	.10089D-02	.25708D-03	= .40229D-04	.18089D-04	= .63736D-05	= .77610D-05
14	- .34145D-05	.35567D-05	.17662D-05	- .17662D-05	- .65194D-03	- .93333D-05	- .43971D-05	- .42516D-05	- .22284D-05
15	.12181D-04	.18662D-04	.21006D-04	.10444D-02	.41367D-03	.61136D-04	.18815D-04	.76615D-05	.80743D-05
16	-16.279	10.969	-4.8173	-15.013	-68.479	-166.53	-166.34	-146.29	-163.96
17	.202465D-04	- .283000D-04	- .39200D-04	.11809D-02	.32143D-03	.43545D-04	.20206D-04	.17703D-04	.86765D-05
18	- .57440D-06	- .19054D-05	- .77411D-05	.25992D-03	.67686D-02	- .17481D-04	- .75718D-05	- .61179D-05	.33150D-05
19	.21225D-06	.28364D-06	.400465D-04	.28559D-02	.74930D-03	.469921D-04	.21578D-06	.18731D-04	.92917D-05
20	178.37	-176.15	-168.85	-65.566	64.596	-21.874	-20.543	-19.064	-20.932

18M 730687

FIGURE 8. Output Format - Bifilar Nonlinear Analysis Time History Results.

VIBRATION LEVELS AT 4 A/C LOCATIONS

COSINE, SINE, TOTAL AMPLITUDE IN G AND PHASE ANGLE IN DEGREES OF POINT 1

	1 P	2 P	3 P	4 P	5 P	6 P	7 P	8 P	9 P
1	.74646D-04	.10540D-03	.16495D-03	.68218D-02	-.17800D-03	-.13764D-03	-.67664D-04	-.77459D-04	-.32567D-04
	-.17197D-04	.10152D-04	.45770D-04	.16337D-01	.15142D-02	.87238D-05	.99550D-05	.72264D-05	.3596D-05
	.76601D-04	.15859D-03	.17105D-03	.17426D-01	.15246D-02	.13811D-03	.70234D-04	.77959D-04	.33389D-04
	-12.973	5.5052	15.381	113.04	-96.705	-176.38	-172.56	174.67	-167.27
2	-.44661D-03	-.23631D-03	-.40666D-01	-.25074D-01	-.26798D-02	-.55354D-03	-.25294D-03	-.10032D-03	-.11363D-03
	-.20551D-03	-.23320D-04	.36511D-05	.11033D-01	.88283D-02	.15354D-03	.87506D-04	-.16269D-04	.54112D-04
	.49145D-03	.23744D-03	.40664D-03	.27394D-01	.92660D-02	.57442D-03	.26763D-03	.10112D-03	.12594D-03
	-155.25	-174.36	179.46	23.751	106.89	15.532	19.083	-7.1226	25.547
3	-.21825D-03	-.39446D-03	-.56827D-03	-.13515D-01	-.38145D-02	.62622D-03	.29075D-03	.10752D-03	.12778D-03
	-.27555D-04	-.88199D-04	-.10098D-03	-.51186D-02	.92417D-02	.19102D-03	.96591D-04	-.33801D-04	.54140D-04
	-.21998D-03	-.40255D-03	-.57717D-03	-.14456D-01	.99380D-02	.65444D-03	.30642D-03	-.10050D-03	.13578D-03
	-172.81	-168.51	-169.92	-20.737	112.43	17.031	18.375	10.218	22.962

COSINE, SINE, TOTAL AMPLITUDE IN G AND PHASE ANGLE IN DEGREES OF POINT 2

	1 P	2 P	3 P	4 P	5 P	6 P	7 P	8 P	9 P
1	.10408D-03	.14141D-03	.21754D-03	-.67874D-02	-.71084D-03	-.18505D-03	-.30701D-04	-.99222D-04	-.40505D-04
	-.70700D-05	-.37834D-05	-.37375D-04	-.18411D-01	-.22560D-02	-.37913D-04	-.16089D-04	-.17450D-04	.68683D-04
	.10402D-03	.14146D-03	.22073D-03	.19622D-01	.23303D-02	.18869D-03	.92117D-04	.10074D-03	.4044D-04
	-3.8905	1.5338	9.7465	110.24	-107.27	168.42	169.94	170.03	170.76
2	-.79628D-03	-.27576D-03	-.32357D-03	.60930D-02	.96273D-02	.59969D-03	.25702D-03	.16243D-03	.93566D-04
	-.39016D-03	.16613D-03	.40307D-03	-.10963D-01	.11193D-01	-.76927D-03	-.39836D-03	-.23443D-03	.21426D-03
	.88443D-03	.32194D-03	.51688D-03	.14543D-01	.14763D-01	.97339D-03	.47408D-03	.27432D-03	.23618D-03
	-153.84	168.93	128.76	-60.936	49.299	-52.061	-57.171	-58.721	-65.120

COSINE, SINE, TOTAL AMPLITUDE IN G AND PHASE ANGLE IN DEGREES OF POINT 3

	1 P	2 P	3 P	4 P	5 P	6 P	7 P	8 P	9 P
3	.11721D-03	-.18746D-03	-.82776D-04	.15241D-01	-.12303D-01	.15987D-03	.82942D-04	-.57137D-05	.47371D-06
	-.22463D-04	-.15717D-03	-.76443D-04	.28371D-01	.86053D-03	.69882D-03	.33232D-03	.12336D-03	-.11070D-03
	.11950D-03	.24449D-03	.11261D-03	.32086D-01	.12335D-01	.71102D-03	.34310D-03	.12350D-03	.11715D-03
	10.839	-140.01	-137.28	61.755	176.00	77.007	76.010	92.652	74.490

IBM Z30687

FIGURE 8 (b). Continued.

INITIAL BIPLAR DISPLACEMENTS (LC.1720-1739)

.348890-01 -16560 .349550-01 .16568

INITIAL BIPLAR VELOCITIES (LC.1740-1759)

13.328 -3.5640 -13.417 3.5655

INITIAL HUB DISPLACEMENTS (LC.1768-1773)

.15065D-02 .35604D-02 .25974D-03 .45858D-04 .59105D-04 .10595D-04

INITIAL HUB VELOCITIES (LC.1774-1779)

-43641 -2.27048D-01 .16799D-01 .33085D-02 .43242D-02 .10283D-02

INITIAL STATE VARIABLES DISPL. (LC.1780-1859)

-.419300-04 .83752D-04 .47216D-04 .38650D-02 .19628D-03 -.44468D-03 -.97618D-03 .25778D-02 -.29684D-03 .10835D-02
-.47164D-04 -.53035D-05 .31298D-07 .36200D-03 -.56627D-02 .10109D-01 -.131128D-02 -.135222D-03 -.92779D-04 .56515D-04
.138300-04 .56357D-02 .207400-01 .11073 .51973D-01

INITIAL STATE VARIABLES. VELOC. (LC.1860-1939)

.476500-01 -.11799D-01 -.21021 .15078 .14798 -.33559D-01 -.99727D-01 -.22058 .18196 .20168D-01
.10169 -.33443D-03 -.11013D-04 -.1.2027 .30740D-01 .67974 -.27664 .92194D-02 .76840D-02 .44570D-03
.279445D-02 .297460 .27402 5.2717 14.502

(c)

FIGURE 8. Concluded.

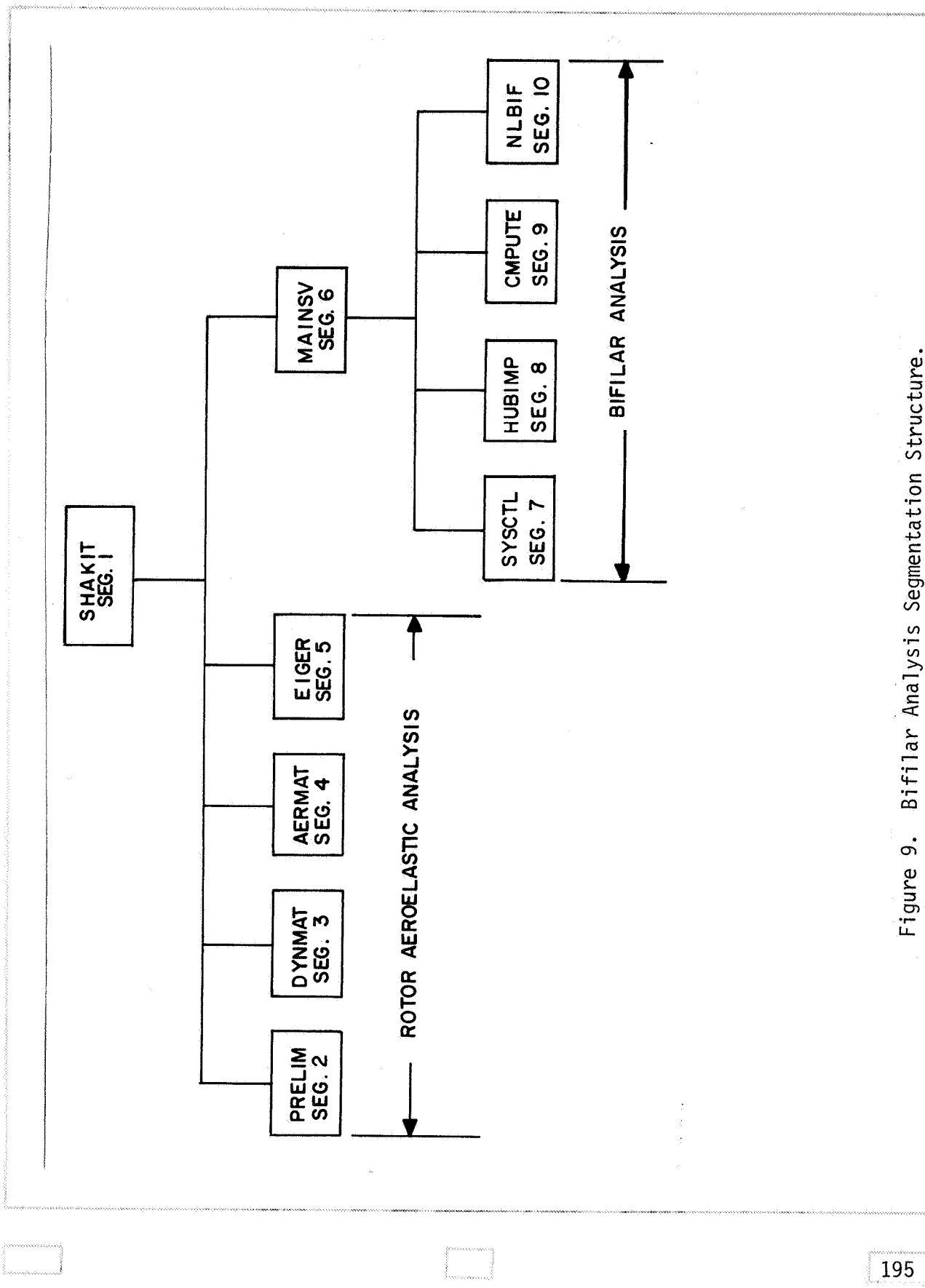


Figure 9. Bifilar Analysis Segmentation Structure.

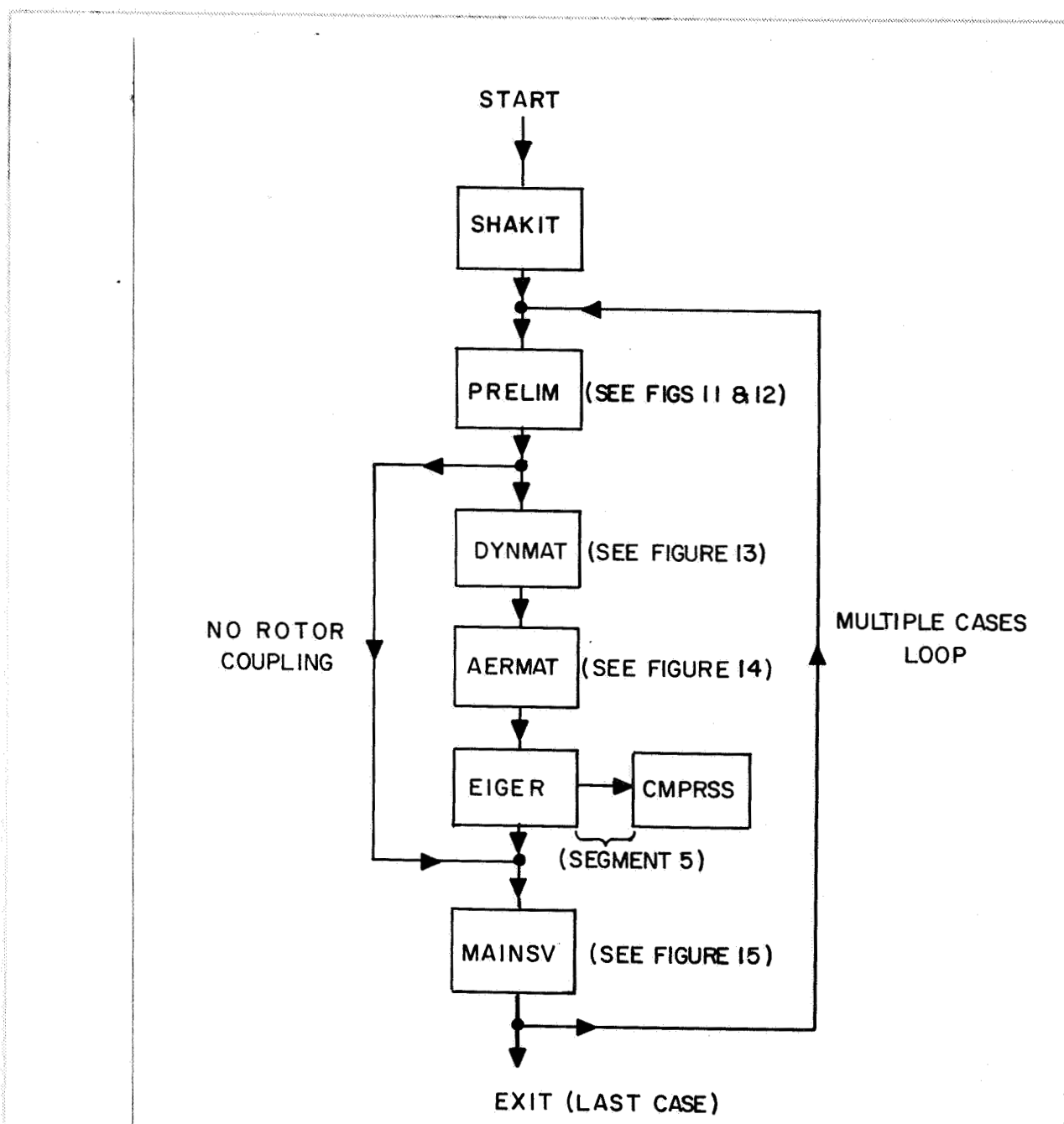


Figure 10. Flow Chart for the Main Program.

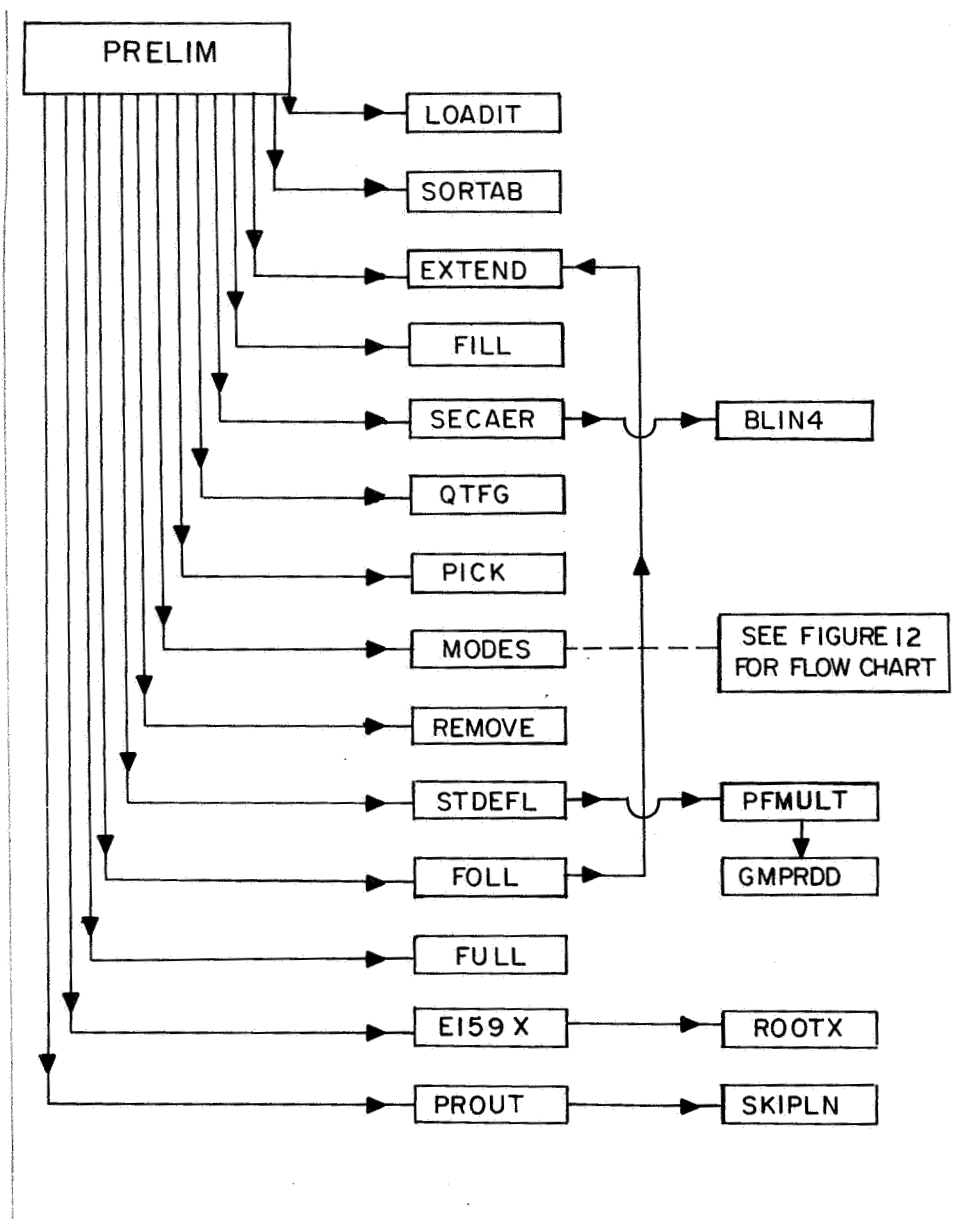


Figure 11. Flow Chart for Subroutine PRELIM.

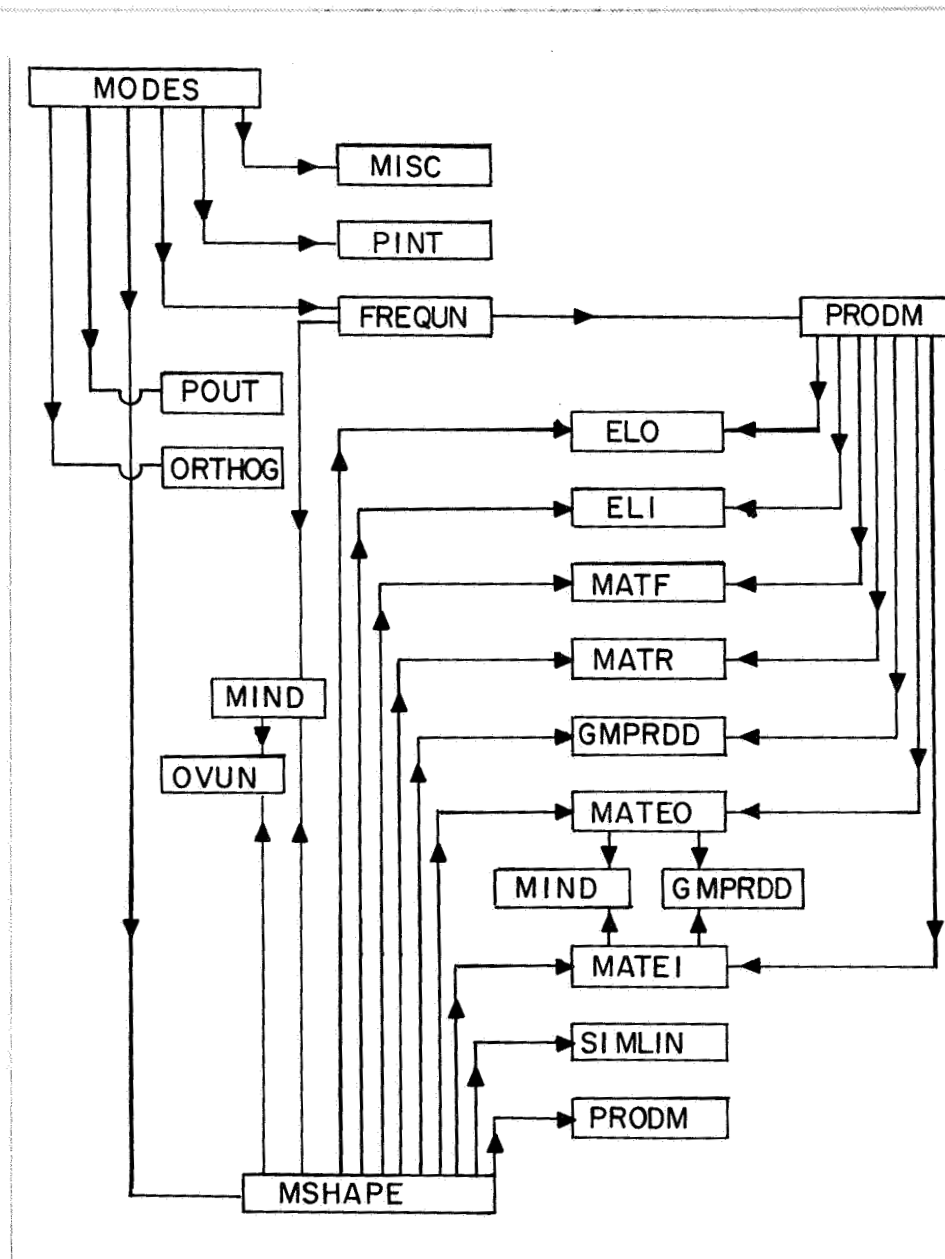


Figure 12. Flow Chart for Subroutine MODES.

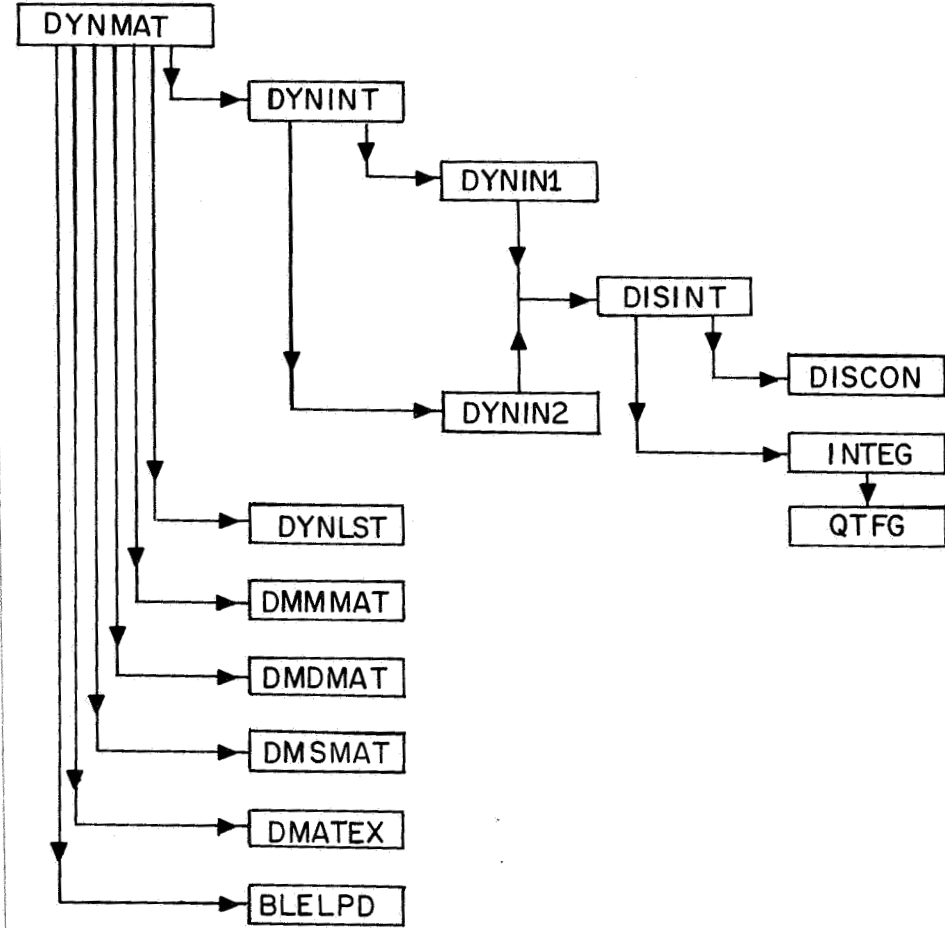


Figure 13. Flow Chart for Subroutine DYNMAT.

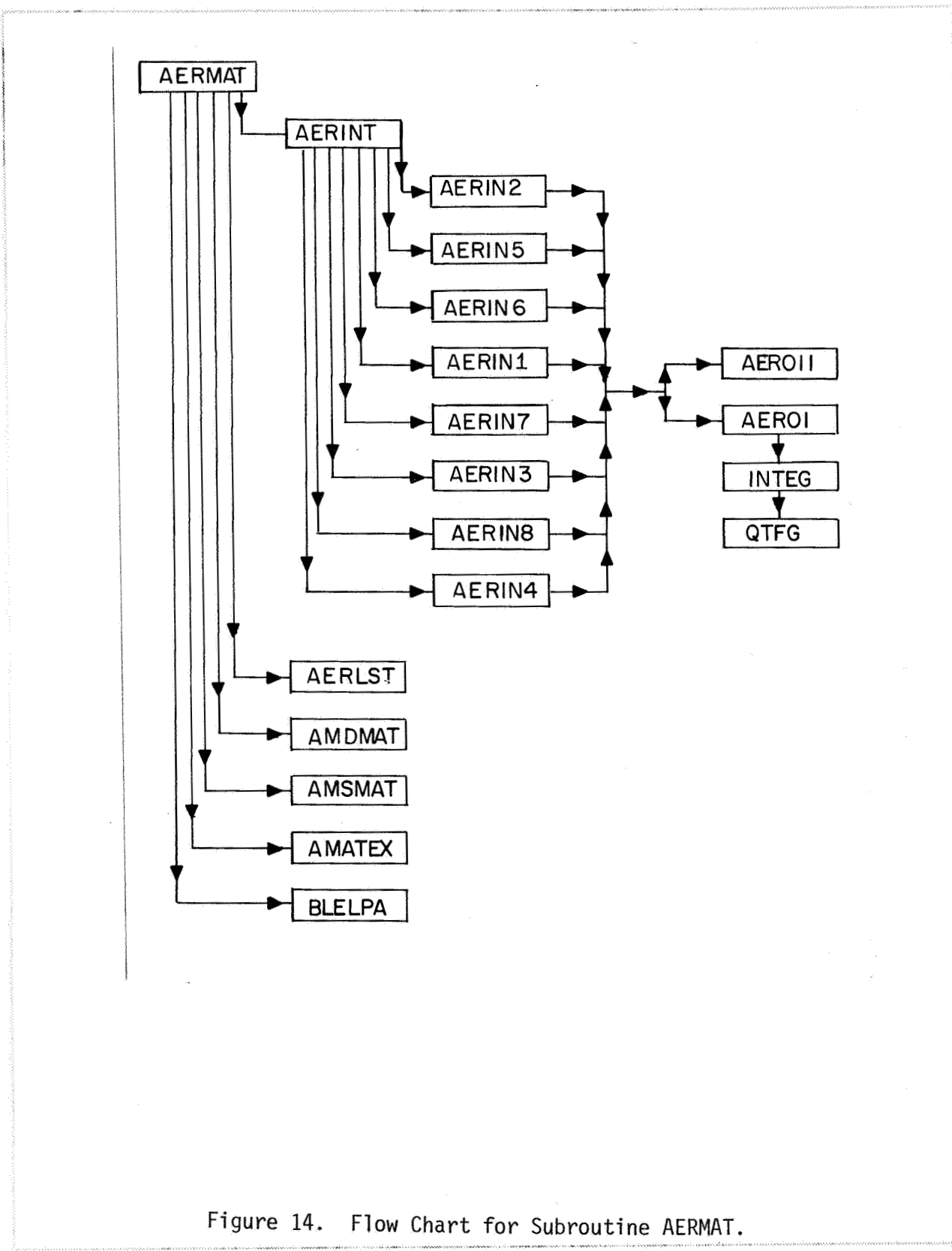


Figure 14. Flow Chart for Subroutine AERMAT.

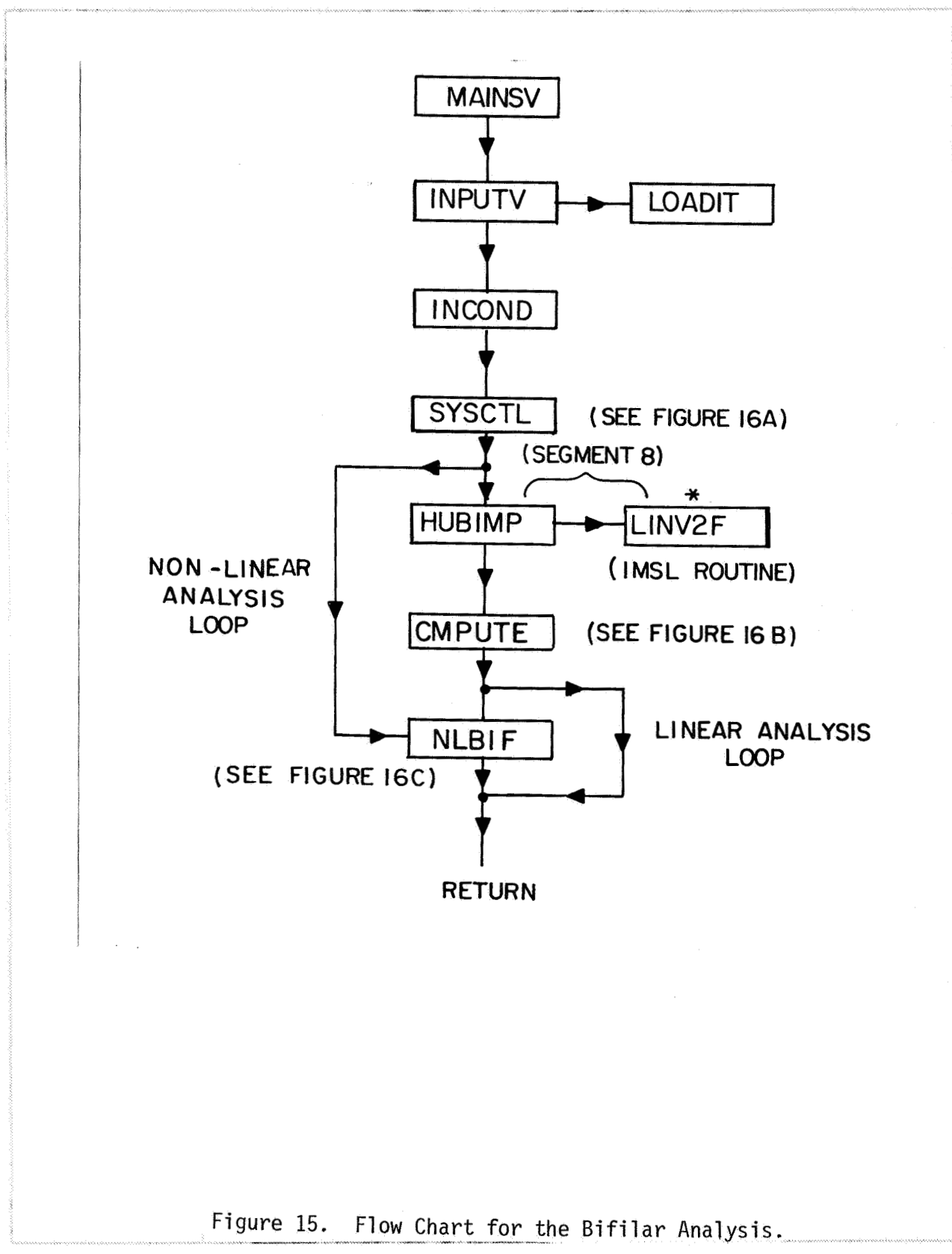
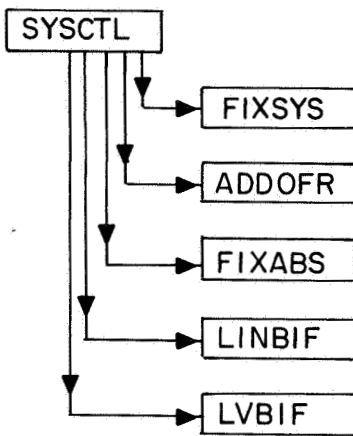
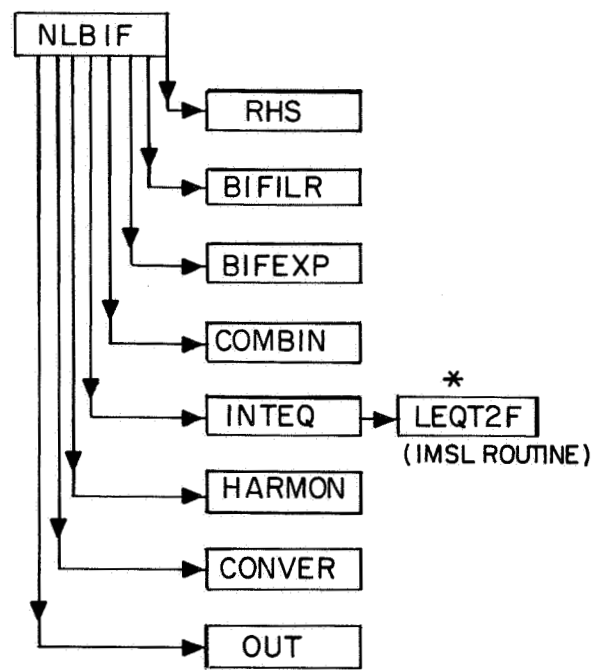


Figure 15. Flow Chart for the Bifilar Analysis.

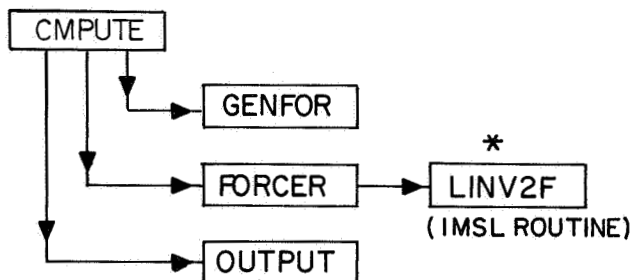




16a. SYSCTL Flow Chart.



16c. NLBIF Flow Chart.



16b. CMPUTE Flow Chart.

Figure 16. Flow Charts for Subroutines SYSCTL, CMPUTE, NLBIF.

		46 47 48 49 50 51 52 53 54 55 56 57 58 59 60 61 62 63 64 65 66 67 68 69 70 71 72 73 74 75 76 77 78 79 80 81 82 83 84 85 86 87 88 89 90 91 92			SUBROUTINE COMMON BLOCK	
		SYSCTL STDEFI SORTAB SKIPLN SIMLIN SHAKIT SECAER ROOTX RHS REMOVE QTFG PROUT PRODM PRELIM POUT PINT PICK PFMULT OVUN OUTPUT OUT ORTHOG NLBIF MSHAPE MODES MISC MIND MATR MATF MATEO MAINSV LVBIF LOADIT LINBIF INTEQ INTEG INPUTV INCOND HUBIMP HARMON GMPROD GENFOR FULL FREQUN FORCER FOLL			BLANK AERO1 AERO2 AERO3 AERO4 AERO5 AERO6 COCAER CONT DAT DNINP DNOUT ENATTI ENATO EOF6 FRAT FREQ HARM INDAT INEIG INEIGN LAGDAM NAMIC NDOF NMIC NLDATA1 NLDATA2 PHONO PHAT PRAMI PANTS PANTS PRSMTH TIDS TORFIN TOTMAT TWISTM WORKA XRDATA	
COMMON BLOCK	SUBROUTINE	BLANK AERO1 AERO2 AERO3 AERO4 AERO5 AERO6 COCAER CONT DAT DNINP DNOUT ENATTI ENATO EOF6 FRAT FREQ HARM INDAT INEIG INEIGN LAGDAM NAMIC NDOF NMIC NLDATA1 NLDATA2 PHONO PHAT PRAMI PANTS PANTS PRSMTH TIDS TORFIN TOTMAT TWISTM WORKA XRDATA	BLANK AERO1 AERO2 AERO3 AERO4 AERO5 AERO6 COCAER CONT DAT DNINP DNOUT ENATTI ENATO EOF6 FRAT FREQ HARM INDAT INEIG INEIGN LAGDAM NAMIC NDOF NMIC NLDATA1 NLDATA2 PHONO PHAT PRAMI PANTS PANTS PRSMTH TIDS TORFIN TOTMAT TWISTM WORKA XRDATA	BLANK AERO1 AERO2 AERO3 AERO4 AERO5 AERO6 COCAER CONT DAT DNINP DNOUT ENATTI ENATO EOF6 FRAT FREQ HARM INDAT INEIG INEIGN LAGDAM NAMIC NDOF NMIC NLDATA1 NLDATA2 PHONO PHAT PRAMI PANTS PANTS PRSMTH TIDS TORFIN TOTMAT TWISTM WORKA XRDATA	BLANK AERO1 AERO2 AERO3 AERO4 AERO5 AERO6 COCAER CONT DAT DNINP DNOUT ENATTI ENATO EOF6 FRAT FREQ HARM INDAT INEIG INEIGN LAGDAM NAMIC NDOF NMIC NLDATA1 NLDATA2 PHONO PHAT PRAMI PANTS PANTS PRSMTH TIDS TORFIN TOTMAT TWISTM WORKA XRDATA	
1	BLANK	X	X	X	X	
2	AERO1	X	X	X	X	
3	AERO2	X	X	X	X	
4	AERO3	X	X	X	X	
5	AERO4	X	X	X	X	
6	AERO5	X	X	X	X	
7	AERO6	X	X	X	X	
8	COCAER	X	X	X	X	
9	CONT	X	X	X	X	
10	DAT	X	X	X	X	
11	DNINP	X	X	X	X	
12	DNOUT	X	X	X	X	
13	ENATTI	X	X	X	X	
14	ENATO	X	X	X	X	
15	EOF6	X	X	X	X	
16	FRAT	X	X	X	X	
17	FREQ	X	X	X	X	
18	HARM	X	X	X	X	
19	INDAT	X	X	X	X	
20	INEIG	X	X	X	X	
21	INEIGN	X	X	X	X	
22	LAGDAM	X	X	X	X	
23	NAMIC	X	X	X	X	
24	NDOF	X	X	X	X	
25	NMIC	X	X	X	X	
26	NLDATA1	X	X	X	X	
27	NLDATA2	X	X	X	X	
28	PHATNO	X	X	X	X	
29	PHAT	X	X	X	X	
30	PRAMI	X	X	X	X	
31	PANTS	X	X	X	X	
32	PANTS	X	X	X	X	
33	TIDS	X	X	X	X	
34	TORFIN	X	X	X	X	
35	TOTMAT	X	X	X	X	
36	TWISTM	X	X	X	X	
37	WORKA	X	X	X	X	
	XRDATA	X	X	X	X	

(a)

Figure 17. COMMON Blocks.

SUBROUTINE		1	2	3	4	5	6	7	8	9	10	11	12	13	14	15	16	17	18	19	20	21	22	23	24	25	26	27	28	29	30	31	32	33	34	35	36	37	38	39	40	41	42	43	44	45
COMMON BLOCK	SUBROUTINE	COMMON BLOCK																																												
1	BLANK	X	X	X	X	X	X	X	X	X	X	X	X	X	X	X	X	X	X	X	X	X	X	X	X	X	X	X	X	X	X	X	X	X	X	X	X	X	X	X						
2	AERO1	X	X	X	X	X	X	X	X	X	X	X	X	X	X	X	X	X	X	X	X	X	X	X	X	X	X	X	X	X	X	X	X	X	X	X	X	X	X							
3	AERO2	X	X	X	X	X	X	X	X	X	X	X	X	X	X	X	X	X	X	X	X	X	X	X	X	X	X	X	X	X	X	X	X	X	X	X	X	X	X							
4	AERO3	X	X	X	X	X	X	X	X	X	X	X	X	X	X	X	X	X	X	X	X	X	X	X	X	X	X	X	X	X	X	X	X	X	X	X	X	X	X							
5	AERO4	X	X	X	X	X	X	X	X	X	X	X	X	X	X	X	X	X	X	X	X	X	X	X	X	X	X	X	X	X	X	X	X	X	X	X	X	X	X							
6	AERO5	X	X	X	X	X	X	X	X	X	X	X	X	X	X	X	X	X	X	X	X	X	X	X	X	X	X	X	X	X	X	X	X	X	X	X	X	X	X							
7	COCACER	X	X	X	X	X	X	X	X	X	X	X	X	X	X	X	X	X	X	X	X	X	X	X	X	X	X	X	X	X	X	X	X	X	X	X	X	X	X							
8	CONT	X	X	X	X	X	X	X	X	X	X	X	X	X	X	X	X	X	X	X	X	X	X	X	X	X	X	X	X	X	X	X	X	X	X	X	X	X	X							
9	DAT	X	X	X	X	X	X	X	X	X	X	X	X	X	X	X	X	X	X	X	X	X	X	X	X	X	X	X	X	X	X	X	X	X	X	X	X	X	X							
10	DYNINP	X	X	X	X	X	X	X	X	X	X	X	X	X	X	X	X	X	X	X	X	X	X	X	X	X	X	X	X	X	X	X	X	X	X	X	X	X	X							
11	DYNOUT	X	X	X	X	X	X	X	X	X	X	X	X	X	X	X	X	X	X	X	X	X	X	X	X	X	X	X	X	X	X	X	X	X	X	X	X	X	X							
12	ENATI	X	X	X	X	X	X	X	X	X	X	X	X	X	X	X	X	X	X	X	X	X	X	X	X	X	X	X	X	X	X	X	X	X	X	X	X	X	X							
13	ENATO	X	X	X	X	X	X	X	X	X	X	X	X	X	X	X	X	X	X	X	X	X	X	X	X	X	X	X	X	X	X	X	X	X	X	X	X	X	X							
14	EOF6	X	X	X	X	X	X	X	X	X	X	X	X	X	X	X	X	X	X	X	X	X	X	X	X	X	X	X	X	X	X	X	X	X	X	X	X	X	X							
15	FMAT	X	X	X	X	X	X	X	X	X	X	X	X	X	X	X	X	X	X	X	X	X	X	X	X	X	X	X	X	X	X	X	X	X	X	X	X	X	X							
16	FREQ	X	X	X	X	X	X	X	X	X	X	X	X	X	X	X	X	X	X	X	X	X	X	X	X	X	X	X	X	X	X	X	X	X	X	X	X	X	X							
17	HARM	X	X	X	X	X	X	X	X	X	X	X	X	X	X	X	X	X	X	X	X	X	X	X	X	X	X	X	X	X	X	X	X	X	X	X	X	X	X							
18	INDAT	X	X	X	X	X	X	X	X	X	X	X	X	X	X	X	X	X	X	X	X	X	X	X	X	X	X	X	X	X	X	X	X	X	X	X	X	X	X							
19	INEIG	X	X	X	X	X	X	X	X	X	X	X	X	X	X	X	X	X	X	X	X	X	X	X	X	X	X	X	X	X	X	X	X	X	X	X	X	X	X							
20	LAGDAM	X	X	X	X	X	X	X	X	X	X	X	X	X	X	X	X	X	X	X	X	X	X	X	X	X	X	X	X	X	X	X	X	X	X	X	X	X	X							
21	NAGDAM	X	X	X	X	X	X	X	X	X	X	X	X	X	X	X	X	X	X	X	X	X	X	X	X	X	X	X	X	X	X	X	X	X	X	X	X	X	X							
22	NAMIC	X	X	X	X	X	X	X	X	X	X	X	X	X	X	X	X	X	X	X	X	X	X	X	X	X	X	X	X	X	X	X	X	X	X	X	X	X	X							
23	NDOF	X	X	X	X	X	X	X	X	X	X	X	X	X	X	X	X	X	X	X	X	X	X	X	X	X	X	X	X	X	X	X	X	X	X	X	X	X	X							
24	NHIC	X	X	X	X	X	X	X	X	X	X	X	X	X	X	X	X	X	X	X	X	X	X	X	X	X	X	X	X	X	X	X	X	X	X	X	X	X	X							
25	NLDAT1	X	X	X	X	X	X	X	X	X	X	X	X	X	X	X	X	X	X	X	X	X	X	X	X	X	X	X	X	X	X	X	X	X	X	X	X	X	X							
26	NLDAT2	X	X	X	X	X	X	X	X	X	X	X	X	X	X	X	X	X	X	X	X	X	X	X	X	X	X	X	X	X	X	X	X	X	X	X	X	X	X							
27	PHITQ	X	X	X	X	X	X	X	X	X	X	X	X	X	X	X	X	X	X	X	X	X	X	X	X	X	X	X	X	X	X	X	X	X	X	X	X	X	X							
28	PMAT	X	X	X	X	X	X	X	X	X	X	X	X	X	X	X	X	X	X	X	X	X	X	X	X	X	X	X	X	X	X	X	X	X	X	X	X	X	X							
29	PRAM1	X	X	X	X	X	X	X	X	X	X	X	X	X	X	X	X	X	X	X	X	X	X	X	X	X	X	X	X	X	X	X	X	X	X	X	X	X	X							
30	PRNTSW	X	X	X	X	X	X	X	X	X	X	X	X	X	X	X	X	X	X	X	X	X	X	X	X	X	X	X	X	X	X	X	X	X	X	X	X	X	X							
31	PRSNTH	X	X	X	X	X	X	X	X	X	X	X	X	X	X	X	X	X	X	X	X	X	X	X	X	X	X	X	X	X	X	X	X	X	X	X	X	X	X							
32	TMDS	X	X	X	X	X	X	X	X	X	X	X	X	X	X	X	X	X	X	X	X	X	X	X	X	X	X	X	X	X	X	X	X	X	X	X	X	X	X							
33	TORFIN	X	X	X	X	X	X	X	X	X	X	X	X	X	X	X	X	X	X	X	X	X	X	X	X	X	X	X	X	X	X	X	X	X	X	X	X	X	X							
34	TOMAT	X	X	X	X	X	X	X	X	X	X	X	X	X	X	X	X	X	X	X	X	X	X	X	X	X	X	X	X	X	X	X	X	X	X	X	X	X	X							
35	TWISTM	X	X	X	X	X	X	X	X	X	X	X	X	X	X	X	X	X	X	X	X	X	X	X	X	X	X	X	X	X	X	X	X	X	X	X	X	X	X							
36	WORKA	X	X	X	X	X	X	X	X	X	X	X	X	X	X	X	X	X	X	X	X	X	X	X	X	X	X	X	X	X	X	X	X	X	X	X	X	X	X							
37	XFRDAT	X	X	X	X	X	X	X	X	X	X	X	X	X	X	X	X	X	X	X	X	X	X	X	X	X	X	X	X	X	X	X	X	X	X	X	X	X	X							

(b)

Figure 17. Concluded.

* * APPENDIX A. JOB CONTROL LANGUAGE

```
CARD NO.      JOB CONTROL LANGUAGE TO RUN ROTOR>BIFLAR COUPLED PROGRAM
=====
1 //E90BCRUN JOB (4045,STAL,02,25),'CASARINO - X-6565',MSGCLASS=T,
   REGION=000K,NGLLEVEL=1,TIME=02,CLASS=,NOTIFY=ET473
   //----- ROTOR/BIFLAR COUPLED PROGRAM
   //----- USES OVERLAY STRUCTURE DOUBLE PRECISION VERSION
   //----- MODULE IS E90BCFIN & IS FOUND IN "ET473.SEBBY.LOAD"
   //----- INPUT COMES FROM "ET473.BIFLAR.DATA(NASARUN)"
```

2 //STEP01 EXEC PGM=E90BCFIN
3 //STEPLIB DD DSN=ET473.SEBBY.LOAD,DISP=SHR
4 //FT05F001 DD DSN=ET473.BIFLAR.DATA(NASARUN),DISP=SHR
5 //-----
6 //FT06F001 DD SYSOUT=TT DUMMY
7 //FT07F001 DD UNIT=NORK,DISP=(NEW,DELETE),SPACE=(TRK,(5,1)),
 DCB=(RECFM=VSB,LRECL=680,BLKSIZE=050)
8 //FT11F001 DD UNIT=NORK,DISP=(NEW,DELETE),SPACE=(TRK,(15,1)),
 DCB=(RECFM=VSB,LRECL=404,BLKSIZE=2050),
9 //-----
*----- END OF JOB CONTROL LANGUAGE

APPENDIX B. TEST CASES INPUT DATA

NASA	TEST	CASES :	WITH ROTOR	LINEAR ANALYSIS OPTION
CASE 1.		CASE 2.	WITH ROTOR	NON-LINEAR ANALYSIS OPTION
CASE 3.		CASE 4.	NO ROTOR	LINEAR ANALYSIS OPTION
			NO ROTOR	NON-LINEAR ANALYSIS OPTION

INPUT TO ROTOR/BIFILAR COUPLED PROGRAM

CARD FORMAT = A,B,C,D E,F,G	
WHERE :	A = COLUMN 2 - 6, NO. OF ITEMS, INTEGER (5 MAXIMUM)
B = COLUMNS 7 - 18, LOCATION NO., INTEGER, (RIGHT ADJUSTED)	
C = COLUMNS 19-30, QUANTITY, REAL	
D = COLUMNS 31-42, QUANTITY, REAL	
E = COLUMNS 43-54, QUANTITY, REAL	
F = COLUMNS 55-66, QUANTITY, REAL	
G = COLUMNS 55-66,	

COLUMN NUMBER		BEGINNING OF INPUT	
123456789012345678901234567890123456789012345678901234567890			
5 1 0.002378	1116. 99	.0	258.
3 6 26.833333	1.25		
5 13 6.4	1.000000.	15.1265	.75
2 19 258.0	2.		
3 107 1.	0.	1.	
1 111 1.	0.		
3 113 01000111.	1.	11.	
1 119 5.			
1 125 1.			
5 126 27.074	11.238	9.178	6.82
3 131 1.	676. 0.		
1 200 20.			
5 201 17.5	17.5	25.	16.8
5 206 16.8	16.8	16.8	17.49
5 211 17.49	17.49	15.9	15.9
5 216 12.97	12.97	7.7	7.7
1 250 20.			
4 251 0.			
4 255 15.01	0.	15.	0.
4 259 50.01	8.3	50.	8.3
4 263 228.97	20.76	228.96	20.76
4 267 276.67	22.317	276.66	22.317
1 350 14.	20.76	322.	20.76
4 351 0.			
4 355 270.	-9.5	50.	-9.5
6 359 305.	1.2	290.	2.8
2 363 322.	3.8	318.	1.2
1 450 14.	1.2		
4 451 0.	-9.5	50.	-9.5
4 455 270.	1.2	290.	2.8
4 459 305.	3.8	318.	1.2
2 463 322.	1.2		

1	550	58.
4	551	.0.
4	555	.75.
4	559	159.01
4	563	192.01
4	567	210.01
4	571	220.01
4	575	228.36
4	579	240.
4	583	270.31
4	587	276.67
4	591	290.
4	595	299.
4	599	301.25
4	603	306.695
2	607	322.
1	650	18.
4	651	.0.
4	655	.50.01
4	659	228.97
4	663	276.67
2	667	322.
1	750	20.
4	751	.0.
4	755	15.01
4	759	50.01
4	763	228.97
4	767	276.67
1	950	52.
4	951	.0.
4	955	2.07
4	959	2.10
4	963	.93
4	967	.56
4	971	.53
4	975	.5812
4	979	.69551
4	983	1.51
4	987	1.6447
4	991	1.46447
4	995	.75
4	999	.25
1	1050	.34.
2	1051	.0.
4	1053	.55.02
4	1057	644.2
4	1061	532.5
4	1065	443.
4	1069	650.
4	1073	900.
4	1077	830.
4	1081	590..
1	11150	.34.
2	11151	.0.
4	11153	.55.02
4	11157	305.5
4	11161	237.
4	11165	54.
4	11169	24.37
4	11173	25.43

41177	27.19	40.	26.95	30.3
41181	24.95	1.7	22.95	50.
41350	32.	15.	.00269	8.3
41351	0	2.8	.00823	3.9
41355	.00479	15.83	.02398	29.17
41359	.01842	15.83	.03474	61.04
41363	.0318	84.96	.04665	12.34
41367	.03971	8.96	.03381	8.3
41371	.04354	36.66	.05861	13.5
41375	.06848	2.	.03805	
41379	.05723	9.5		
41450	32.	15.		
41451	0	2.8	.00269	8.3
41455	.00479	15.83	.00823	3.9
41459	.01842	15.83	.02398	29.17
41463	.0318	84.96	.03474	61.04
41467	.03971	8.96	.04665	12.34
41471	.04354	36.66	.03381	8.3
41475	.06848	2.	.05861	13.5
41479	.05723	9.5	.03805	
41550	12.			
41551	0	15.	70320000.	31.
41555	47600000.		25600000.	9.5
41559	27050000.		27870000.	247.
41773	50000.			
21779	17.4	10.75		
41850	32.	0.000	.0000	.0200
41854	-179.000		.0250	.0650
41858	-172.000		.1100	.6620
41862	-115.000		.1.8800	1.8800
41866	-30.000		.6300	.6300
41870	-10.000		.2500	.0860
41874	-6.0000		.0500	.0390
41878	-4.8000		.0280	.0180
41882	-3.0000		.0110	.0090
41886	-4.0000		.0100	.0130
41890	10.0000		.0140	.0180
41894	12.0000		.0220	.0300
41898	14.0000		.0640	.1780
41902	29.9000		.6300	.6300
41906	65.0000		1.8800	.6420
41910	172.0000		.1.1000	.175.0000
41914	180.0000		.0200	.0050
41925	32.000		.3000	.180.0000
41929	-179.000		.0250	.0200
41933	-172.000		.1100	.6420
41937	-115.000		1.8800	1.8800
41941	-30.000		.6300	.6300
41945	-10.0000		.2500	.0860
41949	-6.0000		.0500	.0390
41953	-4.8000		.0280	.0180
41957	-3.0000		.0110	.0090
41961	4.0000		.0140	.0130
41965	10.0000		.1100	.0180
41969	12.0000		.0220	.0300
41973	14.0000		.0640	.1780
41977	29.9000		.6300	.6300
41981	65.0000		1.8800	.6420
41985	172.0000		.1100	.175.0000
41989	180.0000		.0200	.0050

42000	19.0000	-4000	-30.0000	6300
42004	-10.0000	-2600	-5.0000	1010
42008	-4.5000	-6.0000	-4.0000	0340
42012	-3.0000	-0.0200	-2.0000	0130
42016	1.0000	-0.0100	-0.0800	0080
42020	6.0000	-0.0110	-3.0000	0090
42024	9.0000	-0.0175	-10.0000	0150
42028	11.0000	-0.0500	-12.8000	0270
42032	15.0000	-0.2300	-30.0000	1360
42036	19.0000	-0.5000	-30.0000	6300
42040	-10.0000	-0.0100	-0.0400	0270
42044	-6.0000	-0.0700	-5.0000	01780
42048	-4.0000	-0.0240	-3.0000	0150
42052	-2.0000	-0.0100	-1.0000	0085
42056	4.0000	-0.0080	-2.0000	0080
42060	6.0000	-0.0095	-5.0000	0110
42064	8.0000	-0.0180	-7.0000	01780
42068	15.0000	-0.0440	-30.0000	6300
42072	20.0000	-0.2800	-30.0000	6300
42076	-10.0000	-0.0800	-8.0000	01370
42080	-6.0000	-0.0810	-5.0000	00450
42084	-4.6000	-0.0350	-4.0000	0250
42088	-3.0000	-0.0170	-2.0000	0120
42092	-1.0000	-0.0085	-1.0000	0080
42096	1.0000	-0.0080	-2.0000	0100
42100	3.0000	-0.0160	-4.0000	0250
42104	5.0000	-0.0380	-6.0000	0660
42108	10.0000	-0.1760	15.0000	3000
42112	14.0000	-0.7000	-30.0000	6300
42116	10.0000	-0.3100	-7.0000	1550
42120	-6.0000	-0.0940	-5.0000	0600
42124	-3.0000	-0.0270	-2.0000	0130
42128	-1.0000	-0.0100	-1.0000	0100
42132	1.0000	-0.0115	-2.0000	0250
42136	3.0000	-0.1600	15.0000	3200
42140	15.0000	-0.7500	-30.0000	6300
42144	-10.0000	-0.3260	-7.0000	1680
42148	-1.0000	-0.1090	-5.0000	0850
42152	8.0000	-0.0200	-2.0000	0150
42156	30.0000	-0.1600	-30.0000	6300
42160	75.0000	-0.3200	-7.0000	1550
42164	-10.0000	-0.3260	-8.0000	1680
42168	-2.4000	-0.0200	-2.0000	0150
42172	-1.0000	-0.1200	-1.0000	0135
42176	1.0000	-0.1340	-7.0000	1550
42180	6.0000	-0.3300	-30.0000	6300
42184	15.0000	-0.8000	-30.0000	6300
42188	20.0000	-1.2900	-10.0000	2250
42192	-12.0000	-0.1700	-6.0000	1220
42196	-8.0000	-0.0750	-3.0000	0420
42200	-4.0000	-0.0240	-4.0000	0950
42204	1.0000	-0.2800	-1.0000	0260
42208	6.0000	-0.0255	-1.0000	0420
42212	10.0000	-0.0350	-4.0000	1080
42216	16.0000	-0.0700	-8.0000	1850
42220	30.0000	-0.1480	-12.0000	2850
42224	-9.0000	-0.2300	-11.0000	0180
42228	17.0000	-0.3000	-30.0000	6300
42232	-12.0000	-0.3300	-10.0000	2620

42458	-8.0000	.2100
42462	-6.0000	.1150
42466	-1.0000	.0630
42470	4.0000	.0780
42474	8.0000	.1380
42478	12.0000	.2210
42482	15.0000	.3225
42525	-12.0000	1.0000
42529	-12.0000	-3.7000
42533	-8.0000	-2.6800
42537	-4.0000	-1.5200
42541	4.0000	-1.0000
42545	8.0000	-1.7000
42549	12.0000	-2.5500
42553	15.0000	-3.6300
42600	-12.0000	2.0000
42604	-8.0000	-3.6200
42608	-4.0000	-2.4800
42612	-4.0000	-1.5200
42616	4.0000	-1.0000
42620	4.0000	-1.7000
42624	8.0000	-2.5500
42628	12.0000	-3.425
42750	26.0000	.0000
42754	-1172.0000	.7800
42758	-1156.0000	.6600
42762	-11.7000	-39.0000
42766	6.7000	-8.0000
42770	5.0000	-6.0000
42774	11.0000	-7.4000
42778	15.0000	-1.4900
42782	20.0000	1.2100
42786	30.0000	1.0000
42790	149.0000	30.1000
42794	156.0000	150.0000
42798	160.0000	-7.0000
42802	180.0000	-64.0000
42806	226.0000	-90.0000
42825	-1172.0000	-300.0000
42829	-1158.0000	.7800
42833	-11.7000	.6600
42837	-10.0000	-8.0000
42841	-6.7000	-6.0000
42845	5.0000	-7.4000
42849	11.0000	1.2100
42853	15.0000	1.0000
42857	20.0000	30.1000
42861	149.0000	150.0000
42865	156.0000	-7.0000
42869	160.0000	-64.0000
42873	180.0000	-90.0000
42877	180.0000	-40.0000
42900	13.0000	-10.0000
42904	-10.0000	-7.4000
42908	-7.0000	-6.0000
42912	7.0000	-1.0400
42916	9.0000	1.2200
42920	11.2000	1.1290
42924	18.0000	1.1200
42975	14.0000	-30.0000
42979	-10.0000	-8.5000

42983	-7.0000	4700
42991	6.0000	-5.0000
42995	10.0000	7.0000
42999	12.0000	9.0000
43003	30.0000	11.0000
43005	18.0000	11.0000
43054	-10.0000	16.0000
43058	-6.0000	14.0000
43062	-14.0000	11.0000
43066	-2.0000	-1.0000
43070	-4.0000	-1.0000
43074	4.0000	-1.0000
43078	6.0000	-1.0000
43082	14.0000	-1.0000
43086	30.0000	-1.0000
43125	15.0000	-1.0000
43129	-10.0000	-1.0000
43133	-15.8000	-1.0000
43137	-14.0000	-1.0000
43141	-12.0000	-1.0000
43145	3.0000	-1.0000
43149	5.0000	-1.0000
43153	15.0000	-1.0000
43200	15.0000	-1.0000
43204	-10.0000	-1.0000
43208	-15.7000	-1.0000
43212	-14.0000	-1.0000
43216	-12.0000	-1.0000
43220	-2.0000	-1.0000
43224	4.0000	-1.0000
43228	15.0000	-1.0000
43275	15.0000	-1.0000
43279	-14.0000	-1.0000
43283	-10.0000	-1.0000
43287	-2.0000	-1.0000
43291	2.0000	-1.0000
43295	6.0000	-1.0000
43299	9.0000	-1.0000
43303	19.0000	-1.0000
43350	14.0000	-1.0000
43354	-16.0000	-1.0000
43358	-12.0000	-1.0000
43362	-12.0000	-1.0000
43366	-2.0000	-1.0000
43370	6.0000	-1.0000
43374	9.0000	-1.0000
43378	30.0000	-1.0000
43425	14.0000	-1.0000
43429	-16.0000	-1.0000
43433	-10.0000	-1.0000
43437	-2.0000	-1.0000
43441	1.0000	-1.0000
43445	4.0000	-1.0000
43449	8.0000	-1.0000
43453	30.0000	-1.0000
43500	13.0000	-1.0000
43504	-16.0000	-1.0000
43508	-10.0000	-1.0000
43512	-2.0000	-1.0000

43516	2.0000	.1800	4.0000	.4350
43520	6.0000	.8000	8.0000	.7950
43524	10.0000	.3000	1.0000	1.0000
43528	13.0000	-2.0000	-30.0000	-6.9500
43532	-16.0000	-7.2000	-6.0000	-6.6500
43535	-10.0000	-6.0000	-12.0000	-0.0500
43537	-2.0000	-2.0000	4.0000	-4490
43541	2.0000	2.0000	8.0000	-8060
43545	6.0000	7.0000	30.0000	1.0000
43549	10.0000	8.0000	180.0000	-0.0000
43553	13.0000	33.0000	80.0000	-0.0000
43557	-16.0000	-174.0000	-390.0000	-160.0000
43561	-2.0000	-145.0000	4810	-125.0000
43562	-90.0000	550	-60.0000	-5570
43566	-30.0000	1637	-30.0000	-3950
43569	-10.0000	-7.4000	-7.4000	-1637
43573	-6.0000	1.065	1.065	-0.689
43574	-6.4000	0.052	-5.0000	0.032
43578	4.0000	0.019	14.0000	0.35
43582	15.2000	-1.932	19.0000	-1.303
43586	30.0000	-1.937	30.1000	-1.937
43590	34.9000	-2.920	35.0000	-2.220
43594	45.0000	-2.950	60.0000	-3950
43598	80.0000	-5.000	95.0000	-5550
43602	110.0000	-15.000	125.0000	-5520
43706	135.0000	-1.380	145.0000	-1.810
43710	150.0000	-4.380	160.0000	-3000
43714	174.0000	-3.590	180.0000	-6130
43725	33.0000	-3.000	-180.0000	-1.130
43729	-174.0000	-3.590	-160.0000	-3000
43733	-165.0000	-4.810	-125.0000	-5570
43737	-90.0000	-5.550	-60.0000	-3950
43741	-30.0000	-1.037	-30.0000	-1437
43745	-10.0000	-1.065	-7.4000	0.989
43749	-6.4000	0.052	-5.0000	0.032
43753	4.0000	0.019	14.0000	0.35
43757	15.2000	-0.932	19.0000	-1.303
43761	30.0000	-1.437	30.1000	-1.437
43765	34.9000	-2.220	35.0000	-2.220
43769	45.0000	-1.950	60.0000	-3950
43773	80.0000	-5.600	95.0000	-5550
43777	110.0000	-1.560	125.0000	-5570
43781	135.0000	-5.380	145.0000	-4810
43785	150.0000	-4.380	160.0000	-6000
43789	174.0000	-3.590	180.0000	-6130
43800	10.0000	-1.027	-30.0000	-1437
43804	-10.0000	-1.027	-7.4000	-1.356
43808	-6.0000	0.038	-5.0000	0.019
43812	8.0000	0.124	11.2000	0.115
43816	12.2000	-1.299	18.0000	-1.361
43820	30.0000	-1.437	-7.4000	0.989
43825	9.0000	-5.000	-30.0000	-1437
43879	-10.0000	-1.028	-9.0000	-0.952
43883	-7.0000	-0.683	-5.0000	0.045
43887	8.0000	-0.031	12.0000	-0.800
43891	16.0000	-1.293	30.0000	-1.437
43950	21.0000	-6.000	-30.0000	-1437
43954	-25.000	-1.267	-20.0000	0.707
43958	-15.0000	-0.878	-10.0000	-0.087
43962	-3.0000	-0.004	5.0000	0.0087
43966	8.0000	-0.690	13.0000	-1.1615

		1.0	ROTOR ANALYSIS INPUT - TEST MAIN ROTOR - 4
-1 110	1.0	1.0	ROTOR ANALYSIS INPUT - TEST MAIN ROTOR - 4
1 TITLE 1	-	4.0	4.0
1 TITLE 2	-	2.0	2.0
1 TITLE 1	-	30.	30.
1 TITLE 2	-	15.	15.
1 TITLE 1	-	4.	4.
1 TITLE 2	-	6.	6.
1 TITLE 1	-	1.	1.
1 TITLE 2	-	5.	5.
1 TITLE 1	-	12.	12.
1 TITLE 2	-	1.	1.
443970	15.0000	-1.1352	-1.1437
44025	-15.0000	-1.1352	-1.1397
44029	-25.0000	-1.1352	-1.1306
44033	-35.0000	-1.1352	-1.0073
44037	-45.0000	-1.1352	-0.0019
44041	-55.0000	-1.1352	2.0000
44045	3.0000	-0.0211	-0.0569
44049	6.0000	-1.1105	-0.0000
44053	15.0000	-1.1437	-0.0000
44100	18.0000	-1.1352	-0.0000
44104	-25.0000	-1.1361	-20.0000
44108	-15.0000	-1.1260	-10.0000
44112	-8.0000	-1.1039	-16.0000
44116	-4.0000	-1.0291	-3.0000
44120	-2.0000	-0.0265	-0.0000
44124	1.0000	-0.0197	2.0000
44128	3.0000	-0.0943	4.0000
44132	5.0000	-1.1177	15.0000
44136	30.0000	-1.1437	-30.0000
44175	15.0000	-0.8000	-0.0000
44179	-8.0000	-0.0750	-6.0000
44183	-4.0000	-0.0350	-2.0000
44187	0.0000	-0.0150	-0.5000
44191	1.0000	-0.0120	1.5000
44195	2.0000	-0.0290	4.0000
44199	6.0000	-1.1000	8.0000
44203	18.0000	-1.1300	-30.0000
44250	17.0000	-90000	-30.0000
44254	-8.0000	-1.1200	-6.0000
44258	-4.0000	-0.0430	-2.0000
44262	0.0000	-0.0200	-10.000
44266	2500	-0.0120	-5000
44270	7500	-0.0090	1.0000
44274	1.5000	-0.0300	2.0000
44278	4.0000	-0.0830	6.0000
44282	8.0000	-1.1600	-30.0000
44325	17.0000	1.0000	-30.0000
44329	-8.0000	-1.1200	-6.0000
44333	-4.0000	-0.0430	-2.0000
44337	0.0000	-0.0200	-10.000
44341	2500	-0.0120	-5000
44345	7500	-0.0090	1.0000
44349	1.5000	-0.0300	2.0000
44353	4.0000	-0.0830	6.0000
44357	8.0000	-1.1600	-30.0000
44400	17.0000	2.0000	-30.0000
44404	-8.0000	-1.1200	-6.0000
44408	-4.0000	-0.0430	-2.0000
44412	0.0000	-0.0200	-10.000
44416	2500	-0.0120	-5000
44420	7500	-0.0090	1.0000
44424	1.5000	-0.0300	2.0000
44428	4.0000	-0.0830	6.0000
44432	8.0000	-1.1600	-30.0000

-1110.1.0				- ROTOR ANALYSIS INPUT - TEST MAIN ROTOR - 4 TEST CASES			
TITLE 1				TITLE 2 - BIFILAR ANALYSIS INPUT			
4	1.	4.	4.	4.	4.0	30.	
5	6.	5.	6.	258.	2.	15.	0.
3	12.	1.	4.		0.0		

51030	0.180	6.950	0.0	0.0	0.0
51035	-.054				
31036	-.02632	-.2362	-.135		
31037	-.032	-.04	-.2664		
31038	-.08	-.01855	-.03		
31039	.015	.03522	-.01		
31040	.06	.6	.44		
31041	.032	-.22	.142		
31042	.020665	-.02	.04		
31043	.02065	-.08	.135		
31044	-.1239	-.10875	-.02		
31045	-.04551	0.0	0.0		
51100	1.0	0.0	0.0		
51101	0.0	1.0	0.0		
51112	0.0	0.0	1.0		
51118	0.0	-.566	0.0		
51124	-.566	0.0	2.44		
51130	0.0	9.50	0.0		
11135	-.056				
31136	-.00972	-.52	.00357		
31142	.01847	-.05478	-.42		
31148	-.0795	-.06274	.25		
31154	.0.02	-.031	-.0712		
31160	-.04347	-.08173	.91		
31166	-.001914	-.65	.01		
31172	-.01914	-.015	-.3		
31178	-.137	.1	-.8374		
31184	-.02403	.42	.1227		
51200	1.0	0.0	0.0		
51206	0.0	1.0	0.0		
51212	0.0	0.0	1.0		
51218	0.0	-.1464	0.0		
51224	-.1464	0.0	-.437		
51230	0.0	-.17.0	0.0		
11235	-.054	-.17.0	-.0138		
31236	-.002634	-.01	.04		
31242	-.02794	-.03844	.04		
31248	-.007521	-.14	-.5556		
31254	-.000371	-.07	-.3323		
31260	-.0003	-.402	-.1		
31266	-.000374	-.1.5	.05		
31272	-.000374	-.05	.01		
31278	-.007358	-.00364	.019		
31284	-.003116	-.0764	.03752		
51300	1.0	0.0	0.0		
51306	0.0	1.0	0.0		
51312	0.0	0.0	1.0		
51318	0.0	-.905	0.0		
51324	-.905	0.0	-.0138		
51330	0.0	-.20.34	0.0		
11335	-.054				
31336	-.04543	-.1.75	.07506		
31342	1.6	-.15914	-.1		
31348	-.01	-.0234	.4804		
31354	-.00436	.011	-.0402		
31360	.6	.015	.18		
31366	.05	1.1	-.1		
31372	1.33	1.1	-.1		
31378	-.030532	-.0048	-.016637		
31384	.0923	.0325	-.034		
51490	0.	0.	0.		0.

41495	0.	23.73	23.73	23.73
41500	23.73	.01	.01	.01
41520	.01	.3	.3	.3
41540	.3	.01	.01	.01
41560	18.22	18.22	18.22	18.22
41580	0.	90.	180.	270.
41600	500.			
41627	500.			
51760	5.			
11765	9.			
1	1	1.		
1	1	4	18.	
1	1	8.		
1	1	9.		
1	1	12.		
1	1	18.		
4	50	1.808	3.061	5.13
5	54	2.47	1.941	2.45
4	70	3.06	384.0	918.0
5	74	828.0	696.0	726.0
4	90	.025	.025	.025
5	94	.025	.025	.025
4	450	.001	.15	.001
5	455	.001	.54	.001
4	461	.0028	.001	.11
5	462	1.0	.001	.31
1	467	.0015		
5	468	.001	.54	.001
4	473	.003683		
5	474	.001	.15	.11
1	479	-.004382		
5	480	.05	-.065	.022
1	485	-.06		
5	486	24	-.15	.022
1	491	-.06		
5	492	7	.52	.125
1	497	.0015		
5	498	-.05	.22	.001
1	503	-.05		
4	750	.017	2664	-.03
5	754	1.0	.05	.01
4	770	-.044	.02315	-.013
5	774	-.0175	-.02	.0057
31000	-	0.2632	-.2362	-.0357
31006	-	0.32	-.04	-.2664
31012	-	0.38	-.04	-.03
31018	-	0.5	0.3522	-.01
31024	-	0.6	.6	.44
31030	-	0.665	-.22	.142
31036	-	0.665	-.02	.04
31042	-	1.239	.08	.135
31048	-	0.0551	1.0875	-.102
31100	-	0.0972	-.52	.00357
31106	-	0.0847	-.05478	-.42
31112	-	0.095	-.006274	-.25
31118	-	0.0102	-.031	-.0712
31124	-	0.0347	-.08173	.91
31130	-	0.03914	-.65	-.3
31136	-	0.03914	-.65	-.015

END OF INPUT

APPENDIX C. TEST CASES RESULTS
CASE I. ROTOR RESULTS

TITLE 1 - TEST MAIN ROTOR DATA - COUPLED WITH BIPLAR ANALYSIS

000463

HOVER

MAIN ROTOR

PITCH ANGLE AT .75% RADIUS	=	6.400.000 DEG
CALCULATED THRUST	=	16364.911 LB
CALCULATED CONING ANGLE	=	3.369 DEG
CALCULATED LAG ANGLE	=	5.180 DEG
CALCULATED BLADE TORSIONAL FREQUENCY	=	0.0 RAD/SEC
CALCULATED BLADE BENDING FREQUENCIES : MODE 1 =		77.5 RAD/SEC
		MODE 2 = 126.7 RAD/SEC

STEADY DEFLECTIONS (IN)

RADIUS (IN)	FLATWISE	EDGewise	ANGLE OF ATTACK (DEG)
0.0	0.0	0.0	-74.100
15.000	0.0	0.0	-35.210
23.750	-0.004	0.011	-20.206
41.250	-0.009	0.014	-6.880
62.500	0.041	0.265	-0.159
83.400	0.156	0.505	2.552
100.200	0.256	0.699	3.650
117.000	0.356	0.904	4.219
133.800	0.455	1.119	4.447
150.600	0.546	1.343	4.446
167.745	0.626	1.582	4.277
185.235	0.688	1.835	3.980
202.725	0.723	2.076	3.968
220.215	0.728	2.371	3.124
236.910	0.696	2.641	2.627
252.810	0.631	2.907	2.116
268.710	0.542	3.181	1.574
283.145	0.456	3.437	0.647
296.115	0.397	3.670	-0.156
308.450	0.358	3.957	-0.545
314.150	0.353	3.997	1.274
320.000	0.344	4.103	2.101

MODE NO.	PHIXPH	PHIZPH	PHELD	PHFLD	PHFFLD
1	1.0000	-0.0009	0.0	0.0	0.0
2	-1.0000	0.0010	0.0	0.0	0.0

QEOID	QEOPID	QFOLD	QFOPID	PHID	THTLID	PHOS
0.0	0.0	0.0	0.0	0.0	0.0	0.0

CASE DEFINITION

AIR DENSITY LB.SEC.-SQ.IN.-4TH	SPEED OF SOUND FT./SEC.	TIP LOSS FACTOR	AXIAL VEL. KNOTS	BLADE RADIUS FEET	ROTOR SPEED R.P.M.	PREFCON ANGLE RADIANS
0.114680-06	1116.00000	0.99000	0.0	256.00000	26.83333	
OFFSET FEET	NUMBER OF BLADES	ROOT FLAP SPRING LB.IN./RAD.	ROOT LAG SPRING LB.IN./RAD.	PREFCON ANGLE RADIAN		
1.25000	4	0.0	0.0	0.0	0.0	
BLADE YOUNG'S MOD. LB./IN.-SQ	RADIUS OF PUSH ROD INCHES	LAG DAMPING FRACT CRITICAL	RIGID PITCH DAMP. FRACT CRITICAL	REF. ROTOR SPEED R.P.M.	BLADE BENDING MODES	
0.100000+07	15.12650	0.35000	0.0	258.00000	2	
PITCH HORN LENGTH INCHES	FORWARD FLIGHT SPEED DEG/SEC	WEIGHT AT PUSHROD, LB	ELASTIC PITCH DAMP. FRACT. CRITICAL	PITCH BEAM STIFFNESS ACTUATOR MOM. LB/IN.	PITCH BEAM RADUIS INCHES	
7.25000		0.0	0.0	676.00000	0.0	
ROTEST	FTEST	SYSDEF	ROTDEF	ARTIC	PHASE	
VECT	TRMASC	SUMASC	TSERV	MNMASC	MSERVC	
		111.	1.	1.	111.	
						111.

CIR	CIRN	LAGX
1.	1.	1.

MODE NO.	ZETBID	ZETG	NS	OHF	PHY			PHZ			PHY			PHX			PHY			PHTX		
					STRUCTURAL	AERO-DYNAMIC	AC.	CG	TORSIONAL	EA	MODE SHAPE	TWIST	TWIST	AC.	CG	EA	TWIST	AC.	CG	EA	TWIST	AC.
1	0.0	0.0	0.0	0.0	-9.50000	-9.50000	0.0	0.0	-0.00000	0.0	0.0	0.0	0.0	0.0	0.0	0.0	0.0	0.0	0.0	0.0	0.0	0.0
2	0.0	0.0	0.0	0.0	-9.50000	-9.50000	0.0	0.0	-0.00000	0.0	0.0	0.0	0.0	0.0	0.0	0.0	0.0	0.0	0.0	0.0	0.0	0.0
3	0.0	0.0	0.0	0.0	-9.50000	-9.50000	0.0	0.0	-0.00000	0.0	0.0	0.0	0.0	0.0	0.0	0.0	0.0	0.0	0.0	0.0	0.0	0.0
4	0.0	0.0	0.0	0.0	-8.89205	-8.89205	-0.35000	-0.35000	-0.21759	0.0	0.0	0.0	0.0	0.0	0.0	0.0	0.0	0.0	0.0	0.0	0.0	0.0
5	0.0	0.0	0.0	0.0	-7.87555	-7.87555	0.35000	0.35000	0.92200	0.0	0.0	0.0	0.0	0.0	0.0	0.0	0.0	0.0	0.0	0.0	0.0	0.0
6	0.0	0.0	0.0	0.0	-7.05845	-7.05845	-0.35000	-0.35000	-0.82200	0.0	0.0	0.0	0.0	0.0	0.0	0.0	0.0	0.0	0.0	0.0	0.0	0.0
7	15.00000	8.30000	-9.50000	-9.50000	-9.50000	-9.50000	0.0	0.0	0.0	0.0	0.0	0.0	0.0	0.0	0.0	0.0	0.0	0.0	0.0	0.0	0.0	0.0
8	23.75000	8.30000	-9.50000	-9.50000	-9.50000	-9.50000	0.0	0.0	0.0	0.0	0.0	0.0	0.0	0.0	0.0	0.0	0.0	0.0	0.0	0.0	0.0	0.0
9	41.25000	8.30000	-9.50000	-9.50000	-9.50000	-9.50000	0.0	0.0	0.0	0.0	0.0	0.0	0.0	0.0	0.0	0.0	0.0	0.0	0.0	0.0	0.0	0.0
10	62.50000	20.76000	-8.89205	-8.89205	-8.89205	-8.89205	-0.35000	-0.35000	-0.21759	0.0	0.0	0.0	0.0	0.0	0.0	0.0	0.0	0.0	0.0	0.0	0.0	0.0
11	83.00000	20.76000	-7.87555	-7.87555	-7.87555	-7.87555	0.35000	0.35000	0.92200	0.0	0.0	0.0	0.0	0.0	0.0	0.0	0.0	0.0	0.0	0.0	0.0	0.0
12	100.25000	20.76000	-7.05845	-7.05845	-7.05845	-7.05845	-0.35000	-0.35000	-0.82200	0.0	0.0	0.0	0.0	0.0	0.0	0.0	0.0	0.0	0.0	0.0	0.0	0.0
13	117.00000	20.76000	-6.24136	-6.24136	-6.24136	-6.24136	-0.35000	-0.35000	-0.82200	0.0	0.0	0.0	0.0	0.0	0.0	0.0	0.0	0.0	0.0	0.0	0.0	0.0
14	133.00000	20.76000	-5.42427	-5.42427	-5.42427	-5.42427	-0.35000	-0.35000	-0.82200	0.0	0.0	0.0	0.0	0.0	0.0	0.0	0.0	0.0	0.0	0.0	0.0	0.0
15	150.00000	20.76000	-4.60718	-4.60718	-4.60718	-4.60718	-0.35000	-0.35000	-0.82200	0.0	0.0	0.0	0.0	0.0	0.0	0.0	0.0	0.0	0.0	0.0	0.0	0.0
16	167.74500	20.76000	-3.77331	-3.77331	-3.77331	-3.77331	-0.35000	-0.35000	-0.66700	0.0	0.0	0.0	0.0	0.0	0.0	0.0	0.0	0.0	0.0	0.0	0.0	0.0
17	185.723500	20.76000	-2.92266	-2.92266	-2.92266	-2.92266	-0.35000	-0.35000	-0.66700	0.0	0.0	0.0	0.0	0.0	0.0	0.0	0.0	0.0	0.0	0.0	0.0	0.0
18	202.72500	20.76000	-2.07201	-2.07201	-2.07201	-2.07201	-0.35000	-0.35000	-0.46850	0.0	0.0	0.0	0.0	0.0	0.0	0.0	0.0	0.0	0.0	0.0	0.0	0.0
19	220.215000	20.76000	-1.22136	-1.22136	-1.22136	-1.22136	-0.35000	-0.35000	-0.69851	0.0	0.0	0.0	0.0	0.0	0.0	0.0	0.0	0.0	0.0	0.0	0.0	0.0
20	236.910000	22.31700	-0.40358	-0.40358	-0.40358	-0.40358	0.0	0.0	0.29349	0.0	0.0	0.0	0.0	0.0	0.0	0.0	0.0	0.0	0.0	0.0	0.0	0.0
21	252.610000	22.31700	0.36394	0.36394	0.36394	0.36394	0.0	0.0	0.30385	0.0	0.0	0.0	0.0	0.0	0.0	0.0	0.0	0.0	0.0	0.0	0.0	0.0
22	268.710000	22.31700	1.13726	1.13726	1.13726	1.13726	0.0	0.0	0.30962	0.0	0.0	0.0	0.0	0.0	0.0	0.0	0.0	0.0	0.0	0.0	0.0	0.0
23	283.145000	21.76900	2.25160	2.25160	2.25160	2.25160	-0.35000	-0.35000	-0.36600	0.0	0.0	0.0	0.0	0.0	0.0	0.0	0.0	0.0	0.0	0.0	0.0	0.0
24	296.115000	20.76000	3.20767	3.20767	3.20767	3.20767	-0.35000	-0.35000	2.09000	0.0	0.0	0.0	0.0	0.0	0.0	0.0	0.0	0.0	0.0	0.0	0.0	0.0
25	306.050000	20.76000	3.51000	3.51000	3.51000	3.51000	-1.79128	-1.79128	0.38606	0.0	0.0	0.0	0.0	0.0	0.0	0.0	0.0	0.0	0.0	0.0	0.0	0.0
26	314.050000	20.76000	1.97000	1.97000	1.97000	1.97000	-4.55384	-4.55384	-3.18159	0.0	0.0	0.0	0.0	0.0	0.0	0.0	0.0	0.0	0.0	0.0	0.0	0.0
27	320.000000	20.76000	1.20000	1.20000	1.20000	1.20000	-6.468306	-6.468306	-5.72000	0.0	0.0	0.0	0.0	0.0	0.0	0.0	0.0	0.0	0.0	0.0	0.0	0.0

R	QEO	QFO	QEOP	QFOP
0.0	0.0	0.0	0.0	0.0
15.00000	0.0	0.0	0.0	0.0
23.75000	0.0108	-0.00502	0.00155	-0.00151
41.25000	0.10392	-0.00914	0.00659	-0.00127
62.50000	0.28671	0.04123	0.00916	0.00136
83.40000	0.50523	0.15567	0.01101	0.00444
100.20000	0.69339	0.25565	0.0170	0.00453
117.00000	0.90412	0.35611	0.01231	0.00450
133.80000	1.11881	0.45498	0.01290	0.00420
150.60000	1.35309	0.54645	0.01347	0.00351
167.74500	1.58162	0.62805	0.01404	0.00256
185.23500	1.83470	0.68764	0.01440	0.00133
202.72500	2.09751	0.72338	0.01516	-0.00032
220.21500	2.37055	0.72784	0.01577	-0.00215
236.31000	2.66091	0.69591	0.01635	-0.00418
252.81000	2.90709	0.63050	0.01689	-0.00600
269.71000	3.18148	0.54180	0.01761	-0.00672
283.14500	3.42658	0.45641	0.01779	-0.00611
296.11500	3.66970	0.39875	0.01886	-0.00370
306.45000	3.85694	0.36796	0.01815	-0.00217
314.15000	3.99675	0.35245	0.01816	-0.00171
320.00000	4.10300	0.34363	0.01816	-0.00167

R	D(DT)/DUT	D(DT)/DUP	D(DH)/DUT	D(DH)/DUP	D(DH)/DVT
0.0	0.0	0.0	0.0	0.0	0.0
15.00000	0.0	0.0	0.0	0.0	0.0
23.75000	-0.00040	-0.00073	0.33155	-0.00001	-0.16668
41.25000	0.00140	-0.00516	6.52470	0.00034	-0.00021
62.50000	0.00414	-0.01307	23.85057	0.00109	-0.00130
83.40000	0.00710	-0.01753	41.71577	-0.00107	-0.00327
100.20000	0.00745	-0.02118	59.83550	0.00103	-0.00244
117.00000	0.00859	-0.02483	61.23457	0.00100	-0.00180
133.80000	0.00954	-0.02851	105.97988	0.00096	-0.00133
150.60000	0.01102	-0.03221	134.44925	0.00100	-0.00056
167.74500	0.01192	-0.03662	169.58604	0.00098	-0.00031
185.23500	0.01269	-0.04126	210.32202	0.00095	-0.00015
202.72500	0.01218	-0.04602	255.52919	0.00083	-0.00014
220.21500	0.01210	-0.05052	304.00663	0.00078	-0.00027
236.31000	0.01266	-0.05901	381.23640	0.00078	-0.00053
252.81000	0.01374	-0.06489	447.37186	0.00099	-0.00125
269.71000	0.01276	-0.07412	541.85065	0.00086	-0.00173
283.14500	0.00878	-0.07731	593.92714	0.00095	-0.00250
296.11500	0.00549	-0.08701	697.52874	0.00039	-0.00370
306.45000	0.01024	-0.08279	771.89881	0.00079	-0.00407
314.15000	0.01876	-0.07562	817.74876	0.00168	-0.00494
320.00000	0.02305	-0.08673	756.49209	0.00288	-0.00730

R	D(M1)/DUT	D(M1)/DUP	D(DM1)/DUT	DT	DH	DM
0.0	0.0	0.0	0.0	0.0	0.0	0.0
15.00000	0.00044	0.00073	0.025554	-0.29732	-0.05191	0.1267
23.75000	-0.00948	-0.02382	-30.90563	-0.42541	-0.11705	0.28950
41.50000	0.00011	0.00040	-0.67797	0.43651	0.15563	0.19019
62.50000	0.00014	0.00051	-1.00320	2.76689	0.63533	0.27625
83.40000	0.00014	0.00051	-1.53569	5.12602	0.97658	0.16335
100.20000	0.00017	0.00051	16.77181	7.77250	1.27228	0.54370
117.00000	0.000111	-0.00514	21.82340	10.56367	1.53142	0.79426
133.80000	0.00120	-0.00586	27.06373	13.41433	1.74900	1.17383
150.60000	0.00351	-0.00625				
167.74500	0.00455	-0.00613	29.92084	16.53455	1.95691	2.61935
185.23500	0.00574	-0.00540	29.70216	19.55134	2.12554	4.59828
202.72500	-0.00221	-0.00559	30.5412	22.08643	2.22559	6.18703
220.21500	-0.00107	-0.00339	19.66104	23.60544	2.24479	5.50461
236.91000	-0.00210	-0.00102	5.55483	26.25026	2.37083	5.39755
252.81000	0.00344	-0.00014	6.66406	26.27911	2.30451	5.25127
268.71000	0.00322	-0.00493	37.29655	25.35963	2.20955	6.39255
283.14500	0.00180	-0.00851	65.92044	16.98756	1.59790	4.49944
296.11500	0.00092	-0.01286	101.55111	6.78590	1.13260	4.42266
306.45000	-0.10627	-0.01835	148.14500	7.69474	1.13389	2.42266
314.15000	-0.01425	-0.00576	43.94727	31.97936	2.69876	1.07474
320.00000	-0.02523	0.008714	-765.20454	66.45986	4.15806	-2.40277

R	D(CL1)/DAD	D(CL1)/DA	D(CL1)/DM	D(CL1)/DH	D(CL1)/DM
0.0	-0.42808	1.86000	0.47020	-0.74305	0.0
15.00000	-0.98372	0.74466	0.17059	-0.74305	0.0
23.75000	-0.90206	0.43932	0.12586	-0.24628	-0.30558
41.50000	-0.69222	0.08167	0.05016	-0.08862	-0.10657
62.50000	0.12646	0.0913	0.02051	-0.62625	-0.36861
83.40000	0.49191	0.0964	0.0231	-0.60930	-0.00828
100.20000	0.50170	0.0991	0.0195	-0.1432	-0.00828
117.00000	0.64789	0.01013	0.0215	6.76090	0.0
133.80000	0.67479	0.01027	0.0042	6.76090	0.0
150.60000	0.67339	0.0025	0.00283	6.78151	0.03460
167.74500	0.67371	0.01004	0.00511	6.90300	0.03591
185.23500	0.65183	0.00974	0.00736	7.02707	0.03627
202.72500	0.67704	0.00937	0.00829	7.13287	0.03870
220.21500	0.59106	0.00897	0.00625	7.19567	0.04038
236.91000	0.49999	0.00854	0.00459	7.25523	0.04000
252.81000	0.43973	0.00838	0.00592	7.48130	0.07675
268.71000	0.35132	0.00850	0.00423	8.02034	0.14954
283.14500	0.24346	0.00800	0.00797	8.50984	0.0
296.11500	0.11559	0.00808	0.00285	9.13770	0.02865
306.45000	0.09463	0.00852	0.0143	9.44286	-0.02314
314.15000	0.09295	0.00860	0.00143	9.54040	0.34354
320.00000	0.55272	0.01837	-0.00130	8.53200	0.78367

R	PHE(1,I)	PHE(1,I)	PHE(2,I)	PHE(2,I)	PHE(3,I)	PHE(3,I)	PHE(4,I)	PHE(4,I)
0.0	0.0	0.0	0.0	0.0	0.0	0.0	0.0	0.0
15.00000	-0.00000	-0.00000	-0.00000	-0.00000	-0.00000	-0.00000	-0.00000	-0.00000
23.75000	-0.01443	-0.01443	-0.05550	-0.11533	-0.11533	-0.06307	-0.06307	-0.06307
41.25000	0.04265	0.04265	-0.19633	-0.31760	-0.31760	0.20035	0.20035	0.20035
62.50000	-0.07436	-0.07436	-0.34180	-0.51612	-0.51612	0.32001	0.32001	0.32001
83.40000	-0.09919	-0.09919	-0.46391	-0.64142	-0.64142	0.33810	0.33810	0.33810
100.20000	-0.11385	-0.11385	-0.51923	-0.69542	-0.69542	0.28228	0.28228	0.28228
117.00000	0.12353	0.12353	-0.59883	-0.71296	-0.71296	0.17523	0.17523	0.17523
133.80000	0.12988	0.12988	-0.63689	-0.69571	-0.69571	0.02932	0.02932	0.02932
150.60000	0.12652	0.12652	-0.64399	-0.64607	-0.64607	-0.13980	-0.13980	-0.13980
167.75000	-0.11694	-0.11694	-0.62318	-0.56599	-0.56599	-0.31638	-0.31638	-0.31638
185.23500	0.10502	0.10502	-0.58974	-0.45975	-0.45975	-0.47719	-0.47719	-0.47719
202.75000	-0.08697	-0.08697	-0.48154	-0.33637	-0.33637	-0.52626	-0.52626	-0.52626
220.21500	0.05695	0.05695	-0.35641	-0.19443	-0.19443	-0.63587	-0.63587	-0.63587
236.31000	-0.02880	-0.02880	-0.20108	-0.05016	-0.05016	-0.58155	-0.58155	-0.58155
252.81000	-0.04619	-0.04619	-0.02128	-0.09481	-0.09481	-0.44739	-0.44739	-0.44739
268.71000	-0.04047	-0.04047	0.15885	0.24975	0.24975	-0.21509	-0.21509	-0.21509
283.14500	-0.07552	-0.07552	0.39359	0.38317	0.38317	0.06636	0.06636	0.06636
296.11500	-0.10802	-0.10802	0.59156	0.50845	0.50845	0.38215	0.38215	0.38215
306.45000	-0.13423	-0.13423	0.75377	0.60848	0.60848	0.61391	0.61391	0.61391
314.15000	-0.15381	-0.15381	0.87562	0.68303	0.68303	0.80485	0.80485	0.80485
320.00000	-0.16870	-0.16870	0.96831	0.73966	0.73966	0.95027	0.95027	0.95027

R	PHE(1,I)	PHE(1,I)	PHE(2,I)	PHE(2,I)	PHE(3,I)	PHE(3,I)	PHE(4,I)	PHE(4,I)
0.0	0.0	0.0	0.0	0.0	0.0	0.0	0.0	0.0
15.00000	0.00165	0.00165	-0.00750	-0.01376	-0.01376	0.00793	0.00793	0.00793
23.75000	-0.00164	-0.00164	-0.00746	-0.01289	-0.01289	-0.00789	-0.00789	-0.00789
41.25000	0.00155	0.00155	-0.00724	-0.01060	-0.01060	0.00697	0.00697	0.00697
62.50000	0.00133	0.00133	-0.00637	-0.00765	-0.00765	0.00296	0.00296	0.00296
83.40000	0.00100	0.00100	-0.00512	-0.00430	-0.00430	-0.00192	-0.00192	-0.00192
100.20000	0.00070	0.00070	-0.00396	-0.00201	-0.00201	-0.00538	-0.00538	-0.00538
117.00000	0.00039	0.00039	-0.00265	0.00012	0.00012	-0.00616	-0.00616	-0.00616
133.80000	0.00006	0.00006	-0.00117	0.00213	0.00213	-0.01046	-0.01046	-0.01046
150.60000	-0.00030	-0.00030	0.00052	0.00396	0.00396	-0.01093	-0.01093	-0.01093
167.75000	-0.00066	-0.00066	0.00225	0.00551	0.00551	-0.01466	-0.01466	-0.01466
185.23500	-0.00101	-0.00101	0.00439	0.00674	0.00674	-0.02395	-0.02395	-0.02395
202.72500	-0.00136	-0.00136	0.00637	0.00767	0.00767	-0.03058	-0.03058	-0.03058
220.21500	-0.00163	-0.00163	0.00854	0.00839	0.00839	-0.03609	-0.03609	-0.03609
236.91000	-0.00198	-0.00198	0.01062	0.00892	0.00892	-0.04580	-0.04580	-0.04580
252.81000	-0.00221	-0.00221	0.01246	0.00930	0.00930	0.01181	0.01181	0.01181
268.71000	-0.00239	-0.00239	0.01401	0.00953	0.00953	0.01743	0.01743	0.01743
285.15000	-0.00249	-0.00249	0.01597	0.00953	0.00953	0.02186	0.02186	0.02186
306.45000	-0.00254	-0.00254	0.01533	0.00967	0.00967	0.02392	0.02392	0.02392
314.15000	-0.00255	-0.00255	0.01534	0.00968	0.00968	0.02485	0.02485	0.02485
320.00000	-0.00255	-0.00255	0.01535	0.00968	0.00968	0.02486	0.02486	0.02486

M. OF I. ABOUT C.G. LB./IN. SEC-SQ/IN.	BLADE EDGewise IN.	BLADE FLATwise IN.	DELTA R IN.	M. OF I. ABOUT C.G. LB./IN. SEC-SQ/IN.	BLADE TORSIONAL IN.	DELTA R IN.
0.0	15.000				0.0	15.000
0.00269	8.300				0.00269	8.300
0.00472	2.800				0.00479	2.800
0.00823	3.900				0.00823	3.900
0.01842	15.630				0.01862	15.630
0.02398	29.170				0.02398	29.170
0.03180	—	89.000			0.03180	—
0.03474	—	61.000			0.03474	—
0.03971	—	8.960			0.03971	—
0.04650	—	11.040			0.04650	—
0.04359	—	36.660			0.04354	—
0.03881	12.340				0.03881	12.340
0.06848	—	2.000			0.06848	—
0.05861	—	6.000			0.05861	—
0.05723	—	9.500			0.05723	—
0.03805	—	13.500			0.03805	—
						13.500

BLADE MASS LB.SEC-SQ/IN.-SQ	DELTA R IN.	BLADE ENDGENESE SECOND MOMENT OF AREA-IN.4TH	DELTA R IN.	BLADE FLATWISE SECOND MOMENT OF AREA-IN.4TH	DELTA R IN.
0.0	15.00000	0.80587E+02	17.50000	0.87085F+02	17.50000
0.00749	17.50000	0.3794E+03	17.50000	0.93636E+02	17.50000
0.00423	17.50000	0.46303E+03	25.00000	0.27533E+02	25.00000
0.00165	25.00000	0.71842E+03	16.80000	0.23430E+02	16.80000
0.00144	16.80000	0.85000E+03	16.80000	0.23430E+02	16.80000
0.00138	16.80000	0.85000E+03	16.80000	0.23430E+02	16.80000
0.00137	16.80000	0.85000E+03	16.80000	0.23430E+02	16.80000
0.00137	16.80000	0.85000E+03	16.80000	0.23430E+02	16.80000
0.00137	16.80000	0.90000E+03	17.49000	0.27065E+02	17.49000
0.00145	17.49000	0.90000E+03	17.49000	0.27430E+02	17.49000
0.00146	17.49000	0.869279E+03	17.49000	0.27222E+02	17.49000
0.00150	17.49000	0.73952E+03	17.49000	0.27190E+02	17.49000
0.00162	17.49000	0.66334E+03	15.90000	0.27116E+02	15.90000
0.00170	15.90000	0.59000E+03	15.90000	0.26590E+02	15.90000
0.00190	15.90000	0.56444E+03	15.90000	0.25533E+02	15.90000
0.00190	15.90000	0.56444E+03	15.90000	0.25533E+02	15.90000
0.00186	15.90000	0.53000E+03	12.97000	0.22950E+02	12.97000
0.00176	12.97000	0.53000E+03	12.97000	0.22950E+02	12.97000
0.00153	12.97000	0.53000E+03	7.70000	0.12950E+02	7.70000
0.00133	7.70000	0.53000E+03	7.70000	0.22950E+02	7.70000
0.00139	7.70000	0.53000E+03	4.00000	0.22950E+02	4.00000
0.00036	4.00000				

BLADE RIGID BODY PROPERTIES

FLAPPING MASS 1ST MOL ABOUT HINGE	LB SEC-SQ/IN	LB SEC-SQ/IN	LB SEC-SQ/IN	LB SEC-SQ/IN
MODE(1) = .60383				
MODE(2) = .861467				
FLAPPING INERTIA = 18190.6				
MAG.FREQUENCY. = .246517				CYCLES/REV.

BLADE MODAL PROPERTIES

BENDING MODE GENERALIZED MASSES				
MODE(1) = .125382				
MODE(2) = .209446				

BENDING MODE (M)(PHE)

..... MODE(1) = .193469D-01 LB SEC-SQ/IN. MODE(1) = .942375D-01. LB SEC-SQ/IN

MODE(2) = -.115519 LB SEC-SQ/IN

BENDING MODE (M)(PHE)(R)

..... MODE(1) = .805651D-01 LB SEC-SQ MODE(1) = .621710. LB SEC-SQ

MODE(2) = .663062 LB SEC-SQ

MODE(2) = -3.94313 LB SEC-SQ

17 DEGREES OF FREEDOM ARE USED IN THIS RUN

1 2 7 8 9 10 11 12 21 22 23 24 25 26 27 28 29

FINAL STIFFNESS MATRIX

12	.0	.0	.0	.0	-859.306	389.188	-391.226	-1701.58	-.2179000+07	242365.
	.272896D+07	-.123761D+08	.0	.0	.0	-.161865D+07	208359.			
13	.0	.0	.0	.0	-33.0894	1.71156	-8.44605	-5.12357	-1732.55	-4083.65
	.755.359	.755.296	.0	.0	.0	.125.043	-.16335.3			
14	.0	.0	.0	.0	1.71156	33.0894	-5.12357	-8.49605	-4083.65	1732.55
	.753.296	.756.359	.0	.0	.0	.16335.3	-.125.043			
15	-112.328	-112.808	-10129.7	3811.79	.0	.0	.0	.0	.0	0
	.0	.0	.0	.0	.0	.0	.0	.0	.0	0
16	.0	.0	.0	.0	7143.69	-32606.9	-3102.89	-35682.5	.17431D+08	-4156790+07
	-.235881D+07	.118284D+07	.0	.0	.0	.0	-.153513.	-.515991.		
17	.0	.0	.0	.0	-32606.9	-7143.69	-35682.5	3102.89	-.4156790+07	-17431D+08
	-.118284D+07	.235881D+07	.0	.0	.0	.0	-.130249.	-.153513.		

FINAL DAMPING MATRIX

12	.0 983657.	.0 10.006.	.0 -88.5144	.0 19.0341	-5.19222 .0	-31.8052 -4.3258.5	40.9471 17771.1	-14.4804 -132.618	-132.618 -80650.8
13	.0 -33.9177	.0 -44.5914	.0 .531516	.0 .267172	-.547965D-01 .0	.221337D-01 163.720	-.147067D-01 .310.191	.195906 154.845	84.7249
14	.0 -44.5914	.0 33.9177	.0 -267172	.0 .531516	-.221337D-01 .0	-.547965D-01 -310.191	-.195906 163.720	-.147067D-01 -310.191	84.7249 -154.845
15	-.613499 .0	-.366813 .0	2584.08 .0	-.516.957 49.4160	.0 .0	.0 .0	.0 .0	.0 .0	.0 .0
16	.0 -10154.6	.0 -117905.	.0 1100.99	.0 -328.002	-.8.16080 .0	261.645 .136682D+07	-.211.864 .229132D+07	-.73.6610 .111417D+07	.540907.
17	.0 -117905.	.0 10154.6	.0 328.002	.0 1100.99	261.645 .0	8.16080 -.229132D+07	-.73.6610 .136682D+07	211.864 .540907.	-.111417D+07

FINAL MASS. MATRIX

12	.0	.0	.0	.0	.0	-.960889D-01	.0	.757761	.0	-2.45428
	.0	.0	.0	.0	.0	-6.14694	-2230.99			
13	.0	.0	.0	.0	.0	-.400246D-02	-194931D-01	.455219D-02	.116169	5.27690 .0
	.0	.0	.0	.0	.0					-5.27690 .0
14	-.86324	-.86324	-.86324	-.86324	-.86324	-.194931D-01	.400246D-02	-.116169	-.455219D-02	-.0
15	-.942375D-01	.385765D-02	.861467	.0	.0	.0	.0	.0	.0	.0
16	.0	.0	.0	.0	.0	181437D-01	-.802058	-.363098	-.3.86923	1868.37 19461.1
17	.0	.0	.0	.0	.0	-.802058	-.181437D-01	-.3.88923	.363098	19461.1 -1868.37

CASE 1: BIFILAR RESULTS

TITLE 2: BIFILAR DATA - WITH ROTOR - 9 FIX. SYS-3P FORCES-LINEAR CASE

BIFILAR ANALYSIS RESULTS

ALL DISPLACEMENTS ARE IN G AND ALL ANGLES ARE IN DEGREES

NUMBER OF FIXED SYSTEM MODES IS 9

NUMBER OF FIXED SYSTEM ABSORBERS IS 1

NUMBER OF INPLANE BIFILARS IS 1

NUMBER OF VERTICAL BIFILARS IS 1

TOTAL NO. OF DEGREES-OF-FREEDOM
(WITH NO. ROTOR) IS 16

NUMBER OF A.C. STATIONS IS 4

ROTOR COUPLING SWITCH (0=NO,1=YES) IS 1

ROTOR MATRICES PRINTOUT(0=NO,1=YES) IS 0

FIXED SYSTEM MATRICES PRINTOUT " IS 0

ADD ROTOR MATRICES PRINTOUT " IS 0

ADD FIX.SYS. ABSORBER PRINTOUT " IS 0

ADD INPLANE BIFILAR PRINTOUT " IS 0

ADD VERTICAL BIFILAR PRINTOUT " IS 0

INPLANE BIFILAR (9X9) PRINTOUT " IS 0

VERTICAL BIFILAR (9X9) PRINTOUT " IS 0

GAMMAS PRINTOUT " IS 0

ROTOR NO. OF DEGREES-OF-FREEDOM IS 12

TOTAL NO. OF DEGREES-OF-FREEDOM IS 28

PRESENT NO. OF DEGREES-OF-FREEDOM (NP) = 9

ADDITIONAL NO. DEGREES-OF-FREEDOM (NA) = 12

TOTAL NO. OF DEGREES-OF-FREEDOM (NP+NA) = 21

ORDER OF MATRIX TO BE ADDED (NL) = 18

ORDER = D.O.F. OF ADDED MATRIX (NL-NA) = 6

PRESENT NO. OF DEGREES-OF-FREEDOM (NP) = 21

ADDITIONAL NO. DEGREES-OF-FREEDOM (NA) = 1

TOTAL NO. OF DEGREES-OF-FREEDOM (NP+NA) = 22

ORDER OF MATRIX TO BE ADDED (NL) = 2

ORDER = D.O.F. OF ADDED MATRIX (NL-NA) = 1

INPLANE BIPLAR PARAMETERS

TOTAL NO. OF BIPLIARS (N) = 4.00000

BIPLAR MASS (M) = .6140000-01

BIPLAR ARM (RER) = 18.2200

BIPLAR FREQUENCY (H) = 3.00000

BIPLAR RADIUS (RER*NA/4) = 2.02444

NPHRRR = 1.00656

14MM = 10.00000

NPHRRM(1,NA/4) = 10.0656

NPHRRM(1,NA/4)*2 = 100.656

PRESENT NO. OF DEGREES-OF-FREEDOM (NP)	= 22
ADDITIONAL NO. DEGREES-OF-FREEDOM (NA)	= 3
TOTAL NO. OF DEGREES-OF-FREEDOM (NP+NA)	= 25
ORDER OF MATRIX TO BE ADDED (NL)	= 9
ORDER - D.O.F. OF ADDED MATRIX (NL-NA)	= 6

VERTICAL...BIFFILAR...PARAMETERS

TOTAL NO. OF BIFFILARS (N)	= 4.00000
BIFFILAR MASS (M)	= .608000D-01
DISTANCE FROM C.R. (R)	= 18.5000
BIFFILAR FREQUENCY (W)	= 4.00000
R1=R/(NP+NA-1)	= 1.23333
R1=R1	= 1.52111
R+R1	= 19.7333
(R+R1)*#2	= 389.404
MNN(R+R1)	= 4.79915
MNN((R+R1)*#2)	= 94.7032
MNNR1*(R+R1)	= 5.91695

PRESENT NO. OF DEGREES-OF-FREEDOM (NP)	= 25
ADDITIONAL NO. DEGREES-OF-FREEDOM (NA)	= 3
TOTAL NO. OF DEGREES-OF-FREEDOM (NP+NA)	= 28
ORDER OF MATRIX TO BE ADDED (NL)	= 9
ORDER - D.O.F. OF ADDED MATRIX (NL-NA)	= 6

GENERALIZED FORCES - ORDER IS = 9

COSINE COMPONENT

.500000	-170.000	500.000	.500000	-201.000	25.0000	120.000	350.000
.110.000							
-25.0000							

SINE COMPONENT

75.0000	.500000	.500000	270.000	75.0000	-32.5000	-75.0000	260.000
.110.000							
-25.0000							

(GAMMAS)

COSINE - SINE - AMPLITUDE - PHASE (DEG)

ROTOR

-.420508D-03	.103080D-02						
-.320688D-03	.291653D-04						
.257314D-05	-.300397D-05						
.100956D-06	.705548D-07						
-.123503D-02	.977919D-02						
-.397314D-02	-.137627D-02						
-.915847D-02	-.563780D-02						
.270569D-02	.193891D-02						
.129046D-03	-.147193D-03						
-.666364D-04	.178137D-05						
-.548050D-04	.228122D-05						
-.160107D-04	.750412D-04						

FIXED SYSTEM ABSORBER(S)

-.344875D-02 -.150106D-02 .376126D-02 -156.479

(EQT ORDER IS:O,SIN,COS) (AMPL/PHASE ORDER IS:N,N-1,N+1)
DEG & DEG

.705532D-03	.691230D-03	.161459D-01	44.4215
.3153306	.718392D-01	9.28677	-77.2864
.708454D-01	-.317137	.298438D-01	-118.491

(EQT ORDER IS:O,SIN,COS) (AMPL/PHASE ORDER IS:N,N-1,N+1)
DEG & DEG

-2250140-01 -2135380-01 456860 -137.744
 -510380-02 -366550-02 356881D-01 -30.282
 -1125250-02 .3910580-02 .149276 116.499

MULTI-TEXT SYSTEM ELEMENTS (HZ)

FORCING FREQUENCY (HZ) = 17.2000

THE CONVERSION FACTOR TO G = 30.2259

FUSELAGE NO. OF DEGREES OF FREEDOM

- .2141900-03 - .446165D-04 - .349518D-03 - .295426D-02 - .567524D-03 - .284549D-03 - .641759D-03 - .256691D-02
+ .214383D-03

FIRST A.C. STATION DISPLACEMENT IN G

SINE SINE COSINE SINE COSINE SINE

FIRST A.C. STATION TOTAL DISPLACEMENT IN G

14472D-01 .262493D-01 .168862D-01

SECURITY AND STATION RECONCILIATION IN C

COSINE SINE COSINE SINE COSINE SINE

.112625D-01	-.152913D-01	-.881726D-02	.884320D-02	-.978861D-02	-.282865D-01
-------------	--------------	--------------	-------------	--------------	--------------

SECOND A.C. STATION TOTAL DISPLACEMENT IN G

X	Y	Z
---	---	---

189832D-01	124878D-01	299323D-01
------------	------------	------------

SECOND A.C. STATION PHASE ANGLE IN DEG

-53.6093	134.916	-109.088
----------	---------	----------

THIRD A.C. STATION DISPLACEMENT IN G

X	Y	Z
---	---	---

COSINE	SINE	COSINE	SINE	COSINE	SINE	COSINE	SINE
.566726D-02	-.669938D-02	-.130642D-02	.746452D-02	.160931D-01	.584755D-02		

THIRD A.C. STATION TOTAL DISPLACEMENT IN G

X	Y	Z
---	---	---

.877494D-02	.757798D-02	.171225D-01
-------------	-------------	-------------

THIRD A.C. STATION PHASE ANGLE IN DEG

-49.7708	99.9272	19.9690
----------	---------	---------

FOURTH A.C. STATION DISPLACEMENT IN G

X	Y	Z
---	---	---

COSINE	SINE	COSINE	SINE	COSINE	SINE	COSINE	SINE
.175254D-01	.101499D-01	.224440D-01	.275527D-01	-.131746D-01	.320180D-02		

FOURTH A.C. STATION TOTAL DISPLACEMENT IN G

X	Y	Z
---	---	---

.202524D-01	.355603D-01	.135561D-01
-------------	-------------	-------------

FOURTH A.C. STATION PHASE ANGLE IN DEG

30.0775	50.8648	166.340
---------	---------	---------

ROTOR HEAD DISPLACEMENT IN G

X	Y	Z			
COSINE	SINE	COSINE	SINE	COSINE	SINE
- .528534D-01	.123521	- .941640D-01	.371639D-02	- .398021D-02	.438087D-02

ROTOR HEAD TOTAL DISPLACEMENT IN G

X	Y	Z
.136356	.942383D-01	.591896D-02

ROTOR HEAD DISPLACEMENT PHASE ANGLES IN DEG

113.166	177.725	132.256
---------	---------	---------

CASE 2. BIFILAR RESULTS
BIFILAR...ANALYSIS...RESULTS

ALL DISPLACEMENTS ARE IN G AND ALL ANGLES ARE IN DEGREES

NUMBER OF FIXED SYSTEM MODES	IS 9
NUMBER OF FIXED SYSTEM ABSORBERS	IS 1
NUMBER OF INPLANE BIFILARS	IS 0
NUMBER OF VERTICAL BIFILARS	IS 1
TOTAL NO. OF DEGREES-OF-FREEDOM (WITH NO. ROTOR)	IS 13
NUMBER OF A.C. STATIONS	IS 4
ROTOR COUPLING SWITCH. (0=NO,1=YES)	IS 1
ROTOR MATRICES PRINTOUT(0=NO,1=YES)	IS 0
FIXED SYSTEM MATRICES PRINTOUT "	IS 0
ADD ROTOR MATRICES PRINTOUT "	IS 0
ADD FIX.SYS. ABSORBER PRINTOUT "	IS 1
ADD INPLANE BIFILAR PRINTOUT "	IS 1
ADD VERTICAL BIFILAR PRINTOUT "	IS 0
INPLANE BIFILAR (9X9) PRINTOUT "	IS 0
VERTICAL BIFILAR (9X9) PRINTOUT "	IS 0
GAMMAS PRINTOUT "	IS 0

ROTOR NO. OF DEGREES-OF-FREEDOM IS 12

TOTAL NO. OF DEGREES-OF-FREEDOM IS 25

PRESNT. NO. OF DEGREES-OF-FREEDOM (NP) = 9

ADDITIONAL NO. DEGREES-OF-FREEDOM (NA) = 12

TOTAL NO. OF DEGREES-OF-FREEDOM (NP+NA) = 21

ORDER OF MATRIX TO BE ADDED (NL) = 18

ORDER = D.O.F. OF ADDED MATRIX (NL-NA) = 6

PRESNT. NO. OF DEGREES-OF-FREEDOM (NP) = 21

ADDITIONAL NO. DEGREES-OF-FREEDOM (NA) = 1

TOTAL NO. OF DEGREES-OF-FREEDOM (NP+NA) = 22

ORDER OF MATRIX TO BE ADDED (NL) = 2

ORDER = D.O.F. OF ADDED MATRIX (NL-NA) = 1

VERTICAL BIPIALAR PARAMETERS

TOTAL NO. OF BIPILARS (N) = 4.00000

BIPIALAR MASS (M) = .600000D-01

DISTANCE FROM C.R. (R) = 18.5000

BIPIALAR FREQUENCY (W) = 4.00000

R1=R/(N*H-1.1) = .1.23333

R1*R1 = 1.52111

R+R1 = 19.7333

(R+R1)*2 = 389.404

M=N*M(R+R1) = 4.7915

M=M*(R+R1)*2 = 94.7032

N=N*R1*(R+R1) = 5.91895

PRESENT NO. OF DEGREES-OF-FREEDOM (NP) = 22

ADDITIONAL NO. DEGREES-OF-FREEDOM (NA) = 3

TOTAL NO. OF DEGREES-OF-FREEDOM (NP+NA) = 25

ORDER OF MATRIX TO BE ADDED (NLU) = 9

ORDER = D.O.F. OF ADDED MATRIX (NP-NA) = 6

D.Q.E.E.29.NE.....9,KROTRE..12.NFABSE..1.KINDS.OF INPL..BIF.E...0,KINDS.OF VERT..BIF.E...1,NUMB.OF N.L.INPL..BIF...4

FIXED SYSTEM + ROTOR + FIXED ABSORBERS (R.H.S.) OF ORDER 25

卷之三

THE MASS (L.H.S.) MATRIX OF ORDER 18

THE BIFFLAR FORCE VECTOR OF ORDER 10

* 2556260-04 - 2556260-04 .0 .0 .0 .0 .0 .0 .0 .0 .0 IBM Z30687

THE ROTOR HEAD MODE SHAPES, TRANSPOSE(PHI), OF ORDER 9 X 6

.10000D-02	.15000	.10000D-02	-.51200D-02	.47400D-03	.15680D-02
-.156000	.10000D-02	.11000	-.12000D-03	-.51830D-02	.28000D-03
1.10000	.10000D-02	.31000	-.53950D-02	.15000D-02	.15000D-03
-.10000D-02	.15000	.10000D-02	.12140D-01	.77200D-04	.36830D-03
-.40200	.15000	-.10000D-02	-.80100D-02	.32520D-02	.43820D-03
.50000D-01	-.65000D-01	.22000D-01	-.12440D-02	-.47300D-03	.60000D-02
-.24000	-.15000	.22000D-01	-.12440D-02	-.47300D-03	.60000D-02
.70000	.52000	-.12500	-.70000D-04	.23100D-01	.15000D-03
-.50000D-01	.22000	.10000D-02	.63500D-02	.22000D-03	-.12700D-02

THE EXPANDED BIFFLAR MASS MATRIX OF ORDER = 13

.57749D-02	-.24725D-05	.30618D-03	.19956D-01	.53592D-02	-.33300D-02	-.64154D-02	.19357D-01	.76938D-02	*.22596D-01
.38622D-02	-.14703D-01	.40703D-02	.83517D-01	.59513D-04	.33600D-01	-.43612D-02	-.20251D-01	-.58333D-01	.41943D-02
-.24725D-05	.28460D-01	-.41567D-01	.42976D-01	.59041D-03	.30618D-03	-.41567D-01	.40703D-02	.83517D-01	.42976D-01
.30618D-03	-.83517D-01	.24565	-.36367D-03	-.98722D-01	-.12176D-01	.58682D-01	.17209	-.12244D-01	.50187D-03
-.12395	.25322D-03	.15470	-.19566D-01	.59513D-04	.33600D-01	-.43612D-02	-.20251D-01	-.58333D-01	.41943D-02
.19956D-01	.59513D-04	.33600D-01	.71646D-01	.19783D-01	.45245D-01	-.70680D-02	-.20061D-01	.69570D-01	.29124D-01
.80266D-03	-.66610D-01	.10513D-02	.33600D-01	.98722D-01	.19783D-01	-.70680D-02	-.20061D-01	.69570D-01	.17546D-01
.53592D-02	.33600D-01	-.98722D-01	.48877D-01	.19783D-01	.45245D-01	-.70680D-02	-.20061D-01	.69570D-01	.17546D-01
-.33300D-02	-.43612D-02	.12176D-01	-.88326D-02	-.70680D-02	.52764D-02	.89673D-02	.20417D-03	-.33598D-02	-.23183D-01
-.11318D-01	-.70203D-02	-.88853D-02	-.12244D-01	.29124D-01	.13100D-01	-.33598D-02	.22330D-01	.22018D-01	-.10287D-01
-.64154D-02	-.20251D-01	.58822D-01	-.20061D-01	-.28963D-01	.89673D-02	.23301D-01	.22018D-01	.22330D-01	-.33751D-01
-.64940D-01	.35475D-02	.16737D-01							
.89774D-01	.32940D-02	.19940D-02	.27042	.69712D-01	-.92108D-01	-.15409	.25836	.95972D-01	1.0000
.0	.0	.0	.0	.0	.0	.0	.0	.0	.0
1.51864D-01	-.17075	-.49246	-.31690D-02	-.19419	-.84698D-01	-.17855	-.34427	-.112137	.0
1.00000	1.00000	.0	.0	.0	.0	.0	.0	.0	.0
-.56414D-01	.23060D-02	.10061D-02	-.26306	-.78476D-01	-.27892D-01	.14994D-01	-.25536	-.12137	.0
.16174D-01	-.16515	.49546	.41770D-02	-.20295	-.35302D-01	.58551D-01	.34727	-.37398D-01	.0
.0	.0	1.00000	.0	.0	.0	.0	.0	.0	IBM Z30687

THE EXPANDED BIFFLAR FORCE VECTOR OF ORDER = 13

- .38036D-05 - .87050D-05 .25502D-04 -.13759D-04 -.14091D-04 .29357D-05 .99558D-05 .45950D-05 -.68925D-05 .0
0 .0

FINAL COMBINED MASS MATRIX OF ORDER 29 FOR PSI= .0

1	.30344	-.81765D-01	-2.9687	-2.3651	1.7839	.22624	.17970	.79122	+1.2707	.94238D-04
	.38577D-05	.86147D-01	.0	-.34010D-02	.46788D-02	.17445D-01	.19518D-01	-.33621	-101.32	
	.75043	.10999D-02	.74987D-04	-.75763D-02	-.70140D-03	.22596D-01	.38222D-02	-.14703D-01	.40709D-02	-18.629
2										
	-.81765D-01	4.6785	-.11174	-.77927D-01	1.2008	.60633D-01	-.16217	-6.0335	-.21990D-01	-1.0366D-01
	.42434D-03	9.4761	.0	.54962D-02	.66219D-02	.18770D-01	.40917D-01	-.102.89	7.3431	2.8095
	.35.0468	-.12234D-01	.82485D-02	-.17757D-03	...66925D-02	.82307D-03	-.62976D-01	...58044D-03	-.41567D-01	...
	2.9687	-.11174	16.746	6.5549	-.4.9101	-.44102	.15529	-2.9867	3.2545	.29214D-01
	1.11955D-02	26.705	.0	.54192D-03	-.10372D-01	.20323D-01	.63568D-01	-.75.389	263.46	5.5910
	-.80.063	-.19410D-02	-.23246D-01	.19266D-01	.79832D-02	.50187D-03	-.12395	.25322D-03	.12470	
3										
	-.2.3651	-.77927D-01	6.5542	9.1646	-.3.8371	-.72238	-.84356	-.78956	3.5180.	.94238D-04
	-.38577D-05	.86147D-01	.0	-.10372D-01	-.75966D-02	.58028D-01	-.49522D-01	24.190	233.26	-32.934
	4.5767	-.64700D-03	-.74987D-04	.17964D-01	-.11424D-03	.68664D-01	.80266D-03	-.66210D-01	.10513D-02	
4										
	1.7839	1.2008	-.4.9101	-3.8371	6.7034	.38945	.76440D-01	-3.9865	-2.0075	.10366D-01
	-.42434D-03	-9.4761	.0	.11440D-02	.14920D-01	.31152D-01	-.17411D-01	-80.374	150.60	-18.270
	39.574	-.64700D-01	-.82485D-02	-.11883D-01	.48121D-02	.17546D-01	.48877D-01	-.19752D-01	-.51068D-01	
5										
	22634	.60633D-01	-.44102	-.72238	.38545	2.0415	.14325	-.41731	-.37564	-.20732D-02
	.84868D-04	1.8952	.0	.14227D-02	-.22847D-03	.50321D-02	.10771D-01	-.11.265	-22.983	3.7638
	4.3473	-.32350D-02	.16492D-02	-.18448D-02	.83929D-02	-.23183D-01	-.21318D-01	-.70203D-02	-.88953D-02	
6										
	1.7970	-.16217	.15529	-.84336	.76440D-01	.14325	2.3217	-.47330D-01	-.45179	-.20732D-02
	.84868D-04	1.8952	.0	.23246D-02	-.42724D-02	-.14042D-01	-.33230D-01	-.10.263	-22.534	
	21.450	-.64700D-03	.16497D-02	-.18408D-02	.69926D-03	-.33751D-01	-.44940D-01	.35477D-02	.14737D-01	
7										
	79122	-6.0335	-2.9867	.78956	-.3.9865	-.41731	-.47330D-01	30.528	.35510	-.11760D-01
	.48221D-03	10.768	.0	.31467D-01	-.11927D-01	.26212D-01	.87611D-01	433.11	-.47.266	
	-61.393	.12940D-01	.93733D-02	-.10558D-03	-.34182D-01	.65025D-01	-.86552D-01	-.66273D-01	.87427D-01	-.51.099
8										
	-.1.2707	-.21990D-01	3.2545	3.5180	-.2.0075	-.37584	-.45179			
	.38577D-05	.86147D-01	.0	.41496D-02	-.32419D-02	.22168D-01	-.31427D-01	15.882	122.01	-11.405
	5.9875	-.12940D-02	.74987D-04	.93963D-02	-.32554D-03	.24155D-01	.30199D-02	-.30549D-01	-.94129D-02	
9										
	10									
	-.37655D-03	-.41465D-01	.11685	.37695D-03	.41465D-01	-.82929D-02	-.82929D-02	-.47119D-01	-.37695D-03	.12446
	-.25186D-03	.62860	-.96089D-01	.0	.0	.0	.0	.0	.0	
	0	0	0	0	0	0	0	0	0	
11										
	.15431D-04	1.6974D-02	-.47835D-02	-.15431D-04	-.16974D-02	.33947D-03	.19288D-02	.15431D-04	-.25186D-03	
	20956	-.3.9359	.75778	.0	.0	.0	.0	.0	.0	
	0	0	0	0	0	0	0	0	0	

IBM 230687

12

IBM Z30687

FINAL COMBINED FORCE VECTOR OF ORDER 29 FOR PSI = .0

STATE VARIABLES (DISP&VEL) FOR PSI = .0

STATE VARIABLES (DISP&VEL) FOR PSI = .0	
- .25286D-11	- 1.9571D-08
- .26472D-11	- .2049D-08
.46451D-11	.3593D-08
- .7143D-11	- .5529D-08
- .15220D-11	- .4043D-08
.16185D-11	.1257D-08
.5132D-11	.3973D-08
.23666D-12	.1831D-09
- .12391D-11	- .9599D-09
.12391D-11	.9599D-09
- .30384D-11	- .2357D-08
.41981D-12	.3429D-09
.18716D-13	.1446D-10
- .30990D-16	- .2398D-13
- .11555D-11	- .8945D-09
.36247D-11	.2805D-08
.63628D-11	.4949D-08

.10919D-0	=	.845100-08
.11122D-13	-	.148010-10
.31698D-13	-	.24534D-10
.50001D-13	-	.38701D-10
.93811D-13	-	.72810D-10
.44216D-11	-	.34222D-08
.31637D-11	-	.24487D-08
.40165D-12	-	.31088D-09
.18836D-12	-	.14578D-09

BIFFLAR. INITIAL DISP. & VEL. FOR PST. = 0

.36172D-11	.	.26449D-08
.69642D-11	.	.38423D-08
.25522D-11	-	.19754D-08
.40992D-11	-	.31728D-08

FIXED SYSTEM + ROTOR + FIXED ABSORBERS (R.H.S.) OF ORDER 25 ($\psi = 2 \text{ DEC}$)

.13624D-07	.	.44860D-07	-	.22938D-06	.	.23600D-06	.	.13370D-06	-	.28865D-07	-	.92330D-07	-	.10942D-06	.	.20289D-06	*	.41028D-08
.27024D-09	-	.50329D-06	-	.84167D-06	.	.94017D-08	.	.19417D-07	-	.12205D-16	-	.45731D-08	.	.16607D-05	-	.36607D-05	.	.73551D-04
.30634D-04	=	.70809D-07	-	.492443D-07	.	.50507D-07	.	.235338D-08	-	.235338D-08								

STATE VARIABLES (DISP&VEL) FOR PSI = 30.000

.....	25048D-14	38904D-02
.....	.11111D-0429375D-03
.....	-.12945D-0460366D-03
.....	-.61756D-04	-.87113D-02
.....	-.34311D-05	-.23132D-02
.....	-.69925D-1513406D-02
.....	.10632D-0438400D-02
.....	-.37044D-06	-.35237D-02
.....	-.73576D-05	-.102882D-02
.....	.24983D-05	-.90190D-03
.....	-.12617D-0616874D-03
.....	-.25183D-0741743D-05
.....	-.94686D-09	-.10165D-05
.....	-.41310D-04	-.35801D-02
.....	-.20113D-0435268D-03
.....	.59878D-0649570D-02
.....	-.44100D-05	-.61698D-02
.....	-.20268D-0518932D-03
.....	-.15160D-0518076D-03
.....	-.61764D-06	-.77497D-04
.....	-.22019D-0632475D-06
.....	-.12211D-0425428D-02
.....	-.12016D-0511571D-02
.....	-.20069D-0411886D-02

STETIAB TINITAI DISB' & VEL EOB BST = 30 000

REV= 2, G1=.183D-01, G2=.160D-01, XHUB=.412D-02, YHUB=.317D-02, THZH=.301D-05, DXHUB=.315, DYHUB=.224

NREV=	3,	G1=	183D-01,	G2=	288D-01,	XHUB=	439D-02,	YHUB=	484D-02,	TH2I=	698D-05,	DXHUB=	534	DYHUB=	197
NREV=	4,	G1=	116D-01,	G2=	351D-01,	XHUB=	397D-02,	YHUB=	569D-02,	TH2I=	976D-05,	DXHUB=	686	DYHUB=	117

```

NREV= 5, G1= .462D-02, G2= .344D-01, XHUB= .333D-02, YHUB= .592D-02, THZH= .122D-04, DXHUB= .770..., DYHUB= .486D-01.

NREV= 6, G1= .185D-02, G2= .301D-01, XHUB= .321D-02, YHUB= .601D-02, THZH= .131D-04, DXHUB= .812..., DYHUB= .176D-01.

NREV= 7, G1= .437D-02, G2= .219D-01, XHUB= .105D-02, YHUB= .526D-02, THZH= .146D-04, DXHUB= .749..., DYHUB= .140.

NREV= 8, G1= .128D-01, G2= .984D-02, XHUB= .271D-02, YHUB= .371D-02, THZH= .128D-04, DXHUB= .614..., DYHUB= .183.

NREV= 9, G1= .124D-01, G2= .213D-02, XHUB= .247D-02, YHUB= .261D-02, THZH= .103D-04, DXHUB= .468..., DYHUB= .148.

NREV= 10, G1= .653D-02, G2= .821D-02, XHUB= .455D-02, YHUB= .226D-02, THZH= .844D-05, DXHUB= .382..., DYHUB= .608D-02.

NREV= 11, G1= .454D-03, G2= .813D-02, XHUB= .141D-02, YHUB= .257D-02, THZH= .723D-05, DXHUB= .361..., DYHUB= .176D-01.

NREV= 12, G1= .452D-02, G2= .419D-02, XHUB= .191D-02, YHUB= .312D-02, THZH= .781D-05, DXHUB= .399..., DYHUB= .573D-01.

NREV= 13, G1= .483D-02, G2= .310D-03, XHUB= .201D-02, YHUB= .356D-02, THZH= .846D-05, DXHUB= .450..., DYHUB= .470D-01.

NREV= 14, G1= .252D-02, G2= .298D-02, XHUB= .174D-02, YHUB= .374D-02, THZH= .932D-05, DXHUB= .483..., DYHUB= .131D-01.

NREV= 15, G1= .123D-01, G2= .309D-02, XHUB= .147D-02, YHUB= .371D-02, THZH= .989D-05, DXHUB= .486..., DYHUB= .195D-01.

NREV= 16, G1= .179D-02, G2= .148D-02, XHUB= .135D-02, YHUB= .363D-02, THZH= .1040D-04, DXHUB= .464..., DYHUB= .327D-01.

```

THE NUMBER OF REVOLUTIONS REQUIRED TO CONVERGE = 16

INPUT FIXED SYSTEM MODES FREQUENCIES IN HZ

5,10	6,40	15,3	14,2	13,8	11,6	12,1	17,4	21,1
------	------	------	------	------	------	------	------	------

THE CONVERGENCE FACTOR TO G = 30.2

BIFILAR HARMONIC OUTPUT - AMPLITUDE AND PHASE

IBM Z30687

	1 P	2 P	3 P	4 P	5 P	6 P	7 P	8 P	9 P
	1 P	2 P	3 P	4 P	5 P	6 P	7 P	8 P	9 P
1	.725760-02	.203050D-01	.9.7569	-.559910D-01	-.164460D-01	-.299650D-02	-.515150D-02	-.39280D-02	-.279980D-02
	52.592	53.478	96.204	-124.06	29.256	-124.17	-103.32	-100.26	-132.76
2	.130260D-01	.273970D-01	.9.7675	-.361920D-01	-.371970D-01	-.334460D-02	-.416630D-02	-.290310D-02	-.313040D-02
	167.32	-177.75	-172.99	-49.115	-46.272	30.184	-45.499	-31.080	-18.104
3	.338070D-02	-.87900D-02	.9.7962	-.347740D-01	-.216690D-01	-.130220D-01	-.674880D-02	-.602910D-02	-.329220D-02
	-107.27	-66.614	-83.966	83.358	-154.00	18.479	79.690	75.105	63.689
4	.122760-01	-.122590D-01	.9.7978	-.476730D-01	-.35955D-01	-.138660D-01	-.316020D-02	-.231910D-02	-.324950D-02
	5.5568	-31.531	6.2263	167.95	139.47	-166.74	154.27	124.83	170.57
HARMONIC HUB OUTPUT - COSINE , SINE AND TOTAL RESPONSE AND PHASE ANGLE IN DEGREES									
	1 P	2 P	3 P	4 P	5 P	6 P	7 P	8 P	9 P
1	-.353870D-03	-.713320D-03	-.10783D-02	.13513D-01	-.11137D-01	-.43362D-03	.23521D-03	.59209D-03	.93772D-04
	.717860-04	.157370D-03	.1343-03	-.13798	-.16454D-02	-.48493D-03	-.21450D-03	-.17708D-03	-.62981D-03
	.36100D-03	-.73468D-03	-.10866D-02	.13864	-.11314D-01	-.98551D-03	-.54069D-03	-.29251D-03	-.21521D-03
	168.53	167.56	172.90	-86.407	10.158	-63.896	-64.214	-19.929	-71.303
2	.84053D-04	-.17284D-03	-.40974D-03	-.494763D-01	-.98815D-02	-.10481D-03	-.62883D-04	-.22187D-03	-.38672D-04
	12153D-03	-.11195D-03	-.552D-03	-.31934D-01	-.16442D-02	-.19251D-03	-.23191D-03	-.30311D-14	-.42152D-04
	.147760-03	-.20570D-03	.68215D-03	.99988D-01	-.10017D-01	-.21915D-03	-.65026D-04	-.31522D-03	-.49135D-04
	55.331	-146.37	-128.92	-18.623	9.44668	-61.433	-14.750	-45.263	38.090
3	-.18544D-03	-.12556D-03	-.20801D-03	.49658D-02	-.29709D-02	-.36247D-03	-.16057D-03	-.73182D-04	-.68470D-04
	-.20083D-04	-.20287D-03	-.12629D-03	-.23223D-03	-.82157D-02	-.74049D-02	-.37798D-03	-.16333D-03	-.73886D-04
	1.8653D-03	-.12429D-03	-.23223D-03	-.82157D-02	-.74049D-02	-.37798D-03	-.16333D-03	-.68586D-04	-.68586D-04
	-173.82	-170.53	-153.60	-52.813	66.346	-16.471	-10.552	-21.891	-3.0290
4	.11692D-04	-.18351D-04	-.20934D-04	-.20934D-04	-.10068D-02	-.25708D-03	-.40228D-04	-.18089D-04	-.63736D-05
	-.34145D-05	.35367D-05	-.17642D-05	-.17642D-05	-.65194D-03	-.76333D-05	-.43971D-04	-.55117D-05	-.77610D-05
	.12181D-04	1.86920D-04	-.21003D-04	-.10444D-02	-.70180D-03	-.61367D-04	-.18615D-04	-.43516D-05	-.82224D-15
	-16.279	10.969	-4.3173	-15.013	-68.479	-116.53	-166.34	-146.29	-163.98
5	-.20246D-04	-.28350D-04	-.33290D-04	-.11186D-02	-.32143D-03	-.43543D-04	-.20260D-04	-.17703D-04	-.86785D-05
	.17520D-05	-.63393D-06	-.17411D-05	-.17411D-05	-.17726D-13	-.17718D-04	-.17411D-05	-.17411D-05	-.17411D-05
	.21604D-05	1.01020D-05	-.28203D-05	-.34176D-03	-.55692D-04	-.26203D-05	-.11028D-05	-.13328D-05	-.16885D-16
	54.189	-141.44	3.5747	31.243	-65.566	64.598	-21.874	-20.543	-20.932
6	.12641D-05	-.79781D-06	.20154D-05	-.29220D-03	-.44537D-04	-.11795D-05	-.42701D-06	-.17881D-06	-.21827D-06

VIBRATION LEVELS AT 4 A/C LOCATIONS.

COSINE,SINE,TOTAL AMPLITUDE IN G AND PHASE ANGLE IN DEGREES OF POINT 1

	1 P	2 P	3 P	4 P	5 P	6 P	7 P	8 P	9 P
1	.746460-04	.10500D-03	.16495D-03	-.68216D-02	-17400D-03	-.11784D-03	-.6963D-04	-.77459D-04	-.35567D-04
	-.17197D-04	.10153D-04	.45374D-04	.16337D-01	-.15142D-02	-.82238D-05	.90956D-05	.72264D-05	.75590D-05
	.76610D-04	.10583D-03	.17108D-03	.17423D-01	-.15242D-02	-.15811D-03	.70234D-04	.77795D-04	.33389D-04
	-12.973	5.5052	15.381	113.04	-.96.705	-176.38	-172.56	174.67	-167.27

2	-.446641D-03	-.23631D-03	-.40666D-03	-.26798D-02	-.25074D-01	-.26798D-02	-.55354D-03	-.10032D-03	-.11363D-03
	-.20510D-03	-.23326D-04	.38911D-05	.11033D-01	.88283D-02	.15384D-03	.87506D-04	.12696D-04	.56310D-06
	.49145D-03	.23746D-03	.40668D-03	.27394D-01	.92260D-02	.57452D-03	.26765D-03	.10112D-03	.12594D-03
	-155.28	-174.36	179.46	23.751	106.89	15.532	19.083	-7.2126	25.547

3	-.21825D-03	-.39446D-03	-.13510D-01	-.38145D-02	.62622D-03	.29079D-03	.18752D-03	.12778D-03	
	-.27545D-04	-.80199D-04	-.10098D-03	.51186D-02	.92417D-02	.19182D-03	.96591D-04	.33601D-04	.56114D-04
	-.21928D-03	-.10258D-03	-.57717D-03	-.94656D-01	.92998D-02	.65394D-03	.30644D-03	.19054D-03	.13878D-03
	-172.81	-168.51	169.92	-20.737	112.43	17.031	18.375	10.218	22.962

COSINE,SINE,TOTAL AMPLITUDE IN G AND PHASE ANGLE IN DEGREES OF POINT 2

1	.10408D-03	.14141D-03	.21754D-03	-.67876D-02	-.71064D-03	-.16505D-03	-.90701D-04	-.99222D-04	-.40506D-04
	-.70720D-05	.37854D-15	.37775D-09	.18411D-04	-.22860D-02	.37913D-04	.16083D-04	.17450D-04	.65686D-05
	.10433D-03	.141416D-03	.22073D-03	.19622D-01	.23939D-02	.18889D-03	.92117D-04	.10074D-03	.41041D-04
	-3.8905	1.5338	9.7485	110.24	-107.27	168.42	169.94	170.03	170.76

2	-.75268D-03	-.27576D-03	-.32357D-03	.60933D-02	.96273D-02	.59963D-03	.25702D-03	.14243D-03	.99366D-04
	-.39016D-03	.16613D-03	.40307D-01	-.10196D-01	-.11193D-01	-.76927D-03	-.59836D-03	-.23445D-03	-.21426D-03
	.88693D-03	.32194D-03	.51668D-03	.12543D-01	.14763D-01	.97539D-03	.47408D-03	.27432D-03	.24613D-03
	-153.84	168.93	128.76	-60.936	49.299	52.061	-57.171	-58.721	-65.120

3	.11722D-03	-.18744D-03	-.82776D-04	.15241D-01	-.12303D-01	.15987D-03	.82946D-04	-.57137D-05	.47371D-04
	-.22443D-04	-.15777D-13	-.76443D-04	-.88377D-01	-.86195D-01	.61282D-05	.35292D-05	.12336D-03	.17070D-03
	.11935D-03	.24445D-03	.11267D-03	.32205D-01	.12333D-01	.71102D-03	.34310D-03	.12350D-03	.17715D-03
	10.839	-140.01	-137.28	61.755	176.00	77.007	76.010	92.652	74.490

COSINE,SINE,TOTAL AMPLITUDE IN G AND PHASE ANGLE IN DEGREES OF POINT 3

COSINE,SINE,TOTAL AMPLITUDE IN G AND PHASE ANGLE IN DEGREES OF POINT 3

	1 P	2 P	3 P	4 P	5 P	6 P	7 P	8 P	9 P
1	.63665D-04	.99252D-06	.13585D-03	-.39269D-02	-.89703D-03	-.14680D-03	-.68826D-04	-.60697D-04	-.29305D-04
2	-.39462D-05	.71563D-05	.22363D-04	.83731D-02	-.22399D-02	.52889D-04	.23639D-04	.19217D-04	.10721D-04
3	-.63787D-04	.99510D-04	.13767D-03	.92482D-02	-.24129D-02	.15612D-03	.72237D-04	.63666D-04	.31205D-04
4	-3.5476	4.1240	9.3461	115.13	-111.82	160.21	160.90	162.43	159.90

COSINE, SINE, TOTAL AMPLITUDE IN G AND PHASE ANGLE IN DEGREES OF POINT 4

1	-604560-03	.587790-03	-438290-03	-193490-01	-138830-01
	-2.272740-03	.151030-03	-212400-04	-702850-02	-422470-02
	.663330-03	.606880-03	.438810-03	.205860-01	.145120-01
	-455.72	14.410	-177.23	-160.04	-163.07
				94.313	90.405
					102.51
					.87.165

-14666D-02 : 50814D-03 : 1911D-03 :-28815D-01 : 11971D-01 :-6144D-03 :-2915D-03 :-14729D-03

3	.42239D-03	-.38248D-03	-.12887D-04	.79289D-02	-.66865D-03	-.24120D-04	-.935673D-05	.11985D-03	-.49814D-05
	.18832D-03	-.15771D-03	-.43586D-03	.48224D-02	-.18224D-02	-.12142D-03	-.96211D-04		
	.46267D-03	-.41296D-03	4.3605D-03	.88044D-02	.17733D-02	.18383D-03	.13764D-03	.17058D-03	.96340D-04
	.24.095	-.157.85	91.69%	-.25.769	-.112.16.	-.97.552	-.93.894	-.45.380	-.92.964

INTIAL STATEMENT OF DISREAGEMENTS (IF 1720-1739)

WILSON, JR., ROBERT C. 16500

INITIAL BIFILAR VEHICLES (IC-1748-1759)

Z Z30 -7 E440 -13 617 3 5655

卷之三

INITIAL_HUB_DISPLACEMENTS [(LC.1768-1773)]**.15065D-02 .35604D-02 .25974D-03 .45856D-04 .59105D-04 .10595D-04****INITIAL_HUB_VELOCITIES** [(LC.1774-1779)]**-43641 -2.7046D-01 -16799D-01 -33085D-02 -43242D-02 -10283D-02****INITIAL_STATE_VARIABLES_DISP** [(LC.1780-1859)]

-.41930D-04 .83752D-04 .47216D-04 .38650D-02 .19628D-03 -.44669D-03 -.97616D-03 .25776D-02 -.29864D-03 -.92779D-04 .59510D-04
-.47164D-04 -.53035D-05 .31295D-07 .39200D-03 -.10109D-01 -.13128D-02 -.13922D-03 -.13922D-04
1.3630D-04 -.56352D-02 -.20740D-01 -.11073 -.51973D-01

INITIAL_STATE_VARIABLES_VELOC [(LC.1860-1939)]

.47650D-01 -.11795D-01 -.21021 .15078 .14798 -.33559D-01 -.99727D-01 -.22058 .20160D-01 -.18196 .44570D-03
-.10169 -.33443D-03 -.11013D-04 -.1.2027 .30764D-01 .6774 -.27664 .92194D-02 -.76840D-02
-.79449D-02 -.23740 2.7402 5.2117 14.502

CASE 3. BIFILAR RESULTS
BIFILAR ANALYSIS RESULTS

ALL DISPLACEMENTS ARE IN G AND ALL ANGLES ARE IN DEGREES

NUMBER OF FIXED SYSTEM MODES	IS 9
NUMBER OF FIXED SYSTEM ABSORBERS	IS 1
NUMBER OF INPLANE BIFILARS	IS 1
NUMBER OF VERTICAL BIFILARS	IS 1
TOTAL NO. OF DEGREES-OF-FREEDOM (WITH,NO,ROTOR)	IS 16
NUMBER OF A.C. STATIONS	IS 4
ROTOR COUPLING SWITCH (0=NO,1=YES) IS 0	
ROTOR MATRICES PRINTOUT (0=NO,1=YES) IS 0	
FIXED SYSTEM MATRICES PRINTOUT " IS 0	
ADD ROTOR MATRICES PRINTOUT " IS 0	
ADD FIX.SYS. ABSORBER PRINTOUT " IS 0	
ADD INPLANE BIFILAR PRINTOUT " IS 0	
ADD VERTICAL BIFILAR PRINTOUT " IS 0	
INPLANE BIFILAR (9X9) PRINTOUT " IS 0	
VERTICAL BIFILAR (9X9) PRINTOUT " IS 0	
GAMMAS PRINTOUT " IS 0	

PRESENT NO. OF DEGREES-OF-FREEDOM (NP) = 9
 ADDITIONAL NO. DEGREES-OF-FREEDOM (NA) = 1
 TOTAL NO. OF DEGREES-OF-FREEDOM (NP+NA) = 10
 ORDER OF MATRIX TO BE ADDED (NL) = 2
 ORDER = D.O.F. OF ADDED MATRIX (NL-NA) = 1

INPLANE BIPLIAR PARAMETERS

TOTAL NO. OF BIPLIARS (N)	=	4.00000
BIPLIAR MASS (M)	=	.614000D-01
BIPLIAR ARM (RCR)	=	18.2200
BIPLIAR FREQUENCY (W)	=	3.00000
BIPLIAR RADIUS (R=RCR/W)	=	2.02444
NHMR*R	=	1.00656
1+NHMR	=	10.0000
NHMR*RH(1.+NHMR)	=	10.0656
NHMR*RH(1.+NHMR)*RH2	=	100.656

PRESENT NO. OF DEGREES-OF-FREEDOM (NP) = 10
 ADDITIONAL NO. DEGREES-OF-FREEDOM (NA) = 3
 TOTAL NO. OF DEGREES-OF-FREEDOM (NP+NA) = 13
 ORDER OF MATRIX TO BE ADDED (NL) = 9
 ORDER = D.O.F. OF ADDED MATRIX (NL-NA) = 6

VERTICAL BIELLAB PARAMETERS

TOTAL NO. OF BIFILARS (N)	=	4,00000
BIFILAR MASS	(M)	= .6080000-01
DISTANCE FROM C.R.	(R)	= 18.5000
BIFILAR FREQUENCY	(N)	= 4,00000

$R1=R/(NM-1,1)$	$= -1.23333$
$R1*R1$	$= 1.52111$
$R1*R1$	$= 19.7333$
$(R1+R1)*R2$	$= 389.404$
$MNN*(R1+R1)$	$= 4.72915$
$MNN*(R1+R1)*R2$	$= 94.7032$
$MNN*(R1+R1)$	$= 91805$

PRESENT NO. OF DEGREES-OF-FREEDOM (N.F.) = 13

ADDITIONAL NO. DEGREES-OF-FREEDOM (NA) = 3 TOTAL... NO. OF DEGREES-OF-FREEDOM (NP+NA) = 16. ORDER OF MATRIX TO BE ADDED	[NLM] = 9 ORDER NO. OF ADDED MATRICES ORDER NO. OF ADDED MATRICES
---	--

GENERALIZED FORCES - ORDER IS 9

COSINE COMPONENT

.500000	-170.000	500.000	.500000	-201.000	25.0000	120.000	350.000
-25.0000							

SINE COMPONENT

75.0000	.500000	.500000	270.000	75.0000	-32.5000	-75.0000	260.000
110.000							

(GAMMAS)

COSINE - SINE - AMPLITUDE - PHASE (DEG)

FIXED SYSTEM ABSORBER(S)

-166206D-02 .216652D-02 .273066D-02 127.493

INPLANE BIPILAR PENDULUM(S)

(EQT ORDER IS:0,SIN,COS) (AMPL & PHASE ORDER IS:N,N-1,N+1) DEG & DEG

.346150D-03 .243546D-03 .606250D-02 35.1296
.329375 .265358D-01 9.55124 -85.7598
.228424D-01 -.3333496 .792694D-01 -131.867

VERTICAL BIPILAR PENDULUM(S)

(EQT ORDER IS:0,SIN,COS) (AMPL & PHASE ORDER IS:N,N-1,N+1) DEG & DEG

-.373716D-01 .363299D-01 .746566 135.810
.504592D-02 .162357D-02 -.488249D-01 -61.7531
.764629D-04 .516534D-02 .190785 97.3330

INPUT FIXED SYSTEM FREQUENCIES (HZ)

5.10000 6.40000 15.3000 14.3000 13.8000 11.6000 12.1000 17.4000 21.1000

FORCING FREQUENCY (HZ) = 17.2000

THE CONVERSION FACTOR TO G = 30.2259

FUSELAGE NO. OF DEGREES OF FREEDOM E 9

COSINE COMPONENT

	X	Y	Z
COSINE	.137705D-03	.105885D-03	-.185943D-02
SINE	-.198076D-03	-.188549D-03	.153812D-02
	.182804D-03		-.441784D-03

	X	Y	Z
COSINE	.166214D-03	.218335D-03	-.169248D-02
SINE	.878125D-04	.389724D-03	.533932D-02

SINE COMPONENT

	X	Y	Z
COSINE	-.198076D-03	-.188549D-03	.153812D-02
SINE	.182804D-03		-.441784D-03

	X	Y	Z
COSINE	.166214D-03	.218335D-03	-.169248D-02
SINE	.878125D-04	.389724D-03	.533932D-02

FIRST A.C. STATION DISPLACEMENT IN G

	X	Y	Z
COSINE	.878210D-02	-.232140D-01	-.861884D-02
SINE	.248196D-01	.901561D-02	.264515D-02

	X	Y	Z
COSINE	.878210D-02	-.232140D-01	-.861884D-02
SINE	.248196D-01	.901561D-02	.264515D-02

FIRST A.C. STATION TOTAL DISPLACEMENT IN G

	X	Y	Z
COSINE	.248196D-01	.901561D-02	.189416D-01
SINE			

	X	Y	Z
COSINE	.248196D-01	.901561D-02	.189416D-01
SINE			

FIRST A.C. STATION PHASE ANGLE IN DEG

-69.2778 162.939 112.966

SECOND A.C. STATION DISPLACEMENT IN G

	X	Y	Z
COSINE	.961892D-02	-.257500D-01	-.631791D-02
SINE	.274873D-01	.192127D-01	.142074D-01

	X	Y	Z
COSINE	.961892D-02	-.257500D-01	-.631791D-02
SINE	.274873D-01	.192127D-01	.142074D-01

SECOND A.C. STATION TOTAL DISPLACEMENT IN G

-69.5168 109.198 -127.711

THIRD A.C. STATION DISPLACEMENT IN G

IBM Z30687
261

ROTOR HEAD DISPLACEMENT PHASE ANGLES IN DEG

113.199 136.580

45.8099

CASE 4. BIFILAR RESULTS

BIFILAR...ANALYSIS...RESULTS

ALL DISPLACEMENTS ARE IN G AND ALL ANGLES ARE IN DEGREES

NUMBER OF FIXED SYSTEM MODES	IS 9
NUMBER OF FIXED SYSTEM ABSORBERS	IS 1
NUMBER OF INPLANE BIFILARS	IS 0
NUMBER OF VERTICAL BIFILARS	IS 1
TOTAL NO. OF DEGREES-OF-FREEDOM (WITH NO. ROTOR)	IS 13
NUMBER OF A.C. STATIONS	IS 4
ROTOR COUPLING SWITCH.....(0=NO,1=YES) IS ...0	
ROTOR MATRICES PRINTOUT(0=NO,1=YES) IS 0	
FIXED SYSTEM MATRICES PRINTOUT " IS 0	
ADD ROTOR MATRICES PRINTOUT " IS 0	
ADD FIX.SYS. ABSORBER PRINTOUT " IS 1	
ADD INPLANE BIFILAR PRINTOUT " IS 1	
ADD VERTICAL BIFILAR PRINTOUT " IS 0	
INPLANE BIFILAR (9X9) PRINTOUT " IS 0	
VERTICAL BIFILAR (9X9) PRINTOUT " IS 0	
GAMMAS PRINTOUT " IS 0	

PRESENT NO. OF DEGREES-OF-FREEDOM (NP) = 9
 ADDITIONAL NO. DEGREES-OF-FREEDOM (NA) = 1
 TOTAL NO. OF DEGREES-OF-FREEDOM (NP+NA) = 10
 ORDER OF MATRIX TO BE ADDED (NL) = 2
 ORDER D.O.F. OF ADDED MATRIX (NL=NA) = 1

VERTICAL BIFLAR PARAMETERS

TOTAL NO. OF BIFLARS (N) =	4.00000
BIFLAR MASS (M) =	.6080000-01
DISTANCE FROM C.R. (R) =	16.5000
BIFLAR FREQUENCY (W) =	4.00000
R1=R/(W*NA-1)	
R1*RI	= 1.52111
R+RI	= 19.7333
(R*RI)*2	= 389.404
M=M*(R*RI)	= 4.79915
M=M*(R*RI)*2	= 94.7032
M=M*(R*RI)	= 5.91895

PRESENT NO. OF DEGREES-OF-FREEDOM (NP) = 10
 ADDITIONAL NO. DEGREES-OF-FREEDOM (NA) = 3
 TOTAL NO. OF DEGREES-OF-FREEDOM (NP+NA) = 13
 ORDER OF MATRIX TO BE ADDED (NL) = 9
 ORDER D.O.F. OF ADDED MATRIX (NL=NA) = 6

D.Q.E.=1.17,NEF=2,KROTR=0,NFABSE=1,KINDS.OF.INPL.BIF=0,KINDS.OF.VERT.BIF=1,NUMB.OF.N.L.INPL.BIF=4

FIXED SYSTEM + ROTOR + FIXED ABSORBERS (R.H.S.) OF ORDER 13

THE MASS (L.H.S.) MATRIX OF ORDER 10

THE ROTOR HEAD MODE SHAPES, TRANSPOSE(PHI), OF ORDER 9 X 6

.10000D-02	.15000	.10000D-02	.51200D-02	.47400D-03	.15680D-02
-.34000	.10000D-02	.11000	-.12000D-03	-.11630D-02	.28000D-03
1.0000	.10000D-02	.31000	.13020D-01	-.53950D-02	.15000D-03
.10000D-02	.64000	.10000D-02	.12400D-01	.77200D-06	.36830D-03
-.40200	.15000	.11000	-.80100D-02	-.32520D-02	-.43820D-03
.50000D-01	-.65000D-01	.22000D-01	-.12440D-02	-.47300D-03	-.60000D-02
.24000	.15000	.22000D-01	-.12440D-02	-.47300D-03	-.60000D-02
-.70000	.32000	.12500	-.20000D-04	.23100D-01	.15000D-03
-.50000D-01	.22000	.10000D-02	.63500D-02	.22000D-03	-.12700D-02

THE EXPANDED BIFILAR MASS MATRIX OF ORDER = 13

.57749D-02	-.24725D-05	.30618D-03	.19956D-01	.53592D-02	-.33300D-02	-.64154D-02	.19357D-01	.76938D-02	.22596D-01
.38222D-02	-.14703D-01	.40703D-02	.59213D-01	.59213D-04	.13660D-01	-.43361D-02	-.20251D-01	-.58333D-01	.41945D-02
-.24725D-05	.28406D-01	-.83517D-01	.41567D-01	.42976D-01	.42976D-03	.82907D-01			
.42976D-01	.58041D-03	-.41567D-01	.30618D-03	.38387D-03	-.98772D-01	.12176D-01	.58829D-01	.17209	-.12246D-01
.30618D-03	-.83517D-01	.245565	.12470	.19956D-01	.19783D-01	-.88326D-02	-.20061D-01	.69157D-01	.29124D-01
-.12335	.25332D-03	.38387D-03	.71646D-01	.58829D-01	.58829D-03	.19357D-01	.59513D-04	.68664D-01	
.19956D-01	.59513D-04	.38387D-03	.10513D-02	.19783D-01	.19783D-01	-.88326D-02	-.20061D-01	.69157D-01	.29124D-01
.80266D-03	-.66210D-01	.19783D-01	.98722D-01	.98722D-01	.98722D-01	-.70680D-02	-.70680D-02	-.28963D-01	.17546D-01
.53592D-02	.33600D-01	-.98722D-01	.19783D-01	.45245D-01	.45245D-01	-.70680D-02	-.70680D-02	-.49972D-01	.13100D-01
.48877D-01	-.19783D-01	-.51082D-01	-.51082D-01	.19783D-01	.19783D-01	-.88326D-02	-.88326D-02	-.89673D-02	.213183D-01
-.33300D-02	-.63612D-02	-.13176D-01	-.88853D-02	-.88853D-02	-.88853D-02	-.52764D-02	-.52764D-02	-.89673D-02	.20417D-01
.21318D-01	-.70203D-02	-.88853D-02	-.88853D-02	-.88853D-02	-.88853D-02	.23301D-01	.23301D-01	.22018D-01	-.10287D-01
-.64154D-02	-.20251D-01	.58829D-01	-.20061D-01	-.28963D-01	-.28963D-01	.89673D-02	.89673D-02	.22018D-01	-.33751D-01
-.44940D-01	.35475D-02	.16737D-01	.16737D-01	.16737D-01	.16737D-01	.20417D-03	.20417D-03	.186680	.186680
.19357D-01	-.58333D-01	.17209	.69157D-01	-.49972D-01	-.49972D-01	.22018D-01	.22018D-01	.14946D-01	.65028D-01
-.86652D-01	-.64273D-01	.67407D-01	.67407D-01	.67407D-01	.67407D-01	.10287D-01	.10287D-01	.19486D-01	.12666D-01
-.78938D-02	.41945D-02	-.12246D-01	.29124D-01	.13100D-01	.13100D-01	-.33598D-02	-.33598D-02	.10287D-01	.24155D-01
.30199D-02	-.30549D-01	-.94123D-02	-.94123D-02	-.94123D-02	-.94123D-02	.19486D-01	.19486D-01	.12666D-01	.12666D-01
.89774D-01	.32944D-02	.19946D-02	.27042	.49712D-01	.49712D-01	-.92108D-01	-.92108D-01	.25836	.95972D-01
.0	.0	.0	.0	.0	.0				1.0000
.15186D-01	.17075	-.49246	.31890D-02	.19419	.19419	-.84698D-01	-.17855	-.34427	.11998D-01
1.0000	.0	.0	.0	.0	.0				
-.58414D-01	.23060D-02	.10061D-02	-.26306	-.78476D-01	-.78476D-01	.14094D-01	.14094D-01	.25536	-.12137
.0	1.0000	.0	.0	.0	.0				
.16174D-01	-.16515	.49546	.41770D-02	-.20295	-.35302D-01	.58551D-01	.34727	-.37398D-01	.0

IBM Z30687

THE EXPANDED BIFILAR FORCE VECTOR OF ORDER = 13

.380360-05 -.870500-05 .255020-04 -.137590-04 .293570-05 .995580-05 .45950D-05 -.68925D-05 .0
.0 ,0 ,0 ,0 ,0 ,0 ,0 ,0

FINAL COMBINED MASS MATRIX OF ORDER 17 FOR PSIM=.0

1.	.8208	-.36060D-03	-.27779D-02	.36758D-01	.13611D-01	-.62287D-02	-.12413D-01	.39304D-01	.141e2D-01	.10999D-02
2.	.79867D-04	-.75763D-02	-.70149D-03	.22598D-01	.38322D-02	-.14703D-01	.40703D-02			
3.	.36060D-03	3.1263	-.17273	.17560D-03	*47531D-01	-.88206D-02	-.39753D-01	-.12186		.86300D-02
	.82485D-02	-.17757D-03	.76695D-02	.82970D-03	.42976D-01	.58041D-03	-.41567D-01			.17236D-01
4.	-.27779D-02	-.17273	5.6517	.33232D-02	-.19421	.2183D-01	.11475	.32670	-.20550D-01	-.19410D-02
	-.23246D-01	.19266D-01	.79832D-02	.50187D-03	.12395	.25322D-03	.12470			
5.	.36758D-01	.17560D-03	.83232D-02	2.4176	-.34132D-01	-.18321D-01	-.40640D-01	.61524D-01	-.64700D-03	
	-.74987D-04	.17964D-01	-.11424D-03	.68064D-01	.80266D-03	-.66210D-01	.10513D-02			
6.	.13611D-01	*47531D-01	-.19421	.34132D-01	2.9082	-.10887D-01	-.57047D-01	-.93380D-01	.22304D-01	.64700D-01
	.82485D-02	-.11853D-01	.48112D-02	.17546D-01	.46877D-01	-.19752D-01	-.51082D-01			
7.	-.32287D-02	-.88206D-02	.2183D-01	-.18321D-01	-.10887D-01	1.9517	.17900D-01	.12133D-02	-.71620-02	.32350D-02
	.16497D-02	-.18408D-02	.69992D-03	-.23183D-01	-.21313D-01	-.170203D-02	-.88853D-02			
8.	-.12413D-01	-.39753D-01	.11475	-.40664D-01	-.57047D-01	.17900D-01	2.0464	.44106D-01	-.20896D-01	-.12940D-03
	.16497D-02	-.18408D-02	.69992D-03	-.33751D-01	.44940D-01	.35475D-02	.14737D-01			
9.	.39304D-01	-.12186	.32670	13751	-.93380D-01	.12133D-02	.44106D-01	5.1534		.38769D-01
	.93733D-02	-.10358D-03	-.34182D-01	.65028D-01	-.386652D-01	-.64273D-01	.87407D-01			
10.	.14162D-01	.86300D-02	-.20550D-01	.61624D-01	.22304D-01	-.71622D-02	-.20896D-01	.38769D-01	6.3181	-.12940D-02
	.74987D-04	.93963D-02	-.32554D-03	.24155D-01	.30193D-02	-.30549D-01	-.94129D-02			
11.	-.17000D-01	-.26640	-.30000D-01	-.10000D-01	1.0000	.50000D-01	.10000D-01	.20000	-.20000D-01	1.0000
	0.	0.	0.	0.	0.	0.	0.	0.		
12.	-.16384	-.38400D-02	*41664	.38648	-.5632	-.39808D-01	-.39808D-01			
	0.	0.	1.0000	0.	0.	0.	0.			
13.	-.15168D-01	1.6586	-.17264	-.24704D-02	*10406	0.	0.	0.		
	0.	0.	1.0000	0.	1.0000	0.	0.			
14.	.89774D-01	.32940D-02	*19940D-02	.27042	.69712D-01	-.92108D-01	-.13409	.25836		.95972D-01
	0.	0.	1.0000	0.	1.0000	0.	0.			

15	.15186D-01	.17075	-.49246	.31890D-02	.19419	-.94698D-01	-.17855	-.34427	.11980D-01	.0
	.0	.0	.0	.0	1.0000	.0	.0			
16	-.58414D-01	.23060D-02	.10061D-02	-.28306	-.78476D-01	-.27892D-01	.14094D-01	-.25536	-.12137	.0
	.0	.0	.0	.0	.0	1.0000	.0			
17	.16174D-01	-.16515	.49546	.41770D-02	-.20295	-.35302D-01	.50557D-01	.34727	-.37338D-01	.0
	.0	.0	.0	.0	.0	.0	1.0000			

FINAL COMBINED FORCE VECTOR OF ORDER 17 FOR PSI = .0

-.38036D-05	-.87050D-05	.25502D-04	.13759D-04	-.14091D-04	.29357D-05	.99558D-05	.45950D-05	-.68925D-05	.0
.0	.0	.0	.0	.0	.0	.0	.0		

STATE VARIABLES (DISPVEL) FOR PSI = .0

-.32735D-11	-.25337D-08								
-.41550D-11	-.32163D-08								
-.72632D-11	-.56217D-08								
-.94506D-11	-.73168D-08								
-.76307D-11	-.59062D-08								
.22745D-11	.17605D-08								
.78403D-11	.57528D-08								
.11433D-11	.88514D-09								
-.16862D-11	-.13067D-08								
-.62521D-11	-.48391D-08								
-.48912D-11	-.37858D-08								
-.11305D-11	-.67507D-09								
.86278D-12	.65231D-09								

BIFFLAR INITIAL DISP & VEL FOR PSI = .0

-.64545D-11	-.34478D-08								
.77832D-11	-.60242D-08								
-.32261D-11	-.24986D-08								
-.65566D-11	-.50750D-08								

FIXED SYSTEM, + ROTOR + FIXED ABSORBERS (R.H.S.) OF ORDER 13 ($\Psi=2$ DEG)

-.13417D-07	.40363D-07	-.48276D-06	.24756D-07	-.12980D-06	-.35905D-07	.22793D-06	-.87310D-07	.24116D-06	-.10012D-06
-.62330D-07	.14320D-07	-.10572D-07							

STATE VARIABLES (DISP&VEL) FOR PSI = 30.000

```

-.31667D-04   -.47168D-02
-.18040D-04   .44986D-03
-.57305D-04   .68663D-03
-.79735D-04   -.11020D-01
-.13172D-06   -.28642D-02
.60914D-05   .16604D-02
.35590D-05   .37338D-02
-.49960D-04   -.36824D-02
-.13070D-05   .13032D-02
.13845D-04   .33312D-02
-.47531D-05   .15521D-02
.28783D-04   .13254D-02
-.24459D-04   -.46604D-03

```

BIFILAR INITIAL DISP & VEL FOR PSI = 30.000

```

.31746D-04   .49550D-02
-.30011D-04   .17144D-03
.28218D-04   -.41782D-02
.33540D-04   .60549D-03

```

NREV= 2, G1= .6134D-02, G2= .327D-01, YHUB= .310D-02, THZH= .462D-05, DXHUB= -.863 , DYHUB= -.249

NREV= 4, G1= .480D-03, G2= .238D-01, XHUB= .411D-02, YHUB= .246D-02, THZH= .308D-05, DXHUB= -.829 , DYHUB= -.256

NREV= 5, G1= .532D-02, G2= .273D-01, XHUB= .482D-02, YHUB= .350D-02, THZH= .533D-05, DXHUB= -1.01 , DYHUB= -.286

NREV= 6, G1= .233D-02, G2= .310D-01, XHUB= .429D-02, YHUB= .363D-02, THZH= .699D-05, DXHUB= -1.16 , DYHUB= -.368

```

NREV= 7, G1= .743D-02, G2= .172D-01, XHUB= .161D-03, YHUB= .161D-02, THZH= .475D-05, DXHUB= -.790 , DYHUB= -.416
NREV= 8, G1= .607D-02, G2= .605D-02, XHUB= .152D-02, YHUB= .109D-02, THZH= .268D-05, DXHUB= -.439 , DYHUB= -.163

NREV= 9, G1= .601D-02, G2= .596D-02, XHUB= .266D-02, YHUB= .230D-02, THZH= .421D-05, DXHUB= -.554 , DYHUB= -.976D-01

NREV= 10, G1= .264D-02, G2= .390D-02, XHUB= .187D-02, YHUB= .230D-02, THZH= .567D-05, DXHUB= -.688 , DYHUB= -.216

NREV= 11, G1= .376D-02, G2= .145D-02, XHUB= .134D-02, YHUB= .160D-02, THZH= .452D-05, DXHUB= -.623 , DYHUB= -.234

NREV= 12, G1= .106D-02, G2= .314D-02, XHUB= .217D-02, YHUB= .178D-02, THZH= .371D-05, DXHUB= -.563 , DYHUB= -.186

NREV= 13, G1= .199D-02, G2= .108D-02, XHUB= .272D-02, YHUB= .227D-02, THZH= .459D-05, DXHUB= -.610 , DYHUB= -.195

THE NUMBER OF REVOLUTIONS REQUIRED TO CONVERGE = 13

INPUT FIXED SYSTEM MODES FREQUENCIES IN HZ

      5.10   6.40   15.3   14.3   13.8   11.6   12.1   17.4   21.1

THE CONVERGENCE FACTOR TO G = 30.2

BIFFILAR HARMONIC OUTPUT - AMPLITUDE AND PHASE

      1 P    2 P    3 P    4 P    5 P    6 P    7 P    8 P    9 P

      1 .670490-02 .12416D-01 9.5710 .27991D-01 .87991D-01 .11213D-01 .35755D-02 .44867D-02 .38823D-02
      167.18 52.740 87.610 -124.05 35.044 70.857 41.773 39.427 70.457

      2 .41905D-02 .24610D-01 9.5752 .23692D-01 .76112D-01 .10635D-01 .26310D-02 .41733D-02 .30317D-02
      9.1624 -127.52 177.26 -29.191 -55.124 76.653 98.182 66.658 54.734

      3 .11155D-01 .33980D-01 9.6299 .22214D-01 .89253D-01 .13026D-01 .23000D-02 .36565D-03 .26055D-02
      8.6491 25.261 -92.716 82.317 -146.67 -57.202 -173.77 94.511 -126.83

      4 .61652D-02 .24692D-01 9.6216 .28710D-01 .73455D-01 .16500D-01 .50300D-02 .36359D-02 .36387D-02
      129.49 -168.30 -2.4178 179.05 127.26 -141.71 -88.468 -53.766 -121.85

```

HARMONIC HUB OUTPUT - COSINE , SINE AND TOTAL RESPONSE AND PHASE ANGLE IN DEGREES

	1 P	2 P	3 P	4 P	5 P	6 P	7 P	8 P	9 P
1	-65430D-03	.58575D-03	.11120D-02	-.35980D-01	-.17899D-01	-.60414D-03	-.30550D-03	-.56524D-03	-.14283D-03
	-.18117D-04	-.47222D-03	-.95122D-03	-.18974	.2803D-03	-.13125D-03	-.96796D-04	.31223D-04	-.12377D-03
	.65454D-03	.75440D-03	.14700D-02	.19312	.17901D-01	.61622D-03	.32333D-03	.56607D-03	.18901D-03
	-1.5860	-38.875	-40.327	-79.257	.76189	-167.74	162.58	3.1630	139.08
2	.60527D-03	.78265D-03	.12837D-02	.48661D-01	.11867D-01	-.78696D-03	-.42562D-03	-.23171D-03	-.20902D-03
	.45630D-04	.93018D-04	.37411D-03	-.71377D-01	-.16023D-02	-.62218D-03	-.28682D-03	-.61975D-03	-.14193D-03
	.85594D-04	.11003D-03	.21633D-03	.95751D-02	.51245D-02	.30477D-03	.14770D-03	.10852D-03	.56165D-03
	-171.88	109.54	113.77	-133.67	56.787	-58.825	-67.411	-104.08	-76.589
3	-.84736D-04	-.36787D-04	-.67202D-04	-.66114D-02	-.28616D-02	-.15570D-01	-.56732D-04	-.23395D-04	-.17736D-04
	-.12055D-04	-.10567D-03	-.19792D-03	-.69261D-02	-.42874D-02	-.25734D-03	-.14537D-03	-.10525D-03	-.74383D-04
	.85594D-04	.11003D-03	.21633D-03	.95751D-02	.51245D-02	.30477D-03	.14770D-03	.10852D-03	.56165D-03
	-171.88	109.54	113.77	-133.67	56.787	-58.825	-67.411	-104.08	-76.589
4	.23402D-04	.25569D-04	.42111D-04	.10883D-02	.15794D-03	-.39211D-04	-.18225D-04	-.53425D-05	-.78922D-05
	-.63601D-06	-.28533D-05	-.31023D-05	-.52730D-03	-.52730D-03	-.29290D-05	-.29290D-05	-.22750D-05	-.21201D-05
	-.23411D-04	-.25728D-04	-.42234D-04	-.11568D-02	-.5945D-03	-.39321D-04	-.18466D-04	-.58063D-05	-.81720D-05
	-1.5567	-6.3567	-4.2126	-19.816	-73.326	175.73	170.79	-156.93	164.96
5	.45204D-05	.31244D-05	.68570D-05	-.32059D-03	-.47232D-03	-.66731D-05	-.11688D-05	-.61159D-05	-.27882D-06
	.21109D-05	-.15778D-05	-.99350D-06	-.39548D-02	-.42771D-03	-.24576D-04	-.10588D-04	-.10509D-04	-.50560D-05
	.49890D-05	.34999D-05	.86434D-05	.39678D-02	.64241D-03	.25466D-04	.10921D-04	.15549D-04	.50636D-05
	25.032	-26.797	-6.6125	-65.366	41.744	-74.809	-83.856	-63.167	-93.156
6	.46929D-06	.14676D-05	.37222D-05	.12354D-03	.31970D-04	-.60135D-06	-.50591D-06	-.23036D-05	-.28873D-06
	.61710D-06	.13014D-05	.34197D-06	.63566D-04	.15021D-04	-.39844D-05	-.33523D-05	-.34068D-05	-.13859D-05
	.77524D-06	.19815D-05	.37388D-05	.13924D-03	.35323D-04	.40300D-05	.23191D-05	.14157D-05	
	52.748	41.564	5.2491	27.189	25.166	-98.582	-102.60	-124.49	-101.77

VIBRATION LEVELS AT 4 A/C LOCATIONS

COSINE,SINE,TOTAL AMPLITUDE IN G AND PHASE ANGLE IN DEGREES OF POINT 1

	1 P	2 P	3 P	4 P	5 P	6 P	7 P	8 P	9 P
1	-.27695D-04	-.59704D-04	-.90025D-04	-.36910D-02	-.17996D-02	-.17336D-04	-.12665D-04	-.12113D-04	-.60542D-05
	.21059D-04	.16551D-04	.31845D-04	.26162D-01	-.10014D-02	.25157D-04	-.10014D-02	.25157D-04	-.15632D-04
	.34762D-04	.62337D-04	.12864D-03	.64621D-01	.17496D-04	.20278D-04	.34446D-04	.16810D-04	
	142.82	164.24	134.43	98.030	-144.42	8.2244	-51.351	136.82	-68.890

	COSINE,SINE,TOTAL AMPLITUDE IN G AND PHASE ANGLE IN DEGREES OF POINT 2								
	1 P	2 P	3 P	4 P	5 P	6 P	7 P	8 P	9 P
2	-.720840-04	-.165970-03	-.372260-02	-.637840-02	-.101200-02	.368560-03	.144590-03	-.666940-04	.549190-04
	.652235D-04	.655100-06	.282220-03	.510760-02	.656460-02	-.322690D-03	-.149680-03	-.183750-03	-.594960D-04
	.952330-04	-.178460-03	-.467140-03	-.817130-02	-.664160-02	.444860D-03	.207970-03	.195270-03	.109700-03
	139.19	158.43	142.83	-35.686	98.765	-32.840	.66.031	-109.78	-59.957
3	-.960800=06	-.263150D-03	-.375730D-03	-.256610D-02	-.534340D-02	-.384770-02	-.165730-03	-.831070-04	.650150D-04
	.999930-04	-.629860-04	.755630-04	-.202420-01	.713740-02	-.131110D-03	-.855650D-04	-.106250-03	-.516310-04
	.137290-03	.270570-03	.388480D-03	-.204240D-01	.715730-02	.406560D-03	.186560D-03	.136890-03	.830220D-04
	133.26	-166.54	168.62	-85.782	94.281	-16.821	-77.302	-51.368	-38.454
	166.41	149.56	134.66	97.962	143.74	83.601	18.189	146.12	-47.564

COSINE,SINE,TOTAL AMPLITUDE IN G AND PHASE ANGLE IN DEGREES OF POINT 3

	COSINE,SINE,TOTAL AMPLITUDE IN G AND PHASE ANGLE IN DEGREES OF POINT 3								
	1 P	2 P	3 P	4 P	5 P	6 P	7 P	8 P	9 P
1	1	-.366860D-04	-.498050D-04	-.873750D-04	-.604960D-02	-.2048870-02	.456642D-05	.886780-05	-.467290-04
		.954150D-05	.292650D-04	.886040D-04	.289950D-01	-.152270-02	.406930D-04	.291370-05	.313370-04
		.406200D-04	.577690D-04	.124300D-03	.292530D-01	-.409530D-02	.409530D-04	.466860D-04	.627440D-05
		35.062	130.69	120.61	-83.522	40.002	-71.669	-78.705	-85.694
2	2	.118620D-03	-.296710D-04	-.122650D-03	.227500D-02	.820100-02	.216900D-03	.68740D-04	.376440D-04
		.812540D-04	-.345460D-04	-.207310D-03	-.603510D-03	-.682310D-02	-.634660D-03	-.344170D-03	-.191070D-03
		.144920D-03	.455570D-04	-.204870D-03	.201660D-01	.107060D-01	.619660D-03	.350560D-03	.191610D-03
		35.062	130.69	120.61	-83.522	40.002	-71.669	-78.705	-85.694
3	3	.116160D-03	-.363960D-03	-.457860D-03	.691600D-02	-.893670-02	.335060D-03	.168160D-03	-.613720-04
		.149580D-03	-.135460D-03	-.161470D-03	.10198D-01	.220780-02	.233920D-03	.989740D-04	.788820D-04
		.189350D-03	-.388370D-03	-.495450D-03	.121750D-01	-.144950D-02	-.267870D-04	-.624230D-05	.314350D-04
		127.83	-.459.59	-.160.57	55.373	16.12	50.277	30.580	-.147.92
		116.23	161.72	95.933	-135.87	109.12	100.34	121.82	90.515
	2	2	.380690D-03	-.485550D-03	.368840D-03	.520290D-02	-.4558860D-02	-.515170D-03	-.241870D-03
		.269190D-04	-.831760D-04	-.296120D-04	-.12030D-01	-.676430D-04	-.733140D-04	-.804770D-05	-.359460D-05
		.381640D-03	.492530D-03	-.389970D-03	131070D-01	.817940D-02	.520360D-03	.242010D-03	.158650D-03
		4.0437	-9.7225	-4.3549	-66.612	-55.791	-171.90	-178.09	-153.57
3	3	.224440D-04	-.312980D-03	-.337620D-03	-.138670D-01	.1838820-02	.226170D-03	.116760D-03	.111700D-03
		.195630D-03	-.164030D-03	-.348560D-05	.409630D-02	.427250D-02	-.228170D-03	-.137530D-03	-.438350D-04
									-.832620D-04

COSINE, SINE, TOTAL AMPLITUDE IN G AND PHASE ANGLE IN DEGREES OF POINT 4

	1. P.	2. P.	3. P.	4. P.	5. P.	6. P.	7. P.	8. P.
1. -55953D-03	.20750D-03	-.87139D-03	-.16897D-01	-.12049D-01	.27150D-03	.16522D-03	.29958D-04	.96836D-04
2. -6.1893D-03	.44420D-03	-.65862D-03	-.95565D-02	-.44070D-03	.95565D-03	.53245D-03	.55112D-03	.31675D-03
3. 83456D-03	.49027D-03	.10293D-02	.19263D-01	.12075D-01	.99447D-03	.57571D-03	.33065D-03	
4. 1132.11	64.961	142.92	151.28	177.91	74.140	72.755	86.859	73.332

2	.53055D-03	.13844D-03	-.11454D-01	-.45731D-02	-.42195D-03	-.10200D-04
	.53056D-04	.16442D-03	-.22733D-03	-.11566D-01	-.80284D-02	-.10840D-03
	.52275D-03	.21492D-03	.27379D-03	.18505D-01	.92355D-02	.44147D-03
	.5	.8231	-.130.09	-.56.130	-.161.32	-.60.334

3	.40576D-03	.12381D-04	.29263D-04	.19887D-01	.19565D-02	.-1.10307D-03	.-6.6633D-04	.-3.1805D-04
	.52326D-03	.-44204D-03	.27250D-03	.-32513D-01	.-10863D-01	.-78669D-02	.-42298D-04	.-32332D-04
	.52286D-03	.44221D-03	.-26760D-03	.22223D-01	.-11820D-01	.-78935D-03	.-18567D-04	.-43320D-04
39.100	-88.396	-83.927	-51.852	-29.176	-148.82	-147.59	-50.585	-134.53

INITIAL BIFILAR DISPLACEMENTS (LC.1720-1739)

1500-02 - 16587 96961D-02 16657

13.629 -1.6505 -13.697 1.7168

INITIAL HUB DISPLACEMENTS (IC.1768-1773)

~~262910-02 23900D-02 30123D-04 44863D-04 44663D-04 55143D-05~~

卷之三

INITIAL STATE VARIABLES DISPL. (LC.1780-1859)

INITIAL STATE VARIABLES VELOC. ILC.1860-1929)

.439790-01	.548500-02	-.22847	.10464	.81171D-01	-.44101D-02	-.38748D-01	-.52990	-.13892	-.63792
-4.4349	6.5571	9.2272.							

Appendix D. Details of Coupled Rotor/Bifilar/Airframe Analysis

TABLE OF CONTENTS

<u>Section</u>		<u>Page</u>
D.1	Inplane Bifilar Equations of Motion	278
D.2	Vertical Bifilar Equations of Motion	291
D.3	Rotor Equations with Hover Aerodynamics	303
D.4	Fuselage Dynamic Representation	339
D.5	Fixed System Absorber	341
D.6	Assembly of Coupled Equations	344
D.7	Forced Response Solution	348
D.8	Time History Solution	351
D.9	List of Symbols	356

D.1 Inplane Bifilar Equations of Motion

The inplane bifilar rotor head absorber is a single degree-of-freedom system. It can be represented as a one degree-of-freedom pendulum as shown in Figure D.1-1. The rotating coordinate system shown here is located on the main rotor hub. The equivalent pendulum arm, r , and the distance from the center of rotation, R , are related by equation (1) (see Figure D.1-2), often referred to as tuning equation. The location of the c.g. relative to the inertia frame system is given by equation (2) shown in Figure D.1-2. Substituting equation (2) into the Lagrange's equations, the non-linear equations of motion are derived, equations (3)-(6), and shown in Figure D.1-3.

To obtain the linear set of equations of motion, equations (7)-(10) (see Figure D.1-4), small angle assumptions were made, e.g. $\sin\gamma_k \sim \gamma_k$, and $\cos\gamma_k \sim 1$. Also, the second order terms were neglected. For identical bifilars, further simplification of these equations can be made by transferring the rotating bifilar coordinate, γ_k , into the fixed system coordinates. The equation for the coordinate transformation used is shown in Figure D.1-5, equation (11). Thus the transformed equations of motion are derived, equations (12)-(17) shown in Figure D.1-5.

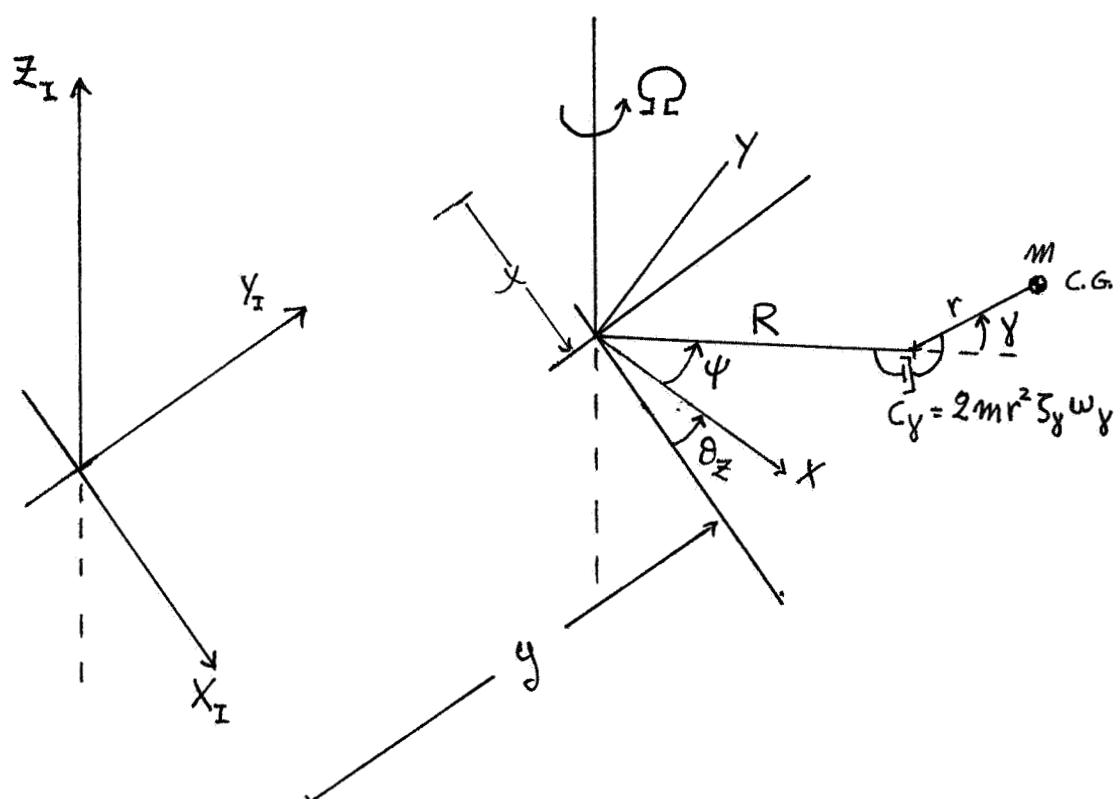


FIGURE D.1-1: INPLANE BIFILAR MATH MODEL

$$n = \sqrt{\frac{R}{r}} \quad (\text{TUNING} \sim \text{PER REV}) \quad (1)$$

$$\{X_i\} = \{X\} + [\Theta_z] \cdot [\Psi] \cdot \{R\{V_i\} + r[\Gamma] \cdot \{V_i\}\} \quad (2)$$

WHERE:

$$[\Theta_z] = \begin{bmatrix} \cos \theta_z & -\sin \theta_z & 0 \\ \sin \theta_z & \cos \theta_z & 0 \\ 0 & 0 & 1 \end{bmatrix}$$

$$[\Psi] = \begin{bmatrix} \cos \psi & -\sin \psi & 0 \\ \sin \psi & \cos \psi & 0 \\ 0 & 0 & 1 \end{bmatrix}; \quad [\Gamma] = \begin{bmatrix} \cos \gamma & -\sin \gamma & 0 \\ \sin \gamma & \cos \gamma & 0 \\ 0 & 0 & 1 \end{bmatrix}$$

$$\{V_i\} = \begin{Bmatrix} 1 \\ 0 \\ 0 \end{Bmatrix}$$

FIGURE D.1-2: POSITION VECTOR FOR INPLANE BIFILAR MASS

X-EQUATION

$$\begin{aligned}
 & (m_G + M_T) \ddot{x} + 2m_G \omega_x S_x \dot{x} + m_G \dot{\omega}_x^2 x \\
 & + \sum_{k=1}^N m_k \left\{ -[r_k \sin(\psi_k + \theta_z + \gamma_k) + R_k \sin(\psi_k + \theta_z)] \ddot{\theta}_z - [r_k \sin(\psi_k + \theta_z + \gamma_k)] \ddot{\gamma}_k \right. \\
 & \quad \left. - 2\Omega [r_k \cos(\psi_k + \theta_z + \gamma_k)] \dot{\gamma}_k - [r_k \cos(\psi_k + \theta_z + \gamma_k)] \dot{\theta}_z^2 \right. \\
 & \quad \left. - 2[r_k \cos(\psi_k + \theta_z + \gamma_k)] \dot{\theta}_z \dot{\gamma}_k - 2\Omega [r_k \cos(\psi_k + \theta_z + \gamma_k) + R_k \cos(\psi_k + \theta_z)] \dot{\theta}_z \right. \\
 & \quad \left. - [r_k \cos(\psi_k + \theta_z + \gamma_k) + R_k \cos(\psi_k + \theta_z)] \dot{\theta}_z^2 \right\} = F_x \quad (3)
 \end{aligned}$$

FIGURE D.1-3: NON-LINEAR EQUATIONS OF MOTION FOR INPLANE BIFILAR

Y EQUATION

$$(m_g + M_r) \ddot{y} + 2m_g w_y \dot{\gamma}_y \dot{y} + m_g \dot{w}_y^2 y$$

$$+ \sum_{k=1}^N m_k \left\{ [r_k \cos(\psi_k + \theta_z + \dot{\gamma}_k) + R_k \cos(\psi_k + \theta_z)] \ddot{\theta}_z + [r_k \cos(\psi_k + \theta_z + \dot{\gamma}_k)] \ddot{\gamma}_k \right.$$

$$- 2\Omega [r_k \sin(\psi_k + \theta_z + \dot{\gamma}_k)] \dot{\gamma}_k - [r_k \sin(\psi_k + \theta_z + \dot{\gamma}_k)] \dot{\gamma}_k^2$$

$$- 2[r_k \sin(\psi_k + \theta_z + \dot{\gamma}_k)] \dot{\theta}_z \dot{\gamma}_k - 2\Omega [r_k \sin(\psi_k + \theta_z + \dot{\gamma}_k) + R_k \sin(\psi_k + \theta_z)] \dot{\theta}_z$$

$$- [r_k \sin(\psi_k + \theta_z + \dot{\gamma}_k) + R_k \sin(\psi_k + \theta_z)] \dot{\theta}_z^2$$

$$- \Omega^2 [r_k \sin(\psi_k + \theta_z + \dot{\gamma}_k) + R \sin(\psi_k + \theta_z)] \} = F_y \quad (4)$$

FIGURE D.1-3: NON-LINEAR EQUATIONS OF MOTION FOR INPLANE BIFILAR (CONTINUED)

∂_z - EQUATION

$$\begin{aligned}
 & \left\{ M_G + \left[\sum_{k=1}^N m_k (r_k + R_k + 2r_k R_k \cos \gamma_k) \right] \right\} \ddot{\theta}_z \\
 & + 2m_G \omega_{\theta z} \dot{\gamma}_z \dot{\theta}_z + m_G \omega_{\theta z}^2 \theta_z \\
 & + \sum_{k=1}^N m_k \left\{ - [r_k \sin(\psi_k + \theta_z + \gamma_k) + R_k \sin(\psi_k + \theta_z)] \ddot{x} \right. \\
 & \quad \left. + [r_k \cos(\psi_k + \theta_z + \gamma_k) + R_k \cos(\psi_k + \theta_z)] \ddot{y} + r_k [r_k + R_k \cos \gamma_k] \ddot{\gamma}_k \right. \\
 & \quad \left. - [2r_k R_k \Omega \sin \gamma_k] \dot{\gamma}_k - [2r_k R_k \sin \gamma_k] \dot{\theta}_z \dot{\gamma}_k \right. \\
 & \quad \left. + [r_k \sin \gamma_k (2r_k \sin \gamma_k + R_k)] \dot{\gamma}_k^2 \right\} = M_z \quad (5)
 \end{aligned}$$

FIGURE D.1-3: NON-LINEAR EQUATIONS OF MOTION FOR INPLANE BIFILAR (CONTINUED)

γ_k - EQUATION

$$\begin{aligned}
 m_k r_k \left\{ -[\sin(\psi_k + \theta_z + \gamma_k)] \ddot{x} + [\cos(\psi_k + \theta_z + \gamma_k)] \ddot{y} \right. \\
 + [r_k + R_k \cos \gamma_k] \ddot{\theta}_z + r_k \ddot{\gamma}_k + [2 r_k \dot{\gamma}_k w_{\gamma_k}] \dot{\gamma}_k \\
 + [2 \Omega R_k \sin \gamma_k] \dot{\theta}_z + [R_k \sin \gamma_k] \dot{\theta}_z^2 \\
 \left. + R_k \Omega^2 \sin \gamma_k \right\} = 0.0 \quad (6)
 \end{aligned}$$

FIGURE D.1-3: NON-LINEAR EQUATIONS OF MOTION FOR INPLANE BIFILAR (CONCLUDED)

X-EQUATION

$$\begin{aligned}
 & (m_g + M_T) \ddot{x} + 2m_g w_x \dot{s}_x \dot{x} + m_g \dot{w}_x^2 x \\
 & + \sum_{k=1}^N m_k \left\{ -[(r_k + R_k) \sin \psi_k] \ddot{\theta}_z - [r_k \sin \psi_k] \ddot{y}_k \right. \\
 & \quad \left. - [2\Omega(r_k + R_k) \cos \psi_k] \dot{\theta}_z - [2\Omega r_k \cos \psi_k] \dot{y}_k \right. \\
 & \quad \left. - \Omega^2 [(r_k + R_k) \cos \psi_k - r_k \dot{y}_k \sin \psi_k - (r_k + R_k) \dot{\theta}_z \sin \psi_k] \right\} = F_x
 \end{aligned} \tag{7}$$

FIGURE D.1-4: LINEAR EQUATIONS OF MOTION FOR INPLANE BIFILAR

Y-EQUATION

$$\begin{aligned}
 & (m_G + M_T) \ddot{y} + 2m_G \omega_y \dot{\gamma}_y \dot{y} + m_G \omega_y^2 y \\
 & + \sum_{k=1}^N m_k \left\{ [(r_k + R_k) \cos \psi_k] \ddot{\theta}_z + [r_k \cos \psi_k] \ddot{\gamma}_k \right. \\
 & \quad \left. - [2\Omega(r_k + R_k) \sin \psi_k] \dot{\theta}_z - [2\Omega r_k \sin \psi_k] \dot{\gamma}_k \right. \\
 & \quad \left. - \Omega^2 [(r_k + R_k) \sin \psi_k + r_k \dot{\gamma}_k \cos \psi_k + (r_k + R_k) \dot{\theta}_z \cos \psi_k] \right\} = F_y
 \end{aligned} \tag{8}$$

FIGURE D.1-4: LINEAR EQUATIONS OF MOTION FOR INPLANE BIFILAR (CONTINUED)

θ_z - EQUATION

$$\begin{aligned}
 & \left\{ m_G + \left[\sum_{k=1}^N m_k (r_k + R_k)^2 \right] \right\} \ddot{\theta}_z \\
 & + 2m_G \omega_{\theta z} \dot{\theta}_z \dot{\varphi}_z + m_G \dot{\omega}_{\theta z}^2 \theta_z \\
 & + \sum_{k=1}^N m_k \left\{ -[(r_k + R_k) \sin \psi_k] \ddot{x} + [(r_k + R_k) \cos \psi_k] \ddot{y} \right. \\
 & \quad \left. + [r_k (r_k + R_k)] \ddot{\varphi}_k \right\} = M_{\theta z} \tag{9}
 \end{aligned}$$

FIGURE D.1-4: LINEAR EQUATIONS OF MOTION FOR INPLANE BIFILAR (CONTINUED)

γ_k - EQUATION

$$m_k r_k \left\{ [-\sin \psi_k] \ddot{x} + [\cos \psi_k] \ddot{y} \right. \\ \left. + [r_k + R_k] \ddot{\theta}_z + r_k \ddot{\gamma}_k \right. \\ \left. + [2r_k \dot{\gamma}_k \omega_{y_k}] \dot{\gamma}_k + R_k \Omega^2 \gamma_k \right\} = 0.0 \quad (10)$$

FIGURE D.1-4: LINEAR EQUATIONS OF MOTION FOR INPLANE BIFILAR (CONCLUDED)

$$\gamma = \frac{1}{N} \gamma_0 + \frac{2}{N} \gamma_s \sin \psi + \frac{2}{N} \gamma_c \cos \psi \quad (11)$$

X-EQUATION

$$(m_G + M_T) \ddot{x} + (2m_G \omega_x \dot{\gamma}_x) \dot{x} + (m_G \omega_x^2) x - m r \ddot{\gamma}_s = F_x \quad (12)$$

Y-EQUATION

$$(m_G + M_T) \ddot{y} + (2m_G \omega_y \dot{\gamma}_y) \dot{y} + (m_G \omega_y^2) y + m r \ddot{\gamma}_c = F_y \quad (13)$$

Z-EQUATION

$$[m_G + M_T(r+R)^2] \ddot{\theta}_z + (2m_G \omega_{\theta_z} \dot{\gamma}_{\theta_z}) \dot{\theta}_z + (m_G \omega_{\theta_z}^2) \theta_z + [m(r+R)r] \ddot{\gamma}_0 = M_z \quad (14)$$

FIGURE D.1-5: INPLANE BIFILAR EQUATIONS IN FIXED SYSTEM COORDINATES

γ_0 - EQUATION

$$N\left(1 + \frac{R}{r}\right)\ddot{\theta}_z + \ddot{\gamma}_0 + \frac{R}{r}\Omega^2\gamma_0 + 2S_y\omega_y\dot{\gamma}_0 = 0 \quad (15)$$

γ_s - EQUATION

$$\left(-\frac{N}{2r}\right)\ddot{x} + \ddot{\gamma}_s + 2S_y\dot{\gamma}_s - 2\Omega\dot{\gamma}_c + \Omega^2\left(\frac{R}{r}-1\right) - 2S_y\Omega\dot{\gamma}_c = 0 \quad (16)$$

γ_c - EQUATION

$$\left(\frac{N}{2r}\right)\ddot{y} + \ddot{\gamma}_c + 2S_y\dot{\gamma}_c + 2\Omega\dot{\gamma}_s + \Omega^2\left(\frac{R}{r}-1\right)\gamma_c + 2S_y\Omega\dot{\gamma}_s = 0 \quad (17)$$

FIGURE D.1-5 INPLANE BIFILAR EQUATIONS IN FIXED SYSTEM COORDINATES (CONCLUDED)

D.2 Vertical Bifilar Equations of Motion

The vertical bifilar rotor head absorber is a single degree of freedom system. The math model is presented in Figure D.2-1. The equivalent pendulum arm, r , and the distance from the center of rotation, R , are related by the tuning equation (18), shown in Figure D.2-2. The vector location of the dynamic mass (c.g.) is given by equation (19), shown in Figure D.2-2. Substituting equation (19) into the Lagrange's equation, also assuming small motions and neglecting second order terms, the linear set of equations of motion with six hub degrees-of-freedom are derived. They are shown in Figure D.2-3, equations (20)-(26).

For identical vertical bifilars, further simplification of these equations can be made by transferring the rotating coordinate, β_k , into the fixed system coordinates. The equation for the coordinate transformation used is shown in Figure D.2-4, equation (27). Thus the transformed equations of motions are derived, equations (28)-(36), shown in Figure D.2-4.

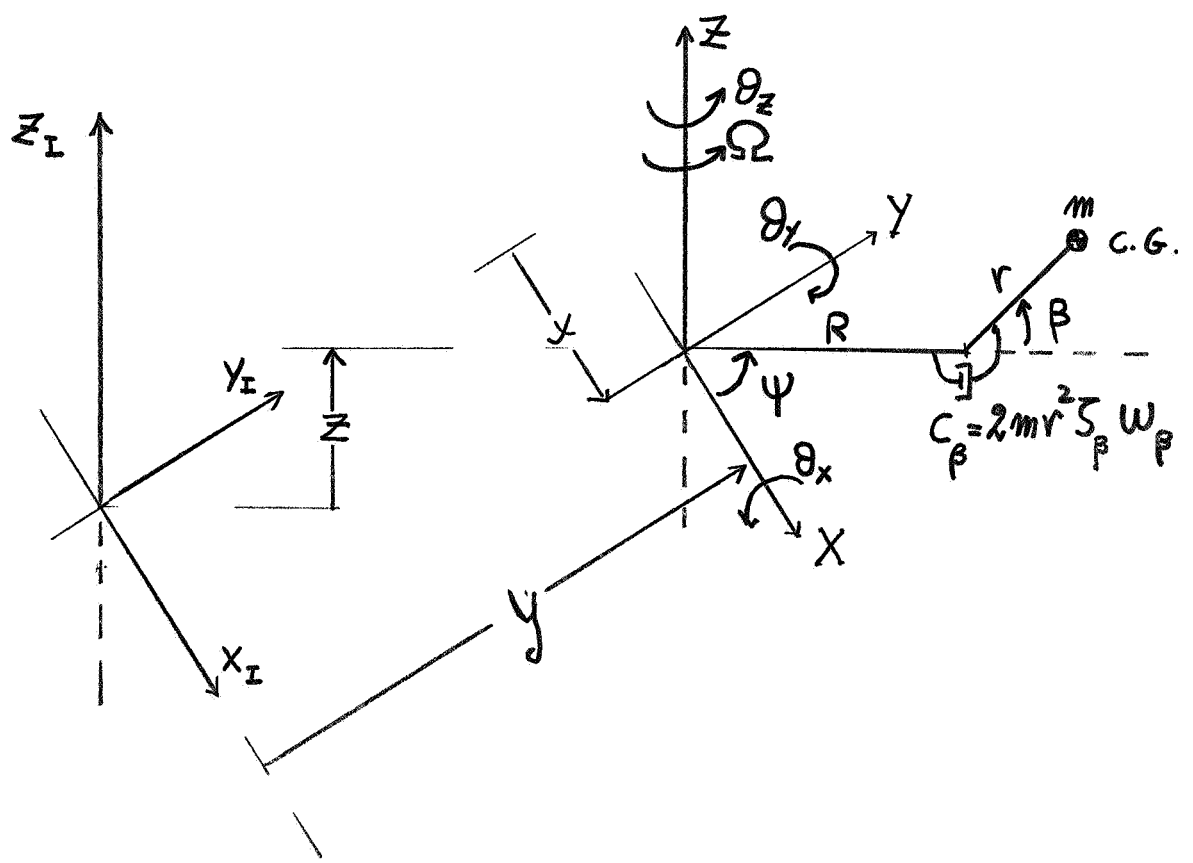


FIGURE D.2-1: VERTICAL BIFILAR MATH MODEL

$$n = \sqrt{\frac{R+r}{r}} \quad (\text{TUNING } \sim \text{PER REV}) \quad (18)$$

$$\{X_I\} = \{X\} + [\Theta_z] \cdot [\Theta_x] \cdot [\Theta_y] \cdot [\Psi] \cdot \{R\{V_i\} + r[B] \cdot \{V_i\}\} \quad (19)$$

WHERE:

$$[\Theta_z] = \begin{bmatrix} \cos \theta_z & -\sin \theta_z & 0 \\ \sin \theta_z & \cos \theta_z & 0 \\ 0 & 0 & 1 \end{bmatrix}$$

$$[\Theta_x] = \begin{bmatrix} 1 & 0 & 0 \\ 0 & \cos \theta_x & -\sin \theta_x \\ 0 & \sin \theta_x & \cos \theta_x \end{bmatrix}$$

$$[\Theta_y] = \begin{bmatrix} \cos \theta_y & 0 & \sin \theta_y \\ 0 & 1 & 0 \\ -\sin \theta_y & 0 & \cos \theta_y \end{bmatrix}$$

$$[\Psi] = \begin{bmatrix} \cos \psi & -\sin \psi & 0 \\ \sin \psi & \cos \psi & 0 \\ 0 & 0 & 1 \end{bmatrix}$$

$$[B] = \begin{bmatrix} \cos \beta & 0 & -\sin \beta \\ 0 & 1 & 0 \\ \sin \beta & 0 & \cos \beta \end{bmatrix}$$

$$\{V_i\} = \begin{bmatrix} 1 \\ 0 \\ 0 \end{bmatrix}$$

FIGURE D.2-2: POSITION VECTOR FOR VERTICAL BIFILAR MASS

X-EQUATION

$$\begin{aligned}
 & (m_G + M_T) \ddot{x} + (2m_G \omega_x \varsigma_x) \dot{x} + (m_G \omega_x^2) x \\
 & + \sum_{k=1}^N m_k \left\{ -[(r_k + R_k) \sin \psi_k] \ddot{\theta}_z - [2\Omega(r_k + R_k) \cos \psi_k] \dot{\theta}_z \right. \\
 & \quad \left. + [\Omega^2(r_k + R_k) \sin \psi_k] \theta_z - \Omega^2(r_k + R_k) \cos \psi_k \right\} = F_x
 \end{aligned} \tag{20}$$

Y-EQUATION

$$\begin{aligned}
 & (m_G + M_T) \ddot{y} + (2m_G \omega_y \varsigma_y) \dot{y} + (m_G \omega_y^2) y \\
 & + \sum_{k=1}^N m_k \left\{ [(r_k + R_k) \cos \psi_k] \ddot{\theta}_z - [2\Omega(r_k + R_k) \sin \psi_k] \dot{\theta}_z \right. \\
 & \quad \left. - [\Omega^2(r_k + R_k) \cos \psi_k] \theta_z - \Omega^2(r_k + R_k) \sin \psi_k \right\} = F_y
 \end{aligned} \tag{21}$$

FIGURE D.2-3: LINEAR EQUATIONS OF MOTION FOR VERTICAL BIFILAR

Z - EQUATION

$$\begin{aligned}
 & (m_G + M_T) \ddot{Z} + (2m_G \omega_z S_z) \dot{Z} + (m_G \omega_z^2) Z \\
 & + \sum_{k=1}^N m_k \left\{ (r_k) \ddot{\beta}_k + [(r_k + R_k) \sin \psi_k] \ddot{\partial}_x + [-(r_k + R_k) \cos \psi_k] \ddot{\partial}_y \right. \\
 & + [2\Omega(r_k + R_k) \cos \psi_k] \dot{\partial}_x + [2\Omega(r_k + R_k) \sin \psi_k] \dot{\partial}_y \\
 & \left. - [\Omega^2(r_k + R_k) \sin \psi_k] \partial_x + [\Omega^2(r_k + R_k) \cos \psi_k] \partial_y \right\} = F_Z
 \end{aligned} \tag{22}$$

FIGURE D,2-3: LINEAR EQUATIONS OF MOTION FOR VERTICAL BIFILAR (CONTINUED)

$\ddot{\theta}_x$ - EQUATION

$$\begin{aligned}
 & \left\{ m_G + \left[\sum_{k=1}^N m_k (r_k + R_k)^2 \sin^2 \psi_k \right] \right\} \ddot{\theta}_x \\
 & + \left\{ 2m_G \omega_{\theta_x} \dot{\theta}_x + \left[\sum_{k=1}^N 2m_k \Omega (r_k + R_k)^2 \cos \psi_k \sin \psi_k \right] \right\} \dot{\theta}_x \\
 & + (m_G \omega_{\theta_x}^2) \theta_x \\
 & + \sum_{k=1}^N m_k \left\{ [r_k (r_k + R_k) \sin \psi_k] \ddot{\beta}_k + [(r_k + R_k) \sin \psi_k] \ddot{z} \right. \\
 & \left. + [-(r_k + R_k)^2 \cos \psi_k \sin \psi_k] \ddot{\theta}_y + [2\Omega (r_k + R_k) \cos \psi_k] \dot{z} \right. \\
 & \left. + [2\Omega (r_k + R_k)^2 \sin^2 \psi_k] \dot{\theta}_y + [r_k \Omega^2 (r_k + R_k) \sin \psi_k] \beta_k \right. \\
 & \left. + [\Omega^2 (r_k + R_k)^2 \sin \psi_k \cos \psi_k] \dot{\theta}_y \right\} = M_x \quad (23)
 \end{aligned}$$

FIGURE D.2-3: LINEAR EQUATIONS OF MOTION FOR VERTICAL BIFILAR (CONTINUED)

θ_y -EQUATION

$$\left\{ m_G + \left[\sum_{k=1}^N m_k (r_k + R_k)^2 \cos^2 \psi_k \right] \right\} \ddot{\theta}_y + (m_G w_{\theta y}^2) \dot{\theta}_y$$

$$+ \left\{ 2m_G w_{\theta y} \dot{\theta}_y - 2\Omega \left[\sum_{k=1}^N m_k (r_k + R_k)^2 \sin \psi_k \cos \psi_k \right] \right\} \dot{\theta}_y$$

$$+ \sum_{k=1}^N m_k \left\{ - [r_k (r_k + R_k) \cos \psi_k] \ddot{\beta}_k - [(r_k + R_k) \cos \psi_k] \ddot{z} \right.$$

$$- \left. [(r_k + R_k)^2 \cos \psi_k \sin \psi_k] \ddot{\theta}_x + [2\Omega (r_k + R_k) \sin \psi_k] \dot{z} \right]$$

$$- [2\Omega (r_k + R_k)^2 \cos^2 \psi_k] \dot{\theta}_x + [r_k \Omega^2 (r_k + R_k) \cos \psi_k] \dot{\beta}_k = M_y$$

(24)

FIGURE D. 2-3: LINEAR EQUATIONS OF MOTION FOR VERTICAL BIFILAR (CONTINUED)

$\dot{\theta}_Z$ - EQUATION

$$\begin{aligned}
 & \left[m_G + \sum_{k=1}^N m_k (r_k + R_k)^2 \right] \ddot{\theta}_Z \\
 & + [2m_G \omega_{\theta_Z} \dot{\theta}_Z] \dot{\theta}_Z + (m_G \omega_{\theta_Z}^2) \theta_Z \\
 & + \sum_{k=1}^N m_k \left\{ -[(r_k + R_k) \sin \psi_k] \ddot{x} + [(r_k + R_k) \cos \psi_k] \ddot{y} \right. \\
 & \quad \left. - [2\Omega(r_k + R_k) \cos \psi_k] \dot{x} - [2\Omega(r_k + R_k) \sin \psi_k] \dot{y} \right\} = M_Z
 \end{aligned} \tag{25}$$

FIGURE D.2-3: LINEAR EQUATIONS OF MOTION FOR VERTICAL BIFILAR (CONTINUED)

β_k - EQUATION

$$\begin{aligned}
 & (m_k r_k) \ddot{\zeta} + [m_k r_k (r_k + R_k) \sin \psi_k] \ddot{\theta}_x + (m_k r_k^2) \ddot{\beta} \\
 & - [m_k r_k (r_k + R_k) \cos \psi_k] \ddot{\theta}_y + [2 m_k r_k^2 S_{\beta_k} w_{\beta_k}] \dot{\beta}_k \\
 & + [2 m_k r_k \Omega (r_k + R_k) \cos \psi_k] \dot{\theta}_x \\
 & + [2 m_k r_k \Omega (r_k + R_k) \sin \psi_k] \dot{\theta}_y + [m_k r_k \Omega^2 (r_k + R_k)] \dot{\beta}_k = 0
 \end{aligned} \tag{26}$$

FIGURE D.2-3: LINEAR EQUATIONS OF MOTION FOR VERTICAL BIFILAR (CONCLUDED)

$$\beta = \frac{1}{N} \beta_0 + \frac{2}{N} \beta_s \sin \psi + \frac{2}{N} \beta_c \cos \psi \quad (27)$$

X-EQUATION

$$(m_G + M_T) \ddot{x} + (2m_G \omega_x S_x) \dot{x} + (m_G \omega_x^2) x = F_x \quad (28)$$

Y-EQUATION

$$(m_G + M_T) \ddot{y} + (2m_G \omega_y S_y) \dot{y} + (m_G \omega_y^2) y = F_y \quad (29)$$

Z-EQUATION

$$(m_G + M_T) \ddot{z} + (2m_G \omega_z S_z) \dot{z} + (m_G \omega_z^2) z + m r \ddot{\beta}_0 = F_z \quad (30)$$

FIGURE D.2-4: VERTICAL BIFILAR EQUATIONS IN FIXED SYSTEM COORDINATES

θ_x - EQUATION

$$\left[m_G + \frac{1}{2} M_T (r+R)^2 \right] \ddot{\theta}_x + (2m_G \omega_{\theta_x} \zeta_{\theta_x}) \dot{\theta}_x + (m_G \omega_{\theta_x}^2) \theta_x \\ + [m(r+R)r] \ddot{\beta}_s - [2mr\Omega(r+R)] \dot{\beta}_c + [M_T \Omega(r+R)^2] \dot{\theta}_y = M_x \quad (31)$$

θ_y - EQUATION

$$\left[m_G + \frac{1}{2} M_T (r+R)^2 \right] \ddot{\theta}_y + (2m_G \omega_{\theta_y} \zeta_{\theta_y}) \dot{\theta}_y + (m_G \omega_{\theta_y}^2) \theta_y \\ + [-mr(r+R)] \ddot{\beta}_c - [2mr\Omega(r+R)] \dot{\beta}_s - [M_T \Omega(r+R)^2] \dot{\theta}_x = M_y \quad (32)$$

θ_z - EQUATION

$$\left[m_G + M_T (r+R)^2 \right] \ddot{\theta}_z + (2m_G \omega_{\theta_z} \zeta_{\theta_z}) \dot{\theta}_z + (m_G \omega_{\theta_z}^2) \theta_z = M_z \quad (33)$$

FIGURE D.2-4: VERTICAL BIFILAR EQUATIONS IN FIXED SYSTEM COORDINATES (CONTINUED)

β_o -EQUATION

$$(M_I r) \ddot{z} + (mr^2) \ddot{\beta}_o + (2mr^2 S_p \omega_p) \dot{\beta}_o + [mr \Omega^2 (r+R)] \beta_o = 0 \quad (34)$$

β_s -EQUATION

$$\begin{aligned} & \left[\frac{M_I}{2} r(r+R) \right] \ddot{\theta}_x + (mr^2) \ddot{\beta}_s + (2mr^2 S_p \omega_p) \dot{\beta}_s \\ & - (2mr^2 \Omega) \dot{\beta}_c + [M_I r \Omega (r+R)] \dot{\theta}_y + (mr R \Omega^2) \beta_s \\ & - (2mr^2 S_p \omega_p \Omega) \beta_c = 0 \end{aligned} \quad (35)$$

β_c -EQUATION

$$\begin{aligned} & - \left[\frac{M_I}{2} r(r+R) \right] \ddot{\theta}_y + (mr^2) \ddot{\beta}_c + (2mr^2 S_p \omega_p) \dot{\beta}_c + (2mr^2 \Omega) \dot{\beta}_s \\ & + [M_I r \Omega (r+R)] \dot{\theta}_x + (mr R \Omega^2) \beta_c + (2mr^2 S_p \omega_p \Omega) \beta_s = 0 \end{aligned} \quad (36)$$

FIGURE D.2-4: VERTICAL BIFILAR EQUATIONS IN FIXED SYSTEM COORDINATES (CONCLUDED)

D.3 Rotor Equations With Hover Aerodynamics

The rotor equations of motion have been derived with five hub degrees of freedom (X , Y , Z , θ_X , θ_Y), as well as with four coupled flap-lag flexible blade bending, two torsional, a rigid flapping and a rigid lead-lag degrees of freedom. Definition of the coordinate system is shown in Figure D.3-1. A detailed derivation of the rotor equations of motion are presented in Reference 1. For completeness sake, these equations are included herewith.

The equations of motion are shown on pp 305 to 331. The airframe generalized coordinates have been utilized for the hub flexibilities. The first equation is for the fixed system, and the other four are rotor equations, i.e. bending, torsion, rigid flapping and rigid lead-lag equations (37)-(41) respectively. These equations consist of the acceleration, velocity and displacement coefficients which account for the left-hand-side of the Lagrange's equations of motion. The right-hand-side of the Lagrange's equations of motion, the generalized forces, are shown by equations (42)-(46). In every equation, all generalized coordinates and physical properties associated with the rotor system have a subscript n , the blade number. The definition of all parameters used in all rotor equations are described in the list of symbols immediately following the equations (pp 332 to 338).

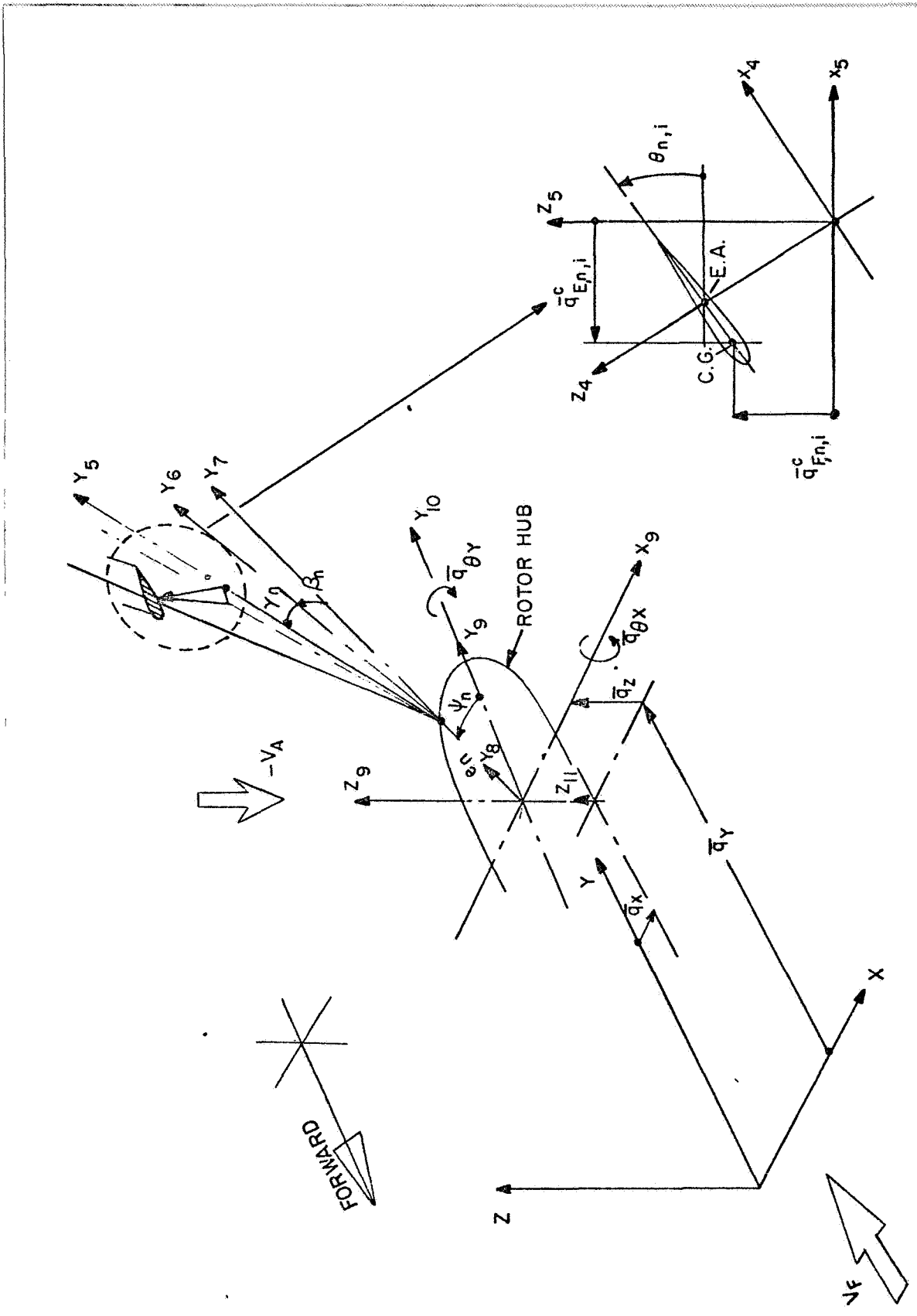


Figure D.3-1: Aeroelastic Rotor Stability Analysis Coordinate System

Airframe Mode Equations

$$\begin{aligned}
 & \left\{ \sum_{n=1}^N \sum_{i=1}^{NA} \left[\delta^{R-e} \text{mdr} \{ \phi_{X,j} (\phi_{X,i} + \phi_{\theta Y,i} [b_2 + r\beta_o]) + \phi_{Y,j} (\phi_{Y,i} - \phi_{\theta X,i} [b_2 + r\beta_o]) \right. \right. \\
 & + \phi_{Z,j} (\phi_{Z,i} + \phi_{\theta X,i} [(a_2 - r\gamma_o) \sin\psi + (e + r + a_2\gamma_o - b_2\beta_o) \cos\psi] \\
 & + \phi_{\theta Y,i} [(e + r + a_2\gamma_o - b_2\beta_o) \sin\psi - (a_2 - r\gamma_o) \cos\psi]) + \phi_{\theta Y,j} ((b_2 + r\beta_o) \phi_{X,i} \\
 & + \phi_{Z,i} [(e + r + a_2\gamma_o - b_2\beta_o) \sin\psi - (a_2 - r\gamma_o) \cos\psi]) + \phi_{\theta X,j} (-b_2 + r\beta_o) \phi_{Y,i} \\
 & + \phi_{Z,i} [(e + r + a_2\gamma_o - b_2\beta_o) \cos\psi + (a_2 - r\gamma_o) \sin\psi]) \\
 & + \phi_{\theta Y,j} (\phi_{\theta Y,i} [(-a_2(a_2\gamma_o - b_2\beta_o) - (r+e)(a_2 - r\gamma_o)) \sin 2\psi + ((r+e)^2 \\
 & + 2(r+e)(a_2\gamma_o - b_2\beta_o)) \sin^2\psi + a_2(a_2 - 2r\gamma_o) \cos^2\psi + b_2(b_2 + 2r\beta_o)] \\
 & + \phi_{\theta X,i} [\frac{1}{2}(-a_2(a_2 - 2r\gamma_o) + (r+e)^2 + 2(r+e)(a_2\gamma_o - b_2\beta_o)) \sin 2\psi \\
 & + (-(r+e)(a_2 - r\gamma_o) - a_2(a_2\gamma_o - b_2\beta_o)) \cos 2\psi]) + \phi_{\theta X,j} (\phi_{\theta Y,i} [\frac{1}{2}(-a_2(a_2 - 2r\gamma_o) \\
 & + (r+e)^2 + 2(r+e)(a_2\gamma_o - b_2\beta_o)) \sin 2\psi + (-(r+e)(a_2 - r\gamma_o) \\
 & - a_2(a_2\gamma_o - b_2\beta_o)) \cos 2\psi] + \phi_{\theta X,i} [(a_2(a_2\gamma_o - b_2\beta_o) + (r+e)(a_2 - r\gamma_o)) \sin 2\psi \\
 & + ((r+e)^2 + 2(r+e)(a_2\gamma_o - b_2\beta_o)) \cos 2\psi + a_2(a_2 - 2r\gamma_o) \sin^2\psi \\
 & + b_2(b_2 + 2r\beta_o)])] + I_X dr \{ \phi_{\theta Y,j} q'_{EO} (-\phi_{\theta Y,i} \cos\theta_o \sin 2\psi - \phi_{\theta X,i} \cos\theta_o \cos 2\psi) \\
 & + \phi_{\theta X,j} q'_{EO} (-\phi_{\theta Y,i} \cos\theta_o \cos 2\psi + \phi_{\theta X,i} \cos\theta_o \sin 2\psi) + \phi_{\theta Y,j} (\phi_{\theta Y,i} (\cos^2\theta_o \sin^2\psi \\
 & + (\gamma_o \cos^2\theta_o - \frac{1}{2}\beta_o \sin 2\theta_o) \sin 2\psi) + \phi_{\theta X,i} (\frac{1}{2}\cos^2\theta_o \sin 2\psi \\
 & + (\gamma_o \cos^2\theta_o - \frac{1}{2}\beta_o \sin 2\theta_o) \cos 2\psi) + \phi_{\theta X,j} (\phi_{\theta Y,i} (\frac{1}{2}\cos^2\theta_o \sin 2\psi + (\gamma_o \cos^2\theta_o \\
 & - \frac{1}{2}\beta_o \sin 2\theta_o) \cos 2\psi) + \phi_{\theta X,i} (\cos^2\theta_o \cos 2\psi - (\gamma_o \cos^2\theta_o - \frac{1}{2}\beta_o \sin 2\theta_o) \sin 2\psi))\} \\
 & + I_Y dr \{ \phi_{\theta Y,j} (\phi_{\theta Y,i} (q'_{EO} \cos\theta_o - q'_{FO} \sin\theta_o) \sin 2\psi + \phi_{\theta X,i} (q'_{EO} \cos\theta_o \\
 & - q'_{FO} \sin\theta_o) \cos 2\psi) + \phi_{\theta X,j} (\phi_{\theta Y,i} (q'_{EO} \cos\theta_o - q'_{FO} \sin\theta_o) \cos 2\psi - q'_{FO} \sin\theta_o \cos 2\psi) \quad 1
 \end{aligned}$$

$$\begin{aligned}
& + \phi_{\theta X,i} (-q'_{EO} \cos \theta_0 + q'_{FO} \sin \theta_0) \sin 2\psi + \phi_{\theta Y,j} (\phi_{\theta Y,i} (\cos^2 \psi - \gamma_0 \sin 2\psi) \\
& + \phi_{\theta X,i} (-\gamma_0 \cos 2\psi - \frac{1}{2} \sin 2\psi)) + \phi_{\theta X,j} (\phi_{\theta Y,i} (-\gamma_0 \cos 2\psi - \frac{1}{2} \sin 2\psi) \\
& + \phi_{\theta X,i} (\sin^2 \psi + \gamma_0 \sin 2\psi)) \} + I_Z dr \{ \phi_{\theta Y,j} q'_{FO} (\phi_{\theta Y,i} \sin \theta_0 \sin 2\psi \\
& + \phi_{\theta X,i} \sin \theta_0 \cos 2\psi) + \phi_{\theta X,j} q'_{FO} (\phi_{\theta Y,i} \sin \theta_0 \cos 2\psi - \phi_{\theta X,i} \sin \theta_0 \sin 2\psi) \\
& + \phi_{\theta Y,j} (\phi_{\theta Y,i} (\sin^2 \theta_0 \sin^2 \psi + (\gamma_0 \sin^2 \theta_0 + \frac{1}{2} \beta_0 \sin 2\theta_0) \sin 2\psi) \\
& + \phi_{\theta X,i} (\frac{1}{2} \sin^2 \theta_0 \sin 2\psi + (\gamma_0 \sin^2 \theta_0 + \frac{1}{2} \beta_0 \sin 2\theta_0) \cos 2\psi)) \\
& + \phi_{\theta X,j} (\phi_{\theta Y,i} (\frac{1}{2} \sin^2 \theta_0 \sin 2\psi + (\gamma_0 \sin^2 \theta_0 + \frac{1}{2} \beta_0 \sin 2\theta_0) \cos 2\psi) \\
& + \phi_{\theta X,i} (\sin^2 \theta_0 \cos^2 \psi - (\gamma_0 \sin^2 \theta_0 + \frac{1}{2} \beta_0 \sin 2\theta_0) \sin 2\psi)) \} \Big] \ddot{q}_i \Big\} \\
& + \left\{ \sum_{i=1}^{NA} [\phi_{\theta X,i} \phi_{\theta X,j} I_{FA} + \phi_{\theta Y,i} \phi_{\theta Y,j} I_L + \phi_{Z,i} \phi_{Z,j} M_S] \ddot{q}_i \right\} + \left\{ M_{A,j} \ddot{q}_j \right\} \\
& + \left\{ \sum_{n=1}^N \left[\int_0^{R-e} m dr \{ \phi_{X,j} ((b_2 \gamma_0 + a_2 \beta_0) \sin \psi - b_2 \cos \psi) + \phi_{Y,j} (- (b_2 \gamma_0 \right. \right. \\
& \left. \left. + a_2 \beta_0) \cos \psi - b_2 \sin \psi) + \phi_{Z,j} a_2 + \phi_{\theta Y,j} [((a_2^2 + b_2^2) \gamma_0 + a_2(r + e)) \sin \psi \right. \right. \\
& \left. \left. - (a_2(a_2 - r \gamma_0) + b_2(b_2 + r \beta_0)) \cos \psi] + \phi_{\theta X,j} [(a_2(a_2 - r \gamma_0) \right. \right. \\
& \left. \left. + b_2(b_2 + r \beta_0)) \sin \psi + ((a_2^2 + b_2^2) \gamma_0 + a_2(r + e)) \cos \psi] \} \right. \right. \\
& \left. \left. + I_X dr \{ \phi_{\theta Y,j} q'_{EO} \cos \theta_0 \sin \psi + \phi_{\theta X,j} q'_{EO} \cos \theta_0 \cos \psi \} + I_Y dr \{ \phi_{\theta Y,j} (-q'_{EO} \cos \theta_0 \right. \right. \\
& \left. \left. + q'_{FO} \sin \theta_0) \sin \psi + \phi_{\theta X,j} (-q'_{EO} \cos \theta_0 + q'_{FO} \sin \theta_0) \cos \psi + \phi_{\theta Y,j} (\gamma_0 \sin \psi \right. \right. \\
& \left. \left. - \cos \psi) + \phi_{\theta X,j} (\gamma_0 \cos \psi + \sin \psi) \} + I_Z dr \{ - \phi_{\theta Y,j} q'_{FO} \sin \theta_0 \sin \psi \right. \right. \\
& \left. \left. - \phi_{\theta X,j} q'_{FO} \sin \theta_0 \cos \psi \} \right] \phi_{\theta T} \ddot{\theta}_T \right\} + \left\{ \sum_{n=1}^N \left[\int_0^{R-e} m dr \{ \phi_{X,j} (b_2 + r \beta_0) \sin \psi - \phi_{Y,j} (b_2 \right. \right. \\
& \left. \left. + r \beta_0) \cos \psi + \phi_{Z,j} (r + a_2 \gamma_0 - b_2 \beta_0) + \phi_{\theta Y,j} [(e(a_2 \gamma_0 - b_2 \beta_0) + r(r + e + 2a_2 \gamma_0) \right. \right. \\
& \left. \left. + b_2^2) \sin \psi - (a_2(a_2 \gamma_0 - b_2 \beta_0) + r(a_2 - r \gamma_0)) \cos \psi] + \phi_{\theta X,j} [(a_2(a_2 \gamma_0 - b_2 \beta_0) \right. \right. \\
& \left. \left. + r(a_2 - r \gamma_0)) \sin \psi + (e(a_2 \gamma_0 - b_2 \beta_0) + r(r + e + 2a_2 \gamma_0) + b_2^2) \cos \psi] \} \right. \right. \\
& \left. \left. + I_X dr \{ - \phi_{\theta Y,j} q'_{EO} \cos \theta_0 \cos \psi + \phi_{\theta X,j} q'_{EO} \cos \theta_0 \sin \psi + \phi_{\theta Y,j} (\cos^2 \theta_0 \sin \psi \right. \right. \\
& \left. \left. - \frac{1}{2} \sin^2 \theta_0) \right] \right\}
\end{aligned}$$

$$\begin{aligned}
& + (\gamma_0 \cos^2 \theta_0 - \frac{1}{2} \beta_0 \sin 2 \theta_0) \cos \psi) + \phi_{\theta X, j} (\cos^2 \theta_0 \cos \psi - (\gamma_0 \cos^2 \theta_0 \\
& - \frac{1}{2} \beta_0 \sin 2 \theta_0) \sin \psi) + I_Y dr \{ \phi_{\theta Y, j} (q'_{EO} \cos \theta_0 - q'_{FO} \sin \theta_0) \cos \psi \\
& + \phi_{\theta X, j} (-q'_{EO} \cos \theta_0 + q'_{FO} \sin \theta_0) \sin \psi + \phi_{\theta X, j} \gamma_0 \sin \psi - \phi_{\theta Y, j} \gamma_0 \cos \psi \} \\
& + I_Z dr \{ \phi_{\theta Y, j} q'_{FO} \sin \theta_0 \cos \psi - \phi_{\theta X, j} q'_{FO} \sin \theta_0 \sin \psi + \phi_{\theta Y, j} (\sin^2 \theta_0 \sin \psi \\
& + (\gamma_0 \sin^2 \theta_0 + \frac{1}{2} \beta_0 \sin 2 \theta_0) \cos \psi) + \phi_{\theta X, j} (\sin^2 \theta_0 \cos \psi - (\gamma_0 \sin^2 \theta_0 \\
& + \frac{1}{2} \beta_0 \sin 2 \theta_0) \sin \psi) \} \Big] \ddot{\beta} \Big\} + \left\{ \sum_{n=1}^N \left[\int_0^{R-e} m dr \{ \phi_{X, j} (-(\alpha_2 - r \gamma_0) \sin \psi - (\alpha_2 \gamma_0 \\
& + r) \cos \psi) + \phi_{Y, j} (-(\alpha_2 \gamma_0 + r) \sin \psi + (\alpha_2 - r \gamma_0) \cos \psi) + \phi_{Z, j} \alpha_2 \beta_0 \\
& + \phi_{\theta Y, j} [(-b_2 (\alpha_2 - r \gamma_0) + \alpha_2 e \beta_0) \sin \psi + (-(\alpha_2^2 + r^2) \beta_0 - b_2 (\alpha_2 \gamma_0 + r)) \cos \psi] \\
& + \phi_{\theta X, j} [(a_2^2 + r^2) \beta_0 + b_2 (\alpha_2 \gamma_0 + r)] \sin \psi + (-b_2 (\alpha_2 - r \gamma_0) + \alpha_2 e \beta_0) \cos \psi] \} \right. \\
& + I_X dr \{ -\phi_{\theta Y, j} q'_{EO} \sin \theta_0 \cos \psi + \phi_{\theta X, j} q'_{EO} \sin \theta_0 \sin \psi + \phi_{\theta Y, j} [\frac{1}{2} \sin 2 \theta_0 \sin \psi \\
& + (\frac{1}{2} \gamma_0 \sin 2 \theta_0 - \beta_0 \sin^2 \theta_0) \cos \psi] + \phi_{\theta X, j} [\frac{1}{2} \sin 2 \theta_0 \cos \psi - (\frac{1}{2} \gamma_0 \sin 2 \theta_0 - \beta_0 \sin^2 \theta_0) \sin \psi] \} \\
& + I_Y dr \{ \phi_{\theta Y, j} (q'_{EO} \sin \theta_0 + q'_{FO} \cos \theta_0) \cos \psi + \phi_{\theta X, j} (-q'_{EO} \sin \theta_0 \\
& - q'_{FO} \cos \theta_0) \sin \psi \} + I_Z dr \{ -\phi_{\theta Y, j} q'_{FO} \cos \theta_0 \cos \psi + \phi_{\theta X, j} q'_{FO} \cos \theta_0 \sin \psi \\
& + \phi_{\theta Y, j} [-\frac{1}{2} \sin 2 \theta_0 \sin \psi - (\frac{1}{2} \gamma_0 \sin 2 \theta_0 + \beta_0 \cos^2 \theta_0) \cos \psi] + \phi_{\theta X, j} [-\frac{1}{2} \sin 2 \theta_0 \cos \psi \\
& + (\frac{1}{2} \gamma_0 \sin 2 \theta_0 + \beta_0 \cos^2 \theta_0) \sin \psi] \} \Big] \ddot{\gamma} \Big\} + \left\{ \sum_{n=1}^N \sum_{i=1}^{NE} \left[\int_0^{R-e} m dr \{ \phi_{X, j} (\phi_{E, i} (\gamma_0 \sin \psi - \cos \psi) \right. \\
& + v_{1,i} \sin \psi + \phi_{F, i} \beta_0 \sin \psi) + \phi_{Y, j} (\phi_{E, i} (-\sin \psi - \gamma_0 \cos \psi) - v_{1,i} \cos \psi \\
& - \phi_{F, i} \beta_0 \cos \psi) + \phi_{Z, j} \phi_{F, i} + \phi_{\theta Y, j} [(\phi_{F, i} (\alpha_2 \gamma_0 + r + e) + \phi_{E, i} b_2 \gamma_0) \sin \psi \\
& + (-\phi_{F, i} (\alpha_2 - r \gamma_0) - \phi_{E, i} (b_2 + r \beta_0)) \cos \psi] + \phi_{\theta X, j} [(\phi_{F, i} (\alpha_2 - r \gamma_0) + \phi_{E, i} b_2 \\
& + r \beta_0) \sin \psi + (\phi_{E, i} b_2 \gamma_0 + \phi_{F, i} (\alpha_2 \gamma_0 + r + e)) \cos \psi] + \phi_{\theta Y, j} v_{1,i} b_2 \sin \psi \\
& + \phi_{\theta X, j} v_{1,i} b_2 \cos \psi \} + I_X dr \{ \phi_{\theta Y, j} [\cos \theta_0 \sin \psi + (\gamma_0 \cos \theta_0 - \beta_0 \sin \theta_0 \\
& - q'_{EO}) \cos \psi] \phi'_{F, i} + \phi_{\theta X, j} [\cos \theta_0 \cos \psi - (\gamma_0 \cos \theta_0 - \beta_0 \sin \theta_0 - q'_{EO}) \sin \psi] \phi'_{F, i} \} \right. \Big\} \quad 3
\end{aligned}$$

$$\begin{aligned}
& + I_Y \text{dr} \{ (\phi_{\theta Y, j} q'_{FO} \cos \psi - \phi_{\theta X, j} q'_{FO} \sin \psi) \phi'_{E,i} \} \\
& + I_Z \text{dr} \{ \phi_{\theta Y, j} [- \sin \theta_0 \sin \psi - (\gamma_0 \sin \theta_0 + \beta_0 \cos \theta_0 + q'_{FO}) \cos \psi] \phi'_{E,i} \\
& + \phi_{\theta X, j} [- \sin \theta_0 \cos \psi + (\gamma_0 \sin \theta_0 + \beta_0 \cos \theta_0 + q'_{FO}) \sin \psi] \phi'_{E,i} \} \}_{q_T, i} \\
& + \left\{ \frac{1}{R_S} [\phi_{\theta X, j} I_{FA} - \phi_{\theta Y, j} I_L] + \phi_{Z, j} M_S \right\} \ddot{x}_A \left\{ + \left\{ \frac{1}{R_S} [- \phi_{\theta X, j} I_{FA} - \phi_{\theta Y, j} I_L] \right. \right. \\
& + \left. \left. \phi_{Z, j} M_S \right\} \ddot{x}_F \right\} + \left\{ \frac{1}{R_S} \phi_{\theta Y, j} I_L \ddot{x}_L \right\} + \left\{ \sum_{n=1}^N \sum_{i=1}^{N_A} \left[\int_0^{R-e} \text{mdr} \{ 2\Omega \phi_{Z, j} [\phi_{\theta X, i} ((a_2 - r\gamma_0) \cos \psi \right. \right. \\
& - (e + r + a_2 \gamma_0 - b_2 \beta_0) \sin \psi) + \phi_{\theta Y, i} ((e + r + a_2 \gamma_0 - b_2 \beta_0) \cos \psi \\
& + (a_2 - r\gamma_0) \sin \psi)] + \Omega \phi_{\theta Y, j} [\phi_{\theta Y, i} [(r + e)^2 + 2(r + e)(a_2 \gamma_0 - b_2 \beta_0) \\
& - a_2 (a_2 - r\gamma_0)] \sin 2\psi + [-(r + e)(a_2 - r\gamma_0) - a_2 (a_2 \gamma_0 - b_2 \beta_0)] 2 \cos 2\psi) \\
& + \phi_{\theta X, i} [(a_2 (a_2 \gamma_0 - b_2 \beta_0) + (r + e)(a_2 - r\gamma_0)] 2 \sin 2\psi + [(r + e)^2 \\
& - a_2 (a_2 - 2r\gamma_0) + 2(r + e)(a_2 \gamma_0 - b_2 \beta_0)] \cos 2\psi - a_2 (a_2 - 2r\gamma_0) - (r + e)^2 \\
& - 2(r + e)(a_2 \gamma_0 - b_2 \beta_0)] + \Omega \phi_{\theta X, j} [\phi_{\theta Y, i} [(a_2 (a_2 \gamma_0 - b_2 \beta_0) + (r + e)(a_2 \\
& - r\gamma_0)] 2 \sin 2\psi + [-a_2 (a_2 - 2r\gamma_0) + (r + e)^2 + 2(r + e)(a_2 \gamma_0 - b_2 \beta_0)] \cos 2\psi \\
& + a_2 (a_2 - 2r\gamma_0) + (r + e)^2 + 2(r + e)(a_2 \gamma_0 - b_2 \beta_0)] + \phi_{\theta X, i} [- (r + e)^2 \\
& - 2(r + e)(a_2 \gamma_0 - b_2 \beta_0) + a_2 (a_2 - r\gamma_0)] \sin 2\psi + [(r + e)(a_2 - r\gamma_0) \\
& + a_2 (a_2 \gamma_0 - b_2 \beta_0)] 2 \cos 2\psi \}] + I_X \text{dr} \{ 2\Omega q'_{EO} (\phi_{\theta Y, j} [- \phi_{\theta Y, i} \cos \theta_0 \cos 2\psi \\
& + \phi_{\theta X, i} \cos \theta_0 \sin 2\psi] + \phi_{\theta X, j} [\phi_{\theta Y, i} \cos \theta_0 \sin 2\psi + \phi_{\theta X, i} \cos \theta_0 \cos 2\psi]) \\
& + \Omega (\phi_{\theta Y, j} [\phi_{\theta Y, i} (\cos^2 \theta_0 \sin 2\psi + (2\gamma_0 \cos^2 \theta_0 - \beta_0 \sin 2\theta_0) \cos 2\psi) \\
& + \phi_{\theta X, i} (\cos^2 \theta_0 \cos 2\psi - (2\gamma_0 \cos^2 \theta_0 - \beta_0 \sin 2\theta_0) \sin 2\psi) - \phi_{\theta X, i} \sin^2 \theta_0] \\
& + \phi_{\theta X, j} [\phi_{\theta Y, i} (\cos^2 \theta_0 \cos 2\psi - (2\gamma_0 \cos^2 \theta_0 - \beta_0 \sin 2\theta_0) \sin 2\psi) \\
& + \phi_{\theta X, i} (-\cos^2 \theta_0 \sin 2\psi - (2\gamma_0 \cos^2 \theta_0 - \beta_0 \sin 2\theta_0) \cos 2\psi) + \phi_{\theta Y, i} \sin^2 \theta_0] \} \\
& + I_Y \text{dr} \{ 2\Omega (\phi_{\theta Y, j} [\phi_{\theta Y, i} (q'_{EO} \cos \theta_0 - q'_{FO} \sin \theta_0) \cos 2\psi + \phi_{\theta X, i} (-q'_{EO} \cos \theta_0
\end{aligned}$$

$$\begin{aligned}
& + q'_{FO} \sin \theta_0) \sin 2\psi] + \phi_{\theta X,j} [\phi_{\theta Y,i} (-q'_{EO} \cos \theta_0) \quad \text{4} \\
& + q'_{FO} \sin \theta_0) \sin 2\psi + \phi_{\theta X,i} (-q'_{EO} \cos \theta_0 + q'_{FO} \sin \theta_0) \cos 2\psi]) \\
& + \Omega (\phi_{\theta Y,j} [\phi_{\theta Y,i} (-2\gamma_0 \cos 2\psi - \sin 2\psi) + \phi_{\theta X,i} (-\cos 2\psi + 2\gamma_0 \sin 2\psi)] \\
& + \phi_{\theta X,j} [\phi_{\theta Y,i} (-\cos 2\psi + 2\gamma_0 \sin 2\psi) + \phi_{\theta X,i} (2\gamma_0 \cos 2\psi + \sin 2\psi)]) \\
& + I_Z dr \{ 2\Omega q'_{FO} (\phi_{\theta Y,j} [\phi_{\theta Y,i} \sin \theta_0 \cos 2\psi - \phi_{\theta X,i} \sin \theta_0 \cos 2\psi] + \phi_{\theta X,j} [\\
& - \phi_{\theta Y,i} \sin \theta_0 \sin 2\psi - \phi_{\theta X,i} \sin \theta_0 \cos 2\psi]) + \Omega (\phi_{\theta Y,j} [\phi_{\theta Y,i} (\sin^2 \theta_0 \sin 2\psi + (2\gamma_0 \sin^2 \theta_0 \\
& + \beta_0 \sin 2\theta_0) \cos 2\psi) + \phi_{\theta X,i} (\sin^2 \theta_0 \cos 2\psi - (2\gamma_0 \sin^2 \theta_0 + \beta_0 \sin 2\theta_0) \sin 2\psi) \\
& - \phi_{\theta X,i} \cos^2 \theta_0] + \phi_{\theta X,j} [\phi_{\theta Y,i} (\sin^2 \theta_0 \cos 2\psi - (2\gamma_0 \sin^2 \theta_0 + \beta_0 \sin 2\theta_0) \sin 2\psi) \\
& + \phi_{\theta X,i} (-\sin^2 \theta_0 \sin 2\psi - (2\gamma_0 \sin^2 \theta_0 + \beta_0 \sin 2\theta_0) \cos 2\psi) \\
& + \phi_{\theta Y,i} \cos^2 \theta_0]) \} \dot{q}_j \} + \left\{ 2\zeta_{A,j} M_{A,j} \omega_{A,j} \dot{q}_j \right\} \\
& + \left\{ \sum_{n=1}^N \left[\int_0^{R-e} m dr \{ 2\Omega (\phi_{X,j} ((b_2 \gamma_0 + a_2 \beta_0) \cos \psi + b_2 \sin \psi) \right. \\
& + \phi_{Y,j} ((b_2 \gamma_0 + a_2 \beta_0) \sin \psi - b_2 \cos \psi) + \phi_{\theta Y,j} (b_2 (b_2 \\
& + r \beta_0) \sin \psi + b_2 (a_2 \beta_0 + b_2 \gamma_0) \cos \psi) + \phi_{\theta X,j} (-b_2 (b_2 \gamma_0 + a_2 \beta_0) \sin \psi \\
& \left. + b_2 (b_2 + r \beta_0) \cos \psi)) \} + I_X dr \{ \Omega (\phi_{\theta Y,j} [\cos 2\theta_0 \sin \psi + (\gamma_0 \cos 2\theta_0 \\
& - \beta_0 \sin 2\theta_0) \cos \psi] + \phi_{\theta X,j} [\cos 2\theta_0 \cos \psi - (\gamma_0 \cos 2\theta_0 - \beta_0 \sin 2\theta_0) \sin \psi]) \} \\
& + I_Y dr \{ \Omega (\phi_{\theta Y,j} (\gamma_0 \cos \psi + \sin \psi) + \phi_{\theta X,j} (\cos \psi - \gamma_0 \sin \psi)) \} \\
& + I_Z dr \{ \Omega (\phi_{\theta Y,j} [-\cos 2\theta_0 \sin \psi - (\gamma_0 \cos 2\theta_0 - \beta_0 \sin 2\theta_0) \cos \psi] \\
& + \phi_{\theta X,j} [-\cos 2\theta_0 \cos \psi + (\gamma_0 \cos 2\theta_0 - \beta_0 \sin 2\theta_0) \sin \psi]) \} \dot{\phi}_{\theta T} \} \\
& + \left\{ \sum_{n=1}^N \left[\int_0^{R-e} m dr \{ 2\Omega (\phi_{X,j} (b_2 + r \beta_0) \cos \psi + \phi_{Y,j} (b_2 + r \beta_0) \sin \psi \right. \right. \\
& + \phi_{\theta Y,j} b_2 (b_2 + 2r \beta_0) \cos \psi - \phi_{\theta X,j} b_2 (b_2 + 2r \beta_0) \sin \psi) \} \\
& \left. + I_X dr \{ \Omega (\phi_{\theta Y,j} \cos 2\theta_0 \cos \psi - \phi_{\theta X,j} \cos 2\theta_0 \sin \psi) \} + I_Y dr \{ \Omega (\phi_{\theta Y,j} \cos \psi \quad \text{5} \right. \\
& \left. - \phi_{\theta X,j} \sin 2\theta_0) \} \right\}
\end{aligned}$$

$$\begin{aligned}
& - \phi_{\theta X,j} \sin\psi \}) + I_Z dr \{ \Omega (- \phi_{\theta Y,j} \cos 2\theta_0 \cos\psi + \phi_{\theta X,j} \cos 2\theta_0 \sin\psi) \} \Big] \dot{\beta} \Big\} \\
& + \left\{ \sum_{n=1}^N \left[\int^{R-e}_{0} mdr \{ 2\Omega (\phi_{X,j} [- (a_2 - r\gamma_0) \cos\psi + (a_2 \gamma_0 + r) \sin\psi] \right. \right. \\
& + \phi_{Y,j} [- (a_2 \gamma_0 + r) \cos\psi - (a_2 - r\gamma_0) \sin\psi] + \phi_{\theta Y,j} [(r^2 \beta_0 + b_2 (a_2 \gamma_0 \\
& + r)) \sin\psi - (b_2 (a_2 - r\gamma_0) + a_2 r \beta_0) \cos\psi] + \phi_{\theta X,j} [(r^2 \beta_0 + b_2 (a_2 \gamma_0 + r)) \cos\psi \\
& \left. \left. + (b_2 (a_2 - r\gamma_0) + a_2 r \beta_0) \sin\psi] \right) \} + I_X dr \{ 2\Omega q'_{EO} (\phi_{\theta Y,j} \sin\theta_0 \sin\psi \\
& + \phi_{\theta X,j} \sin\theta_0 \cos\psi) + \Omega (\phi_{\theta Y,j} [\sin 2\theta_0 \cos\psi - (\gamma_0 \sin 2\theta_0 - \beta_0) \sin\psi] \\
& + \phi_{\theta X,j} [- \sin 2\theta_0 \sin\psi - (\gamma_0 \sin 2\theta_0 - \beta_0) \cos\psi]) \} \\
& + I_Y dr \{ 2\Omega (\phi_{\theta Y,j} (- q'_{EO} \sin\theta_0 - q'_{FO} \cos\theta_0) \sin\psi + \phi_{\theta X,j} (- q'_{EO} \sin\theta_0 \\
& - q'_{FO} \cos\theta_0) \cos\psi) + \Omega (- \phi_{\theta Y,j} \beta_0 \sin\psi - \phi_{\theta X,j} \beta_0 \cos\psi) \} \\
& + I_Z dr \{ 2\Omega q'_{FO} (\phi_{\theta Y,j} \cos\theta_0 \sin\psi + \phi_{\theta X,j} \cos\theta_0 \cos\psi) + \Omega (\phi_{\theta Y,j} (- \sin 2\theta_0 \cos\psi \\
& + (\gamma_0 \sin 2\theta_0 + \beta_0) \sin\psi) + \phi_{\theta X,j} (\sin 2\theta_0 \sin\psi + (\gamma_0 \sin 2\theta_0 + \beta_0) \cos\psi) \} \Big] \dot{\gamma} \Big\} \\
& + \left\{ \sum_{n=1}^N \sum_{i=1}^{NE} \left[\int^{R-e}_{0} mdr \{ 2\Omega (\phi_{X,j} [\phi_{E,i} (\gamma_0 \cos\psi + \sin\psi) + v_{1,i} \cos\psi \right. \right. \\
& + \phi_{F,i} \beta_0 \cos\psi] + \phi_{Y,j} [- \phi_{E,i} (\cos\psi - \gamma_0 \sin\psi) + v_{1,i} \sin\psi \\
& + \phi_{F,i} \beta_0 \sin\psi] + \phi_{\theta Y,j} [\phi_{E,i} (b_2 + r \beta_0) \sin\psi + b_2 (\phi_{F,i} \beta_0 \\
& + \phi_{E,i} \gamma_0) \cos\psi] + \phi_{\theta X,j} [- b_2 (\phi_{F,i} \beta_0 + \phi_{E,i} \gamma_0) \sin\psi + \phi_{E,i} (b_2 + r \beta_0) \cos\psi] \\
& + \phi_{\theta Y,j} v_{1,i} b_2 \cos\psi - \phi_{\theta X,j} v_{1,i} b_2 \sin\psi \} \} + I_X dr \{ \Omega (\phi_{\theta Y,j} [(\sin\theta_0 \cos\psi \\
& + (q'_{EO} \sin 2\theta_0 - \gamma_0 \sin 2\theta_0 + \beta_0 \cos 2\theta_0) \sin\psi) \phi'_{E,i} \\
& + (\cos\theta_0 \cos\psi + (q'_{EO} - \gamma_0 \cos\theta_0 + \beta_0 \sin\theta_0) \sin\psi) \phi'_{F,i}] \\
& + \phi_{\theta X,j} [(- \sin\theta_0 \sin\psi + (q'_{EO} \sin 2\theta_0 - \gamma_0 \sin 2\theta_0 + \beta_0 \cos 2\theta_0) \cos\psi) \phi'_{E,i} \\
& \left. \left. + (- \cos\theta_0 \sin\psi + (q'_{EO} - \gamma_0 \cos\theta_0 + \beta_0 \sin\theta_0) \cos\psi) \phi'_{F,i} \right] \right) \} \quad (6)
\end{aligned}$$

$$\begin{aligned}
& + I_Y dr \{ \Omega (\phi_{\theta Y, j} [\phi'_{E,i} (- \sin \theta_0 \cos \psi + (- 2q'_{FO} \cos^2 \theta_0 - q'_{EO} \sin 2\theta_0 \\
& - \beta_0 \cos \theta_0 + \gamma_0 \sin \theta_0) \sin \psi) + \phi'_{F,i} (\cos \theta_0 \cos \psi + (- q'_{FO} \sin 2\theta_0 + q'_{EO} \cos 2\theta_0 \\
& - \beta_0 \sin \theta_0 - \gamma_0 \cos \theta_0) \sin \psi)] + \phi_{\theta X, j} [\phi'_{E,i} (\sin \theta_0 \sin \psi + (- 2q'_{FO} \cos^2 \theta_0 \\
& - q'_{EO} \sin 2\theta_0 - \beta_0 \cos \theta_0 + \gamma_0 \sin \theta_0) \cos \psi) + \phi'_{F,i} (- \cos \theta_0 \sin \psi + (q'_{EO} \cos 2\theta_0 \\
& - q'_{FO} \sin 2\theta_0 - \beta_0 \sin \theta_0 - \gamma_0 \cos \theta_0) \cos \psi)]) + I_Z dr \{ \Omega (\phi_{\theta Y, j} [(- \sin \theta_0 \cos \psi \\
& + (2q'_{FO} \cos^2 \theta_0 + \gamma_0 \sin \theta_0 + \beta_0 \cos \theta_0) \sin \psi) \phi'_{E,i} + (- \cos \theta_0 \cos \psi \\
& + (q'_{FO} \sin 2\theta_0 + \gamma_0 \cos \theta_0 + \beta_0 \sin \theta_0) \sin \psi) \phi'_{F,i}] + \phi_{\theta X, j} [(\sin \theta_0 \sin \psi \\
& + (2q'_{FO} \cos^2 \theta_0 + \gamma_0 \sin \theta_0 + \beta_0 \cos \theta_0) \cos \psi) \phi'_{E,i} + (\cos \theta_0 \sin \psi + (q'_{FO} \sin 2\theta_0 \\
& - q'_{EO} \cos 2\theta_0 + \gamma_0 \cos \theta_0 + \beta_0 \sin \theta_0) \cos \psi) \phi'_{F,i}]) \} \} \ddot{q}_T, \} \\
& + \left\{ \sum_{n=1}^N \sum_{i=1}^{NA} \left[\int_{R-e}^{R-e} m dr \{ \Omega^2 \phi_{Z,j} [\phi_{\theta X, i} (- (a_2 - r\gamma_0) \sin \psi - (e + r + a_2 \gamma_0 \\
& - b_2 \beta_0) \cos \psi) + \phi_{\theta Y, i} (- (e + r + a_2 \gamma_0 - b_2 \beta_0) \sin \psi \\
& + (a_2 - r\gamma_0) \cos \psi)] \} \right] \bar{q}_i \right\} + \left\{ M_{A,j} \omega^2 A_{A,j} \bar{q}_j \right\} \\
& + \left\{ \sum_{n=1}^N \left[\int_{R-e}^{R-e} m dr \{ \Omega^2 (\phi_{X,j} [(- (b_2 \gamma_0 + a_2 \beta_0) \sin \psi + b_2 \cos \psi] \\
& + \phi_{Y,j} [(b_2 \gamma_0 + a_2 \beta_0) \cos \psi + b_2 \sin \psi] + \phi_{\theta Y, j} [(a_2 (a_2 \gamma_0 + r + e - 2b_2 \beta_0) \\
& - b_2^2 \gamma_0) \sin \psi + (- a_2 (a_2 - r\gamma_0) + b_2 (b_2 + r\beta_0)) \cos \psi] \\
& + \phi_{\theta X, j} [(a_2 (a_2 - r\gamma_0) - b_2 (b_2 + r\beta_0)) \sin \psi + (a_2 (a_2 \gamma_0 + r + e - 2b_2 \beta_0) \\
& - b_2^2 \gamma_0) \cos \psi]) + I_X dr \{ \Omega^2 q'_{EO} (\phi_{\theta Y, j} \cos \theta_0 \sin \psi + \phi_{\theta X, j} \cos \theta_0 \cos \psi) \\
& + \Omega^2 [\phi_{\theta Y, j} (\cos 2\theta_0 \cos \psi - (\gamma_0 \cos 2\theta_0 - \beta_0 \sin 2\theta_0) \sin \psi) + \phi_{\theta X, j} (- \cos 2\theta_0 \sin \psi \\
& - (\gamma_0 \cos 2\theta_0 - \beta_0 \sin 2\theta_0) \cos \psi)]\} + I_Y dr \{ \Omega^2 [\phi_{\theta Y, j} (- q'_{EO} \cos \theta_0 + q'_{FO} \sin \theta_0) \sin \psi \\
& + \phi_{\theta X, j} (- q'_{EO} \cos \theta_0 + q'_{FO} \sin \theta_0) \cos \psi]\} + I_Z dr \{ \Omega^2 q'_{FO} (- \phi_{\theta Y, j} \sin \theta_0 \sin \psi \right. \}
\end{aligned}$$

$$\begin{aligned}
& - \phi_{\theta X, j} \sin \theta_0 \cos \psi) + \Omega^2 [\phi_{\theta Y, j} (- \cos 2\theta_0 \cos \psi + (\gamma_0 \cos 2\theta_0 - \beta_0 \sin 2\theta_0) \sin \psi) \\
& + \phi_{\theta X, j} (\cos 2\theta_0 \sin \psi + (\gamma_0 \cos 2\theta_0 - \beta_0 \sin 2\theta_0) \cos \psi)] \} \Big] \phi_{\theta T} \Big\} \\
& + \left\{ \sum_{n=1}^N \left[\int^{R-e} \text{mdr} \{ \Omega^2 [- \phi_{X, j} (b_2 + r\beta_0) \sin \psi + \phi_{Y, j} (b_2 + r\beta_0) \cos \psi \right. \right. \\
& + \phi_{\theta Y, j} [(r+e)(a_2 \gamma_0 + r - b_2 \beta_0) + r(a_2 \gamma_0 - b_2 \beta_0) - b_2(2r\beta_0 + b_2)] \sin \psi \\
& + [-a_2(a_2 \gamma_0 + r - b_2 \beta_0) - b_2(b_2 + 2r\beta_0) + r^2 \gamma_0] \cos \psi \\
& + \phi_{\theta X, j} [a_2(a_2 \gamma_0 + r - b_2 \beta_0) + b_2(2r\beta_0 + b_2) - r^2 \gamma_0] \sin \psi \\
& + [(r+e)(a_2 \gamma_0 + r - b_2 \beta_0) + r(a_2 \gamma_0 - b_2 \beta_0) - b_2(b_2 + 2r\beta_0)] \cos \psi)] \\
& + I_X \text{dr} \{ \Omega^2 q'_{EO} (-\phi_{\theta Y, j} \cos \theta_0 \cos \psi + \phi_{\theta X, j} \cos \theta_0 \sin \psi) + \Omega^2 [\phi_{\theta Y, j} (\sin^2 \theta_0 \sin \psi \\
& + \gamma_0 \cos^2 \theta_0 \cos \psi) + \phi_{\theta X, j} (\sin^2 \theta_0 \cos \psi + \gamma_0 \cos^2 \theta_0 \sin \psi)] \} \\
& + I_Y \text{dr} \{ \Omega^2 [\phi_{\theta Y, j} (q'_{EO} \cos \theta_0 - q'_{FO} \sin \theta_0) \cos \psi + \phi_{\theta X, j} (-q'_{EO} \cos \theta_0 \\
& + q'_{FO} \sin \theta_0) \sin \psi + \phi_{\theta Y, j} (-\gamma_0 \cos \psi - \sin \psi) + \phi_{\theta X, j} (\gamma_0 \sin \psi - \cos \psi)] \} \\
& + I_Z \text{dr} \{ \Omega^2 q'_{FO} (\phi_{\theta Y, j} \sin \theta_0 \cos \psi - \phi_{\theta X, j} \sin \theta_0 \sin \psi) + \Omega^2 [\phi_{\theta Y, j} (\cos^2 \theta_0 \sin \psi \\
& + \gamma_0 \sin^2 \theta_0 \cos \psi) + \phi_{\theta X, j} (\cos^2 \theta_0 \cos \psi - \gamma_0 \sin^2 \theta_0 \sin \psi)] \} \Big] \beta \Big\} \\
& + \left\{ \sum_{n=1}^N \left[\int^{R-e} \text{mdr} \{ \Omega^2 [\phi_{X, j} ((a_2 - r\gamma_0) \sin \psi + (a_2 \gamma_0 + r) \cos \psi) \right. \right. \\
& + \phi_{Y, j} ((a_2 \gamma_0 + r) \sin \psi - (a_2 - r\gamma_0) \cos \psi) + \phi_{\theta Y, j} [(r(a_2 \beta_0 - b_2 \gamma_0) \\
& - b_2(a_2 \gamma_0 + r) + a_2([r+e]\beta_0 + b_2) - r^2 \beta_0) \sin \psi + (b_2(a_2 - r\gamma_0) \\
& + b_2(a_2 \gamma_0 + r) - a_2(a_2 \beta_0 - r\beta_0) + r^2 \beta_0) \cos \psi] + \phi_{\theta X, j} [(-b_2(a_2 - r\gamma_0) \\
& - b_2(a_2 \gamma_0 + r) + a_2(a_2 \beta_0 - r\beta_0) - r^2 \beta_0) \sin \psi + (r(a_2 \beta_0 - b_2 \gamma_0) - b_2(a_2 \gamma_0 + r) \\
& + a_2([r+e]\beta_0 + b_2) - r^2 \beta_0) \cos \psi]] \} \Big] \Big\}
\end{aligned}$$

$$\begin{aligned}
& + I_X dr \{ \Omega^2 q'_E (\phi_{\theta Y, j} \sin \theta_o \cos \psi - \phi_{\theta X, j} \sin \theta_o \sin \psi) + \Omega^2 [\phi_{\theta Y, j} (\beta_o \cos^2 \theta_o \cos \psi \\
& - \frac{1}{2} \sin 2 \theta_o \sin \psi) + \phi_{\theta X, j} (- \beta_o \cos^2 \theta_o \sin \psi - \frac{1}{2} \sin 2 \theta_o \cos \psi)] \} \\
& + I_Y dr \{ \Omega^2 [\phi_{\theta Y, j} (- q'_E \sin \theta_o - q'_F \cos \theta_o) \cos \psi + \phi_{\theta X, j} (q'_E \sin \theta_o \\
& + q'_F \cos \theta_o) \sin \psi - \phi_{\theta Y, j} \beta_o \cos \psi + \phi_{\theta X, j} \beta_o \sin \psi] \} \\
& + I_Z dr \{ \Omega^2 q'_F (\phi_{\theta Y, j} \cos \theta_o \cos \psi - \phi_{\theta X, j} \cos \theta_o \sin \psi) + \Omega^2 [\phi_{\theta Y, j} (\frac{1}{2} \sin 2 \theta_o \sin \psi \\
& + \beta_o \sin^2 \theta_o \cos \psi) + \phi_{\theta X, j} (\frac{1}{2} \sin 2 \theta_o \cos \psi - \beta_o \sin^2 \theta_o \sin \psi)] \} \} \\
& + \left[\sum_{n=1}^N \sum_{i=1}^{N_E} \left[\delta^{R-e} mdr \{ \Omega^2 [\phi_{X, j} (- \phi_{E, i} (\gamma_o \sin \psi - \cos \psi) - v_{1,i} \sin \psi \\
& - \phi_{F, i} \beta_o \sin \psi) + \phi_{Y, j} (\phi_{E, i} (\sin \psi + \gamma_o \cos \psi) + v_{1,i} \cos \psi + \phi_{F, i} \beta_o \cos \psi) \\
& + \phi_{\theta Y, j} ((\phi_{F, i} (a_2 \gamma_o + r + e - 2b_2 \beta_o) - \phi_{E, i} b_2 \gamma_o) \sin \psi + (- \phi_{F, i} (a_2 - r \gamma_o) \\
& + \phi_{E, i} (b_2 + r \beta_o)) \cos \psi) + \phi_{\theta X, j} ((\phi_{F, i} (a_2 - r \gamma_o) - \phi_{E, i} (b_2 + r \beta_o)) \sin \psi \\
& + (\phi_{F, i} (a_2 \gamma_o + r + e - 2b_2 \beta_o) - \phi_{E, i} b_2 \gamma_o) \cos \psi) - \phi_{\theta Y, j} v_{1,i} b_2 \sin \psi \\
& - \phi_{\theta X, j} v_{1,i} b_2 \cos \psi] \} + I_X dr \{ \Omega^2 [\phi_{\theta Y, j} (- \sin \theta_o \sin \psi - (\gamma_o \sin \theta_o \\
& - \beta_o \cos \theta_o) \cos \psi) \phi'_{E, i} + \phi_{\theta X, j} (- \sin \theta_o \cos \psi + (\gamma_o \sin \theta_o - \beta_o \cos \theta_o) \sin \psi) \phi'_{E, i}] \} \\
& + I_Y dr \{ \Omega^2 [\phi'_{E, i} (\sin \theta_o \sin \psi + (- q'_E \sin 2 \theta_o - \beta_o \cos \theta_o - q'_F \cos 2 \theta_o \\
& + \gamma_o \sin \theta_o) \cos \psi) + \phi'_{F, i} (- \cos \theta_o \sin \psi + (- q'_F \sin 2 \theta_o - \beta_o \sin \theta_o \\
& + q'_E \cos 2 \theta_o - \gamma_o \cos \theta_o) \cos \psi) + \phi_{\theta X, j} (\phi'_{E, i} (\sin \theta_o \cos \psi + (q'_E \sin 2 \theta_o \\
& + \beta_o \cos \theta_o + q'_F \cos 2 \theta_o - \gamma_o \sin \theta_o) \sin \psi) + \phi'_{F, i} (- \cos \theta_o \cos \psi + (- q'_E \cos 2 \theta_o \\
& + \beta_o \sin \theta_o + q'_F \sin 2 \theta_o + \gamma_o \cos \theta_o) \sin \psi)] \} + I_Z dr \{ \Omega^2 [\phi_{\theta Y, j} ((\cos \theta_o \sin \psi \\
& + (- q'_E \cos 2 \theta_o + \gamma_o \cos \theta_o + \beta_o \sin \theta_o) \cos \psi) \phi'_{F, i} + \phi'_{E, i} q'_F \cos 2 \theta_o \cos \psi) \\
& + \phi_{\theta X, j} ((\cos \theta_o \cos \psi + (q'_F \cos 2 \theta_o - \gamma_o \cos \theta_o - \beta_o \sin \theta_o) \sin \psi) \phi'_{F, i} \\
& - \phi'_{E, i} q'_F \cos 2 \theta_o \sin \psi)] \} \} q_{T', i} \} = 0 \quad g \quad (37)
\end{aligned}$$

Blade Pitch Equations

$$\begin{aligned}
 & \sum_{i=1}^{NA} \left[\int_0^{R-e} mdr \{ \phi_{X,i} ((b_2 \gamma_o + a_2 \beta_o) \sin \psi - b_2 \cos \psi) + \phi_{Y,i} (- (b_2 \gamma_o + a_2 \beta_o) \cos \psi - b_2 \sin \psi) + a_2 \phi_{Z,i} + \phi_{\theta Y,i} [(a_2^2 + b_2^2) \gamma_o + a_2(r + e) \sin \psi + (- a_2(a_2 - r \gamma_o) - b_2(b_2 + r \beta_o)) \cos \psi] + \phi_{\theta X,i} [(a_2(a_2 - r \gamma_o) + b_2(b_2 + r \beta_o)) \sin \psi + ((a_2^2 + b_2^2) \gamma_o + a_2(r + e) \cos \psi)] \right. \\
 & + I_X dr \{ q'_{EO} (\phi_{\theta Y,i} \cos \theta_o \sin \psi + \phi_{\theta X,i} \cos \theta_o \cos \psi) \} + I_Y dr \{ \phi_{\theta Y,i} (-q'_{EO} \cos \theta_o + q'_{FO} \sin \theta_o) \sin \psi + \phi_{\theta Y,i} (\gamma_o \sin \psi - \cos \psi) + \phi_{\theta X,i} (\gamma_o \cos \psi + \sin \psi) \} + I_Z dr \{ q'_{FO} (-\phi_{\theta Y,i} \sin \theta_o \sin \psi - \phi_{\theta X,i} \sin \theta_o \cos \psi) \} \left. \ddot{\phi}_{\theta i} \right\} \\
 & + \left\{ \left[\int_0^{R-e} mdr \{ (a_2^2 + b_2^2) \} + I_Y dr \{ l \} \right] \ddot{\phi}_\theta \ddot{\theta}_T \right\} + \left\{ M_1 L_2^2 \phi_{\theta PR}^2 \ddot{\theta}_T \right\} \\
 & + \left\{ \left[\int_0^{R-e} mdr \{ (a_2^2 + b_2^2) \gamma_o + a_2 r \} + I_X dr \{ q'_{EO} \cos \theta_o \} + I_Y dr \{ -q'_{EO} \cos \theta_o + q'_{FO} \sin \theta_o + \gamma_o \sin \theta_o + \gamma_o \} \right. \right. \\
 & + I_Z dr \{ -q'_{FO} \sin \theta_o \} \left. \ddot{\phi}_{\theta \beta} \right\} + \left\{ -M_1 L_2 \tan \delta_3 \phi_{\theta PR} \ddot{\beta} \right\} \\
 & + \left\{ \left[\int_0^{R-e} mdr \{ b_2 r \} + I_X dr \{ q'_{EO} \sin \theta_o \} + I_Y dr \{ -q'_{EO} \sin \theta_o - q'_{FO} \cos \theta_o \} + I_Z dr \{ q'_{FO} \cos \theta_o \} \right] \ddot{\phi}_{\theta \gamma} \right\} + \left\{ -M_1 L_2^2 \tan \alpha_1 \phi_{\theta PR} \ddot{\gamma} \right\} \\
 & + \left\{ \sum_{i=1}^{NE} \left[\int_0^{R-e} mdr \{ a_2 \phi_{F,i} + b_2 \phi_{E,i} \} + I_X dr \{ q'_{EO} \phi'_{F,i} \} + I_Y dr \{ -q'_{FO} \phi'_{E,i} \} + I_Z dr \{ q'_{FO} \phi'_{E,i} \} \right] \ddot{\phi}_{\theta} \ddot{a}_{T,i} \right\} + \left\{ \sum_{i=1}^{NE} (-M_1 L_2 (\phi_{FPR,i} \right. \\
 & \left. + [L_2 \tan \alpha_1 / (R-e)] \phi_{ET,i})) \phi_{\theta PR} \ddot{a}_{T,i} \right\} \\
 & + \left\{ \sum_{i=1}^{NA} \left[\int_0^{R-e} mdr \{ 2\Omega [\phi_{\theta Y,i} (a_2(a_2 - r \gamma_o) \sin \psi + a_2(a_2 \gamma_o + r + e - b_2 \beta_o) \cos \psi) + \phi_{\theta X,i} (-a_2(a_2 \gamma_o + r + e - b_2 \beta_o) \sin \psi + a_2(a_2 - r \gamma_o) \cos \psi)] \} \right. \right. \quad 10
 \end{aligned}$$

$$\begin{aligned}
& + I_X dr \{ 2\Omega q'_{EO} [\phi_{\theta Y,i} \cos \theta_0 \cos \psi - \phi_{\theta X,i} \cos \theta_0 \sin \psi] + \Omega [\phi_{\theta Y,i} (-\cos 2\theta_0 \sin \psi \\
& - (\gamma_0 \cos 2\theta_0 - \beta_0 \sin 2\theta_0) \cos \psi) + \phi_{\theta X,i} (-\cos 2\theta_0 \cos \psi + (\gamma_0 \cos 2\theta_0 \\
& - \beta_0 \sin 2\theta_0) \sin \psi)] \} + I_Y dr \{ \Omega [\phi_{\theta Y,i} (-q'_{EO} \cos \theta_0 + q'_{FO} \sin \theta_0) 2 \cos \psi \\
& + \phi_{\theta X,i} (q'_{EO} \cos \theta_0 - q'_{FO} \sin \theta_0) 2 \sin \psi + \phi_{\theta Y,i} (\gamma_0 \cos \psi + \sin \psi) + \phi_{\theta X,i} (-\gamma_0 \sin \psi \\
& + \cos \psi)] \} + I_Z dr \{ 2\Omega q'_{FO} [-\phi_{\theta Y,i} \sin \theta_0 \cos \psi + \phi_{\theta X,i} \sin \theta_0 \sin \psi] \\
& + \Omega [\phi_{\theta Y,i} (\cos 2\theta_0 \sin \psi + (\gamma_0 \cos 2\theta_0 - \beta_0 \sin 2\theta_0) \cos \psi) + \phi_{\theta X,i} (\cos 2\theta_0 \cos \psi \\
& - (\gamma_0 \cos 2\theta_0 - \beta_0 \sin 2\theta_0) \sin \psi)] \} \dot{\phi}_{\theta q_i} \left\{ (2\zeta_\theta I_T \Omega + C_1 L_2^2 \phi_{\theta PR}^2) \dot{\theta}_T \right\} \\
& + \left\{ \left[\int_0^{R-e} dr \{ 2\Omega [-b_2 (b_2 + r\beta_0)] \} + I_X dr \{ -\Omega \cos 2\theta_0 \} + I_Y dr \{ -\Omega \right. \right. \\
& \left. \left. + I_Z dr \{ \Omega \cos 2\theta_0 \} \right] \phi_{\theta \beta} \right\} + \left\{ -C_1 L_2^2 \tan \delta_3 \phi_{\theta PR} \dot{\beta} \right\} + \left\{ \left[\int_0^{R-e} dr \{ 2\Omega [a_2 (b_2 + r\beta_0)] \} \right. \right. \\
& \left. \left. + I_X dr \{ -\Omega \sin 2\theta_0 \} + I_Z dr \{ \Omega \sin 2\theta_0 \} \right] \phi_{\theta \gamma} \right\} + \left\{ -C_1 L_2^2 \tan \alpha_1 \phi_{\theta PR} \dot{\gamma} \right\} \\
& + \left\{ \sum_{i=1}^{NE} \left[\int_0^{R-e} dr \{ 2\Omega (-\phi_{F,i} b_2 \beta_0 + \phi_{E,i} a_2 \beta_0) - 2\Omega v_{1,i} b_2 \} + I_X dr \{ \Omega [-\phi'_{E,i} \sin \theta_0 \right. \right. \\
& \left. \left. - \phi'_{F,i} \cos \theta_0] \} + I_Y dr \{ \Omega [\phi'_{E,i} \sin \theta_0 - \phi'_{F,i} \cos \theta_0] \} + I_Z dr \{ \Omega [\phi'_{E,i} \sin \theta_0 \right. \right. \\
& \left. \left. + \phi'_{F,i} \cos \theta_0] \} \right] \phi_{\theta q_{T,i}} \right\} + \left\{ \sum_{i=1}^{NE} (-C_1 L_2^2 (\phi_{FPR,i} \right. \right. \\
& \left. \left. + [L_2 \tan \alpha_1 / (R-e)] \phi_{ET,i}) \phi_{\theta PR} \dot{q}_{T,i} \right\} + \left\{ \left[\int_0^{R-e} dr \{ \Omega^2 [e(a_2 \gamma_0 - b_2 \beta_0) \right. \right. \\
& \left. \left. - b_2 (b_2 + r\beta_0) + a_2^2] \} + I_X dr \{ -\Omega^2 \cos 2\theta_0 \} + I_Z dr \{ \Omega^2 \cos 2\theta_0 \} \right] \phi_{\theta T}^2 \right\} \\
& + \left\{ (\int_0^{R-e} K \phi_{\theta}^2) \theta_T \right\} + \left\{ K_1 L_2^2 \phi_{\theta PR}^2 \theta_T \right\} \\
& + \left\{ \left[\int_0^{R-e} dr \{ \Omega^2 [a_2 (a_2 \gamma_0 + r + e) - b_2 (b_2 \gamma_0 - 2a_2 \beta_0)] \} + I_X dr \{ \Omega^2 [q'_{EO} \cos \theta_0 \right. \right. \\
& \left. \left. - \gamma_0 \cos 2\theta_0] \} + I_Y dr \{ \Omega^2 (-q'_{EO} \cos \theta_0 + q'_{FO} \sin \theta_0) \} + I_Z dr \{ \Omega^2 [-q'_{FO} \sin \theta_0 \right. \right. \\
& \left. \left. + \gamma_0 \cos 2\theta_0] \} \right] \phi_{\theta \beta} \right\} + \left\{ -K_1 L_2^2 \tan \delta_3 \phi_{\theta PR} \beta \right\} + \left\{ \left[\int_0^{R-e} dr \{ \Omega^2 [- (a_2^2 + b_2^2) \beta_0 \right. \right. \\
& \left. \left. + eb_2] \} + I_X dr \{ -\Omega^2 \beta_0 \cos 2\theta_0 \} + I_Z dr \{ \Omega^2 \beta_0 \cos 2\theta_0 \} \right] \phi_{\theta \gamma} \right\} \quad 11
\end{aligned}$$

$$\begin{aligned}
& + \left\{ - K_1 L_2^2 \tan \alpha_1 \phi_{\theta PR} \gamma \right\} + \left\{ \sum_{i=1}^{NE} \left[\int_0^{R-e} dr \{ \Omega^2 [\phi_{F,i}(a_2 + e\gamma_0) - \phi_{E,i}(b_2 \right. \right. \\
& + (r + e)\beta_0)] + I_X dr \{ - \Omega^2 \beta_0 \phi'_{E,i} \cos \theta_0 \} + I_Y dr \{ \Omega^2 \beta_0 (\phi'_{E,i} \cos \theta_0 + \phi'_{F,i} \sin \theta_0) \} \\
& \left. \left. + I_Z dr \{ \Omega^2 [- \phi'_{E,i} q'_{F0} \cos 2\theta_0 + (q'_{E0} \cos 2\theta_0 - \beta_0 \sin \theta_0) \phi'_{F,i}] \} \right] \phi_{\theta} q_{T,i} \right\} \\
& + \left\{ \sum_{i=1}^{NE} (- K_1 L_2 (\phi_{FPR,i} + [L_2 \tan \alpha_1 / (R-e)] \phi_{ET,i})) \phi_{\theta PR} q_{T,i} \right\} = 0 \quad (38)
\end{aligned}$$

Blade Rigid-Body Flapping Equations

$$\begin{aligned}
 & \left\{ \sum_{i=1}^{NA} \left[\int_0^{R-e} m dr \{ \phi_{X,i} (b_2 + r\beta_0) \sin\psi - \phi_{Y,i} (b_2 + r\beta_0) \cos\psi + \phi_{Z,i} (r + a_2 \gamma_0 \right. \right. \\
 & - b_2 \beta_0) + \phi_{\theta Y,i} [(e(a_2 \gamma_0 - b_2 \beta_0) + r(r + e + 2a_2 \gamma_0) + b_2^2) \sin\psi + (-a_2(a_2 \gamma_0 \\
 & - b_2 \beta_0) - r(a_2 - r\gamma_0)) \cos\psi] + \phi_{\theta X,i} [(a_2(a_2 \gamma_0 - b_2 \beta_0) + r(a_2 - r\gamma_0)) \sin\psi \\
 & + (e(a_2 \gamma_0 - b_2 \beta_0) + r(r + e + 2a_2 \gamma_0) + b_2^2) \cos\psi] \} + I_X dr \{ q'_{EO} (\\
 & - \phi_{\theta Y,i} \cos\theta_0 \cos\psi + \phi_{\theta X,i} \cos\theta_0 \sin\psi) + \phi_{\theta Y,i} (\cos^2\theta_0 \sin\psi + (\gamma_0 \cos^2\theta_0 \\
 & - \frac{1}{2}\beta_0 \sin 2\theta_0) \cos\psi) + \phi_{\theta X,i} (\cos^2\theta_0 \cos\psi - (\gamma_0 \cos^2\theta_0 - \frac{1}{2}\beta_0 \sin 2\theta_0) \sin\psi) \} \\
 & + I_Y dr \{ \phi_{\theta Y,i} (q'_{EO} \cos\theta_0 - q'_{FO} \sin\theta_0 - \gamma_0) \cos\psi \\
 & + \phi_{\theta X,i} (-q'_{EO} \cos\theta_0 + q'_{FO} \sin\theta_0 + \gamma_0) \sin\psi \} + I_Z dr \{ q'_{FO} (\phi_{\theta Y,i} \sin\theta_0 \cos\psi \\
 & - \phi_{\theta X,i} \sin\theta_0 \sin\psi) + \phi_{\theta Y,i} (\sin^2\theta_0 \sin\psi + (\gamma_0 \sin^2\theta_0 + \frac{1}{2}\beta_0 \sin 2\theta_0) \cos\psi) \\
 & + \phi_{\theta X,i} (\sin^2\theta_0 \cos\psi - (\gamma_0 \sin^2\theta_0 + \frac{1}{2}\beta_0 \sin 2\theta_0) \sin\psi) \} \ddot{q}_i \Big\} \\
 & + \left\{ \left[\int_0^{R-e} m dr \{ ((a_2^2 + b_2^2)\gamma_0 + a_2 r) \} + I_X dr \{ q'_{EO} \cos\theta_0 \} + I_Y dr \{ -q'_{EO} \cos\theta_0 \right. \right. \\
 & \left. \left. + q'_{FO} \sin\theta_0 + \gamma_0 \} \right] \ddot{\phi}_{\theta T} \right\} + \left\{ -M_1 \frac{L^2}{2} \tan\delta_3 \dot{\phi}_{PR} \ddot{\theta}_T \right\} \\
 & + \left\{ \left[\int_0^{R-e} m dr \{ r^2 + b_2^2 + 2a_2 r\gamma_0 \} + I_X dr \{ \cos^2\theta_0 \} + I_Z dr \{ \sin^2\theta_0 \} \right] \ddot{\beta} \right\} \\
 & + \left\{ M_1 \frac{L^2}{2} \tan^2\delta_3 \ddot{\beta} \right\} + \left\{ \left[\int_0^{R-e} m dr \{ -b_2(a_2 - r\gamma_0) \} + I_X dr \{ \frac{1}{2} \sin 2\theta_0 \} \right. \right. \\
 & \left. \left. + I_Z dr \{ -\frac{1}{2} \sin 2\theta_0 \} \right] \ddot{\gamma} \right\} + \left\{ M_1 \frac{L^2}{2} \tan\delta_3 \tan\alpha_1 \ddot{\gamma} \right\} + \left\{ \sum_{i=1}^{NE} \left[\int_0^{R-e} m dr \{ \phi_{F,i} (a_2 \gamma_0 \right. \right. \\
 & \left. \left. + r) + \phi_{E,i} b_2 \gamma_0 + v_{1,i} b_2 \} + I_X dr \{ \phi'_{F,i} \cos\theta_0 \} + I_Z dr \{ -\phi'_{E,i} \sin\theta_0 \} \right] \ddot{q}_{T,i} \right\} \\
 & + \left\{ \sum_{i=1}^{NE} (M_1 \frac{L}{2} \tan\delta_3 (\phi_{FPR,i} + [L_2 \tan\alpha_1 / (R-e)] \phi_{ET,i})) \ddot{q}_{T,i} \right\} \\
 & + \left\{ \sum_{i=1}^{NA} \left[\int_0^{R-e} m dr \{ 2\Omega [\phi_{\theta Y,i} ((r(r + e + 2a_2 \gamma_0) + e(a_2 \gamma_0 - b_2 \beta_0) + b_2^2) \cos\psi \right. \right. \\
 & \left. \left. + (a_2(a_2 \gamma_0 - b_2 \beta_0) - r^2 \gamma_0) \sin\psi) + \phi_{\theta X,i} ((-r(r + e + 2a_2 \gamma_0) - e(a_2 \gamma_0) \right. \right. \\
 & \left. \left. - b_2^2) \cos\psi \right] \right\} \quad 13
 \end{aligned}$$

$$\begin{aligned}
& - b_2 \beta_0) - b_2^2 \sin \psi + (a_2 (a_2 \gamma_0 - b_2 \beta_0) - r^2 \gamma_0) \cos \psi)] \} \\
& + I_X dr \{ 2 \Omega q'_{EO} (\phi_{\theta Y,i} \cos \theta_0 \sin \psi + \phi_{\theta X,i} \cos \theta_0 \cos \psi) \\
& + \Omega [\phi_{\theta Y,i} (\cos \psi - 2 (\gamma_0 \cos^2 \theta_0 - \frac{1}{2} \beta_0 \sin 2 \theta_0) \sin \psi) + \phi_{\theta X,i} (- \sin \psi - 2 (\gamma_0 \cos^2 \theta_0 \\
& - \frac{1}{2} \beta_0 \sin 2 \theta_0) \cos \psi)] \} + I_Y dr \{ \Omega [\phi_{\theta Y,i} (- q'_{EO} \cos \theta_0 + q'_{FO} \sin \theta_0) 2 \sin \psi \\
& + \phi_{\theta X,i} (- q'_{EO} \cos \theta_0 + q'_{FO} \sin \theta_0) 2 \cos \psi \\
& + \phi_{\theta Y,i} (2 \gamma_0 \sin \psi - \cos \psi) + \phi_{\theta X,i} (2 \gamma_0 \cos \psi + \sin \psi)] \} + I_Z dr \{ 2 \Omega q'_{FO} [\\
& - \phi_{\theta Y,i} \sin \theta_0 \sin \psi - \phi_{\theta X,i} \sin \theta_0 \cos \psi] + \Omega [\phi_{\theta Y,i} (\cos \psi - (2 \gamma_0 \sin^2 \theta_0 \\
& + \beta_0 \sin 2 \theta_0) \sin \psi) + \phi_{\theta X,i} (- \sin \psi - (2 \gamma_0 \sin^2 \theta_0 + \beta_0 \sin 2 \theta_0) \cos \psi)] \} \dot{q}_i \} \\
& + \left\{ \left[\int_0^{R-e} m dr \{ 2 \Omega b_2 (b_2 + r \beta_0) \} + I_X dr \{ \Omega \cos 2 \theta_0 \} + I_Y dr \{ \Omega \} + I_Z dr \{ - \Omega \cos 2 \theta_0 \} \right] \phi_{\theta T} \dot{\theta}_T \right\} \\
& + \left\{ - C_1 L_2^2 \tan \delta_3 \phi_{\theta PR} \dot{\theta}_T \right\} + \left\{ C_1 L_2^2 \tan^2 \delta_3 \dot{\beta} \right\} + \left\{ \int_0^{R-e} m dr \{ 2 \Omega (b_2 (a_2 \gamma_0 + r) \\
& + r^2 \beta_0) \} + I_X dr \{ \Omega (2 q'_{EO} \sin \theta_0 + \beta_0 - \gamma_0 \sin 2 \theta_0) \} + I_Y dr \{ \Omega (- 2 q'_{EO} \sin \theta_0 \\
& - 2 q'_{FO} \cos \theta_0 - \beta_0) \} + I_Z dr \{ \Omega (2 q'_{FO} \cos \theta_0 + \gamma_0 \sin 2 \theta_0 + \beta_0) \} \right\} \dot{r} \} \\
& + \left\{ C_1 L_2^2 \tan \delta_3 \tan \alpha_1 \dot{r} \right\} + \sum_{i=1}^{NE} \left[\int_0^{R-e} m dr \{ 2 \Omega [\phi_{E,i} (b_2 + r \beta_0)] \} \right. \\
& + I_X dr \{ \Omega [\phi'_{E,i} (q'_{EO} \sin 2 \theta_0 + \beta_0 \cos \theta_0 - \gamma_0 \sin \theta_0) + \phi'_{F,i} (q'_{EO} + \beta_0 \sin \theta_0 \\
& - \gamma_0 \cos \theta_0)] \} + I_Y dr \{ \Omega [\phi'_{E,i} (- q'_{EO} \sin 2 \theta_0 - 2 q'_{FO} \cos^2 \theta_0 + \gamma_0 \sin \theta_0 - \beta_0 \cos \theta_0) \\
& + \phi'_{F,i} (q'_{EO} \cos 2 \theta_0 - q'_{FO} \sin 2 \theta_0 - \gamma_0 \cos \theta_0 - \beta_0 \sin \theta_0)] \} \\
& + I_Z dr \{ \Omega [\phi'_{E,i} (2 q'_{FO} \cos^2 \theta_0 + \gamma_0 \sin \theta_0 + \beta_0 \cos \theta_0) + \phi'_{F,i} (q'_{FO} \sin 2 \theta_0 + \gamma_0 \cos \theta_0 \\
& + \beta_0 \sin \theta_0)] \} \dot{q}_{T,i} \} + \left\{ \sum_{i=1}^{NE} (C_1 L_2^2 \tan \delta_3 (\phi_{FPR,i} + [L_2 \tan \alpha_1 / (R-e)] \phi_{ET,i})) \dot{q}_{T,i} \right\} \\
& + \left\{ \sum_{i=1}^{NA} \left[\int_0^{R-e} m dr \{ \Omega^2 [\phi_{\theta Y,i} (- b_2 (b_2 + 2r\beta_0)) \cos \psi + \phi_{\theta X,i} (b_2 (b_2 + 2r\beta_0)) \sin \psi] \} \right] \dot{q}_i \right\} \\
& + \left\{ \int_0^{R-e} m dr \{ \Omega^2 [a_2 (a_2 \gamma_0 + r + e) - b_2 (b_2 \gamma_0 - 2a_2 \beta_0)] \} + I_X dr \{ \Omega^2 [q'_{EO} \cos \theta_0 \\
& - \gamma_0 \cos 2 \theta_0 + \beta_0 \sin 2 \theta_0] \} + I_Y dr \{ \Omega^2 [- q'_{EO} \cos \theta_0 - q'_{FO} \sin \theta_0] \} + I_Z dr \{ \Omega^2 [q'_{FO} \sin \theta_0 \right. \\
& \left. - \gamma_0 \cos 2 \theta_0 - \beta_0 \sin 2 \theta_0] \} \right\} \quad 14
\end{aligned}$$

$$\begin{aligned}
& \left. + \gamma_0 \cos 2\theta_0 - \beta_0 \sin 2\theta_0 \right] \phi_{\theta T} \right\} + \left\{ - K_1 L_2^2 \tan \delta_3 \phi_{\theta PR} \theta_T \right\} \\
& + \left\{ \left[\int^{R-e}_{0} dr \{ \Omega^2 [e(a_2 \gamma_0 - b_2 \beta_0) + r(r+e) - 4r\beta_0 b_2 + 2a_2 r \gamma_0 - b_2^2] \} \right. \right. \\
& + I_X dr \{ \Omega^2 \sin^2 \theta_0 \} + I_Y dr \{ -\Omega^2 \} + I_Z dr \{ \Omega^2 \cos^2 \theta_0 \} \left. \right] \beta \left. \right\} + \left\{ K_1 L_2^2 \tan^2 \delta_3 \beta \right\} \\
& + \left\{ K_B \beta \right\} + \left\{ \left[\int^{R-e}_{0} dr \{ \Omega^2 [b_2 (a_2 - r \gamma_0) + a_2 \beta_0 (2r + e)] \} + I_X dr \{ \right. \right. \\
& \left. \left. - \frac{1}{2} \Omega^2 \sin 2\theta_0 \} + I_Z dr \{ \frac{1}{2} \Omega^2 \sin 2\theta_0 \} \right] \gamma \right\} + \left\{ K_1 L_2^2 \tan \delta_3 \tan \alpha_1 \gamma \right\} \\
& + \left\{ \sum_{i=1}^{NE} \left[\int^{R-e}_{0} dr \{ \Omega^2 [-\phi_{E,i} b_2 \gamma_0 + \phi_{F,i} (a_2 \gamma_0 + r + e + 2b_2 \beta_0) - v_{1,i} b_2] \} \right. \right. \\
& + I_X dr \{ -\Omega^2 \phi'_{E,i} \sin \theta_0 \} + I_Y dr \{ \Omega^2 [\phi'_{E,i} \sin \theta_0 + \phi'_{F,i} \cos \theta_0] \} \\
& + I_Z dr \{ -\Omega^2 [\phi'_{F,i} \cos \theta_0] \} \left. \right] q_{T,i} \left. \right\} + \left\{ \sum_{i=1}^{NE} (K_1 L_2 \tan \delta_3 (\phi_{FPR,i} \right. \\
& \left. + [L_2 \tan \alpha_1 / (R-e)] \phi_{ET,i})) q_{T,i} \right\} = 0 \quad 15
\end{aligned} \tag{39}$$

Blade Rigid-Body Lagging Equations

16

$$\begin{aligned}
 & \left\{ \sum_{i=1}^{NA} \left[\int_0^{R-e} m dr \{ \dot{\phi}_{X,i} (- (a_2 - r\gamma_0) \sin\psi - (a_2 \gamma_0 + r) \cos\psi) + \dot{\phi}_{Y,i} (- (a_2 \gamma_0 + r) \sin\psi \right. \right. \\
 & + (a_2 - r\gamma_0) \cos\psi) + \dot{\phi}_{Z,i} a_2 \beta_0 + \dot{\phi}_{\theta Y,i} (([e\beta_0 - b_2] (a_2 - r\gamma_0)) \sin\psi \\
 & + (- b_2 (a_2 \gamma_0 + r) - (a_2^2 + r^2) \beta_0) \cos\psi) + \dot{\phi}_{\theta X,i} ((b_2 (a_2 \gamma_0 + r) + (a_2^2 \\
 & + r^2) \beta_0) \sin\psi + ([e\beta_0 - b_2] (a_2 - r\gamma_0)) \cos\psi) \} + I_X dr \{ q'_{EO} (- \dot{\phi}_{\theta Y,i} \sin\theta_0 \cos\psi \\
 & + \dot{\phi}_{\theta X,i} \sin\theta_0 \sin\psi) + \dot{\phi}_{\theta Y,i} (\frac{1}{2} \sin 2\theta_0 \sin\psi + (\frac{1}{2} \gamma_0 \sin 2\theta_0 - \beta_0 \sin^2 \theta_0) \cos\psi) \\
 & + \dot{\phi}_{\theta X,i} (\frac{1}{2} \sin 2\theta_0 \cos\psi - (\frac{1}{2} \gamma_0 \sin 2\theta_0 - \beta_0 \sin^2 \theta_0) \sin\psi) \} + I_Y dr \{ \dot{\phi}_{\theta Y,i} (q'_{EO} \sin\theta_0 \\
 & + q'_{FO} \cos\theta_0) \cos\psi + \dot{\phi}_{\theta X,i} (- q'_{EO} \sin\theta_0 - q'_{FO} \cos\theta_0) \sin\psi \} + I_Z dr \{ q'_{FO} \\
 & - \dot{\phi}_{\theta Y,i} \cos\theta_0 \cos\psi + \dot{\phi}_{\theta X,i} \cos\theta_0 \sin\psi \} + \dot{\phi}_{\theta Y,i} (- \frac{1}{2} \sin 2\theta_0 \sin\psi - (\frac{1}{2} \gamma_0 \sin 2\theta_0 \\
 & + \beta_0 \cos^2 \theta_0) \cos\psi) + \dot{\phi}_{\theta X,i} (- \frac{1}{2} \sin 2\theta_0 \cos\psi + (\frac{1}{2} \gamma_0 \sin 2\theta_0 + \beta_0 \cos^2 \theta_0) \sin\psi) \} \dot{\bar{q}}_i \Bigg\} \\
 & + \left\{ \left[\int_0^{R-e} m dr \{ b_2 r \} + I_X dr \{ q'_{EO} \sin\theta_0 \} + I_Y dr \{ - q'_{EO} \sin\theta_0 - q'_{FO} \cos\theta_0 \} \right. \right. \\
 & + I_Z dr \{ q'_{FO} \cos\theta_0 \} \Big] \ddot{\phi}_{\theta T} \Big\} + \left\{ - M_1 L_2^2 \tan \alpha_1 \ddot{\phi}_{\theta PR} \right\} + \left\{ \left[\int_0^{R-e} m dr \{ - b_2 (a_2 \right. \right. \\
 & - r\gamma_0) \} + I_X dr \{ \frac{1}{2} \sin 2\theta_0 \} + I_Z dr \{ - \frac{1}{2} \sin 2\theta_0 \} \Big] \ddot{\beta} \Big\} + \left\{ M_1 L_2^2 \tan \delta_3 \tan \alpha_1 \ddot{\beta} \right\} \\
 & + \left\{ \left[\int_0^{R-e} m dr \{ a_2^2 + r^2 \} + I_X dr \{ \sin^2 \theta_0 \} + I_Z dr \{ \cos^2 \theta_0 \} \right] \ddot{\gamma} \right\} \\
 & + \left\{ M_1 L_2^2 \tan^2 \alpha_1 \ddot{\gamma} \right\} + \left\{ \sum_{i=1}^{NE} \left[\int_0^{R-e} m dr \{ \dot{\phi}_{E,i} r - a_2 v_{1,i} \} + I_X dr \{ \dot{\phi}'_{F,i} \sin\theta_0 \} \right. \right. \\
 & + I_Z dr \{ \dot{\phi}'_{E,i} \cos\theta_0 \} \Big] \ddot{q}_{T,i} \Big\} + \left\{ \sum_{i=1}^{NE} (M_1 L_2 \tan \alpha_1 (\dot{\phi}_{FPR,i} \right. \\
 & + [L_2 \tan \alpha_1 / (R-e)] \dot{\phi}_{ET,i}) \ddot{q}_{T,i} \Big\} + \left\{ \sum_{i=1}^{NA} \left[\int_0^{R-e} m dr \{ 2\Omega [\dot{\phi}_{\theta Y,i} (a_2^2 \beta_0 \sin\psi \right. \right. \\
 & + (r + e) a_2 \beta_0 \cos\psi) + \dot{\phi}_{\theta X,i} (-(r + e) a_2 \beta_0 \sin\psi + a_2^2 \beta_0 \cos\psi)] \} \\
 & + I_X dr \{ \Omega [- \dot{\phi}_{\theta Y,i} \beta_0 \cos 2\theta_0 \sin\psi - \dot{\phi}_{\theta X,i} \beta_0 \cos 2\theta_0 \cos\psi] \} + I_Y dr \{ \Omega \beta_0 (\dot{\phi}_{\theta Y,i} \sin\psi \\
 & + \dot{\phi}_{\theta X,i} \cos\psi) \} + I_Z dr \{ \Omega \beta_0 (\dot{\phi}_{\theta Y,i} \cos 2\theta_0 \sin\psi + \dot{\phi}_{\theta X,i} \cos 2\theta_0 \cos\psi) \} \} \dot{\bar{q}}_i \Bigg\} \\
 & + \left\{ \left[\int_0^{R-e} m dr \{ - 2\Omega a_2 (b_2 + r\beta_0) \} + I_X dr \{ \Omega \sin 2\theta_0 \} + I_Z dr \{ - \Omega \sin 2\theta_0 \} \right] \dot{\phi}_{\theta T} \right\}
 \end{aligned}$$

$$\begin{aligned}
& + \left\{ - C_1 L_2^2 \tan \alpha_1 \dot{\phi}_\theta \dot{\theta}_T \right\} \\
& + \left\{ \int_0^{R-e} dr \left[- 2\Omega(r^2 \beta_o + b_2(a_2 \gamma_o + r)) \right] + I_X dr \left[\Omega(-2q'_{E0} \sin \theta_o + \gamma_o \sin 2\theta_o \right. \right. \\
& \left. \left. - \beta_o) \right] + I_Y dr \left[\Omega \beta_o \right] + I_Z dr \left[\Omega(-2q'_{F0} \cos \theta_o - \gamma_o \sin 2\theta_o - \beta_o) \right] \right\} \dot{\beta} \\
& + \left\{ C_1 L_2^2 \tan \delta_3 \tan \alpha_1 \dot{\beta} \right\} + \left\{ (2\zeta_Y \omega_Y + C_1 L_2^2 \tan^2 \alpha_1) \dot{\gamma} \right\} \\
& + \sum_{i=1}^{NE} \left[\int_0^{R-e} dr \left[- 2\Omega(a_2 \phi_{E,i} + r \beta_o \phi_{F,i}) - 2\Omega r v_{1,i} \right] + I_X dr \left[\Omega[\phi'_{E,i} (2q'_{E0} \sin^2 \theta_o \right. \right. \\
& \left. \left. + \beta_o \sin \theta_o) - \phi'_{F,i} \beta_o \cos \theta_o] \right] + I_Y dr \left[\Omega[\phi'_{E,i} (-2q'_{E0} \sin^2 \theta_o - q'_{F0} \sin 2\theta_o \right. \right. \\
& \left. \left. - \beta_o \sin \theta_o) + \phi'_{F,i} (q'_{E0} \sin 2\theta_o + 2q'_{F0} \cos^2 \theta_o + \beta_o \cos \theta_o)] \right] \right. \\
& \left. + I_Z dr \left[\Omega[\phi'_{E,i} (q'_{F0} \sin 2\theta_o + \beta_o \sin \theta_o) + \phi'_{F,i} (-2q'_{F0} \cos^2 \theta_o \right. \right. \\
& \left. \left. - \beta_o \cos \theta_o)] \right] \dot{q}_{T,i} \right\} + \left\{ \sum_{i=1}^{NE} (C_1 L_2 \tan \alpha_1 (\phi_{FPR,i} + [L_2 \tan \alpha_1 / (R-e)] \phi_{ET,i})) \dot{q}_{T,i} \right\} \\
& + \left\{ \sum_{i=1}^{NA} \left[\int_0^{R-e} dr \left[\Omega^2 [\phi_{\theta Y,i} ((-b_2(a_2 \gamma_o + r) - r^2 \beta_o) \sin \psi + (b_2(a_2 - r \gamma_o) \right. \right. \\
& \left. \left. + a_2 r \beta_o) \cos \psi) + \phi_{\theta X,i} ((-b_2(a_2 - r \gamma_o) - a_2 r \beta_o) \sin \psi + (-b_2(a_2 \gamma_o + r) \right. \right. \\
& \left. \left. - r^2 \beta_o) \cos \psi)] \right] \bar{q}_i \right\} + \left\{ \int_0^{R-e} dr \left[\Omega^2 [- (b_2^2 + a_2^2) \beta_o + e b_2] \right] + I_X dr \left[\right. \right. \\
& \left. \left. - \Omega^2 \beta_o \cos 2\theta_o \right] + I_Z dr \left[\Omega^2 \beta_o \cos 2\theta_o \right] \right\} \dot{\phi}_\theta \dot{\theta}_T \right\} + \left\{ - K_1 L_2^2 \tan \alpha_1 \dot{\phi}_\theta \dot{\theta}_{PR} \right\} \\
& + \left\{ \int_0^{R-e} dr \left[\Omega^2 [b_2(a_2 - r \gamma_o) + a_2 \beta_o (2r + e)] \right] + I_X dr \left[- \frac{1}{2} \Omega^2 \sin 2\theta_o \right] \right. \\
& \left. + I_Z dr \left[\frac{1}{2} \Omega^2 \sin 2\theta_o \right] \right\} \dot{\beta} + \left\{ K_1 L_2^2 \tan \delta_3 \tan \alpha_1 \dot{\beta} \right\} + \left\{ \int_0^{R-e} dr \left[\Omega^2 [e(r - a_2 \gamma_o) \right. \right. \\
& \left. \left. - b_2 r \beta_o] \right] + I_Z dr \left[- \Omega^2 \beta_o \sin^2 \theta_o \right] \right\} \dot{\gamma} + \left\{ K_1 L_2^2 \tan^2 \alpha_1 \dot{\gamma} \right\} + \left\{ K_Y \dot{\gamma} \right\} \\
& + \left\{ \sum_{i=1}^{NE} \int_0^{R-e} dr \left[\Omega^2 [- \phi_{E,i} (b_2 \beta_o - e) - a_2 \beta_o \phi_{F,i}] \right] q_{T,i} \right\} \\
& + \left\{ \sum_{i=1}^{NE} (K_1 L_2 \tan \alpha_1 (\phi_{FPR,i} + [L_2 \tan \alpha_1 / (R-e)] \phi_{ET,i})) q_{T,i} \right\} = 0 \quad (40)
\end{aligned}$$

Blade Bending Equations

$$\begin{aligned}
& - \beta_o \sin \theta_o \sin \psi) + \phi_{\theta X, i} (- \cos \theta_o \sin \psi - (\gamma_o \cos \theta_o - q'_{EO} - \beta_o \sin \theta_o) \cos \psi)) \\
& + \phi'_{E, j} (\phi_{\theta Y, i} (- \sin \theta_o \cos \psi + (\gamma_o \sin \theta_o - \beta_o \cos \theta_o - q'_{EO} \sin 2\theta_o) \sin \psi)) \\
& + \phi_{\theta X, i} (\sin \theta_o \sin \psi + (\gamma_o \sin \theta_o - \beta_o \cos \theta_o - q'_{EO} \sin 2\theta_o) \cos \psi)) \} \\
& + I_Y dr \{ \Omega [\phi'_{E, j} (\phi_{\theta Y, i} (\sin \theta_o \cos \psi + (q'_{EO} \sin 2\theta_o - 2q'_{FO} \sin^2 \theta_o \\
& + \beta_o \cos \theta_o - \gamma_o \sin \theta_o) \sin \psi) + \phi_{\theta X, i} (- \sin \theta_o \sin \psi + (q'_{EO} \sin 2\theta_o - 2q'_{FO} \sin^2 \theta_o \\
& + \beta_o \cos \theta_o - \gamma_o \sin \theta_o) \cos \psi)) + \phi'_{F, j} (\phi_{\theta Y, i} (- \cos \theta_o \cos \psi + (- q'_{EO} \cos 2\theta_o \\
& + q'_{FO} \sin 2\theta_o + \beta_o \sin \theta_o + \gamma_o \cos \theta_o) \sin \psi) + \phi_{\theta X, i} (\cos \theta_o \sin \psi + (- q'_{EO} \cos 2\theta_o \\
& + q'_{FO} \sin 2\theta_o + \beta_o \sin \theta_o + \gamma_o \cos \theta_o) \cos \psi)) \} + I_Z dr \{ \Omega [\phi'_{F, j} (\phi_{\theta Y, i} (\cos \theta_o \cos \psi \\
& - (q'_{FO} \sin 2\theta_o - q'_{EO} \cos 2\theta_o + \gamma_o \cos \theta_o + \beta_o \sin \theta_o) \sin \psi) + \phi_{\theta X, i} (- \cos \theta_o \sin \psi \\
& - (q'_{FO} \sin 2\theta_o - q'_{EO} \cos 2\theta_o + \gamma_o \cos \theta_o + \beta_o \sin \theta_o) \cos \psi)) + \phi'_{E, j} ((- \sin \theta_o \cos \psi \\
& + (2q'_{FO} \sin^2 \theta_o + \gamma_o \sin \theta_o + \beta_o \cos \theta_o) \sin \psi) \phi_{\theta Y, i} + \phi_{\theta X, i} (\sin \theta_o \sin \psi \\
& + (2q'_{FO} \sin^2 \theta_o + \gamma_o \sin \theta_o + \beta_o \cos \theta_o) \cos \psi)) \} \} \dot{q}_1 \} + \left\{ \int_0^{R-e} m dr \{ 2\Omega (\phi_{F, j} b_2 \beta_o \right. \\
& \left. - \phi_{E, j} a_2 \beta_o) + 2\Omega v_{1, j} b_2 \} + I_X dr \{ \Omega (\phi'_{F, j} \cos \theta_o + \phi'_{E, j} \sin \theta_o) \} \right. \\
& \left. + I_Y dr \{ \Omega (- \phi'_{E, j} \sin \theta_o + \phi'_{F, j} \cos \theta_o) \} + I_Z dr \{ \Omega \right. \\
& \left. - \phi'_{E, j} \sin \theta_o - \phi'_{F, j} \cos \theta_o) \} \} \dot{\phi}_{\theta T} \} \} + \left\{ - C_1 L_2 \phi_{\theta PR} (\phi_{FPR, j} \right. \\
& \left. + [L_2 \tan \alpha_1 / (R-e)] \phi_{ET, j}) \right. \dot{\theta}_T \} + \left\{ \int_0^{R-e} m dr \{ - 2\Omega \phi_{E, j} (b_2 + r \beta_o) \} \right. \\
& \left. + I_X dr \{ \Omega [\phi'_{F, j} (\gamma_o \cos \theta_o - \beta_o \sin \theta_o - q'_{EO}) + \phi'_{E, j} (\gamma_o \sin \theta_o - \beta_o \cos \theta_o \right. \\
& \left. - q'_{EO} \sin 2\theta_o) \} \} + I_Y dr \{ \Omega [\phi'_{E, j} (q'_{EO} \sin 2\theta_o + 2q'_{FO} \cos^2 \theta_o - \gamma_o \sin \theta_o \\
& + \beta_o \cos \theta_o) + \phi'_{F, j} (- q'_{EO} \cos 2\theta_o + q'_{FO} \sin 2\theta_o + \gamma_o \cos \theta_o + \beta_o \sin \theta_o) \} \} \\
& + I_Z dr \{ \Omega [\phi'_{E, j} (- 2q'_{FO} \cos^2 \theta_o - \gamma_o \sin \theta_o - \beta_o \cos \theta_o) + \phi'_{F, j} (- q'_{FO} \sin 2\theta_o \quad 19
\end{aligned}$$

$$\begin{aligned}
& + q'_{EO} \cos 2\theta_0 - \gamma_0 \cos \theta_0 - \beta_0 \sin \theta_0) \} \} \dot{\phi}_{FPR,j} \\
& + [L_2 \tan \alpha_1 / (R-e)] \phi_{ET,j} \dot{\phi}_{FPR,j} \left\{ + \left\{ \int^{R-e} \text{mdr} \{ 2\Omega (a_2 \phi_{E,j} + r \beta_0 \phi_{F,j} + v_{1,j} r) \} \right. \right. \\
& + I_X^d r \{ \Omega [\phi'_{F,j} \beta_0 \cos \theta_0 - \phi'_{E,j} (\beta_0 \sin \theta_0 + 2q'_{EO} \sin^2 \theta_0)] \} \\
& + I_Y^d r \{ \Omega [\phi'_{E,j} (2q'_{EO} \sin^2 \theta_0 + q'_{FO} \sin 2\theta_0 + \beta_0 \sin \theta_0) + \phi'_{F,j} (-q'_{EO} \sin 2\theta_0 \\
& - 2q'_{FO} \cos^2 \theta_0 - \beta_0 \cos \theta_0)] \} + I_Z^d r \{ \Omega [\phi'_{E,j} (-q'_{FO} \sin 2\theta_0 - \beta_0 \sin \theta_0) \\
& + \phi'_{F,j} (2q'_{FO} \cos^2 \theta_0 + q'_{EO} \sin 2\theta_0 + \beta_0 \cos \theta_0)] \} \dot{\gamma} \left\{ + \left\{ C_1 L_2 \tan \alpha_1 (\phi_{FPR,j} \right. \right. \\
& + [L_2 \tan \alpha_1 / (R-e)] \phi_{ET,j} \dot{\gamma} \left\{ \sum_{i=1}^{NE} \left[\int^{R-e} \text{mdr} \{ 2\Omega (v_{1,j} \phi_{E,i} - v_{1,i} \phi_{E,j} \right. \right. \\
& + \beta_0 (\phi_{F,j} \phi_{E,i} - \phi_{F,i} \phi_{E,j})] \} + I_X^d r \{ \Omega (\beta_0 \\
& + q'_{EO} \sin \theta_0) (\phi'_{F,j} \phi'_{E,i} - \phi'_{E,j} \phi'_{F,i}) \} \\
& + I_Y^d r \{ \Omega (q'_{EO} \sin \theta_0 + 2q'_{FO} \cos \theta_0 + \beta_0) (\phi'_{E,j} \phi'_{F,i} - \phi'_{F,j} \phi'_{E,i}) \} \\
& + I_Z^d r \{ \Omega (q'_{EO} \sin \theta_0 - 2q'_{FO} \cos \theta_0 - \beta_0) (-\phi'_{F,j} \phi'_{E,i} + \phi'_{E,j} \phi'_{F,i}) \} \dot{q}_{T,i} \left\{ \right. \\
& + \left\{ C_1 (\phi_{FPR,j} + [L_2 \tan \alpha_1 / (R-e)] \phi_{ET,j}) \sum_{i=1}^{NE} (\phi_{FPR,i} \right. \\
& + [L_2 \tan \alpha_1 / (R-e)] \phi_{ET,i}) \dot{q}_{T,i} \left\{ + \left\{ 2\zeta_{q,j} M_{q,j} \omega_{q,j} \dot{q}_{T,j} \right\} \right. \\
& + \left\{ \left[\int^{R-e} \text{mdr} \{ \Omega^2 [\phi_{F,j} (a_2 + e \gamma_0) - \phi_{E,j} (\beta_0 (r + e) + b_2)] \} \right. \right. \\
& + I_X^d r \{ -\Omega^2 \phi'_{E,j} (q'_{EO} \sin 2\theta_0 + \beta_0 \cos \theta_0) \} + I_Y^d r \{ \Omega^2 [\phi'_{E,j} (q'_{EO} \sin 2\theta_0 \\
& + q'_{FO} \cos 2\theta_0 + \beta_0 \cos \theta_0) + \phi'_{F,j} (-q'_{EO} \cos 2\theta_0 + q'_{FO} \sin 2\theta_0 + \beta_0 \sin \theta_0)] \} \\
& + I_Z^d r \{ \Omega^2 [-\phi'_{E,j} q'_{FO} \cos 2\theta_0 + \phi'_{F,j} (-q'_{FO} \sin 2\theta_0 + q'_{EO} \cos 2\theta_0 \\
& - \beta_0 \sin \theta_0)] \} \dot{\phi}_{FPR,j} \left\{ + \left\{ -K_1 L_2 \phi_{FPR,j} + [L_2 \tan \alpha_1 / (R-e)] \phi_{ET,j} \right\} \theta_T \right\} \\
& + \left\{ \left[\int^{R-e} \text{mdr} \{ \Omega^2 [-\phi_{E,j} b_2 \gamma_0 + \phi_{F,j} (a_2 \gamma_0 + r + e + 2b_2 \beta_0) - v_{1,j} b_2] \} \right. \right. \\
& + I_X^d r \{ -\Omega^2 \phi'_{E,j} \sin \theta_0 \} + I_Y^d r \{ \Omega^2 (\phi'_{E,j} \sin \theta_0 - \phi'_{F,j} \cos \theta_0) \} \quad 20
\end{aligned}$$

$$\begin{aligned}
& + I_Z dr \{ \Omega^2 \phi_{F,j}^l \cos \theta_0 \} \Big] \beta \Big\} + \Big\{ K_1 L_2 \tan \delta_3 (\phi_{FPR,j} + [L_2 \tan \alpha_1 / (R-e)] \phi_{ET,j}) \beta \Big\} \\
& + \Big\{ \left[\int_0^{R-e} mdr \{ \Omega^2 [- \phi_{E,j} (b_2 \beta_0 - e) - \phi_{F,j} a_2 \beta_0] \} \right] \gamma \Big\} + \Big\{ K_1 L_2 \tan \alpha_1 (\phi_{FPR,j} \\
& + [L_2 \tan \alpha_1 / (R-e)] \phi_{ET,j}) \gamma \Big\} + \Big\{ \sum_{i=1}^{NE} \left[\int_0^{R-e} mdr \{ - \Omega^2 b_2 \beta_0 v_{2,i,j} \} \right. \\
& + I_X dr \{ \Omega^2 \sin^2 \theta_0 \phi'_{E,j} \phi'_{E,i} \} + I_Y dr \{ \Omega^2 [\phi'_{E,j} (- \phi'_{E,i} \sin^2 \theta_0 + \frac{1}{2} \phi'_{F,i} \sin 2 \theta_0) \\
& + \phi'_{F,j} (\frac{1}{2} \phi'_{E,i} \sin 2 \theta_0 - \phi'_{F,i} \cos^2 \theta_0)] \} + I_Z dr \{ \Omega^2 [- \frac{1}{2} \phi'_{E,j} \phi'_{F,i} \sin 2 \theta_0 \\
& + \phi'_{F,j} (- \frac{1}{2} \phi'_{E,i} \sin 2 \theta_0 + \phi'_{F,i} \cos^2 \theta_0)] \} q_{T,i} \Big\} + \Big\{ K_1 (\phi_{FPR,j} \\
& + [L_2 \tan \alpha_1 / (R-e)] \phi_{ET,j}) \sum_{i=1}^{NE} (\phi_{FPR,i} + [L_2 \tan \alpha_1 / (R-e)] \phi_{ET,i}) q_{T,i} \Big\} \\
& + \Big\{ \omega^2 q_{j,M} q_{j,T} \Big\} = 0 \quad 21 \quad (41)
\end{aligned}$$

$$dT = \frac{1}{2} \rho c U [C_L U_T - C_D U_P]$$

$$dH = \frac{1}{2} \rho c U [C_L U_P + C_D U_T]$$

$$dM = \frac{1}{2} \rho c^2 U^2 C_M$$

$$t_1 = \frac{\partial (dT)}{\partial U_T} = \frac{1}{2} \rho c^1 / U [C_L (U^2 + U_T^2) - C_D U_T U_P + C_{L,\alpha} U_T U_P$$

$$- C_{D,\alpha} U_P^2] + \frac{1}{2} \rho c^1 / v [C_{L,M} U_T^2 - C_{D,M} U_T U_P]$$

$$t_2 = \frac{\partial (dT)}{\partial U_P} = \frac{1}{2} \rho c^1 / U [C_L U_T U_P - C_D (U^2 + U_P^2) - C_{L,\alpha} U_T^2$$

$$+ C_{D,\alpha} U_T U_P] + \frac{1}{2} \rho c^1 / v [C_{L,M} U_T U_P - C_{D,M} U_P^2]$$

$$t_3 = \frac{\partial (dT)}{\partial \alpha} = \frac{1}{2} \rho c U [C_{L,\alpha} U_T - C_{D,\alpha} U_P]$$

$$h_1 = \frac{\partial (dH)}{\partial U_T} = \frac{1}{2} \rho c^1 / U [C_L U_T U_P + C_D (U^2 + U_T^2) + C_{L,\alpha} U_P^2$$

$$+ C_{D,\alpha} U_T U_P] + \frac{1}{2} \rho c^1 / v [C_{L,M} U_T U_P + C_{D,M} U_T^2]$$

$$h_2 = \frac{\partial (dH)}{\partial U_P} = \frac{1}{2} \rho c^1 / U [C_L (U^2 + U_P^2) + C_D U_T U_P - C_{L,\alpha} U_T U_P$$

$$- C_{D,\alpha} U_T^2] + \frac{1}{2} \rho c^1 / v [C_{L,M} U_P^2 + C_{D,M} U_T U_P]$$

$$h_3 = \frac{\partial (dH)}{\partial \alpha} = \frac{1}{2} \rho c U [C_{L,\alpha} U_P + C_{D,\alpha} U_T]$$

$$m_1 = \frac{\partial (dM)}{\partial U_T} = \frac{1}{2} \rho c^2 [C_M^2 U_T + C_{M,\alpha} U_P]$$

$$+ \frac{1}{2} \rho c^{21} / v C_{M,M} U_T U$$

$$m_2 = \frac{\partial (dM)}{\partial U_P} = \frac{1}{2} \rho c^2 [C_M^2 U_P - C_{M,\alpha} U_T]$$

$$+ \frac{1}{2} \rho c^{21} / v C_{M,M} U_P U$$

$$m_3 = \frac{\partial (dM)}{\partial \alpha} = \frac{1}{2} \rho c^2 C_{M,\alpha} U^2$$

23

$$\begin{aligned}
\delta U_T &= \frac{\partial U_T}{\partial q} + \frac{\partial U_T}{\partial \dot{q}} \\
&= \sum_{i=1}^{NA} \{ \phi_{\theta Y, i} (U_P \cos \psi - U_P [\gamma_o - q'_{EO}] \sin \psi) \\
&\quad - \phi_{\theta X, i} (U_P [\gamma_o - q'_{EO}] \cos \psi + U_P \sin \psi) \} \bar{q}_i \\
&\quad - \{ \Omega (a \beta_o + b q'_{EO}) \} \phi_{\theta T} \\
&\quad - \{ \Omega (b + r \beta_o) + U_P (\gamma_o - q'_{EO}) \} \beta \\
&\quad - \{ \Omega e (\gamma_o - q'_{EO}) + U_P \beta_o \} \gamma \\
&\quad + \sum_{i=1}^{NE} \{ \Omega [\phi'_{E,i} (-a - e \gamma_o + (r + e) q'_{EO}) - \phi_{E,i} q'_{EO} - \phi_{F,i} \beta_o \\
&\quad + r_i] - U_P [\phi'_{E,i} (\beta_o + q'_{FO}) + \phi'_{F,i} (\gamma_o - q'_{EO})] \} q_{T,i} \\
&\quad + \sum_{i=1}^{NA} \{ \phi_{\theta Y, i} [b (\gamma_o - q'_{EO}) \sin \psi - (b + r \beta_o) \cos \psi] + \phi_{\theta X, i} [b (\gamma_o - q'_{EO}) \cos \psi \\
&\quad + (b + r \beta_o) \sin \psi] + \phi_{X,i} [(\gamma_o - q'_{EO}) \sin \psi - \cos \psi] + \phi_{Y,i} [-(\gamma_o \\
&\quad - q'_{EO}) \cos \psi - \sin \psi] \} \dot{\bar{q}}_i \\
&\quad + \{ b \} \phi_{\theta T} \\
&\quad + \{ b (\gamma_o - q'_{EO}) \} \dot{\beta} \\
&\quad + \{ r + a q'_{EO} \} \dot{\gamma} \\
&\quad + \sum_{i=1}^{NE} \{ \dot{r}_i q'_{EO} + \phi_{E,i} \} \dot{q}_{T,i}
\end{aligned}$$

$$\begin{aligned}
\delta U_P &= \frac{\partial U_P}{\partial q} + \frac{\partial U_P}{\partial \dot{q}} \\
&= \sum_{i=1}^{NA} \{ \phi_{\theta Y, i} (-U_P (\beta_o + q'_{FO}) \sin \psi) - \phi_{\theta X, i} (U_P (\beta_o + q'_{FO}) \cos \psi) \} \bar{q}_i \\
&\quad + \{ \Omega b (\beta_o + q'_{FO}) \phi_{\theta T} \} \\
&\quad - \{ \Omega (a - r \gamma_o) + U_P (\beta_o + q'_{FO}) \} \beta
\end{aligned}$$

24

$$\begin{aligned}
& + \{\Omega(r\beta_0 - eq'_{FO})\}\gamma \\
& + \sum_{i=1}^{NE} \{\Omega[\phi'_{F,i}(-a + r\gamma_0) + \phi_{E,i}(\beta_0 + q'_{FO})] - U_p \phi'_{F,i}(\beta_0 + q'_{FO})\}q_{T,i} \\
& + \sum_{i=1}^{NA} \{(-(a - r\gamma_0)\cos\psi + (r + e + bq'_{FO} + a\gamma_0)\sin\psi)\phi_{\theta Y,i} \\
& + ((a - r\gamma_0)\sin\psi + (r + e + bq'_{FO} + a\gamma_0)\cos\psi)\phi_{\theta X,i} \\
& + \phi_{X,i}(\beta_0 + q'_{FO})\sin\psi - \phi_{Y,i}(\beta_0 + q'_{FO})\cos\psi \\
& + \dot{\phi}_{Z,i}\} \dot{q}_i \\
& + \{a\}\phi_\theta \dot{\theta}_T \\
& + \{a\gamma_0 + r + bq'_{FO}\} \dot{\beta} \\
& - \{aq'_{FO}\} \dot{\gamma} \\
& + \sum_{i=1}^{NE} \{-\dot{r}_i q'_{FO} + \dot{\phi}_{F,i}\} \dot{q}_{T,i} \\
\delta\alpha = \frac{\partial\alpha}{\partial q} + \frac{\partial\alpha}{\partial \dot{q}} & = \{-1\}\phi_\theta \theta_T
\end{aligned}$$

$$\begin{aligned}
\bar{q}_j & = \int_0^{R-e} \left[\sum_{n=1}^N \left\{ \sum_{i=1}^{NA} \{ \phi_{\theta X,i} [\phi_{\theta Y,j} ((-b_1\beta_0 + a_1q'_{EO} + r + e)dH \right. \right. \\
& \quad \left. \left. + a_1(\beta_0 + q'_{FO})dT)] + \phi_{X,j} [\phi_{\theta Y,i} dT] - \phi_{Y,j} [\phi_{\theta X,i} dT] \} \bar{q}_i \right. \\
& \quad \left. + \{ \phi_{\theta X,j} [(-a_1\sin\psi - a_1(\gamma_0 - q'_{EO})\cos\psi)dH - (b_1\sin\psi - (a_1q'_{FO} \right. \right. \\
& \quad \left. \left. - b_1\dot{\gamma}_0)\cos\psi)dT] + \phi_{\theta Y,j} [(a_1\cos\psi - a_1(\gamma_0 - q'_{EO})\sin\psi)dH + (b_1\cos\psi \right. \right. \\
& \quad \left. \left. + (a_1q'_{FO} - b_1\dot{\gamma}_0)\sin\psi)dT] \} \phi_\theta \theta_T \right. \\
& \quad \left. + \{ \phi_{\theta X,j} [((b_1\beta_0 - r - a_1q'_{EO})\sin\psi + e(\gamma_0 - q'_{EO})\cos\psi)dH \right. \right. \\
& \quad \left. \left. - (b_1\dot{\beta}_0)\cos\psi)dT] \} \phi_\theta \theta_T \right]
\end{aligned}$$

$$\begin{aligned}
& - (a_1(\beta_o + q'_{FO}) \sin\psi + e(\beta_o + q'_{FO}) \cos\psi) dT] + \phi_{\theta Y, j} [(- b_1 \beta_o + r \\
& + a_1 q'_{EO}) \cos\psi + e(\gamma_o - q'_{EO}) \sin\psi) dH + (a_1(\beta_o + q'_{FO}) \cos\psi - e(\beta_o \\
& + q'_{FO}) \sin\psi) dT] + \phi_{X, j} \sin\psi dT - \phi_{Y, j} \cos\psi dT + \phi_{Z, j} ((\gamma_o - q'_{EO}) dH \\
& - (\beta_o + q'_{FO}) dT) \beta \\
& + \{\phi_{\theta X, j} [(- b_1(\gamma_o - q'_{EO}) \sin\psi + (e\beta_o - b_1) \cos\psi) dH - ((b_1 q'_{FO} + a_1 \gamma_o \\
& + r) \sin\psi - (a_1 - r\gamma_o) \cos\psi) dT] - \phi_{\theta Y, j} [(- b_1(\gamma_o - q'_{EO}) \cos\psi - (e\beta_o \\
& - b_1) \sin\psi) dH + ((- b_1 q'_{FO} - a_1 \gamma_o - r) \cos\psi - (a_1 - r\gamma_o) \sin\psi) dT] \\
& - \phi_{X, j} [((\gamma_o - q'_{EO}) \cos\psi + \sin\psi) dH - q'_{FO} \cos\psi dT] - \phi_{Y, j} [((\gamma_o - q'_{EO}) \sin\psi \\
& - \cos\psi) dH - q'_{FO} \sin\psi dT] + \phi_{Z, j} \beta_o dH\} \gamma \\
& + \sum_{i=1}^{NE} \{\phi_{\theta X, j} [(- \phi_{F,i} + b_1(\gamma_o - q'_{EO}) \phi'_{E,i} + a_1 \beta_o \phi'_{E,i}) \sin\psi \\
& - (\phi_{F,i}(\gamma_o - q'_{EO}) + b_1 \phi'_{E,i} - e\beta_o \phi'_{E,i}) \cos\psi) dH - ((\phi_{E,i} + b_1(\gamma_o \\
& - q'_{EO}) \phi'_{F,i} + a_1(\beta_o + q'_{FO}) \phi'_{F,i} + b_1 q'_{FO} \phi'_{E,i}) \sin\psi + (\phi_{E,i} \gamma_o \\
& - r_i - q'_{FO} \phi_{F,i} + (r + e) q'_{FO} \phi'_{F,i}) \cos\psi) dT] - \phi_{\theta Y, j} [(- \phi_{F,i} \\
& + b_1(\gamma_o - q'_{EO}) \phi'_{E,i} + a_1 \beta_o \phi'_{E,i}) \cos\psi + (\phi_{F,i}(\gamma_o - q'_{EO}) + b_1 \phi'_{E,i} \\
& - e\beta_o \phi'_{E,i}) \sin\psi) dH + ((- \phi'_{E,i} - b_1(\gamma_o - q'_{EO}) \phi'_{F,i} - a_1(\beta_o + q'_{FO}) \phi'_{F,i} \\
& - b_1 q'_{FO} \phi'_{E,i}) \cos\psi + (\phi_{E,i} \gamma_o - r_i - q'_{FO} \phi_{F,i} + (r + e) q'_{FO} \phi'_{F,i}) \sin\psi) dT] \\
& - \phi_{X, j} [(\phi'_{E,i} \sin\psi + \phi'_{E,i}(\gamma_o - q'_{EO}) \cos\psi) dH + (- \phi'_{F,i} \sin\psi - (\phi'_{F,i}(\gamma_o \\
& - q'_{EO}) + q'_{FO} \phi'_{E,i}) \cos\psi) dT] - \phi_{Y, j} [(- \phi'_{E,i} \cos\psi + \phi'_{E,i}(\gamma_o \\
& - q'_{EO}) \sin\psi) dH + (\phi'_{F,i} \cos\psi - (\phi'_{F,i}(\gamma_o - q'_{EO}) + q'_{FO} \phi'_{E,i}) \sin\psi) dT] \\
& - \phi_{Z, j} [- \beta_o \phi'_{E,i} dH + \phi'_{F,i}(\beta_o + q'_{FO}) dT] \} a_{T,i} + [(\phi_{\theta X, j} (a_1 \gamma_o + r + e)^{26}
\end{aligned}$$

$$\begin{aligned}
& + b_1 q'_{FO}) - \phi_{\theta Y, j} (a_1 - r \gamma_o) \\
& - \phi_{Y, j} (\beta_o + q'_{FO}) \cos \psi + (\phi_{\theta X, j} (a_1 - r \gamma_o) + \phi_{\theta Y, j} (a_1 \gamma_o + r + e \\
& + b_1 q'_{FO}) + \phi_{X, j} (\beta_o + q'_{FO}) \sin \psi + \phi_{Z, j}) [t_1 \delta U_T + t_2 \delta U_P + t_3 \delta \alpha] \\
& + [(-\phi_{\theta X, j} b_1 (\gamma_o - q'_{EO}) + \phi_{\theta Y, j} (b_1 + r \beta_o) + \phi_{Y, j} (\gamma_o - q'_{EO}) \\
& + \phi_{X, j} \cos \psi - (\phi_{\theta X, j} (b_1 + r \beta_o) + \phi_{\theta Y, j} b_1 (\gamma_o - q'_{EO}) + \phi_{X, j} (\gamma_o - q'_{EO}) \\
& - \phi_{Y, j} \sin \psi) [h_1 \delta U_T + h_2 \delta U_P + h_3 \delta \alpha]] dr \Big\} \quad |(42)
\end{aligned}$$

$$\begin{aligned}
Q_{\theta T} = & \left\{ \int_0^{R-e} [(-a_1 dH - b_1 dT) \phi_{\theta T}^2 \right. \\
& + \sum_{i=1}^{NE} ((-\phi_{F,i} - \phi'_{E,i} q'_{EO} b_1) dH - (\phi_{E,i} + \phi'_{E,i} q'_{FO} b_1 \\
& - \phi'_{F,i} (q'_{EO} b_1 - q'_{FO} a_1)) dT) \phi_{\theta} q_{T,i} \\
& + a_1 (t_1 \delta U_T + t_2 \delta U_P + t_3 \delta \alpha) \phi_{\theta} \\
& - b_1 (h_1 \delta U_T + h_2 \delta U_P + h_3 \delta \alpha) \phi_{\theta} \\
& \left. - (m_1 \delta U_T + m_2 \delta U_P + m_3 \delta \alpha) \phi_{\theta} \right] dr \Big\} \quad |(43)
\end{aligned}$$

$$\begin{aligned}
Q_B = & \left\{ \int_0^{R-e} [(-a_1 (\gamma_o - q'_{EO}) dH - (b_1 \gamma_o - a_1 q'_{FO}) dT) \phi_{\theta} \theta_T \right. \\
& - (b_1 dH - (a_1 - r \gamma_o) dT) \gamma \\
& + \sum_{i=1}^{NE} ((-\phi_{F,i} (\gamma_o - q'_{EO}) - \phi'_{E,i} b_1) dH - (\phi_{E,i} \gamma_o - \phi_{F,i} q'_{FO} \\
& - r_i - \phi'_{F,i} (b_1 - r q'_{FO})) dT) q_{T,i} \\
& + (a_1 \gamma_o + r + b_1 q'_{FO}) (t_1 \delta U_T + t_2 \delta U_P + t_3 \delta \alpha) \\
& \left. - (b_1 (\gamma_o - q'_{EO})) (h_1 \delta U_T + h_2 \delta U_P + h_3 \delta \alpha) \right] dr \Big\} \quad |(44)
\end{aligned}$$

$$Q_Y = \left\{ \int_0^{R-e} \left[(b_1 q'_{EO} dH + b_1 q'_{FO} dT) \phi_\theta \theta_T \right. \right. \\ + \sum_{i=1}^{NE} ((\phi_{E,i} q'_{EO} - r_i + \phi'_{E,i} (a_1 - rq'_{EO})) dH \\ + (\phi_{E,i} q'_{FO} - r \phi'_{E,i} q'_{FO} - \phi'_{F,i} (a_1 - rq'_{EO})) dT) q_{T,i} \\ - (a_1 q'_{FO}) (t_1 \delta U_T + t_2 \delta U_P + t_3 \delta \alpha) \\ \left. \left. - (a_1 q'_{EO} + r) (h_1 \delta U_T + h_2 \delta U_P + h_3 \delta \alpha) \right] dr \right\} \quad (45)$$

$$Q_{q_{T,j}} = \left\{ \int_0^{R-e} \left[(-\phi_{F,j} dH - \phi_{E,j} dT) \phi_\theta \theta_T \right. \right. \\ + \sum_{i=1}^{NE} ((-q'_{EO} r_{j,i} - \phi'_{E,i} (q'_{EO} \phi_{E,j} - r_j)) dH \\ - (q'_{FO} \phi_{E,j} \phi'_{E,i} + \phi'_{F,i} (-q'_{EO} \phi_{E,j} + r_j + q'_{FO} \phi_{F,j}) \\ + q'_{FO} r_{j,i}) dT) q_{T,i} \\ + \phi_{F,j} (t_1 \delta U_T + t_2 \delta U_P + t_3 \delta \alpha) \\ \left. \left. - \phi_{E,j} (h_1 \delta U_T + h_2 \delta U_P + h_3 \delta \alpha) \right] dr \right\} \quad (46)$$

28

LIST OF SYMBOLS

a	$= q_{EO} + (C/4 - EA)\cos\theta_0$
a_1	$= q_{EO} - AC\cos\theta_0$
a_2	$= q_{EO} - CG\cos\theta_0$
a_h	$= EA/b_h$
AC	Distance from blade elastic axis to aerodynamic center--positive toward leading edge.
L_2	Distance from blade elastic axis to pushrod: positive toward leading edge.
L_3	Radial location of blade pitch horn.
L_1	Length of one arm of tail rotor blade pitch spider beam.
L_s	Length of tail rotor pitch beam arm.
m	Blade elemental mass
M_G	Airframe mode generalized mass.
M_q	Generalized mass of blade bending modes.
M_A	Generalized mass of fixed system modes.
M_1	Mass at pushrod.
M	Mach number.
m_1	Partial derivative of pitching moment with respect to local blade tangential velocity.
m_2	Partial derivative of pitching moment with respect to local blade vertical velocity.
m_3	Partial derivative of pitching moment with respect to local blade angle of attack.
n	Blade number.
N	Number of blades.
NE	Number of blade bending modes.

NA	Number of fixed system modes.
h_3	Partial derivative of drag with respect to local blade angle of attack.
I	Blade flatwise, edgewise, torsional mass moment of inertia matrix.
I_θ	Blade torsional mass moment of inertia.
I_{YY}	Blade edgewise second moment of area.
I_X	Elemental blade flatwise mass moment of inertia.
I_Y	Elemental blade torsional mass moment of inertia.
I_Z	Elemental blade chordwise mass moment of inertia.
I_T	Total blade torsional mass moment of inertia.
I_γ	Blade mass moment of inertia about lag hinge.
J	Local blade polar second moment of area.
K	Blade torsional stiffness.
K_G	Airframe mode generalized stiffness.
K_γ	Blade lag hinge spring rate.
K_β	Blade flapping hinge spring rate.
K_1	Pitch beam stiffness or stiffness at main or tail rotor blade pushrod.
K_{MA}	Stiffness of tail rotor pitch actuator for pure moment applied at pitch beam end.
$C_{M,M}$	Partial derivative of pitching moment coefficient with respect to Mach number.
CG	Distance from blade elastic axis to center of gravity--positive toward leading edge.
dL	Elemental lift.
dD	Elemental drag.
dM	Elemental pitching moment.

dT	Elemental thrust.
dH	Elemental inplane force.
e	Blade offset.
EA	Distance from blade semi-chord to elastic axis-positive toward trailing edge.
G	Blade torsional modulus of elasticity.
h_1	Partial derivative of drag with respect to local blade tangential velocity.
h_2	Partial derivative of drag with respect to local blade vertical velocity.
\bar{q}_j	Fixed system mode generalized coordinate.
$Q_{T,j}$	Blade bending mode generalized coordinate--bending up and leading positive.
q_{F0}	Steady blade flatwise deflection--up positive.
Q_{E0}	Steady blade inplane deflection--lag positive.
$\bar{q}_{\theta X}$	Hub pitch coordinate.
$\bar{q}_{\theta Y}$	Hub roll coordinate.
\bar{q}_X	Hub lateral coordinate.
\bar{q}_Y	Hub longitudinal coordinate.
\bar{q}_Z	Hub vertical coordinate.
q_0	Collective mode coordinate.
q_D	Reactionless mode coordinate.
q_s	Sine cyclic coordinate.
q_c	Cosine cyclic coordinate.

q'_{F01}	
q'_{F0s}	Blade flatwise bending slope steady, and sine and cosine coefficient components.
q_{F0c}	Generalized forces.
\underline{Q}	
$Q_{\underline{q},j}$	Generalized force on j'th fixed system mode.
$Q_{\theta T}$	Generalized force on blade pitch.
Q_β	Generalized force on blade flapping.
Q_γ	Generalized force on blade lagging.
$Q_{q_T,j}$	Generalized force on j'th blade bending mode.
Q_j	Generalized aerodynamic force.
r	Radius of local blade element from offset.
r_1	Radial location of inner snubber of crossbeam rotor.
r_2	Radial location of outer snubber of crossbeam rotor.
R	Rotor radius.
R_S	Radius to servo connections on main rotor swash plate.
R_B	Radius to pushrod connections on main rotor swash plate.
t_1	Partial derivative of thrust with respect to local blade tangential velocity.
t_2	Partial derivative of thrust with respect to local blade vertical velocity.
t_3	Partial derivative of thrust with respect to local blade angle of attack.
U	Total local blade inflow velocity.
U_p	Local blade vertical velocity.
U_T	Local blade tangential velocity.

v	Speed of sound.
V	Potential energy.
v_A	Rotor axial velocity.
v_F	Forward-flight speed.
x_1	Displacement at blade pushrod.
α	Local blade angle of attack.
α_1	Pitch-lag coupling--lead, pitch-up positive.
β	Blade rigid-body flapping generalized coordinate--up positive.
β_0	Steady blade coning--up positive.
γ	Blade rigid-body lag generalized coordinate--lead positive.
γ_0	Steady blade lag--lead positive.
δ_3	Pitch-flap coupling--flap up, pitch down positive.
ζ_q	Fraction of critical structural damping of blade bending modes--based on modal frequency.
ζ_θ	Fraction of critical structural damping of blade pitch mode--based on rotor speed.
ζ_γ	Fraction of critical rigid-body lag damping--based on uncoupled lag frequency.
ζ_A	Fraction of critical structural damping of fixed system modes--based on modal frequency.
θ	Blade pitch generalized coordinate--leading edge down positive.
θ_0	Steady blade pitch angle--leading edge down positive.
θ_T	Blade pitch normal coordinate.
θ_P	Geometric blade pitch angle--leading edge up positive.
v_1	$= \left(\int_0^r (-\phi' E_{,i} q' E_0 + \phi' F_{,i} q' F_0) dr \right) = -r_i$
v_2	$= \left(\int_0^r (\phi' E_{,i} \phi' E_{,j} + \phi' F_{,i} \phi' F_{,j}) dr \right) = \dot{r}_i = r_{i,j}$
ρ	Air mass density.

ϕ	Local blade inflow angle.
$\phi_{X,Y,Z}$	Fixed system translational mode shapes at hub.
$\phi_{\theta X,\theta Y}$	Fixed system rotational mode shapes at hub.
ϕ_F	Blade flatwise bending mode shape.
ϕ_E	Blade inplane bending mode shape.
ϕ_θ	Blade torsional mode shape.
$\phi_{\theta PR}$	Blade torsional mode shape at pushrod radial station.
ϕ_{FPR}	Blade flatwise bending mode shape at pushrod radial station.
ϕ_{ET}	Blade inplane bending mode shape at tip radius.
ψ	Blade azimuthal angle.
ω_{T1}	Blade asymmetric torsional frequency.
ω_{T2}	Blade symmetric torsional frequency.
ω_p	Hub pitch frequency.
ω_y	Hub yaw frequency.
ω_{EN}	Blade edgewise natural frequency.
ω_q	Frequency of blade bending modes.
ω_γ	Uncoupled rigid-body lag frequency.
ω_A	Frequency of fixed system modes.
ω	Flutter frequency.
Ω	Rotor speed.

Subscripts

i	Refers to blade element or mode number.
j	Refers to mode or force number.

s Refers to mode number.
t
n Refers to blade number.
PR Refers to pushrod.
X
Y Refers to hub lateral, longitudinal, and vertical directions.
Z
 θ_X Refers to hub pitch and roll directions.
 θ_Y

Superscripts

c Means coupled.
u Means uncoupled.

Differential Notation

' Differentiation with respect to radius.
. Differentiation with respect to time.
.. Second differential with respect to time.

D.4 Fuselage Dynamic Representation

The fuselage math model is presented by equation (47), shown in Figure D.4-1. It consists of up to sixteen rigid and/or elastic mode shapes. For this modal representation we need the generalized masses (M_{gi}), frequencies (ω_{ni}) and damping (ζ_i) for these mode shapes. We also need the modal components at any point on the aircraft where forces and moments are applied.

Obtaining the generalized coordinates, q_i , one can then evaluate the response at any point on the aircraft using equation (48), see Figure D.4-1.

$$m_{g_i} \ddot{q}_i + 2\zeta_i m_{g_i} \dot{w}_i \dot{q}_i + m_{g_i} w_i^2 q_i = \phi_{H,i}^T \cdot F_H + \sum_{k=1}^N \phi_{K,i}^T \cdot F_K \quad (47)$$

WHERE:

$\phi_{H,i}^T$ = TRANSPOSE OF MODE SHAPES AT HUB

F_H = FORCES AND MOMENTS AT HUB

$\phi_{K,i}^T$ = TRANSPOSE OF MODE SHAPES AT K^{th} AIRCRAFT POINT

F_K = FORCES AND MOMENTS AT K^{th} AIRCRAFT POINT

N = TOTAL NUMBER OF AIRCRAFT POINTS WHERE EXCITATIONS APPLIED

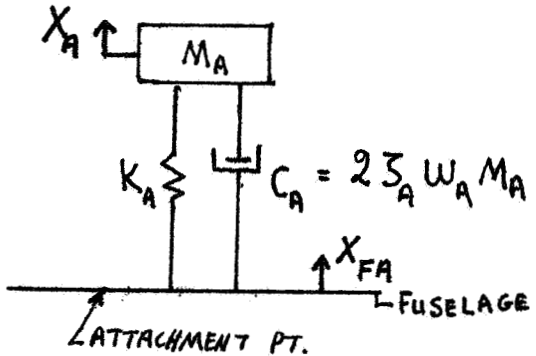
$$X_K = \phi_{K,i} \cdot q_i \quad (48)$$

X_K = RESPONSE VECTOR AT K^{th} POINT ON AIRCRAFT.

FIGURE D.4-1: FUSELAGE MATH MODEL

D.5 Fixed System Absorber

The math model of the fixed system absorber is shown in Figure D.5-1. It is a one degree of freedom spring-mass system. The kinetic and potential energies of the system are given by equations (49) and (50) respectively, shown in Figure D.5-1. Substituting into Lagrange's equation results in the equation of motion for the fixed absorber shown in Figure D.5-1 by equation (51).



$$K.E. = \frac{1}{2} M_A (\dot{X}_A + \dot{X}_{FA})^2 \quad (49)$$

$$P.E. = \frac{1}{2} K_A X_A^2 \quad (50)$$

WHERE :

$$\omega_A^2 = \frac{K_A}{M_A}$$

THUS :

$$[M]\{\ddot{X}\} + [C]\{\dot{X}\} + [K]\{X\} = 0 \quad (51)$$

D.5-1: FIXED SYSTEM ABSORBER

WHERE:

$$\{X\} = \begin{Bmatrix} X_{FA} \\ X_A \end{Bmatrix}$$

$$[M] = \begin{bmatrix} M_A & : & M_A \\ : & \ddots & : \\ M_A & : & M_A \end{bmatrix} ; \quad [C] = \begin{bmatrix} 0 & : & 0 \\ : & \ddots & : \\ 0 & : & 25_A \omega_A M_A \end{bmatrix}$$

4ND

$$[K] = \begin{bmatrix} 0 & : & 0 \\ : & \ddots & : \\ 0 & : & M_A \omega_A^2 \end{bmatrix}$$

D.5-1: FIXED SYSTEM ABSORBER (CONCLUDED)

D.6 Assembly of Coupled Equations

To assemble the coupled equations of motion we need to know the modal components, of the same mode shapes used in Section D.4, at any aircraft point where the rotor, fixed and rotating absorbers are attached.

Here we will demonstrate the procedure used to couple the fixed system with that of the rotor. This same technique is used to couple the bifilar and fixed absorbers with the fixed system.

Equation (52) in Figure D.6-1 shows the rotor equation of motion in general form. We partitioned the mass, stiffness and damping matrices into submatrices associated with the hub (attachment point) and rotor degrees of freedom, see equation (53) Figure D.6-1.

The hub degrees of freedom are related to the fuselage (generalized) degrees of freedom by equation (54) shown in Figure D.6-1. Thus equation (53) can be transformed into equation (55) whose state vector consists of the fuselage and rotor degrees of freedom, as shown in Figure D.6-2.

With the hub degrees of freedom replaced by the generalized degrees of freedom, q 's, we can now combine the rotor and fuselage equations of motion, as shown by equation (56) in Figure D.6-2.

$$[M] \cdot \{\ddot{X}\} + [C]\{\dot{X}\} + [K] \cdot \{X\} = \{F\} \quad (52)$$

$$\begin{bmatrix} M_{HH} & M_{HR} \\ M_{RH} & M_{RR} \end{bmatrix} \begin{Bmatrix} \ddot{X}_H \\ \ddot{X}_R \end{Bmatrix} + \begin{bmatrix} C_{HH} & C_{HR} \\ C_{RH} & C_{RR} \end{bmatrix} \begin{Bmatrix} \dot{X}_H \\ \dot{X}_R \end{Bmatrix} + \begin{bmatrix} K_{HH} & K_{HR} \\ K_{RH} & K_{RR} \end{bmatrix} \begin{Bmatrix} X_H \\ X_R \end{Bmatrix} = \begin{Bmatrix} F_R \\ 0 \end{Bmatrix} \quad (53)$$

WHERE:

$$\{X_H\} = \text{HUB DEGREES OF FREEDOM}, (6 \times 1)$$

$$\{X_R\} = \text{ROTOR DEGREES OF FREEDOM}, (n_R \times 1)$$

$$\{X_H\} = [\phi_H] \cdot \{q\} \quad (54)$$

WHERE :

$$\{q\} = \text{FUSELAGE DEGREES OF FREEDOM } (n_F \times 1)$$

$$[\phi_H] = \text{HUB MODE SHAPES } (6 \times n_F)$$

Figure D.6-1: Uncoupled Equations of Motion

$$\left[\begin{array}{c|c} [\Phi_H]^T \cdot [M_{HH}] \cdot [\Phi_H] & [\Phi_H]^T \cdot [M_{HR}] \\ \hline [M_{RH}] \cdot [\Phi_H] & [M_{RR}] \end{array} \right] \begin{Bmatrix} \ddot{q} \\ \ddot{X}_R \end{Bmatrix} +$$

$$\left[\begin{array}{c|c} [\Phi_H]^T \cdot [C_{HH}] \cdot [\Phi_H] & [\Phi_H]^T \cdot [C_{HR}] \\ \hline [C_{RH}] \cdot [\Phi_H] & [C_{RR}] \end{array} \right] \begin{Bmatrix} \dot{q} \\ \ddot{X}_R \end{Bmatrix} +$$

$$\left[\begin{array}{c|c} [\Phi_H]^T \cdot [K_{HH}] \cdot [\Phi_H] & [\Phi_H]^T \cdot [K_{HR}] \\ \hline [K_{RH}] \cdot [\Phi_H] & [K_{RR}] \end{array} \right] \begin{Bmatrix} \ddot{q} \\ \ddot{X}_R \end{Bmatrix} = \begin{Bmatrix} [\Phi_H]^T \cdot \{F_R\} \\ 0 \end{Bmatrix} \quad (55)$$

$$\left[\begin{array}{c|c} m_g + [\Phi_H]^T \cdot [M_{HH}] \cdot [\Phi_H] & [\Phi_H]^T \cdot [M_{HR}] \\ \hline [M_{RH}] \cdot [\Phi_H] & [M_{RR}] \end{array} \right] \begin{Bmatrix} \ddot{q} \\ \ddot{X}_R \end{Bmatrix} +$$

Figure D.6-2: Procedure to Form Coupled Equations (Continued)

$$\begin{bmatrix}
 \left[25m_g \omega^2 \right] + [\Phi_H]^T [C_{HH}] \cdot [\Phi_H] & | & [\Phi_H]^T [C_{HR}] \\
 \hline
 | & | & | \\
 [C_{RH}] \cdot [\Phi_H] & | & [C_{RR}] \\
 \hline
 \end{bmatrix} \begin{Bmatrix} \dot{q} \\ \dot{x}_R \end{Bmatrix} +
 \begin{bmatrix}
 \left[m_g \omega^2 \right] + [\Phi_H]^T [K_{HH}] \cdot [\Phi_H] & | & [\Phi_H]^T [K_{HR}] \\
 \hline
 | & | & | \\
 [K_{RH}] \cdot [\Phi_H] & | & [K_{RR}] \\
 \hline
 \end{bmatrix} \begin{Bmatrix} q \\ x_R \end{Bmatrix} = \begin{Bmatrix} [\Phi_H]^T \{F_R\} \\ + [\Phi_{AP}]^T \{F_{AP}\} \end{Bmatrix} \quad (56)$$

WHERE:

$[\Phi_{AP}]$ = MODE SHAPES AT ANY AIRCRAFT POINT ($6 \times n_f$)

$\{F\}$ = FORCE APPLIED AT ANY AIRCRAFT POINT (6×1)

Figure D.6-2: Procedure to Form Coupled Equations (Concluded)

D.7 Forced Response Solution

The final math model is represented by equation (57) of Figure D.7-1, where the state vector, X , consists of the fuselage, rotor, fixed and rotating absorbers degrees of freedom.

A solution of the form shown by equation (58) is assumed which after substitution in equation (57) results in equation (59), see Figure D.7-1. Expressing the state vector, X_C and X_S in terms of the sine and cosine components of the fuselage and remaining degrees of freedom, see equation (60) Figure D.7-1, and substituting it into equation (59) gives equation (61) from which equation (62) immediately follows after grouping like degrees of freedom. The form of equation (62) is preferred over that of equation (61) since the size of the inverse matrices involved in the solution is greatly reduced. From equations (62) the solutions for q and γ are expressed by equations (63) and (64) respectively, see Figure D.7-1.

$$[M]\{\ddot{X}\} + [C]\{\dot{X}\} + [K]\{X\} = \{F\} \quad |(57)$$

$$\{X\} = \{X_s\} \sin \omega_f t + \{X_c\} \cos \omega_f t \quad |(58)$$

$$[(K) - \omega_f^2[M]]\{X_c\} + \omega_f[C]\{X_s\} = \{F_c\} \quad |(59)$$

$$-\omega_f[C]\{X_c\} + [(K) - \omega_f^2[M]]\{X_s\} = \{F_s\}$$

WHERE:

$$\{X_c\} = \left\{ \begin{array}{c} q_c \\ \gamma_c \end{array} \right\} \quad \text{AND} \quad \{X_s\} = \left\{ \begin{array}{c} q_s \\ \gamma_s \end{array} \right\} \quad |(60)$$

$\{q\}$ AND $\{q\}$ ARE THE COSINE AND SINE COMPONENTS OF THE FUSELAGE DEGREES OF FREEDOM

$\{\gamma\}$ AND $\{\gamma\}$ ARE THE COSINE AND SINE COMPONENTS OF THE ROTOR, FIXED ABSORBERS AND ROTATING ABSORBERS DEGREES OF FREEDOM

Figure D.7-1: Forced Response Solution (Continued)

$$\begin{bmatrix} [K] - \omega_f^2[M] & | & \omega_f[C] \\ -\omega_f[C] & | & [K] - \omega_f^2[M] \end{bmatrix} \begin{Bmatrix} q_c \\ \dot{q}_c \\ q_s \\ \dot{q}_s \end{Bmatrix} = \begin{Bmatrix} F_c \\ 0 \\ F_s \\ 0 \end{Bmatrix} \quad (61)$$

$$\begin{bmatrix} [E] & | & [F] \\ [G] & | & [H] \end{bmatrix} \begin{Bmatrix} q_c \\ q_s \\ \dot{q}_c \\ \dot{q}_s \end{Bmatrix} = \begin{Bmatrix} F_c \\ F_s \\ 0 \\ 0 \end{Bmatrix} \quad (62)$$

$$[[E] - [F][H]^{-1}[G]] \begin{Bmatrix} q_c \\ q_s \end{Bmatrix} = \begin{Bmatrix} F_c \\ F_s \end{Bmatrix} \quad (63)$$

$$\begin{Bmatrix} \dot{q}_c \\ \dot{q}_s \end{Bmatrix} = [H]^{-1}[G] \begin{Bmatrix} q_c \\ q_s \end{Bmatrix} \quad (64)$$

Figure D.7-1: Forced Response Solution (Concluded)

D.8 Time History Solution

We have shown previously the technique used to couple the equations of motion of the fixed system, rotor, fixed absorber, and the linear bifilar transferred to fixed system coordinates. The final equation we arrived at is of the form shown by equation (65), Figure D.8-1. We can rewrite equation (65) in the form shown by equation (66), Figure D.8-2, where the right-hand-side of the equation is replaced by a forcing vector. The non-linear inplane bifilar equations of motion, shown in Figure D.1-3, can be rewritten in the compact form shown in equation (67), Figure D.8-2. Using the coupling technique described in section D.6 we can also couple equations (66) and (67). The resultant coupled mass matrix and force vector are shown in Figure D.8-2 by equations (68) and (69) respectively. The state vector is expanded and consists of the fuselage, rotor, fixed absorber, linear inplane and/or vertical bifilar in the fixed system coordinate, and non-linear inplane bifilar degrees of freedom. The final equations of motion of the system can be rewritten as shown by equation (70) Figure D.8-2. The reason for partitioning the matrix as shown in equation (70) is that the submatrix D has been reduced to the identity matrix and the only inversion required for solution is that of a matrix whose dimension is much smaller than that of the total mass matrix as shown in equation (9). This saves considerable computer time and in addition it is more stable.

Solving equations (71) and (72), shown in Figure D.8-3, we get the acceleration vector. The velocity and displacement vector are updated by equations (73). This procedure is repeated until the state variable, X , have converged within the specified constraints.

$$\begin{bmatrix} \frac{M_q}{q} & \frac{M_{qR}}{q} & \frac{M_{qFA}}{q} & \frac{M_{qLB}}{q} \\ \frac{M_{Rq}}{q} & \frac{M_R}{q} & 0 & 0 \\ \frac{M_{FAq}}{q} & 0 & \frac{M_{FA}}{q} & 0 \\ \frac{M_{LBq}}{q} & 0 & 0 & \frac{M_{LB}}{q} \end{bmatrix} \begin{Bmatrix} \ddot{q} \\ \ddot{x}_R \\ \ddot{x}_{FA} \\ \ddot{x}_{LB} \end{Bmatrix} =$$

$$\begin{Bmatrix} F_q \\ 0 \\ 0 \\ 0 \end{Bmatrix} - \begin{bmatrix} [C_q] & [C_{qR}] & [C_{qFA}] & [C_{qLB}] \\ [C_{Rq}] & [C_R] & 0 & 0 \\ [C_{FAq}] & 0 & [C_{FA}] & 0 \\ [C_{LBq}] & 0 & 0 & [C_{LB}] \end{bmatrix} \begin{Bmatrix} \dot{q} \\ \dot{x}_R \\ \dot{x}_{FA} \\ \dot{x}_{LB} \end{Bmatrix} -$$

$$\begin{bmatrix} [K_q] & [K_{qR}] & [K_{qFA}] & [K_{qLB}] \\ [K_{Rq}] & [K_R] & 0 & 0 \\ [K_{FAq}] & 0 & [K_{FA}] & 0 \\ [K_{LBq}] & 0 & 0 & [K_{LB}] \end{bmatrix} \begin{Bmatrix} \ddot{q} \\ \ddot{x}_R \\ \ddot{x}_{FA} \\ \ddot{x}_{LB} \end{Bmatrix} \quad (65)$$

FIGURE D.8-1: COUPLED EQUATIONS OF MOTION

$$\begin{bmatrix} [M_q] & | & [M_{qR}] & | & [M_{qFA}] & | & [M_{qLB}] \\ \hline [M_{Rq}] & | & [M_R] & | & 0 & | & 0 \\ \hline [M_{FAq}] & | & 0 & | & [M_{FA}] & | & 0 \\ \hline [M_{LBq}] & | & 0 & | & 0 & | & [M_{LB}] \end{bmatrix} \begin{Bmatrix} \ddot{q} \\ \ddot{x}_R \\ \ddot{x}_{FA} \\ \ddot{x}_{LB} \end{Bmatrix} = \begin{Bmatrix} F_q \\ F_R \\ F_{FA} \\ F_{LB} \end{Bmatrix} \quad (66)$$

$$\begin{bmatrix} [M_H(\psi)] & | & [M_{HB}(\psi)] \\ \hline [M_{BH}(\psi)] & | & [M_B(\psi)] \end{bmatrix} \begin{Bmatrix} \ddot{x}_H \\ \ddot{\gamma} \end{Bmatrix} = \begin{Bmatrix} F_H(\psi) \\ F_\gamma(\psi) \end{Bmatrix} \quad (67)$$

$$\begin{bmatrix} [M_q] + [\Phi_H]^T \cdot [M_H] \cdot [\Phi_H]^{-1} & | & [M_{qR}] & | & [M_{qFA}] & | & M_{qLB} \cdot [\Phi_H]^T \cdot [M_{HB}] \\ \hline [M_{Rq}] & | & [M_R] & | & 0 & | & 0 \\ \hline [M_{FAq}] & | & 0 & | & [M_{FA}] & | & 0 \\ \hline [M_{LBq}] & | & 0 & | & 0 & | & [M_{LB}] \\ \hline [M_{BH}] \cdot [\Phi_H] & | & 0 & | & 0 & | & 0 \end{bmatrix} = [M] \quad (68)$$

FIGURE D.8-2: COUPLED EQUATIONS OF MOTION (CONTINUED)

$$\left\{ \begin{array}{l} \{F_Q\} + [\Phi_H]^T \cdot \{F_H\} \\ \dots F_R \dots \\ \dots F_{FA} \dots \\ \dots F_{LB} \dots \\ [\Phi_H]^T \cdot \{F_B\} \end{array} \right\} = \{F\} \quad (69)$$

$$\begin{bmatrix} [A] & [B] \\ [C] & [D] \end{bmatrix} \begin{bmatrix} \ddot{X}_1 \\ \ddot{X}_2 \end{bmatrix} = \begin{bmatrix} F_1 \\ F_2 \end{bmatrix} \quad (70)$$

WHERE:

$$\{X_1\} = \begin{bmatrix} q \\ X_R \end{bmatrix} \quad \text{AND} \quad \{\dot{X}_2\} = \begin{bmatrix} X_{FA} \\ X_{LB} \\ \gamma \end{bmatrix}$$

X_R = ROTOR DEGREES OF FREEDOM

X_{FA} = FIXED ABSORBER DEGREES OF FREEDOM

X_{LB} AND γ = LINEAR (TRANS. TO FIX SYSTEM) AND N.L. BIFILAR DEGREES OF FREEDOM.

FIGURE D.8-2: COUPLED EQUATIONS OF MOTION (CONCLUDED)

$$\{\ddot{X}_1\} = [A] - [B][C]^{-1} \cdot \{F_1\} - [B] \cdot \{F_2\} \quad (71)$$

$$\{\ddot{X}_2\} = \{F_2\} - [C] \cdot \{\ddot{X}_1\} \quad (72)$$

SINCE :

$$[D] \equiv [I] \quad (\text{IDENTITY MATRIX})$$

$$\{\dot{X}_1\}_{\text{NEW}} = \{\dot{X}_1\}_{\text{OLD}} + (\Delta T) \{\ddot{X}_1\}_{\text{NEW}}$$

$$\{X_1\}_{\text{NEW}} = \{X_1\}_{\text{OLD}} + (\Delta T) \{\dot{X}_1\}_{\text{NEW}} \quad (73)$$

$$\{\dot{X}_2\}_{\text{NEW}} = \{\dot{X}_2\}_{\text{OLD}} + (\Delta T) \{\ddot{X}_2\}_{\text{NEW}}$$

$$\{X_2\}_{\text{NEW}} = \{X_2\}_{\text{OLD}} + (\Delta T) \{\dot{X}_2\}_{\text{NEW}}$$

FIGURE D.8-3: SOLUTION OF COUPLED EQUATIONS OF MOTION

D.9 List of Symbols

M_A	Fixed absorber mass
M_{Gi} , m_{gi}	Generalized masses
M_T	Total bifilar mass
m	Individual bifilar mass
N	Total number of bifilars
n	Bifilar tuning
q_i	Generalized coordinates
R	Distance from center of bifilar tracking hole to center of rotation
r	Equivalent pendulum arm
x_A	Vertical motion of fixed system absorber
x_{FA}	Vertical motion of attachment point of fixed absorber and fuselage
X	Rotating coordinate system
X_I	Inertia coordinate system
w_A	Fixed absorber tuning frequency
w_i	Generalized frequencies
w_β	Vertical bifilar tuning frequency
w_γ	Inplane bifilar tuning frequency
β	Vertical bifilar degree of freedom
γ	Inplane bifilar degree of freedom
ζ_A	Fixed absorber damping
ζ_β	Vertical bifilar damping
ζ_γ	Inplane bifilar damping

ζ_i	Generalized damping
ϕ	Mode shapes
ψ	Bifilar arm angle of rotation
Ω	Rotor speed
θ_x	Hub roll
θ_y	Hub pitch
θ_z	Hub yaw
ζ_x	Hub longitudinal modal damping
ζ_y	Hub lateral modal damping
ζ_z	Hub vertical modal damping
$\zeta_{\theta x}$	Hub roll modal damping
$\zeta_{\theta y}$	Hub pitch modal damping
$\zeta_{\theta z}$	Hub yaw modal damping
w_x	Hub longitudinal modal frequency
w_y	Hub lateral modal frequency
w_z	Hub vertical modal frequency
$w_{\theta x}$	Hub roll modal frequency
$w_{\theta y}$	Hub pitch modal frequency
$w_{\theta z}$	Hub yaw modal frequency

Subscripts

H, h	Hub
HR	Hub-Rotor
i	Fixed system mode
k	k^{th} bifilar
R	Rotor

Differential Notation

- . Differentiation with respect to time
- .. Second differential with respect to time

Matrix Definitions

C	Damping matrix
C_{HH}	Hub damping sub-matrix
C_{HR}	Hub/rotor damping coupled sub-matrix
C_{RH}	Rotor/hub damping coupled sub-matrix
C_{RR}	Rotor damping sub-matrix
C_q	Generalized fuselage damping sub-matrix
C_{qR}	Generalized fuselage/rotor damping coupled sub-matrix
C_{Rq}	Rotor/generalized fuselage damping coupled sub-matrix
C_{qFA}	Generalized fuselage/fixed absorber damping coupled sub-matrix
C_{FAq}	Fixed absorber/generalized fuselage damping coupled sub-matrix
C_{qLB}	Generalized fuselage/linear bifilar damping coupled sub-matrix
C_{LBq}	Linear bifilar/generalized fuselage damping coupled sub-matrix
F	Force vector
F_{AP}	Force vector at any point on the aircraft
F_C	Cosine component of generalized force vector
F_S	Sine component of generalized force vector
F_H	Force vector at hub
F_R	Force vector at hub due to rotor
K	Stiffness matrix
K_{HH}	Hub stiffness sub-matrix
K_{HR}	Hub/rotor stiffness coupled sub-matrix

K_{RH}	Rotor/hub stiffness coupled sub-matrix
K_{RR}	Rotor stiffness sub-matrix
K_q	Generalized fuselage stiffness sub-matrix
K_{qR}	Generalized fuselage/rotor stiffness coupled sub-matrix
K_{Rq}	Rotor/generalized fuselage stiffness coupled sub-matrix
K_{qFA}	Generalized fuselage/fixed absorber stiffness coupled sub-matrix
K_{FAq}	Fixed absorber/generalized fuselage stiffness coupled sub-matrix
K_{qLB}	Generalized fuselage/linear bifilar stiffness coupled sub-matrix
K_{LBq}	Linear bifilar/generalized fuselage stiffness coupled sub-matrix
M	Mass matrix
M_{HH}	Hub mass matrix
M_{HR}	Hub/rotor mass coupled sub-matrix
M_{RH}	Rotor/hub mass coupled sub-matrix
M_{RR}	Rotor mass sub-matrix
M_q	Generalized fuselage mass sub-matrix
M_{qR}	Generalized fuselage/rotor mass coupled sub-matrix
M_{Rq}	Rotor/generalized fuselage mass coupled sub-matrix
M_{qFA}	Generalized fuselage/fixed absorber mass coupled sub-matrix
M_{FAq}	Fixed absorber/generalized fuselage mass coupled sub-matrix
M_{qLB}	Generalized fuselage/linear bifilar mass coupled sub-matrix
M_{LBq}	Linear bifilar/generalized fuselage mass coupled sub-matrix